RADIOIMMUNOASSAY AND CHARACTERIZATION OF LIGANDIN IN THE RAT

by

Nathan Michael Bass

A thesis submitted for the degree, Doctor of Philosophy, in the Faculty of Medicine, University of Cape Town.

November, 1977.

To Wilma

The beautiful relations
Shown only by biochemistry
Replace a stupefied sense of wonder
with something more wonderful
Because natural and understandable.
Nature is more wonderful
When it is at least partly understood.

Hugh MacDiarmid.

ACKNOWLEDGEMENTS

Although I felt the stirrings of something akin to interest in the laboratory bench on many occasions while I was a medical student, my experience of its real essence began in 1975, when Dr. Ralph Kirsch welcomed me to the MRC Liver Research Laboratory, and introduced me to ligandin. In the months that followed, during which time I pursued the work that has provided the material for this thesis, Dr. Kirsch shared in every tribulation and triumph, while providing optimistic encouragement and sound criticism which were at all times invaluable. It has been a privilege and a pleasure to work with him.

During this work, I was decidedly fortunate in having the outstanding technical assistance of Ms. Sheenah Tuff, whose devotion and skill have made a contribution for which I shall remain eternally indebted.

On many occasions I benefitted greatly from the aid, advice and instruction of friends and colleagues, to whom I am deeply grateful. I wish to thank in particular:

Dr. L Purves, of the Department of Chemical Pathology, for introducing me to a host of new skills, including radioimmunoassay, polyacrylamide gel electrophoresis and computers, and for his continuing helpful advice;

Dr. Jack Franks of the University of Colorado Medical School, whose timely presence in our laboratory was a great boon to me, and with whom I spent many stimulating hours discussing and learning about biochemistry, mathematics and life in general;

Professor S.J. Saunders, for the critical appraisal and guidance from which this work has benefitted;

Mr. V.M. Wells, for unfailingly maintaining the supply line of materials, repairing recalcitrant equipment, constructing many pieces of apparatus, and generally being an indispensable man-about-the-laboratory;

Mr. M.F. Parker and Mr. M. Stofile for their expert and cheerful handling of the experimental animals, which they also bred and nurtured with care;

Dr. T. Wainer and Mr. D.A. Scammell of the Medical School Animal House for providing, and tending to the rabbits;

Ms. L. Frith, for the flawless iodine monochloride labelling;

Ms. J. Green and associates, of the Department of Surgery, for numerous SGOT determinations;

Mr. Ian Marks, for a brief, but valuable, period of technical assistance;

Ms. M. Morgan and Dr. W.F. Brandt, of the Department of Biochemistry, who most co-operatively performed the amino acid analyses;

Mr. J. Johnson, who ensured the availability of clean glassware and provided many comforting cups of tea;

Mr. John Billings, for writing the curve fitting programme used in Chapter XVI;

Mr. Gerry Blekkenhorst, for his friendly and most practical advice, which along with the loan of equipment, con-

tributed significantly to the production of this thesis;

Ms. Linda van Schalkwyk, who took many painstaking photographs; and

Ms. Mary Jean McBlain, for a commendable piece of work in typing this thesis.

I express my heartfelt gratitude to my parents for their unflagging support, encouragement, and confidence in me; and to my wife Wilma, to whom this thesis is dedicated, for many things, including patiently sharing me with my work, and so often making light its heavy burden.

This work was made possible through the generous financial assistance of the Medical Research Council, the Cape Provincial Administration, the South African Atomic Energy Board, the Nellie Atkinson Bequest and the Harry Crossley Foundation.

ABBREVIATIONS USED IN THIS THESIS

BSA	Bovine Serum Albumin
BSP	Sulphobromophthalein Sodium
CD	Circular Dichroism
CM-	Carboxymethyl-
CV	Coefficient of Variation
DAB	4-Dimethylaminoazobenzene
DARG	Donkey Anti-Rabbit Globulin
DDT	α,α-Bis(p-Chlorophenyl)-β,β,β-Trichlorethane
DEAE-	Diethylaminoethyl-
DTT	Dithiothreitol
EDTA	Ethylenediaminetetra-acetic Acid (Disodium salt)
GAL-IgG	Goat Anti-Rat Ligandin Immunoglobulin G
GOT	Glutamic-Oxalacetic Transaminase
GSH	Glutathione
Guan. HCl	Guanidine Hydrochloride
^{3}H-BR	Tritiated Bilirubin
HSA	Human Serum Albumin
ICG	Indocyanin Green
NADH	Nicotinamide Adenine Dinucleotide, Reduced Form
NIRS	Non-Immune Rabbit Serum
PAGE	Polyacrylamide Gel Electrophoresis
RIA	Radioimmunoassay
SDS	Sodium Dodecyl Sulphate
SGOT	Serum Glutamic-Oxalacetic Transaminase
T_3	Tri-iodothyronine
T_4	Thyroxine
TCA	Trichloroacetic Acid
TCDD	Tetrachloro-Dibenzo-p-Dioxan
TEAE-	Triethylaminoethyl-
TEMED	N,N,N^{1},N^{1}-Tetramethylethylene Diamine
Tris	Tris-(Hydroxymethyl)-Aminomethane
UCB	Unconjugated Bilirubin
UDPGA	Uridine Diphosphate Glucuronic Acid

TABLE OF CONTENTS

Page

APPENDICES

PART 1

INTRODUCTION AND LITERATURE SURVEY

CHAPTER I

INTRODUCTION

Ligandin, a major soluble hepatic protein with the distinctive property of binding a wide range of organic anions, is a relative newcomer to the field of hepatic physiology and biochemistry, and its importance in relation to various aspects of hepatic and renal function has been given considerable stress (1-13).

Although the first isolation of ligandin and its identification as a discrete entity was achieved by Ketterer in the period 1965-67 (14), the discovery of this protein, its characterization and subsequent naming, were the results of independent studies in three major areas of research in which the liver occupied a central role (1). Thus ligandin emerged from investigations into the enigma of bilirubin uptake by the liver, the nature of carcinogen-binding target proteins and the mechanism of steroid hormone action in the liver. The later discovery of the identity of ligandin with the enzyme glutathione S-transferase B (15) added a further dimension to the understanding of the role of this protein in the liver. Ligandin could thus be regarded as a milestone in several fields, providing a point of convergence between the disciplines of hepatic physiology, enzymology, endocrinology and cancer research.

The present study was prompted by the need for a sensitive and specific method for measuring ligandin in tissues and physiological fluids and is concerned mainly with the development of a radioimmunoassay for this protein in the rat, as well as the applications of this technique. Certain

observations pertaining to the structure of ligandin also emerged during this work and were explored further in relation to the function of this protein as an enzyme and as an organic anion binding protein.

Although the work presented here was commenced in 1975, the review that comprises Part 1 of this thesis, encompasses the pertinent literature available up to the time of writing in 1977, and hopes to provide a clear and in-depth insight into the complex and multifunctional nature of ligandin. Thus I have attempted firstly, to present a perspective of the events and concepts in each field which led to the realization of ligandin. This is followed by an account of the present biochemical understanding of this protein and finally, an examination of the putative function of ligandin in the cell. It is against this background that the aims and scope of the present study will be fully detailed.

A.

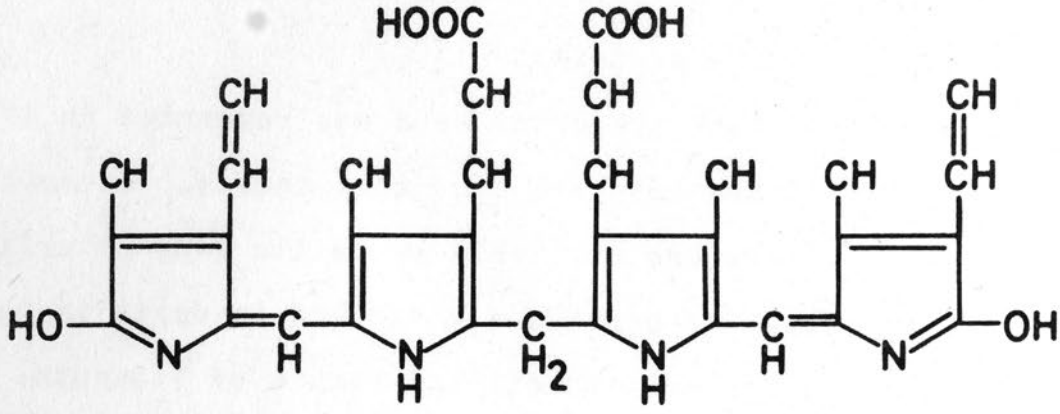

B.

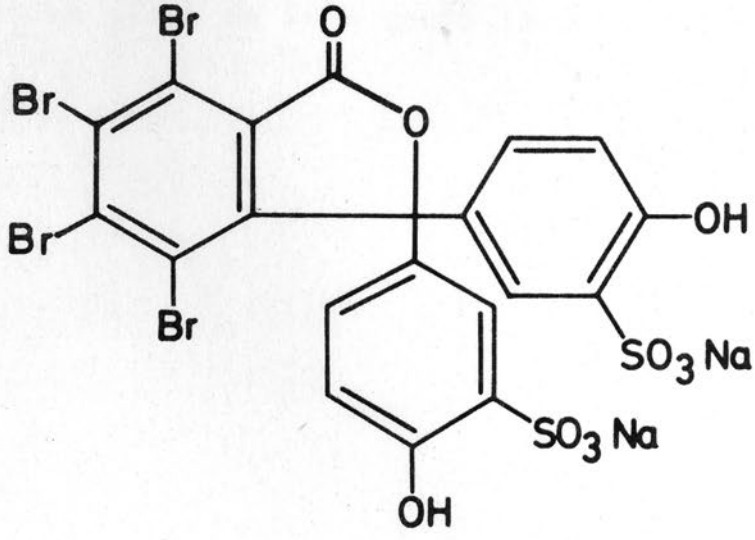

Fig. 1.1. Structural formulae of (A), bilirubin and (B), BSP.

CHAPTER II

HISTORICAL ASPECTS

1. The Uptake of Organic Anions by the Liver

i) Organic anions and the liver:

The organic anions in mammalian bile consist of bile acids, bile pigments derived mainly from bilirubin, porphyrins, metabolites, dyes and drugs which are all believed to be excreted by the liver (16). Bilirubin and the dye sulphobromophthalein sodium (BSP) have been extensively studied as examples of endogenous and exogenous organic anions respectively, in relation to normal and abnormal hepatic function, and will be considered here briefly (see Fig. 1.1):

(a) Bilirubin

The role of the liver in the elimination of a factor responsible for jaundice may have been appreciated since the time of Hippocrates in 400 B.C., while jaundice associated with biliary stones and other causes was dealt with in the writings of Galen and Avicenna (17). The experiments of Tarchanoff (18) in 1874 first demonstrated that intravascular administration of haemoglobin resulted in an increased excretion of bile pigment, but the problem as to whether the liver merely excreted the bilirubin formed at other sites or both formed and excreted the pigment, was only resolved with the achievement of successful hepatectomy in mammals (19). It was then established that formation of bilirubin - the major bile pigment - from haemoglobin, took place in the reticuloendothelial system from whence it was transported in the

plasma to the liver, which then excreted the pigment in the bile.

Bilirubin is a non-polar organic anion, and because of its importance in the clinical syndrome of jaundice, it has been extensively studied in relation to liver function, and these studies have provided insight into the mechanism whereby other organic anions of great biological importance such as steroid hormones and drugs are transported, metabolized and excreted (3,20). Bilirubin is primarily derived from the haemoglobin of senescent erythrocytes in the reticuloendothelial system, while about 10% originates from non-erythroid sources. The mechanisms of conversion of haemoglobin to bilirubin is a complex process which has been exhaustively studied and reviewed (3,21,22). After it is released from the reticuloendothelial system, bilirubin is transported in the plasma bound mainly to albumin (23-26) at a single high affinity binding site, and under certain circumstances, at a series of low affinity sites as well. A small amount of bilirubin may also bind to α_1 and α_2-globulins (23) and a β-lipoprotein (3).

(b) BSP:

The early investigations of Chrzonszczewsky in 1866 (27) demonstrated the importance of the liver in the elimination of administered dyes, while Rosenthal and White (28) in 1924 showed that the tetrahalogenphenolphthaleins were rapidly removed from the blood by the liver and excreted in the bile. The elimination of the brominated compound sulphobromophthalein sodium (BSP) appeared to be most affected by hepatic damage

in rabbits, and was subsequently found to be of value in the detection of hepatocellular damage in man (29). In a manner similar to bilirubin, BSP is transported in the plasma bound to albumin at both high and low affinity sites (30,31) and also to an α_1-lipoprotein (32).

Both bilirubin and BSP disappear very rapidly from the blood after intravenous administration and were used extensively in early investigations of liver function in both experimental and clinical fields (33-38). Although some studies had indicated that other tissues besides the liver, were capable of removing bilirubin (39) and BSP (40,41) from the plasma, it was well established at the time that in the normal mammal, plasma disappearance of these substances occurred primarily through the activity of the liver.

The use of other organic anions including the bile salts (42,43) and dyes such as fluoroscein or its sodium salt, uranin (43), rose bengal (36,44) and indocyanine green (ICG) (45-47) was soon introduced to an extent, to elucidate the mechanism of the hepatic organic anion elimination. Studies utilizing these substances were usually performed however, in conjunction with bilirubin, BSP, or both.

ii) <u>The hepatic cells responsible for organic anion clearance</u>

Mammalian liver is composed of five distinct cell types:

(1) Hepatocytes or parenchymal cells (60-65% of the cell population).

(2) Reticuloendothelial (littoral, von Kupffer) cells (35%

of the cell population.

(3) Bile duct cells.

(4) Connective tissue cells.

(5) Blood vessel endothelial cells.

The latter 3 groups constitute a small percentage of the total cells and a minor component of liver mass (48).

A considerable controversy existed for many years as to which cell types were responsible for the removal of BSP from the plasma. Studies in which India ink injection caused retention of BSP in dogs were interpreted as demonstrating the effect of reticuloendothelial blockade on BSP removal by Kupffer cells (33,49,50), although bilirubin elimination was not affected by this treatment (39). Contrary evidence was presented by Rosenthal and Lillie (51) in 1931. These workers found no effect on BSP removal by prior reticuloendothelial blockade, while the observations of Shore and Zilversmit in 1954 (52) suggested that the effect of India ink on BSP removal was better explained by a hepatotoxic action, rather than by a specific effect on the Kupffer cells. Another view, held by Andrews (53), was that the small bile ducts played an important role in BSP removal, and was based on the observation that BSP was removed more efficiently when introduced into the hepatic artery than into the portal vein of perfused canine liver. Brauer and his associates, however, showed the exact opposite to occur (54).

Perhaps the most convincing evidence that the parenchymal cells are responsible for BSP removal from the plasma, was produced from the studies of Krebs and Brauer in 1949 (55)

which demonstrated by means of autoradiography that radiolabelled BSP was taken up exclusively by the hepatic parenchymal cells. Similar findings for rose bengal were reported by Mendeloff (44) while the classical study by Hanzon in 1952 (43) which utilized intravital fluorescence microscopy, provided a direct demonstration of the uptake of uranin by hepatocytes in the rat. The controversy was raised yet again in 1967, when Tovey (56) stressed the participation of Kupffer cells in the hepatic removal of BSP, but the most recent studies of Stege and co-workers (48) with isolated parenchymal and Kupffer cells are fully in favour of the exclusive role of the parenchymal cells in removing BSP from the plasma.

Less uncertainty has existed for the role of the hepatocyte in bilirubin removal from the plasma, although the belief that bilirubin occurred as colloidal particles in the blood, led Elton (57) to propose in 1935 that the Kupffer cells actively participated in phagocytosis of this substance. However, bile pigment granulations were visualized by histological examination in the hepatocytes by Forsgren (58) and Kremer (59), while Novikoff and Essner (60) in 1960, identified bile pigment appearing in the hepatocytes by electron microscopy, after intravenous administration of bilirubin. The role of the Kupffer cell, if any, in bilirubin uptake, remains undefined (61).

iii) <u>The mechanism of organic anion transfer from blood to bile</u>

The rapid and selective transfer of organic anions from

blood to bile was initially conceived of by early investigators as a relatively simple process involving "secretory activity" of the liver cells, which effected concentration of these substances in the bile (41,43). The process of secretion was not well understood however, but was thought to be governed by the dual factors of cellular permeability for a substance and a driving force acting on that substance (43). Cellular permeability appeared to be related to the lipid solubility and molecular size of the substance under study, while the driving force was seen as composed of gradients created through concentration of the substance, hydrostatic pressure, electrical potential or surface forces.

Although the formation of bile appeared to be dependent on perfusion of the liver cells by blood (62), a hydrostatic pressure filtration mechanism analogous to that found in the glomeruli of the kidney, as proposed by Pavel (63), was found to be untenable as an explanation of the secretory activity of the liver (64). It appeared more likely, that the major determinant of bile formation was the intrinsic ability of the liver cells to secrete organic anions against a concentration gradient by an energy dependent process termed "active transfer" (43,64,65).

The separation of the process of hepatic removal of organic anions into two distinct processes, uptake into the hepatocytes followed by excretion into the bile, became evident from the observations made by several groups (33,34, 66), that both bilirubin and BSP were cleared earlier and at

a more rapid rate than their subsequent appearance and rate of excretion in the bile. The observed difference in the plasma clearance and biliary excretion rates of organic anions further implied that the liver was capable of temporarily storing these compounds after uptake with excretion taking place from this "storage compartment" (34,66). When the phenomenon of uptake was explored by the use of rat liver slices and isolated perfused livers (67,68), it was demonstrated that the in vitro uptake of BSP by the liver was more efficient than that shown by other tissues, and appeared not to be an energy-requiring process. Hanzon (43) visualized the process of hepatocyte extraction of uranin from the plasma by direct microscopy, and described it to consist of diffusion of the dye through the sinusoidal endothelial cells with uptake and concentration close to the endothelial surface of the liver cells, followed by passive diffusion across the cell and concentration close to the bile cannalicular surface,with ultimate excretion in the bile. From these studies, a picture of two "active" concentrating processes residing at the sinusoidal and cannalicular poles of the hepatocyte emerged. These two processes "linked in series" appeared to effect the transfer of organic anions from blood to bile.

The concept of an interim storage phase in the transfer process was developed further with the finding that the liver had a limited capacity for eliminating organic anions into the bile (69-76). This phenomenon borrowed a term from the field of renal physiology and became known as the transfer

maximum or Tm, and referred to the upper limit for the rate of transfer of organic anions from blood to bile. The properties of hepatic storage and maximal transfer were shown to exist for both BSP (75) and bilirubin (43,72-74) and an infusion technique was developed by Wheeler and his associates (76) which allowed measurement of both these parameters for BSP in a number of mammalian species (76,77). It was clear from these studies that BSP underwent a rapid initial flux into the "storage compartment" with maintenance of a maximal biliary excretion rate during periods of decreasing plasma concentration. The multiple-indicator dilution kinetic studies performed by Goresky (78,79) permitted the measurement of the "uptake" capacity for BSP of canine liver prior to subsequent disposal of the dye by the cell. His findings supported the concept of an initial maximal transport capacity (i.e. uptake) much larger than the maximal capacity for excretion into the bile. It emerged clearly therefore, that the Tm reflected the overall rate-limiting capacity of the cannalicular membrane site for excreting BSP into the bile, and that the phenomenon of storage resulted from the discrepancy between the maximal rates at which the liver cell was capable of removing the dye from the plasma and excreting it into the bile (79).

Concepts concerning the nature of the rate-limiting step in the transfer of bilirubin from blood to bile, and the mechanism of biliary excretion of BSP in limiting the disposal of the dye, were considerably expanded by the discovery between 1950 and 1960, that both of these substances undergo metabolic transformation in the hepatocyte. It was found

that once inside the cell, bilirubin was conjugated mainly to glucuronic acid by a microsomal enzyme(s) glucuronyl transferase (9,17,22,61,64). Similarly, BSP was found to be largely conjugated to the tripeptide glutathione (GSH) by a soluble enzyme (see Chapter II.5).

The fact that only the water soluble conjugated form of bilirubin was found in the bile of most mammalian species (61) led to the belief that conjugation was essential to the biliary excretion of bilirubin by the liver. Support for this view, as well as a better understanding of the limiting nature of conjugation in overall transfer of bilirubin from blood to bile, was gained from the work of Schmid (80) and Arias (73) and their respective co-workers on the Gunn rat, a species with inherited glucuronyl transferase deficiency. In this animal, absence of the bilirubin conjugating mechanism led to retention of unconjugated bilirubin in the plasma, with only minute quantities of non-glucuronide conjugates and traces of unconjugated bilirubin appearing in the bile (80). It was shown that the hepatic Tm for bilirubin was the same in Gunn rats, receiving infusions of the conjugated pigment, and normal rats, infused with either conjugated or unconjugated bilirubin (73,80). The significantly greater amounts of bilirubin excreted during the first ten minutes after injection of conjugated as opposed to unconjugated bilirubin into normal rats, was thought to reflect the time required for uptake and conjugation of the pigment by the liver cells (73).

These observations clearly showed that while the conju-

gation of bilirubin was essential to allow biliary excretion of the pigment to occur, it was not normally limiting to the overall transfer of bilirubin from blood to bile. The question concerning whether the phase of cellular uptake or excretion was limiting, assuming that the capacity for uptake of both conjugated and unconjugated bilirubin was the same, was resolved by the finding that when large doses of unconjugated bilirubin were administered intravenously to humans, the serum levels of conjugated bilirubin rose after a period (81). This supported the view that the ability of the liver to excrete conjugated bilirubin was, in fact, the limiting point in transfer. The important question concerning the influence of conjugation in "driving" the uptake process or in determining the extent of uptake remained unanswered at this stage. The inhibition of the process responsible for excretion of conjugated bilirubin and other organic anions, both free and conjugated, by substances such as icterogenin, 17 α-ethyl-19-nortestosterone (61), and bunamiodyl (74) further served to reveal that this process was distinct from conjugation per se.

Despite the observation that most of the BSP excreted in the bile was in the form of its GSH conjugate (64), the finding of appreciable quantities of free BSP in the bile raised the question whether conjugation was important for or merely incidental to hepatic uptake and biliary excretion of BSP. Philp et al (82) and Combes (83) showed that appreciable quantities of free BSP accumulated in the liver within minutes of intravenous injection, suggesting that conjugation was not

obligatory for hepatic BSP uptake per se, nor did it appear to determine the extent of uptake (83). A more complex problem arose concerning the rate-limiting effect of conjugation on biliary excretion of BSP. The above studies (82, 83) demonstrated that mainly conjugated BSP was excreted into the bile even when the liver contained a preponderance of the free dye, while hepatic GSH depletion (83) led to a decrease in BSP excretion. Whelan et al (84) later showed that infusion of conjugated BSP into experimental animals doubled the Tm obtained with similar infusion of the free dye. These findings all suggested that conjugation of BSP was the rate-limiting step in the overall transport of the dye from blood to bile. Combes (64) however, noted that after administration of BSP, a considerable amount of the conjugated dye was retained in the liver even when its delivery into the bile was occurring at a maximal rate. An inhibitory effect of BSP upon the excretion of the conjugated dye rather than a rate-limiting effect of conjugation has been proposed by more recent investigations (85) and affords a satisfactory explanation of all the observations made to date. Furthermore, it is noteworthy that 3,6-dibromophthalein disulphonate (86), an analogue of BSP, is excreted in the bile as readily as BSP but without prior conjugation, suggesting that conjugation may not be obligatory for BSP excretion, although it may enhance this step in the hepatic elimination of the dye.

iv) The hepatocyte model

The investigations into the mechanism of organic anion

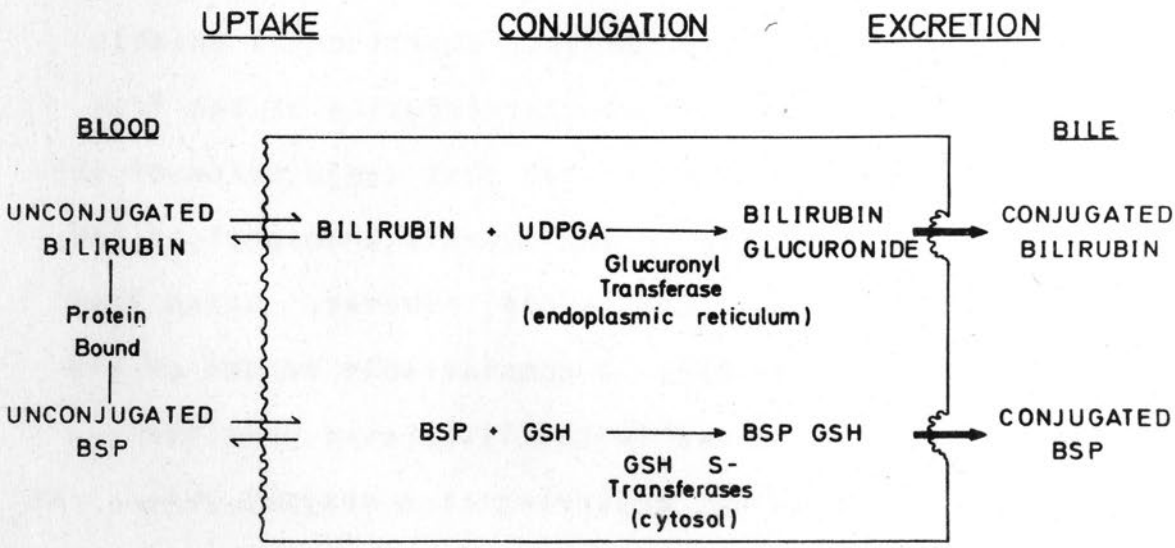

Fig. 1.2 Schematic representation of the three stage model of hepatic transfer of bilirubin and BSP from blood to bile. (Adapted from Arias (61)).

transfer from blood to bile enabled the construction of a conceptual model of the process, in which transfer could be separated into three phases taking place at three distinct sites (see Fig. 1.2):

(1) The phase of uptake into a storage space - at the sinusoidal cell surface.
(2) The phase of conjugation - at the microsomes (bilirubin) or in the cytosol (BSP).
(3) The phase of biliary excretion - at the cannalicular cell surface.

Of great importance, was the fact that certain clinical syndromes as well as their veterinary analogues, could be recognised as resulting from partial or complete defects occurring in each of the above individual phases. Hyperbilirubinaemia and impairment of organic anion clearance in these states were thus seen as manifestations of impaired uptake (Gilbert's disease, mutant Southdown sheep), conjugation (Gilbert's disease, Crigler-Najjar syndrome, Gunn rat), and biliary excretion (Dubin-Johnson syndrome, Rotor syndrome, Corriedale sheep) (3,16,17,21,22,61).

A considerable contribution towards the construction and understanding of this model was made by the theory of compartmental analysis applied to the study of hepatic removal of organic anions from the plasma. The measurement of decreasing organic anion concentration in the plasma following intravenous administration, had lent itself well to the clinical assessment of liver function (35-38,47,87). Ingelfinger et al (35) and Mendeloff et al (36) showed that the disappea-

A.

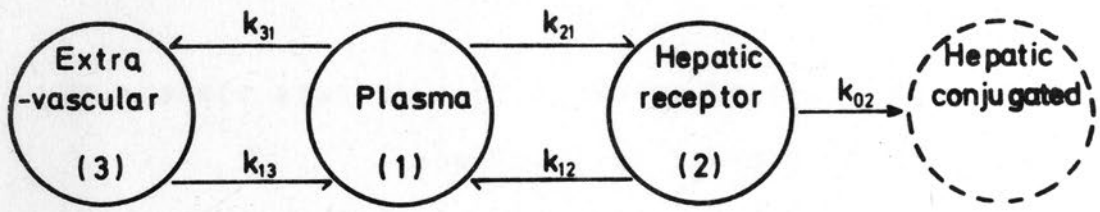

B.

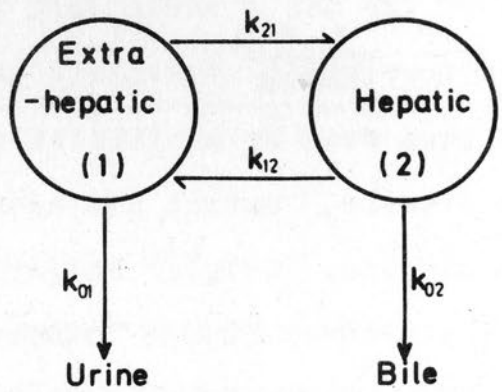

Fig. 1.3. Compartmental models of plasma organic anion turnover. (A), The three compartment model of plasma bilirubin turnover proposed by Berk et al (92), and (B), the two compartment model for plasma BSP turnover proposed by Quarfordt et al (93). k_{ij} Represents the fraction of organic anion in compartment j that is transferred per min to compartment i.

rance of BSP from the plasma six to thirty minutes after intravenous injection was a linear logarithmic function versus time, or in other words, a single exponential function. The slope of the disappearance curve afforded an estimate of the fractional removal rate or clearance of the dye ("K" per cent per minute) by the liver (87). Similar studies of BSP plasma disappearance carried out for longer periods of time (88,89) made it evident that the mathematical description of the disappearance curves required the sum of two exponential functions. Bilirubin plasma disappearance showed identical behaviour to this as well (90,91). Further analysis of organic anion disappearance data permitted the construction of a simple two compartment model consisting of a plasma compartment and a hepatic compartment, with derivation of values for the fractional rate constants for the dynamic transfer between and from each compartment (88-91). Further prolongation of the time period during which the plasma disappearance of ^{14}C-bilirubin was studied, indicated that a third exponential function was required to fit the data adequately, and thus a third compartment representing the extravascular space, was introduced into the model (Fig. 1.3A). This latter model, derived by Berk et al (92) envisages the unconjugated bilirubin in the plasma in a state of dynamic equilibrium with an extravascular compartment and with a hepatic "receptor pool", from which bilirubin is irreversibly cleared by the process of conjugation into an intrahepatic conjugated bilirubin pool. The model derived for BSP is essentially similar (Fig. 1.3B), but disregards the extravascular compartment while emphasizing losses from

the extrahepatic compartment into the urine (93). It is important to emphasise that the uptake process defined by these model systems, and also by the studies of Goresky (78, 79), is bi-directional. This would also suggest that uptake is not governed by a uni-directional active transport system.

v) The phenomena of saturation and competition

Saturation and competition phenomena in biological transport had been extensively studied in the field of renal physiology, prior to the realization that similar events were inherent in the hepatic transfer of organic anions from blood to bile (43,65). The concept of saturation of the hepatic transport mechanism was introduced by Ingelfinger et al (35), in order to explain the departures from linearity of BSP plasma disappearance curves in both normal humans and patients with liver disease. The administration of two doses of BSP thirty minutes apart, reproduced this effect (36), while the administration of successively higher doses of BSP (36,46) and ICG (46) resulted in a progressive reduction in the removal rate of these agents from the plasma. The maximal capacity for biliary excretion of organic anions could have accounted for some of these observations (75), but studies with rat liver slices and isolated perfused livers (67,68) clearly showed in vitro, that the uptake mechanism for phthalein dyes was a saturable process of finite capacity, and that this capacity was greater in the liver than in other tissues. Goresky (78,79) confirmed the saturable nature of BSP hepatic uptake in the dog, and described this process

quantitatively by means of Michaelis-Menten kinetics. He thus found an upper limit for the rate of uptake (Vmax) of 110 mg/min/10 kg body weight; a value greatly in excess of the canine biliary Tm for this dye, of 1.9 mg/min/10 kg (76).

In 1936, Dragstedt and Mills (33) had noted that the removal of BSP from the plasma was impaired by the simultaneous injection of bilirubin. Subsequently, numerous studies were conducted showing a mutual blocking effect between various organic anions on their plasma disappearance, as well as their excretion into the bile. The plasma disappearance of BSP was thus shown to be retarded by bilirubin (33,46), ICG, rose bengal (46), and bile salts (36, 76,46). ICG removal was delayed by BSP, bilirubin (46) and taurocholate (64), while rose bengal clearance was similarly affected by BSP (36) and bilirubin (94). These findings were not however, uniformly reproduced, and Mendeloff et al (36) found no effect on BSP clearance by bilirubin, rose bengal or uranin, while Cantarow et al (34) concluded that hyperbilirubinaemia did not influence the removal of BSP from the plasma.

When the biliary excretion of organic anions was primarily studied, bilirubin excretion was found to be diminished by BSP (34), sodium dehydrocholate and uranin; and excretion of the latter substance was reduced by both bilirubin and bile salts (43). Similarly, rose bengal and BSP exhibited mutual blocking effects on each other's biliary excretion, and both were thus affected by sodium dehydro-

cholate (64, 65).

The above phenomena were interpreted as evidence for competition occurring between organic anions for a common mechanism of limited capacity during transfer from blood to bile. The problem remained, that many of these often conflicting reports failed to define in absolute terms, whether the competition between organic anions occurred during the uptake or excretory phases, or both. In this regard, Hargreaves and Lathe (95) were able to show that numerous organic anions interfered with both uptake and excretion of bilirubin as well as with the conjugation of the pigment! Competitive inhibition during the uptake phase per se, was however, clearly shown by Hanzon (43), in that large doses of bilirubin appeared to limit the entry of uranin into the hepatocytes, while the studies of Wheeler et al (76) suggested that competitive inhibition between BSP and bile salts occurred during uptake, rather than at biliary excretion. This conclusion was also supported by tissue slice experiments (68).

The unconjugated hyperbilirubinaemia caused by cholecystographic agents such as bunamiodyl, iodipamide and iopanoic acid seemed likely to be due to interference with the uptake of bilirubin (74), although inhibition of conjugation was also possible (95). Indeed, the work of Bertelot and Billing (96) strongly indicated that bunamiodyl impaired the hepatic uptake of BSP with no direct effect on the biliary excretion of the dye, while in vitro studies (97) also demonstrated impairment of BSP uptake by rat liver

slices in the presence of iodipamide. It is perplexing however, that Billing et al (74) also found that bunamiodyl inhibited the biliary excretion of conjugated bilirubin. These workers also rejected the possibility that uptake of bilirubin was blocked by this agent after finding that the livers of animals receiving bunamiodyl contained more bile pigment than did control animals. It is possible however, that the high doses of bilirubin and bunamiodyl infused into animals in this study saturated the biliary excretion mechanism to the extent that no effect on uptake could be measured. Convincing evidence for a competitive effect at the uptake site was also reported for the male fern extract flavispidic acid (98), the antifungal agent X5079C (99) and the drug probenecid (100).

The demonstration of phenomena of saturation and competition in the uptake of organic anions by the liver, lent considerable support to the proposal that the cell membrane facing the sinusoids was responsible for uptake. Goresky (79) enlarged on the operational properties of membrane transport systems, in relation to the uptake of BSP. These properties included the demonstration of:

(1) a saturation phenomenon,

(2) countertransport, and

(3) competitive inhibition.

Considerable evidence for the first and last of these properties had been accumulated in terms of BSP and bilirubin uptake. Countertransport had also been demonstrated by the intravenous administration of a large dose of unlabelled BSP,

shortly after ^{35}S-labelled BSP had been given. This resulted in a rise in the plasma radioactivity to a new level, from which it decayed slowly (79). This could be seen as a "flushing out" of labelled material from the cell, due to the effect of the unlabelled dye competing for transport into the cell. The net effect would be that the unidirectional flux of labelled BSP into the cell would be less than that outwards. The interpretation of these data was that a membrane "carrier" transport system removed BSP from the blood stream and concentrated it in the liver cell.

With improvement in the technology of isolating cell plasma membranes, the opportunity arose to study the liver cell membrane directly in relation to organic anion uptake in vitro. Cornelius et al (101) in 1967, demonstrated that BSP was bound by isolated rat liver cell membranes. They further showed that competitive inhibition occurred between BSP and equimolar quantities of iodipamide, ICG and flavispidic acid for binding to these membranes, while taurocholate, bilirubin and uranin had no effect on BSP binding. The conclusion drawn by these workers, however, that the lack of inhibition shown by the latter three substances was in keeping with their lack of competition with BSP for in vivo hepatic uptake, was not entirely in accord with the controversial literature on this subject (33,43,46, 68,76).

vi) <u>The intracellular proteins and uptake</u>

A number of observations had indicated a role for the

intracellular proteins of the liver in the uptake of organic anions, long before isolation and direct study of these proteins was feasible. The concept of uptake resulting from intracellular protein binding was attractive by reason of its simplicity, and was not excluded by the concept of "active transport", as it was recognized that the passage of substances into the cells, even against a concentration gradient, could be accounted for by processes not requiring energy from the cell, through the binding of a substance chemically, or by adsorption, on one side of the cell membrane (43). Indeed, studies with incubated liver slices and isolated perfused livers (67,68,97) defined the uptake of BSP as a purely physico-chemical process, not requiring metabolic energy and capable of surviving the effects of fluoride, cyanide and mercuric ions as well as heat denaturation. Furthermore, Brauer and Pessoti (67) had shown that the efficiency of uptake of various phthalein dyes correlated well with their degree of binding to albumin. This suggested that dye-binding to liver proteins in a manner similar to albumin, was responsible for uptake. Bradley (75) also suggested that the ability of the liver to store considerable quantities of BSP indicated a high affinity of the intrahepatic proteins for this dye.

Unlike BSP, only small amounts of bilirubin are soluble in protein free solutions at physiological pH (102). It was thus apparent, that accumulation of bilirubin in the liver cells after uptake would lead to precipitation of the pigment in the cells, unless a biological acceptor substance -

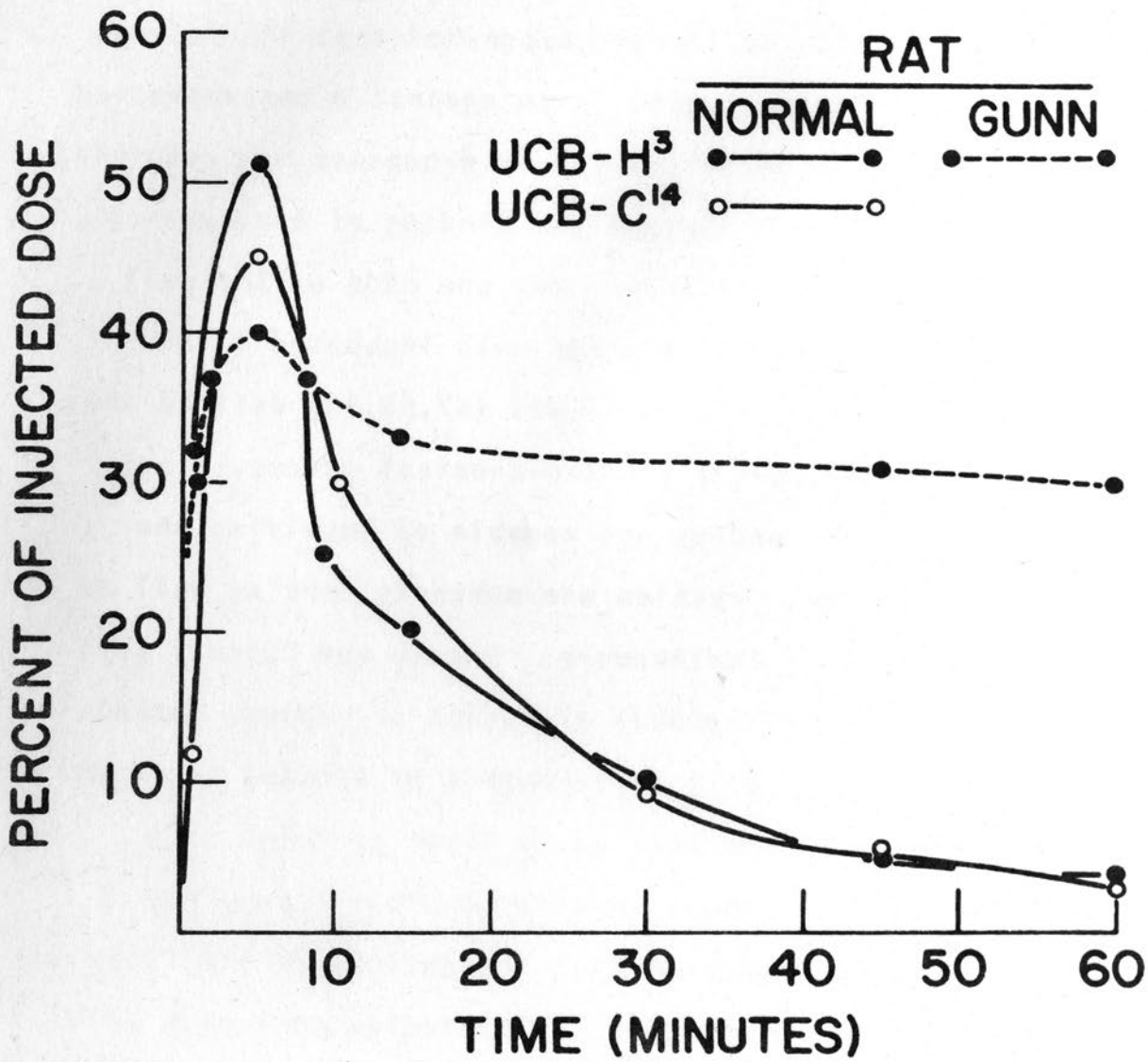

Fig. 1.4. The per cent of an injected dose of radiolabelled unconjugated bilirubin (UCB) in the liver of normal and Gunn rats as a function of time. (Reproduced from Bernstein et al (104)).

most likely a protein - was present in the cell cytoplasm.

Hanzon (43) had reported that uranin taken up by the liver cells was evenly distributed throughout the cells, with no accumulation at any of the subcellular formations. Billing et al (74) also found that on ultracentrifugation of rat liver homogenates, 52% of the intrahepatic bilirubin was associated with the soluble liver proteins, with less than 20% found in the subcellular particles.

The development of techniques for producing tritiated bilirubin (^{3}H-BR) gave a great impetus to the study of bilirubin uptake and intracellular distribution. The investigations of Brown et al (103) in 1964 and Bernstein et al (104) in 1966 with ^{3}H-BR in normal and Gunn rats, confirmed the rapid uptake of bilirubin (Fig. 1.4), with 35% of the injected dose recoverable from the liver two minutes after injection. At this time, no biliary excretion of the pigment was evident (103). The fact that the Gunn rat was capable of rapid hepatic uptake and concentration of unconjugated ^{3}H-BR (104,105), as well as the finding that during the early phase of uptake, most of the intrahepatic ^{3}H-BR in normal rats was unconjugated, firmly established the discrete nature of the uptake process and its independence from bilirubin conjugation.

These studies also confirmed the earlier observations on the intracellular distribution of bilirubin (74) and further showed that no sequential transport of the pigment via an intracellular chain of particles took place after uptake. Rather, at all times up to an hour after injection

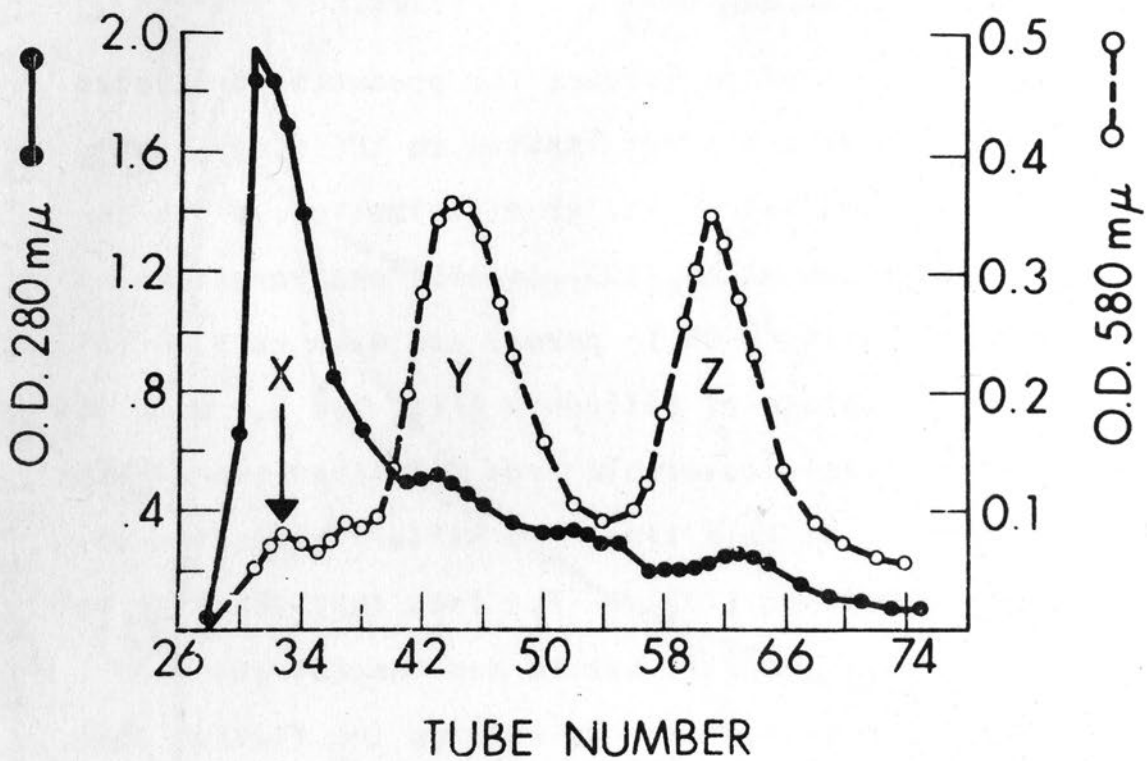

Fig. 1.5. The X, Y and Z BSP-binding protein fractions from 100,000 xg rat liver supernatant obtained on Sephadex G-75 chromatography. (Reproduced from Levi et al (107)).

of ^{3}H-BR, 50-70% of the intrahepatic label was associated with the supernatant fraction, 17-25% being bound to the microsomes, with lesser amounts present in the nuclear, mitochondrial and lysosomal fractions. Similar patterns were obtained when conjugated ^{3}H-BR was used, and also when labelled bilirubin was added to liver homogenates prior to ultracentrifugation. The rapid uptake of ^{3}H-BR could further not be accounted for by a mechanism of transport involving bilirubin bound to albumin (103).

A systematic search for a specific cytoplasmic "acceptor" macromolecule was prompted by these studies. Bernstein et al (104) reported that starch gel electrophoresis of rat liver cytosol with ^{3}H-BR revealed binding of bilirubin to a non-albumin soluble protein or lipoprotein that did not migrate at pH 7 to 8. However, attempts to isolate this protein by means of electrophoresis and ion exchange chromatography failed (106), as the binding relationship did not survive these techniques.

The newly introduced technology of molecular sieve chromatography was used by Grodsky (105) to define a 40 - 50,000 molecular weight non-albumin protein in the hepatic 100,000g supernatant (cytosol) which bound bilirubin. In 1969, Levi et al (107) reported that when BSP or bilirubin were added to rat liver cytosol, which was then separated by Sephadex G-75 column chromatography, organic anion binding was evident in three protein fractions (Fig. 1.5). These were termed X, Y and Z fractions in order of elution. These fractions were distinct from albumin, and apart from

a Z BSP-binding peak in the small intestinal mucosa, no other tissue besides the liver demonstrated Y or Z peaks. Binding of BSP to the X peak was variable and probably represented non-specific adsorption to high molecular weight proteins. Y and Z peaks were seen with a number of organic anions and were present in the hepatic cytosol of a number of mammals including man.

Drugs known to inhibit organic anion uptake, such as flavispidic acid and cholecystographic agents, displaced BSP and bilirubin from the Z but not from the Y peak, suggesting that the Y binding protein had a higher affinity for organic anions that the Z fraction. Novobiocin, probenecid and X5079C however, had no displacement effect.

The hepatic preponderance of the Y and Z organic anion-binding proteins suggested an important role for these proteins in the selective and rapid uptake of organic anions by the liver. Considerable interest was also aroused by the finding that the protein responsible for organic anion-binding in the Y fraction of Levi et al, had a number of other identities and possible intracellular functions. The emergence of these identities is considered next.

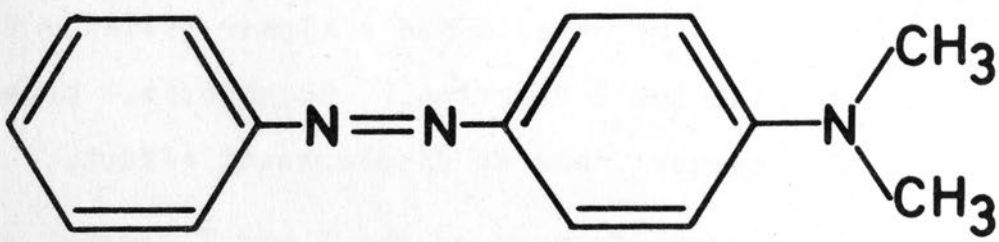

Fig. 1.6. Structural formula of 4-dimethylaminoazobenzene (DAB).

2. The Azodye Carcinogen-Binding Proteins

The production of tumours by chemical carcinogens has been recognized and studied for over two centuries (108,109). The azodye 4-dimethylaminoazobenzene (DAB) (Fig. 1.6) and its derivatives, have been particularly well studied in relation to their metabolism and production of hepatic tumours in the rat (108). Miller and Miller (110,111) first drew attention to the fact that DAB fed to rats was bound by stable chemical linkages to proteins within the liver, and that with few exceptions, there was a good correlation between dye-protein binding and the susceptibility of the liver to azodye carcinogenesis. It was also apparent that although each of the morphological fractions of the liver contained protein bound dye, the major share resided in the soluble proteins (112).

Sorof and his co-workers (113-115) demonstrated that 70 to 90% of the azodye bound to soluble liver proteins was located in a basic, electrophoretically slow fraction (the h_2 fraction), which comprised only 7 to 15% of the soluble liver proteins. This fraction (and concomitantly protein bound azodye) was strikingly reduced in DAB induced tumours (110,112,114,115). This was of considerable interest in relation to the hypothesis that chemical carcinogens induced neoplastic change through the process of gradual deletion of certain proteins which might play a key role in the control of cellular growth (116). These proteins were thought to be deleted as a result of formation of complexes with carcinogens, with inhibition of their further synthesis.

Specific carcinogen-protein interaction also lent itself to proposal that carcinogens were transported to the cell nucleus bound to specific cytoplasmic target proteins, thus allowing alkylation of regulatory nucleoproteins with initiation of carcinogenesis (117).

Ketterer et al (14) first isolated two specific azocarcinogens binding proteins from rats given intraperitoneal DAB. A high degree of purity was obtained with a basic 45,000 molecular weight protein, which appeared to correspond to the azodye-containing h-protein fraction of Sorof (113), when comparisons were made by starch gel electrophoresis. The other protein isolated by Ketterer et al was a neutral, 14,000 molecular weight species, and was initially thought to comprise two separate proteins due to its considerable charge heterogeneity (118). A third, 88,000 molecular weight azocarcinogen-binding protein was subsequently isolated by Sorof et al (119) and was shown to be the principal azodye-binding protein in the hepatic cytoplasm, termed the "slow h_2 5 S" protein. It was shown to consist of two equal subunits, each capable of binding an azocarcinogen residue. The three cytoplasmic azocarcinogen-binding proteins were now classified by the letters: A, B and C, for the 14,000, 45,000 and 88,000 molecular weight proteins respectively (4,118). The interaction of DAB with these proteins was shown to consist of covalent binding via sulfhydryl-containing amino acids, probably consequent to the activation of the dye by microsomal enzymes and cytoplasmic sulfotransferases, to the N-hydroxy sulfuric acid

ester of N-methylaminoazobenzene (13,120).

The relationship between azocarcinogen-binding protein B and a corticosteroid metabolite-binding protein was soon established. This development is discussed below.

3. The Corticosteroid-Binding Proteins

Steroid hormones exert their action at sites distant from their source of production, and much elaborate research has revealed a fascinating and complex series of molecular events underlying the selective mode of action of these hormones within their target tissues (121,122). Early studies employing radiolabelled corticosteroids, established that the liver rapidly concentrated most of an intravenously injected dose of these compounds and retained the activity for considerable periods of time (123-125). Steroid hormone action in the liver appeared to be mediated via the induction of several enzymes (126), and the mechanism of this induction was actively sought.

Litwack et al (127) reported in 1963, that ^{14}C-hydrocortisone was present mainly in the hepatic cytosol 45 minutes after intravenous injection of the labelled hormone. Fractionation of the cytosol by Biogel P-100 chromatography revealed binding of the labelled steroid to macromolecules (128), and this suggested that the induction of enzymes in the liver by steroid hormones might be mediated through macromolecular binding. Indeed, numerous studies performed during the mid-sixties supported the concept of intracellular

protein "receptors" for various steroid hormones which acted as determinants of target organ specificity, and which were connected to the intracellular mechanism of action of these hormones (122). Fiala and Litwack (129) further noted that the macromolecular binding of ^{14}C-hydrocortisone by hepatic cytosol after in vivo steroid hormone administration, could not be reproduced by adding the labelled hormone to cytosol in vitro. This was explained by the discovery that the corticosteroid hormone was rapidly metabolized in vivo to three anionic metabolites, which after extractions demonstrated in vitro macromolecular binding.

In 1968 Morey and Litwack (130) succeeded in separating four cortisol metabolite-binding fractions from rat liver cytosol by DEAE-Sephadex chromatography. The first peak yielded a 37 - 50,000 molecular weight basic protein (corticosteroid metabolite-binder I), which bound the most anionic of the three dominant anionic cortisol metabolites (131). The third peak (binder III) was shown to contain a 4 - 5,000 molecular weight protein, which bound a less anionic derivative of cortisol, while binder II was eventually identified as the true corticosteroid-receptor protein of the liver (132).

The considerable documentation of an endocrine influence on carcinogenesis (see refs. 13,121,133 for reviews) raised the possibility that hepatocarcinogenesis might result from the interaction of carcinogens and corticosteroids at a common molecular site. This prompted studies which revealed

that corticosteroid metabolite-binder I bound ^{14}C-DAB administered to rats (134), and similarly, interacted covalently with the carcinogen 3-methylcholonthrene (135). The remarkably similar properties of binder I and the azo-carcinogen-binding protein B described by Ketterer were recognized (134), and full identity between these two entities and the Y protein described by Levi et al (107) was subsequently established.

4. Ligandin - A Triple Identity

The identity between Y protein, azocarcinogen-binding protein B and corticosteroid metabolite-binder I was fully established in 1971, when Litwack, Ketterer and Arias (1) reported that these proteins exhibited closely similar physico-chemical properties including size, charge and amino acid analyses. The identity was confirmed by the finding that monospecific antisera against each of the proteins cross-reacted with all three. The most striking property of the newly discovered protein, and that which appeared to relate to its major intracellular function, was its ability to bind a large number of organic anions. Thus the name "ligandin" was proposed, to appropriately unite the three identities of this protein. Remarkably, a fourth identity, that of an enzyme, now followed.

5. The GSH S-Transferases and Ligandin

In 1958, Krebs and Brauer (136) observed that a metabolic transformation of most of the BSP administered intravenously took place in the liver. Several chromatographic species of the dye were excreted in the bile, which were subsequently shown to represent amino acid conjugates yielding glycine, glutamic acid and alanine on hydrolysis (75,137,138). The latter group was shown to represent desulphydrylated cysteine (139), and it was demonstrated that the major pathway of BSP metabolism in several species, involved conjugation with the tripeptide GSH (139-142). Combes and Stakelum (140,142) and Javitt et al (139) showed that conjugation of BSP with GSH could occur spontaneously in vitro, but that the reaction was considerably enhanced by a soluble hepatic enzyme. Conjugation of BSP with GSH was found to involve the formation of a thioether linkage through the GSH cysteine sulphydryl group, with release of a bromine residue from BSP at the site of conjugation (139, 140).

It had also been appreciated since 1879 (143), that the administration of monohalogenated benzene compounds led to the urinary excretion of mercapturic acids, which represent thioether conjugates of N-acetylcysteine. Barnes et al (144) found that the levels of hepatic GSH were decreased by the administration of mercapturic acid - forming compounds to rats. This suggested that the metabolism of these compounds involved conjugation with GSH in the liver. Booth et al (145) described the partial purification of a soluble

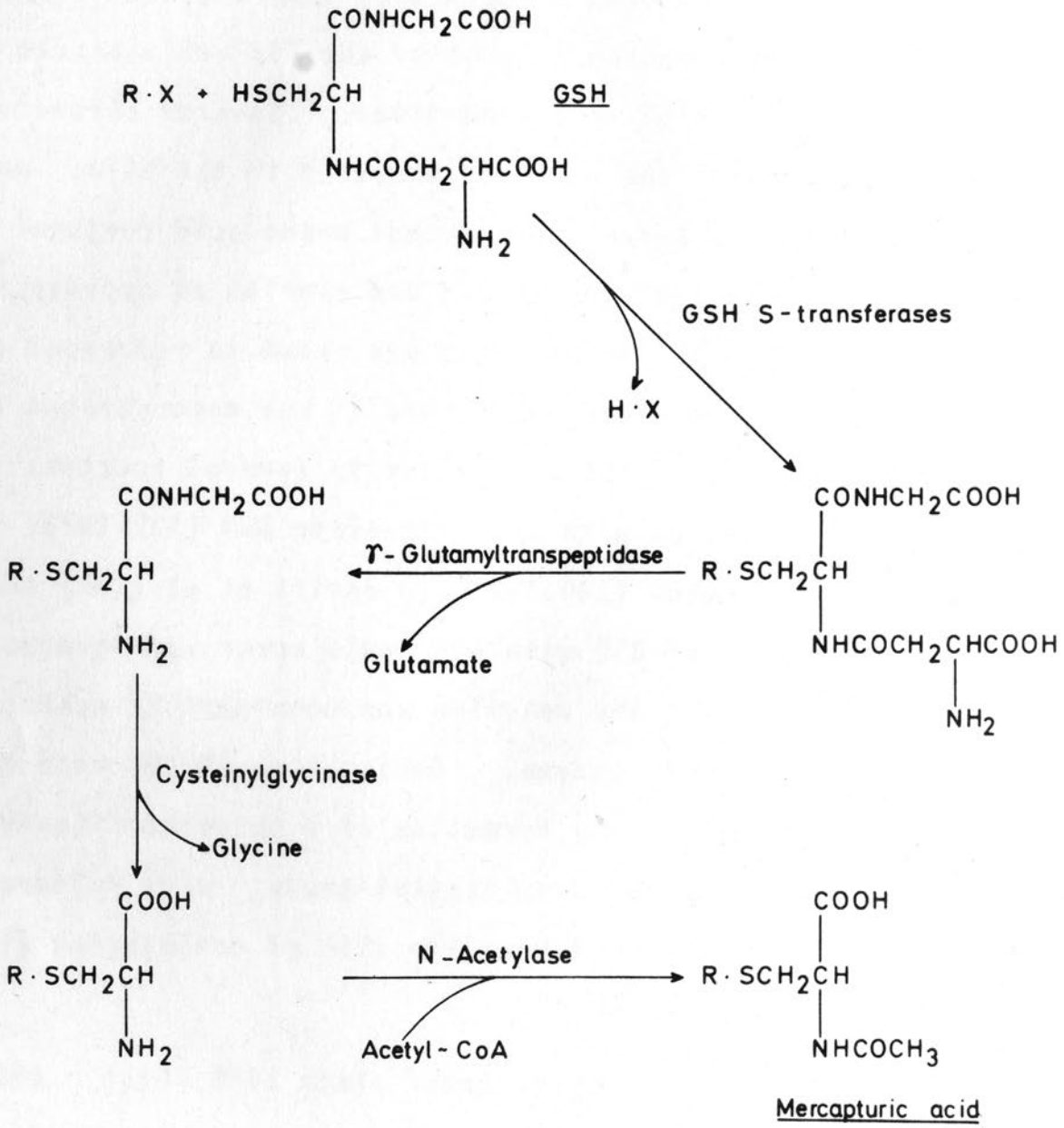

Fig. 1.7. Mercapturic acid biosynthetic pathway. R·X represents an electrophilic compound.

enzyme from rat liver which catalysed the conjugation of a number of these compounds, including the arylhalide 3,4-dichloronitrobenzene, with GSH as a specific co-factor. This enzyme appeared to be involved in the initial step of the mercapturic acid formation pathway. This metabolic pathway has been recently reviewed by Chasseaud (146), and is concerned with the disposal of a large range of foreign compounds (xenobiotics), many of which are highly toxic or carcinogenic (Fig. 1.7).

It soon appeared that several distinct forms of "GSH S-transferase" activities could be distinguished on the basis of activities towards various classes of substrates, tissue distribution, and physico-chemical stabilities. These enzymes were further classified according to their activities based on the carbon skeleton of the substrate involved. Thus aryl-, alkyl-, aralkyl-, alkene- and epoxidetransferase enzymes were proposed (145,147-149), although homogenous forms of all of these substrate-characterized species had not been obtained.

A number of important contributions towards the understanding of the GSH S-transferases were made between 1973 and 1974. Kaplowitz et al (150,151) noted that the BSP-binding Y peak of liver supernatant corresponded to the fraction containing the enzyme catalysing the conjugation of BSP and 3,4-dichloronitrobenzene with GSH. These workers purified GSH S-aryltransferase by the method of Booth et al (145) and found that the partially purified enzyme bore a close resemblance to ligandin in its size,

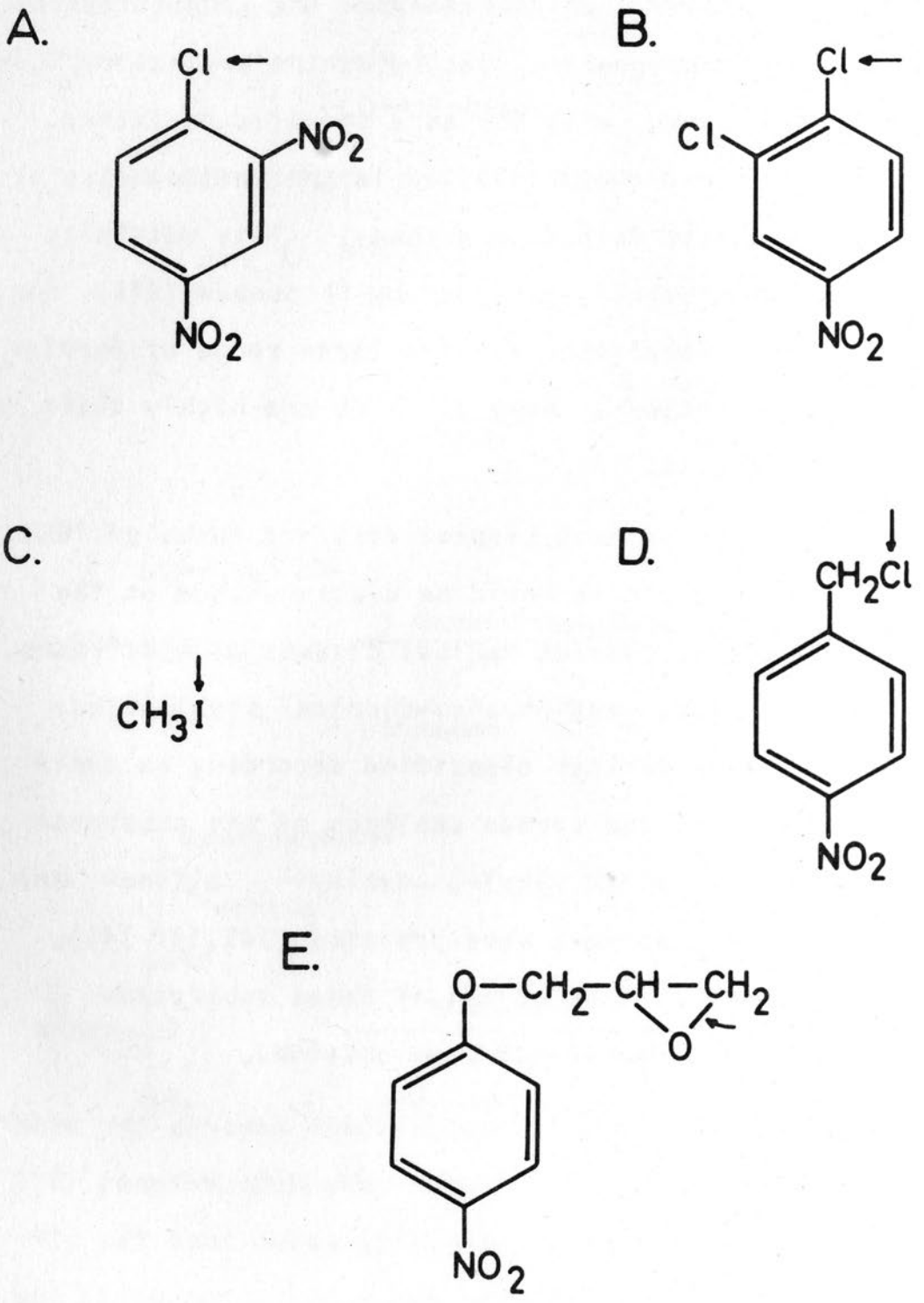

Fig. 1.8. Substrates for the GSH S-transferases. Leaving groups or points of addition of GSH are indicated by the arrows. (A), 1-chloro-2,4-dinitrobenzene; (B), 3,4-dichloronitrobenzene (1,2-dichloro-4-nitrobenzene) - both (A) and (B) are aryl substrates - (C), iodomethane (alkyl substrate); (D), p-nitrobenzyl chloride (aralkyl substrate); (E), 1,2-epoxy-3-(p-nitrophenoxy)-propane (epoxide substrate).

charge, amino acid analysis and organic anion-binding property. These findings appeared to justify the identification of ligandin with the enzyme GSH S-aryltransferase, but this was refuted by Ketterer et al (152), who showed that although the enzyme responsible for BSP and 3,4-dichloronitrobenzene conjugation had the same size and subunit characteristics as ligandin, the two entities were completely separable from one another on isoelectric focusing.

The work of Fjellstedt et al (153) and Pabst et al (154) finally led to the purification of three homogenous GSH S-transferases on the basis of activities towards three major GSH S-transferase substrates: an epoxide (1,2-epoxy- (p-nitrophenoxy)-propane), an arylhalide (3,4-dichloronitrobenzene) and an alkylhalide (iodomethane) (see Fig. 1.8). However, each of the enzymes thus obtained exhibited activity towards substrates of several classes, indicating that rat liver contained several GSH S-transferases of broad and overlapping substrate specificities, thus making the old system of classification untenable. The six homogenous GSH S-transferases which were eventually defined (155,156) were thus each assigned a letter based on the reverse order of their elution from CM - cellulose, a step in the purification common to most of them. In this manner, the separate GSH S-transferases A, B, C, D and E emerged, as well as transferase M which was adsorbed by DEAE-cellulose prior to CM-cellulose chromatography, and which showed activity with menapthyl sulphate as substrate. More recently, a seventh distinct transferase, labelled AA,

found eluting after transferase A from CM-cellulose, was added to the list (157).

All the GSH S-transferases were shown to be 45 - 46,000 molecular weight dimeric proteins, differing in charge with isoelectric points ranging between pH 6.5 to 10 for transferases E to AA (155,157). Their amino acid compositions showed considerable homologies but were not identical. Each of the transferases showed activity with a wide range of substrates but with greatly differing specific activities. This also allowed identification of each of the related enzymes by its characteristic catalytic profile with a number of substrates. Thus transferase B, although isolated on the basis of iodomethane conjugating activity,had much higher activity towards 1-chloro-2,4-dinitrobenzene, yet minimal activity with 3,4-dichloronitrobenzene (see Fig. 1.8). This served to distinguish it from transferase A, an enzyme with a high activity towards both arylhalide substrates. Transferase E had the highest activity towards epoxides and also towards iodomethane. This latter, rather insensitive substrate, allowed preferential identification of transferase B during purification owing to the relatively greater quantity of this enzyme species in the liver. Immunodiffusion studies revealed that transferases A and C share an antigenic determinant, whereas transferase B was immunologically distinct from its fellow enzymes.

The identity between GSH S-transferase B and ligandin was soon established on the basis of identical catalytic

activity profiles, immunological crossreaction studies, binding activity towards non-substrate ligands such as bilirubin, ICG and penicillin, and parallel induction of transferase B activity and immunologically measured ligandin by phenobarbital treatment (15).

In retrospect, it is clear that the earlier controversy regarding the identity of ligandin with a GSH S-transferase (150-152) might not have arisen if 1-chloro-2,4-dinitrobenzene had been used to establish the relationship, rather than the poor transferase B aryl substrates 3,4-dichloronitrobenzene and BSP.

CHAPTER III

THE BIOCHEMISTRY OF LIGANDIN

1. Introduction

A considerable body of data has accumulated concerning the biochemistry of ligandin including its physicochemical properties, binding, catalytic activity, tissue distribution, phylogeny, ontogeny and response to microsomal induction agents and other drugs. These data relate mainly to the protein obtained from the rat, although more recently, the human equivalent has also been studied. The literature concerning both rat and human ligandin will be reviewed below.

2. Purification

A number of methods have been described for the purification of ligandin (14,131,152,155,158-164). Most methods utilize the hepatic 100,000 xg supernatant as starting material, and take advantage of the basic charge of the protein in subsequent steps utilizing anion exchange and cation exchange resins. A molecular sieve step utilizing Sephadex and Biogel column chromatography has been included in most methods, while salting-out procedures (14,155), column isoelectric focusing (152,163,164), and Cellex-phosphate (131) or hydroxylapatite adsorption chromatography (155) have been included by different groups. Binding of specific ligands such as BSP (159), DAB (14), labelled corticosteroid metabolites (131) or GSH S-transferase cata-

lytic activity with iodomethane (155) and 1-chloro-2,4-dinitrobenzene (157,161,163,164) have been utilized as markers for ligandin during purification. A unique one step bioaffinity chromatography method for purifying ligandin using bilirubin-agarose has been described by Koskelo et al (165).

3. Physicochemical Properties

A summary of the physicochemical properties of rat ligandin is given in Table 1.I. Ligandin is a spherical protein (5,163) of molecular size ∿ 46,000 daltons, composed of two ∿ 23,000 dalton subunits which are not disulphide linked (5,131,168). The protein contains no nucleotides (8,131), carbohydrate, or trace metal components (8). Peptide mapping data reported by Ketterer et al (163), indicate that the ligandin subunits have very similar amino acid sequences, but are not identical. This may account for the finding of Listowsky et al (168), who found that analysis of ligandin by polyacrylamide gel electrophoresis in sodium dodecyl sulfate, using a discontinuous buffer system, revealed two subunit components with apparent molecular weight of 22,000 and 25,000 daltons. Human ligandin appears to be a larger molecule than its rat counterpart, with a molecular size of ∿ 50,000 daltons, composed of two ∿25,000 dalton subunits (161).

Circular dichroism (CD) studies with ligandin have revealed a highly ordered secondary structure (see Table 1.I). The CD spectrum is characterized by negative ellipticity

TABLE 1.I

PHYSICOCHEMICAL PROPERTIES OF RAT LIGANDIN

	Range of values	References
Molecular Size (D)		
a) Protomer	37,000 - 50,000	1,4,5,7,14,131, 133,155,162,163
b) Monomers	22,000 - 25,000	1,5,7,155,163,168
Stokes radius (Å)	30.4	133
Calculated partial specific volume ($\bar{v}$)	0.75	4,155
Sedimentation coefficient ($S^{o}_{20,w}$)	3.5 - 3.7	1,4,7,131,133,163
Diffusion coefficient ($D^{o}_{20,w}$)	7.5 -11.8	7,133,163
Frictional coefficient (f/f_o)	1.18- 1.2	4,5,133,163
Conformation estimated from CD spectra (%):		
α - helix	40 - 47	
β - structure	15 - 28	
Random coil	25 - 45	
Free - SH groups (in 6M. Guan. HCl)	4.2	155
Isoelectric point (pI)	8.4 -10.3	1,4,5,7,14,131,133, 155,163,165,168
$E^{1\%}_{280}$	7.6 - 8.1	155,163
Approximate amino acid composition (residues/ mol):		1 (see also 4,5, 14,131,155,159, 162 and 163)

Asp_{34}, Thr_{11}, Ser_{13}, Glu_{39}, Pro_{16}, Gly_{18}, Ala_{26}, Val_{17}, Met_{14}, Leu_{46}, $Ileu_{19}$, Tyr_{12}, Phe_{17}, Lys_{33}, His_{5}, Arg_{21}, Trg_{2}, Cys_{4}

bands at 208 and 222 nm and a positive extreme at 192 nm, while in the spectral region between 150 and 300 nm, six extrema are evident (8,166,167). The intrinsic stability of the molecule is also evident by the lack of significant unfolding in denaturing solvents (168).

Ligandin is a basic protein with an isoelectric point between 8.4 and 10.3 (see Table 1.I). Two major charge species, attributed to microheterogeneity, have been observed from studies with starch-gel electrophoresis (14), CM-cellulose chromatography (163), hydroxylapatite chromatography (155), and isoelectric focusing (152,155). However, up to six charge species have been observed with the latter technique in the pH 7 - 10 range (168). Human ligandin also resolves into five species termed α, β, λ, δ and ε, on isoelectric focusing, with isoelectric points between pH 7.8 and 8.8. Each of these forms has the same amino acid composition and all appear to be products of a single gene; the charge differences are attributed to in vivo deamidation (161).

A number of similar amino acid analyses have been published for ligandin, and a representative analysis is given in Table 1.I. An important discrepancy is the finding of Habig et al (155) of 9 as opposed to 2 tryptophan residues/molecule found by most other workers. This may, however, reflect differences in methodology. The amino acid profile of ligandin shows the presence of almost equal numbers of both acidic and basic amino acids. Considering the basic pI of ligandin, this must indicate that many of the glutamic and aspartic acid residues are present as glutamine and aspa-

ragine. Ketterer et al (14) have been unable to locate a free N-terminal amino acid in ligandin, indicating possible substitution or cyclization of the N-terminal α-amino group. Listowsky et al (168) have, however, reported the N-terminal residue of ligandin to be proline.

4. Enzymatic Properties

As discussed earlier, ligandin belongs to a group of enzymes, the GSH S-transferases, that catalyse the conjugation of GSH with a wide range of electrophoretic compounds. The GSH S-transferases constitute approximately 10% of the soluble liver proteins in the rat, while ligandin. (transferase B), constitutes about half the total concentration of this family of enzymes (169). The six relatively basic GSH S-transferases characterized from rat liver are designated AA, A, B, C, D and E, and show broad and overlapping substrate specificities, and similar physical properties (155-157,169). Ligandin is immunologically distinct from the other transferases (155,157). It also has a profile of catalytic activities with various substrates which may serve to distinguish it from the other transferases (Table 1.II) with the possible exception of transferase AA, which exhibits a catalytic profile remarkably similar to B (157). Transferase AA is the most basic species (pI ∿ 10), followed by ligandin (pI ∿ 9.8).

Ligandin is comparatively the least active of the transferases with a wide range of substrates, and has minimal to no activity with 3,4-dichloronitrobenzene, BSP or alkyl-

TABLE 1.II

COMPARATIVE CATALYTIC ACTIVITIES OF GLUTATHIONE S-TRANSFERASES A AND B (LIGANDIN)

(Refs: 155, 157, 169, 171)

Substrate	Specific activity (μmol/min/mg)		Km (mM)		Vmax (mol/min/mol of enzyme)	
	A	B	A	B	A	B
3,4-Dichloronitrobenzene	4.3	0.003	1.1	2	390	1.3
1-chloro-2,4-dinitrobenzene	62	11	0.06	0.8	3,000	860
p-nitrobenzyl chloride	11.4	0.1	1.4	3.4	1,200	60
iodomethane	0	0.6		40	0	200
ethacrynic acid	0	0.3		nd	0	nd
BSP	0.53	0.006	0.002	0.07	77	0.24
2-nitropropane	0.012	0.005	29	9.2	2.2	0.5
trinitroglycerin	0.06	0.09	6.5	0.8	15	7.0
ethylthiocyanate	0.08	0.02	5.3	1.9	35	3.0

nd: data not available/not determined

epoxides. It does however show significant activity towards the aryl-epoxide benzo (α) pyrene-4,5-oxide (170), and is most active with 1-chloro-2,4-dinitrobenzene. It shares with transferase AA the highest specific activity of all the GSH S-transferases towards the alkene substrate ethacrynic acid (155,157). Despite the overall low and narrow range of ligandin catalytic activity - a factor which has at times led to doubt concerning its role as an enzyme (4,8) - the high concentration of this protein in the liver must make its in vivo contribution towards total GSH S-transferase activity highly significant.

An analogous,yet contrasting situation regarding the GSH S-transferases obtains in the human being (161). Human liver contains five electrophoretically different "ligandins" (α, β, λ, δ and ε) which are all active transferases and probably represent minor post-translational modifications of a single protein (see Chapter III.3). Further support for this hypothesis stems from the finding that each of the human transferases has a similar specific activity for a given substrate, with Km and Vmax values for 1-chloro-2,4-dinitrobenzene differing only slightly. This is in marked contrast to the rat GSH S-transferases, among which the specific activities for a given substrate may differ over several orders of magnitude (155,169).

The GSH S-transferases perform an important role in the detoxification of a variety of non-physiological compounds including epoxides, sulphate esters, alkenes and halogenated and nitro derivatives (146,149-157), by the formation

of their thioether conjugates of glutathione. The general equation describing this reaction is:

$$RX + GSH \rightarrow RSG + HX \quad \{1$$

Most of the transferase substrates will proceed to form GSH adducts in the absence of the enzyme, some at a rate ∿ 10% of the enzymatic rate (169). With the possible exception of homoglutathione, neither rat nor human GSH S-transferases are able to utilize other sulphydryl reagents in place of GSH (161,169).

Two further reactions in which these enzymes participate do not result in thioether formation (171). These are the reduction of organic nitrate esters such as nitroglycerin, with the formation of nitrous acid and oxidised GSH:

$$RCH_2ONO_2 + 2\ GSH \rightarrow RCH_2OH + HNO_2 + GSSG \quad \{2$$

and the cleavage of organic thiocyanate to form cyanide and the respective asymmetric disulphide of GSH:

$$RSCN + GSH \rightleftarrows RSSG + HCN \quad \{3$$

Similar mechanisms may underlie the proposed conversion of prostaglandin endoperoxides to prostaglandins $F_{2\alpha}$, E_2 and D_2 by the GSH S-transferases (172), as well as the hepatic Δ^5-3-ketosteroid isomerase activity recently attributed to ligandin (173).

The property of binding non-substrate ligands which first attracted attention to ligandin, is shared by the other transferases as well (174,175). The individual affinities of transferases AA, A, B and C, for ligands such as bilirubin, ICG, and haem, differ over a wide range, while the human

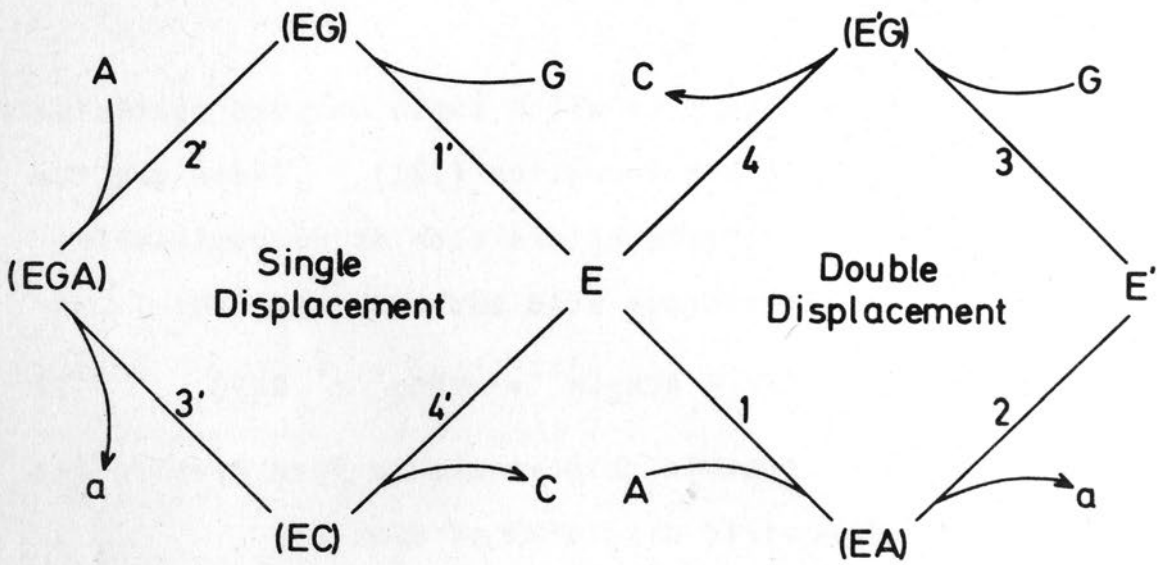

Fig. 1.9. Schematic representation of the kinetic steps for GSH S-transferase A catalysis. The reaction proceeds in a counter-clockwise direction from E, the free enzyme, in each case. The symbols G, A, a, and C represent GSH, the electrophilic substrate, the leaving group and the GSH conjugate respectively. Under normal conditions, the single displacement pathway is followed, whereas the double displacement pathway applies at very low concentrations of GSH. (Reproduced from Pabst et al (156) and Jakoby et al (169)).

transferases show similar to identical affinities with these ligands (161,175). In general, the affinity of transferase B (ligandin) for non-substrate ligands, is the highest of those shown by the GSH S-transferases. In addition, non-substrate ligands are inhibitors of GSH S-transferase catalytic activity (161,174,175) and with some exceptions, the inhibition constants (K_i) approximate the dissociation constants (K_D). Inhibition of rat transferase B, and human ligandin activity towards 1-chloro-2,4-dinitrobenzene by non-substrate ligands is competitive, whereas inhibition of the activities of the other rat transferases is of both the competitive and non-competitive varieties.

The kinetic mechanism of catalysis by the GSH S-transferases has been studied with particular reference to transferase A (156,169) and under physiological conditions is of the sort known as Ordered Bi Bi. This is represented by the "left wing" of the diagram shown in Fig. 1.9. This represents a single displacement mechanism in which GSH is first bound to the enzyme, followed by the addition of the second substrate to form a ternary complex of enzyme and both substrates. The reaction proceeds and the leaving group is removed to form the enzyme thioether complex, which then liberates the thioether to regenerate the enzyme. While this mechanism probably holds for all the transferases in vivo, a different mechanism appears to take place with transferase A at low GSH concentrations (right "wing" of diagram in Fig. 1.9). Under these circumstances, the electrophilic substrate is first on the enzyme and the first product is

released before both substrates have been bound to the enzyme. The existence of this "ping-pong" mechanism has been questioned (176) and is probably of little physiological significance.

The general mechanism underlying the many and diverse reactions catalysed by the GSH S-transferases, has been postulated as an enhancement of GSH thiol nucleophilicity i.e. facilitation of the ionization of GSH to GS^-. Substrates are thought to bind at a non-specific hydrophobic site on the enzyme in close proximity to GS^-, with subsequent non-enzymatic nucleophilic attack of enzyme-bound GS^- on the electrophilic centre of the second substrate (169,177).

5. Binding Properties

Ligandin has stimulated wide interest by virtue of its ability to bind a large number of small molecules. A comprehensive list of organic anions and other compounds, with the available quantitative data on their binding to ligandin, is given in Table 1.III. The wide range of techniques used to study binding to ligandin includes gel filtration (107,159,162,165,178-187), ligand partition between Sephadex beads and protein solutions (188,189), starch gel electrophoresis (14), equilibrium dialysis (5, 163,167,190,191), CD (8,159,164,166,167,182,192,193), fluorescence spectroscopy (164,174,192,194), difference spectrophotometry (164,192), zone electrophoresis, zonal centrifugation and moving boundary sedimentation (195,196).

TABLE 1.III

LIGAND BINDING CHARACTERISTICS OF LIGANDIN

Ligand	K_a (M^{-1})	N	References
Porphyrins and derivatives			
Haem	10^5-10^{10}	1	5,163,167,174 192,196
Protoporphyrin IX*	nd	nd	163
Coproporphyrin III*	nd	nd	165
Haematoporphyrin	10^6	1	167
Bilirubin	10^6-10^9	1	5,164,167,174, 194,195
Bilirubin monoglucuronide	3×10^5	nd	194
Bilirubin diglucuronide	10^5	nd	194
Biliverdin	nd	nd	193
Phylloerythrin	nd	nd	6
Steroid hormones and metabolites			
Cortisol	0 -10^6	1	13,133,163,167, 191
Cortisol disulphate metabolite	nd	nd	133
Oestradiol	10^5	1	163,191
Oestrone	10^5	1	163,191
Oestrone sulphate	6×10^5	1	163,191
Testosterone	2×10^5	1	163,191
Dehydroepiandrosterone sulphate	2.5×10^5	1	163,191
Pregnenolone sulphate	2.5×10^5	1	163,191
2-hydroxyoestradiol-GSH	6×10^5	1	163,191
Oestrone glucuronide	5×10^4	1	163,191
Diethylstilboestrol	5×10^5	nd	163,191

/contd.

TABLE 1.III (continued)

LIGAND BINDING CHARACTERISTICS OF LIGANDIN

Ligand	K_a (M^{-1})	N	References
Antibiotics			
Penicillin	10^3	1	159,162,167
Tetracycline	10^4	nd	162,163
Chloramphenicol	10^4	1	162,167
Cephalothin	10^2	nd	162,174
Cephlexin*	nd	nd	162
Polymyxin B	$0 - 10^2$	nd	162,174
Nitrofurantoin*	nd	nd	162
Sulphonamides	nd	nd	6
Fatty acids			
Palmitate	10^4	1	191
Oleate	$10^4 - 10^6$	1	167,191
Bile salts			
Deoxycholate	5×10^4	1	163,191
Taurodeoxycholate	5×10^4	1	163,191
Chenodeoxycholate	5×10^4	1	163,191
Cholate	2×10^4	1	163,190,191
Lithocholate	nd	nd	167
Radiographic contrast media			
Iopanoic acid*	nd	nd	178
Iodipamide	10^3	1	167,178
Iophenoxic acid	10^2	1	167

/contd.

TABLE 1.III (continued)

LIGAND BINDING CHARACTERISTICS OF LIGANDIN

Ligand	K_a (M^{-1})	N	References
Thyroid hormones			
T_3	10^5 -10^6	1	167,182
T_4	10^4 -10^5	1	167,182
Carcinogens, alkylating agents and metabolites			
DAB	5 x10^4	nd	163,191
N-Hydroxy, N-methylaminoazobenzene sulfate ester†	-	nd	163
N-Methylaminoazobenzene-GSH	4 x10^5	1	163,191
3-Methylcholanthrene	4 x10^5	1	163,191
3-Methylcholanthrene metabolite†	-	nd	1,135
Benzpyrene	10^5	1	167
1-Chloro-2,4-dinitrobenzene†	-	nd	175
Dyes and metabolites			
BSP	10^6 -10^7	1	107,159,167, 191
BSP-GSH	nd	nd	159,167
3,6-Dibromosulphophthalein	6 x10^4	nd	174
Phenolsulphonphthalein*	nd	nd	159
ICG	3.10^5 -10^6	1	167,174
Evans blue (T-1824)	10^6	1	107,167

/contd.

TABLE 1.III (continued)

LIGAND BINDING CHARACTERISTICS OF LIGANDIN

Ligand	K_a (M^{-1})	N	References
Peptides			
Gastrin*	nd	nd	181
GSH	10^4 - 10^5	1	163,167,191
Miscellaneous drugs and anions			
Flavispidic acid	10^5	nd	8
Vasoflavine	nd	nd	6-9
Probenecid	10^3	1	159,167
Phlorizin*	nd	nd	159
Acetylsalicylic acid*	nd	nd	198,199
p-Aminohippurate	10^3	1	159.167,198,199
Furosemide*	nd	nd	199
Tolbutamide*	nd	nd	187
8-Anilinonaphthalene sulphonate	10^4	nd	174
Morphine sulphate	10^2	nd	171
Sulphate	2×10^4	nd	163,191
Glucuronic acid	10^4	nd	163,191

---

* K_a: Association constant for purified ligandin
N: No. of binding sites
nd: Data not available/not determined
* : Binding demonstrated only by gel filtration of whole cytosol
† : Covalent binding in vivo

Many binding studies have been performed using purified ligandin, yielding quantitative affinity and stoichiometric data (163,164,167,174,191,192). Binding to ligandin has also been assessed in many cases by the demonstration of a Y organic anion-binding peak on gel filtration of whole 100,000g supernatant (107,159,162,165,178-187). By this means the binding of some compounds has been shown to occur both in vitro and in vivo, although major quantitative and qualitative differences between in vivo and in vitro binding of haem (183,184), folate (180) and thyroid hormones (182) have been observed. Similarly, binding of the dye Evans blue, occurs readily in vitro, but not in vivo (107,167). Chromatographic elution patterns may be difficult to assess in terms of ligandin binding, as in the case of rose bengal (186), while bile acids, which show binding on equilibrium dialysis (163,190,191), do not show Y protein binding on gel filtration (190). Shortly after intravenous injection, 71-80% of a number of organic anions recovered from the liver, are present in the 100,000g supernatant (2,107). Y and Z binding account for 75% of BSP in the supernatant fraction, and preferential binding occurs to the Y peak (107). Ligandin accounts for 80% of bilirubin binding in this fraction (11).

Ligandin binding of the great majority of the compounds listed in Table 1.III is a non-covalent, freely dissociating interaction, with the notable exception of certain carcinogens and alkylating agents which bind covalently in vivo as well as non-covalently in vitro (1,163,175). Covalent

binding of the DAB metabolite occurs to a cysteine residue in the ligandin polypeptide chain (5,120,163). Non-covalent binding to ligandin is heat labile and destroyed above 50°C (107). Although binding was initially reported to be unaffected between pH 6.5 - 7.5, or by ionic strength and buffer salts (107), pH optima for binding have been subsequently reported as pH 7 - 8 in CD studies (167) and pH 6 - 7 in equilibrium dialysis studies (191). Bilirubin has been shown to bind with higher affinity to ligandin at pH 7 than at pH 8 (164). Meuwissen et al (196) have emphasised that cytosol binding of bilirubin is extremely sensitive to ionic strength, buffer salts and pH, with a binding optimum at the physiological pH of cytosol (pH 6.9).

Competition between various compounds for binding to ligandin is extremely well documented, both in vivo and in vitro (107,159,167,182,191). This has been used to advantage as a means of determining affinity data for many ligands (167,191). Originally, ligandin was thought of as an organic anion-binding protein, a concept supported by the basic charge of the molecule which suggested that electrostatic interaction provided the major force for binding. However, it has been clearly shown that while certain organic anions such as pyruvate (9) do not bind, uncharged and apolar compounds such as steroid hormones and 3-methylcholanthrene bind at a site in common with organic anions (5,163,191). A certain specificity of binding is also apparent in that other neutral compounds such as propranolol (167) and ouabain (185) do not bind to ligandin.

Organic cations such as lidocaine (167) do not bind, whereas the base tetracycline binds to ligandin with reasonable affinity (162,163,191), possibly on the basis of its electronegative conjugated carbonyl groups.

CD studies have yielded much interesting information about the nature of ligandin interaction with bilirubin and other ligands (8,166,167,193). The bilirubin-ligandin complex induces large Cotton effects in the ligandin CD spectrum, with increased ellipticity near 255nm and 3 new ellipticity extrema in the region of bilirubin absorption, centred at 405, 455 and 515nm. Competitive displacement of bilirubin from albumin by various ligands, results in diminution in these ellipticities. The data emerging from these and other studies (164,189) indicate that bilirubin binds to ligandin in an asymmetrically aligned twisted configuration, without altering the configuration of ligandin. Binding occurs at a single high affinity site similar to that of albumin (193). Competition between bilirubin and other ligands occurs at this primary site, which is probably hydrophobic in nature (164,167). Binding of bilirubin (167, 193) and other ligands (191) to an additional site(s) occurs when 1:1 stoichiometry is exceeded, and the binding at this locus or loci appears to involve electrostatic interactions (193).

A hydrophobic primary binding site on ligandin would account for the observations that polar substitution of certain compounds, including bile acids (163,191) and porphyrins (5,165), decreases binding affinity, while increased

ionic strength enhances the binding of oestrone and oestrone sulphate (191). The higher binding affinity of certain anionic conjugates relative to their uncharged parent compounds, as well as the binding of sulphate and glucuronic acid, suggest that electrostatic interaction may reinforce apolar binding at or near the primary binding site.

GSH induces anomalous shifts in the bilirubin-ligandin CD spectrum (167) and competes for binding with oestrone sulphate, but not oestrone, in a manner not compatible with a 1:1 competition model (191). These data support the concept of GSH binding to a hydrophilic site adjacent to, and partially overlapping the primary hydrophobic site. GSH S-transferase B substrates such as iodomethane and 1-chloro-2,4-dinitrobenzene, do not displace bilirubin from the primary site (167), while bilirubin is an effective inhibitor of catalytic activity (174). This would imply that the primary binding site and second substrate catalytic site are the same, but that substrate ligands are rather loosely bound in its vicinity.

The 1:1 stoichiometry of ligand binding to ligandin suggests that the two subunits may co-operate in forming the primary binding site, however direct evidence for this is not available. Haem was originally thought to bind at two sites (4,5,163), but is now believed to bind at the same primary site as bilirubin, as well as at several weaker sites (189,192). This interaction is thought to alter the configuration of ligandin, as evident from CD data (192) and the loss of antigenicity of ligandin when complexed with

haem (163). Binding of haem to ligandin does not involve the iron atom of the porphyrin, and is unlike the specific binding of haem by haemoproteins (192).

When equimolar amounts of albumin, ligandin and bilirubin were studied by CD, over 90% of the bilirubin was transferred from ligandin to albumin (167). A similar phenomenon was observed by Bloomer et al (179) when a 1:1 ratio of albumin to hepatic cytosol protein was eluted from Sephadex G-75. Dynamic flow equilibrium dialysis studies have also indicated that the affinity of hepatic cytosol proteins is lower than that of serum proteins for BSP (197). The affinity of ligandin for bilirubin, and probably other organic anions, would appear to be at least one order of magnitude less than that of albumin for these ligands. This is an important point, as it creates considerable difficulty in explaining how ligandin competes with albumin in the transfer of organic anions from plasma to hepatocyte. Meuwissen, Ketterer and co-workers (163,195,196) have, however, shown that the binding of bilirubin and other compounds by ligandin may be adversely affected by purification, or even fractionation of hepatic cytosol, as this may alter the in vivo milieu of the protein and lead to a loss of an undefined factor required for optimum binding. These workers have studied binding by means of moving boundary sedimentation, which maintains the original cytosol environment, and under these conditions, ligandin completely removed bilirubin off albumin. The presence of mercaptans such as GSH during binding experiments, may indeed enhance the binding of certain ligands (174),

and it is estimated that at least 90% of hepatic ligandin is bound with GSH in vivo (5,163). This still does not account for the very high affinities of ligandin for bilirubin ($10^9 M^{-1}$) and haem ($10^{10} M^{-1}$) reported by Meuwissen et al (195,196), and other factors removed during fractionation of cytosol must be sought in order to explain these findings. Other unexplained discrepancies concerning the binding properties of ligandin also exist regarding the affinities of cortisol (13,133,167,191), oleic acid (167, 191), and haem (167,192,196), for the purified protein (see Table 1.III).

The limited binding studies performed to date with human ligandin, indicate that the affinity of this species for organic anions is an order of magnitude less than that observed in the rat analogue (161). There is also some evidence to suggest that antibiotics bind to a protein similar to Z protein in human liver cytosol, rather than to ligandin (200).

6. Quantitative Aspects of Ligandin

i) Methodology

Measurement of ligandin in the tissues of various species has been achieved by ligand binding techniques utilizing gel filtration (107,186,201-207) and gel adsorption (188), polyacrylamide gel electrophoresis (201,208), quantitative immunodiffusion (158-160,209-211) and immuno fluorescence (211,212). The GSH S-transferase activity of

various tissues has been related to ligandin content (213-215), but the overlapping substrate specificities of the various transferases, makes absolute interpretation of these data extremely difficult in terms of ligandin per se. The ratio of catalytic activities of tissue supernatants towards 1-chloro-2,4-dinitrobenzene and 3,4-dichloronitrobenzene, and immunoprecipitation of catalytic activity to the former substrate by antiserum to ligandin has been used, and appear to be the most specific forms of enzymatic assay for this protein (216,217).

ii) Tissue distribution

The highest concentration of ligandin is present in the liver, where it constitutes 5% of the cytosol protein in the rat (158) and 2% in man (160). Fleischner et al (212) have reported that ligandin is uniformly distributed in the hepatic lobule. In this study, specific ligandin immunofluorescence was confined to the cell cytoplasm and was not detectable in the cell membrane or subcellular organelles. Bannikov et al (211) however, found a higher concentration of ligandin in the centrilobular areas, and their immunofluorescence studies detected this protein in the liver cell nuclei as well as in the cytoplasm. Ligandin is restricted to the hepatocytes within the liver (211,212), as is GSH S-transferase activity (48). The next highest concentrations of ligandin are found in the cytosols of the kidney and small intestinal mucosa, constituting approximately 2% of the soluble proteins in these tissues (158,159,

209-211). In the kidney, ligandin is confined to the proximal tubular cells (212) and its concentration in these cells must therefore be higher than the overall 2% of total renal cytosol proteins. Renal ligandin has been isolated and fully characterized in the rat and shown to be identical with the hepatic protein (159). In the small intestinal mucosa, ligandin occurs predominantly in the proximal portion and is confined to the non-goblet mucosal cells. The concentration of ligandin is also richer in the tips of the villi, than in the crypts (212). Low quantities of ligandin are found in hepatomas (209-212), and the protein is absent in poorly differentiated varieties of this tumour. Ligandin has also been detected by some workers in the testis, ovary (210,211), skin and lungs of the rat (4), but these findings have not been uniformly confirmed (158,212,218).

Antisera to rat ligandin appear highly species specific. Goat anti-rat ligandin cross-reacts only with hamster tissues (212), while rabbit antisera detect this protein in the liver and kidneys of mice (210,211,219). In this regard, an interesting situation has been described in the mouse, in which three basic 40;000 molecular weight dimeric proteins have been isolated from the soluble protein of liver and skin, on the basis of binding 3-methylcholanthrene. Antiserum to rat ligandin cross-reacts with the two most basic of these three proteins (basic proteins II and III), but not with the relatively more acidic species, termed mouse h-protein (109,219,220). All three of these mouse proteins in addition, have GSH S-transferase activity. Antiserum to

human ligandin crossreacts only with rhesus monkey hepatic supernatant (6).

iii) Sex and strain differences

Quantitative differences in the substrate dependent hepatic and renal GSH S-transferase activities have been demonstrated between male and female rats (213,214,221). Reyes et al (201) noted minor strain differences in the concentration of ligandin, measured by gel filtration, among Long-Evans, Gunn and Sprague-Dawley rats, but a sex difference was not clearly established. Foliot et al (203) found no difference in hepatic ligandin levels between adult Wistar and Gunn rats. Hales and Niems (216) have found that ligandin constitutes 4.5% of the hepatic cytosol proteins in female Sprague-Dawley rats and 3.3% in male animals of the same strain.

iv) Phylogeny

Levine et al (204) have shown by means of a dye-binding technique, that ligandin, or a ligandin-like protein, is present in the livers of a large number of air-breathing species including mammals, birds, reptiles and amphibians. It is absent in elasmobranchs and teleost fish and only appears in amphibia after metamorphosis. It thus appears that ligandin is associated with the aquatic to terrestrial evolutionary transition. It is interesting, that although ligandin is absent from elasmobranch liver, this phylum appears to possess GSH S-transferase activity (222), and this enzyme activity is also present in insects, plants, and possibly

bacteria (223), indicating an extremely early phylogenetic appearance of this important detoxifying mechanism. The enzyme has been purified and characterized from the housefly, and bears a remarkable similarity to the rat and human analogues, in that it consists of a series of charge isomers of molecular size ∿ 40,000 daltons (223).

v) Mammalian ontogeny

In the neonate, ligandin has been found in low concentrations in the livers of all species studied, including the rat (185,188,203,210-212,217), guinea-pig (224), monkey (202) and man (6,160), and was undetectable in the kidney of the newborn rat by immunodiffusion (159). Direct quantitative data are lacking in the developing animal, but Grodsky et al (188) reported bilirubin binding of 34% and BSP binding of 24% of adult levels in foetal rats 2 days pre-partum. Klaasen (185) and Foliot et al (203) obtained levels of 10% and 17% of adult values for ligandin in 5 day old rats by dye-binding methods, and similarly, Levi et al (202) estimated the hepatic ligandin concentration in day old primates as 33% of adult levels. Recently, Hales and Niems (217) assessed ligandin concentration in rats soon after birth to be 20% of adult values. Hepatic ligandin concentration increases rapidly postnatally, reaching adult levels in the first 4-5 weeks after birth in the rat (185,188,203, 210,217) and within 5 days in the monkey (202). Foliot et al (203) observed that development of ligandin was more rapid in Gunn rats than in normal Wistar rats, suggesting

that bilirubin might induce ligandin in the newborn.

Related developmental patterns have been reported for hepatic GSH S-transferase activity towards BSP in the rat (225,226). Qualitative differences between these patterns and that of ligandin per se, bearing in mind the inefficiency of ligandin catalytic activity towards BSP, probably indicate that the different transferases develop at different rates. There is in fact evidence to suggest that ligandin matures more rapidly relative to the other GSH S-transferases (217).

vi) Turnover

In an early communication, Levi et al (227) reported a half-life of 19 days for ligandin, determined after pulse-labelling. Later (208), this figure changed to 3-5 days, and most recently, Arias et al (11) have estimated the half-life of ligandin in the liver and kidney as approximately 2 - 2.3 days.

vii) Effects of drugs, hormones and fasting

The induction of enzymes in the hepatic endoplasmic reticulum by various drugs, insecticides and carcinogens, is a well known phenomenon (for Reviews see refs. 126 and 228) which has been found to apply to ligandin, a cytoplasmic protein, as well. Xenobiotics have been reported to induce ligand-binding capacity (185,201,205), immunoreactive ligandin (158-160) and GSH S-transferase activity towards several substrates in rat liver (15,213) and

kidney (214).

Phenobarbital treatment increases ligandin concentration in normal and Gunn rat liver (158,201,205), adult human beings (160) and developing rats (217). This effect is evident within 2 days after commencing treatment (185), and is solely due to increased synthesis of ligandin which reaches a new steady state 120-280% above control levels by the sixth day of treatment (11,158,208). Ligandin levels returned to normal 6-9 days after cessation of phenobarbital treatment. Hepatic ligandin is also induced by allylisopropylacetamide, dieldrin, DDT, 3-methylcholanthrene, benzpyrene (201), 16 α-pregnenecarbonitrile (159), spironolactone (185) and tetrachloro-dibenzo-p-dioxin (TCDD) (6,159). Only the latter agent has been reported to induce ligandin in the kidney, although increases in various substrate-defined renal GSH S-transferase activities have been described with phenobarbital and polycyclic hydrocarbons as well (214).

Hypophysectomy and thyroidectomy, as well as congenital hypopituitarism and hypothyroidism, result in elevated hepatic ligandin levels (11,133,160,201). Thyroidectomy doubles renal ligandin concentration as well (11). The effects of both pituitary and thyroid hormone deprivation on ligandin appear to be mediated through partial stabilization of the protein, and are both reversed by thyroxine administration (11) while further potentiated by phenobarbital treatment. Controversial data have been reported by Hales and Niems (216) and Kaplowitz et al (215) regarding the

effect of hypophysectomy on ligandin levels. The former workers' studies suggest that hypophysectomy lowers hepatic ligandin levels in female rats, effecting a normalization of the ligandin concentration difference between rats of different sexes. The latter group inferred from studies on GSH S-transferase activities, that hypophysectomy had no effect on hepatic or renal ligandin concentrations. However, the data reported by both groups suggest that increases in the other transferases may occur with pituitary hormone deprivation, and it is possible that the increased dye-binding observed by Reyes et al (201) was due to these, rather than ligandin in particular.

Reduction of hepatic ligandin levels is associated with both mechanical and ethinyl oestradiol induced cholestasis (201), fasting (229) and the administration of hypolipidaemic agents such as Clofibrate and Nafenopin (230). The latter agents do not, however, affect total hepatic content of the protein (206,230). The effects of fasting appear to be mediated through diminished synthesis as well as increased degradation of ligandin and can be prevented by prior phenobarbital treatment (229).

Ligandin is not affected in normal animals by the administration of alcohol, thyroid hormone, testosterone or hydrocortisone (201).

CHAPTER IV

THE ROLE OF LIGANDIN IN THE CELL

1. Binding Proteins and Transport

The term "binding" has been commonly used in biological science to describe the often poorly defined interaction between small ligands and macromolecular structures. Binding has been studied as a phenomenon relating to numerous biological transport processes (12,231). Drug-protein binding constitutes a basic principle underlying the pharmacokinetics, transcellular movements, and mode of action of bioactive agents.

Little is really understood of the mechanisms underlying the process of cellular trans-membrane accumulation of nutrients, drugs, hormones and other small molecules, and considerable interest has focused on the role of specific binding proteins in this process. Bacterial binding-protein systems in particular, have been meticulously studied and a large number of these proteins have been isolated. All these proteins are in the 30,000 molecular size range and are highly specific for ligands ranging from sulphate ions to specific sugars and amino acids (231,232). There is strong indirect evidence to support the notion that these bacterial proteins are involved in the active transport of substances across the bacterial membrane. These proteins are not structural components of the membrane, which has an additional transport system associated with it structurally, but reside close to the membrane in the periplasmic space. It is tempting to consider ligandin, a

46,000 molecular weight cytoplasmic protein, as an analogue of the bacterial transport proteins in relation to the hepatic uptake process of advanced life forms.

2. The Role of Ligandin in Hepatic Uptake

i) The Evidence

"Uptake" is a jargon term used to describe the process of rapid and selective transport of small molecules - mainly organic anions - from the sinusoidal plasma across the hepatocyte cell membrane into the cell interior. Uptake has been convincingly shown to occur independently of blood flow (64), subsequent metabolic transformation (104,105,223) and biliary excretion (see discussion ref. 8, 201). The measurement of this dynamic process presents a major problem. Kinetic methods of assessing uptake have employed the measurement of organic anion plasma disappearance rates (K) per se (201,233), resolution of exponential decay (91-93) and complex flow data (78,79) into terms of compartmental analysis (k_{21}) and uptake into "storage" (71,76,86,201). Measurement of the intrahepatic concentration (201,234,235) and "cumulative uptake" (236,237) of organic anions following intravenous administration have also been used. None of these methods is direct, or free of assumptions which may be questioned. Scharschmidt et al (233) have shown, however, that the initial plasma disappearance rate of organic anions (K) agrees well with the compartmental analysis (k_{21}, see Fig. 1.) and direct tissue measurement means of assessing the uptake parameter in the rat.

Thus the evidence pertaining to the role of ligandin in uptake is indirect or "guilt by association" in nature (2,3,6-11,20) and is considered under specific categories below.

(a) Distribution

Ligandin occurs in high concentrations in tissues with overtly active transport functions: the liver, kidney and small intestinal mucosa. It also binds organic anions which are normally cleared from the plasma by the liver and kidney (107,158,159,167). The greater initial uptake of uranin by the centrilobular zones of the liver (43), also concurs with the high centrilobular distribution of ligandin found by Bannikov et al (211), while the distribution of ligandin in the proximal renal tubules coincides with the site of renal organic anion transport (10,11).

The selectivity of hepatic uptake for certain organic anions is conceivable in terms of the high affinity of ligandin for bilirubin and BSP (167), while the fact that ligandin binds cholecystographic but not renographic contrast media (178) is further evidence supporting the role of this protein in selective hepatic uptake. The selectivity of uptake however, is not solely governed by ligandin which also binds Evans Blue, a dye which does not enter the liver (107,167), while ouabain (185) and rose bengal (186), which are taken up rapidly and selectively by the liver, do not bind to ligandin. Furthermore, organic cations are also cleared from the plasma by the liver, but show no

binding to soluble liver proteins (16,238,239).

(b) Phylogeny

The presence of ligandin exclusively in air-breathing vertebrates has been correlated with the capacity of these species to transfer BSP selectively from plasma to liver (204). However, the studies of Boyer et al (222) have shown that virtually an entire dose of BSP given to dog-fish intravenously can be recovered from the liver and bile within 2-24 hours. These findings demonstrate that aquatic vertebrates that lack hepatic ligandin, do not excrete organic anions such as BSP across the gills as previously believed (204). This also suggests that ligandin may correlate better with the rapidity, rather than the selectivity of uptake in terrestrial vertebrates.

(c) Ontogeny

Several studies have demonstrated delayed clearance of bilirubin (21) and BSP (234) in the foetus and healthy newborn. In keeping with the generalised immaturity of enzyme function in neonates (226,240), the enzymes required for conjugation of bilirubin (21,241) and BSP (225,226) are low at this stage of life. However, the immature conjugating mechanism in both cases does not appear to be the limiting factor in the diminished capacity of the newborn liver to excrete organic anions, but rather the mechanism of biliary excretion of conjugates (234,241,242).

The uptake process has also been shown to be immature in the guinea-pig neonate for bilirubin (241) and in the rat neonate for BSP (234), but is probably not an overall limiting factor. The low levels of ligandin in the neonate of various species (see Chapter III.6.v) might explain the reduced uptake capacity observed at this stage of life. Furthermore, the maturation of ligandin appears to correlate well with the maturation of organic anion uptake in developing mammals (202,224) and the disappearance of "physiological jaundice" in non-human primates (202). The apparently normal uptake of BSP in the neonatal guinea-pig (see discussion ref. 234) and ICG in human newborn (47), conflicts with the hypothesis that ligandin immaturity in the newborn leads to diminished uptake of all organic anions. Also, the immaturity of neonatal hepatic clearance of neutral compounds such as ouabain, is not related to low ligandin levels, but rather to the underdeveloped biliary excretion mechanism (185).

Deficiency of renal ligandin may account for the immaturity of p-aminhippurate (PAH) transport in mammalian neonates (10). Pegg et al (243) have shown that penicillin pretreatment of young rabbits enhances the rate of uptake of PAH by the proximal tubules, and the mechanism appears to act via the increase of a soluble carrier protein. A subsequent study (244) however, showed a definite lack of correlation between the development of PAH transport and GSH S-aryltransferase activity in rabbit and rat renal slices. The pitfall of equating total enzyme activity with ligandin

however, must be emphasised as regards these findings.

It would appear therefore, that deficient ligandin in neonatal liver and kidney may contribute to the immature functioning of these organs, but is probably not the most important factor involved.

(d) Induction

Induction of ligandin by various agents (see Chapter III.6.vii) is associated with increased hepatic uptake of organic anions in normal and Gunn rats (201,205), while induction of renal ligandin is concurrent with increased renal clearance and urinary excretion of penicillin (159) and renal PAH transport (10,11). This evidence must be viewed in the light of the fact that phenobarbital enhances the plasma disappearance of numerous drugs, including organic bases and neutral compounds which do not bind to ligandin (245). Phenobarbital treatment induces the enzymes conjugating bilirubin and BSP and also increases liver weight and bile flow. Klaasen (245) has proposed that the latter effect is the most important in determining the increased rate of clearance of numerous substances by the liver, while Scharschmidt et al (233) have shown that the uptake of bilirubin in normal and Gunn rats treated with phenobarbital is increased by a percentage similar to the percentage increase in liver weight, and not to the extent that ligandin is increased by phenobarbital treatment. Also, different microsomal enzyme inducers vary in their potency in effecting

induction of ligandin while affecting clearance of organic anions to a similar degree (185). Fasting reduces ligandin concentration in the liver (229) and concomitantly reduces the uptake of BSP and ICG (229,233), but inexplicably, does not affect bilirubin uptake.

Another unexplained anomaly arises from the finding that although ligandin concentration in the liver is apparently boosted by hypophysectomy and thyroidectomy, the initial plasma disappearance rate of BSP is reduced under these circumstances (201) while the cumulative uptake of bilirubin is normal (236). It is possible that the reduction in bile flow, and hence biliary excretion caused by thyroid hormone deprivation, antagonizes any enhancement of uptake produced by elevated ligandin levels (236). This serves to point out that although uptake occurs independently of more distal processes, these may nevertheless limit the rate at which uptake can occur, and moreover, serves to illustrate the difficulty in assessing the uptake process as an isolated phenomenon. Compartmental analysis studies have shown that induction of ligandin in rats (246) and dogs (11) is not accompanied by an increase in the fractional rate constant for uptake (k_{21}), but rather a decrease in the reflux parameter (k_{12}) (see Fig. 1.3). These findings suggest a mechanism whereby ligandin, by limiting the reflux of organic anions back into the plasma, may influence the net flux of uptake into the liver.

(e) Competition

The competition between various ligands for binding to ligandin provides an attractive explanation for the mechanism of competition shown by these substances for hepatic and renal uptake in vivo. Most ligands studied appear to compete for binding at a single site on ligandin (see Chapter III.5). Thus the retarded uptake of BSP and T_3 in Gunn rats could be accounted for by bilirubin competition for binding to ligandin (182), and the effect of probenecid in retarding the renal clearance of penicillin could be similarly explained (159). However, the degrees of in vivo competition between bilirubin, BSP and ICG (233), are not readily explained in terms of the known affinities of these pigments for ligandin (167). The concept is further undermined by the fact that rifampicin, which competes with BSP (247) and ICG (235) for uptake in vivo, does not bind to ligandin. Also flavispidic acid, which blocks bilirubin uptake in vivo, does not clearly interfere with bilirubin binding to ligandin, although it may effectively displace this compound from Z protein (107). In the case of bile salts, weak binding to ligandin has been demonstrated (191), but the considerable lack of agreement regarding the competitive effects of these agents on the uptake of other organic anions (36,68,76,94,248-250) disallows any meaningful interpretation of the significance of ligandin-bile salt interactions in relation to uptake. The studies of Clarenberg and Kao (237) have also suggested that observed competitive effects between bilirubin and BSP may

not be due to events occurring during uptake, but may rather reflect competition occurring at the site of biliary excretion.

ii) The cell membrane

From the consideration of the arguments both for and against the role of ligandin in the uptake process, it is clear that a simple "unifying hypothesis" for uptake centred around this protein is not at hand. The situation is indeed complex, and a functional role for the cell membrane could be proposed, in order to accommodate all the data which suggest multiple shared and separate modes of transport for molecules into the liver cell.

Kinetic analysis of the hepatic uptake process from whole animal (78,233,235), perfused liver (67,248,251), tissue slice (67,68) and isolated cell studies (252,253), supports the notion of uptake being a high capacity yet saturable process, which can be described in terms of classical Michaelis-Menten kinetics. This precludes simple diffusion as the mechanism underlying uptake and further, fulfils an operational characteristic of a membrane carrier-mediated transport process (see Chapter II.1.v). The other operational characteristics of this mechanism, namely competitive inhibition and countertransport, have also been demonstrated for uptake (79,233). Scharschmidt et al (233) have shown what might be a fourth operational characteristic of membrane carrier-mediated transport inherent in the uptake process. These workers have shown that large doses of bili-

rubin enter the cell more rapidly when the intrahepatic bilirubin concentration is increased by prior infusion (a "preloading effect"). It is difficult to explain this phenomenon in terms of uptake governed by ligandin. However, this phenomenon could not be demonstrated in isolated perfused liver studies (251). The complexity of whole animal or even isolated liver perfusion studies, introduces variables of multiple processes such as extravascular distribution, blood flow, plasma protein binding, storage, conjugation and biliary excretion occurring prior to and beyond uptake, which makes interpretation of these studies difficult. These difficulties are to some extent obviated in tissue slice and isolated cell studies, but there have been few of these reported and the results have been conflicting to the extent of defining the organic anion uptake process either as a membrane carrier-mediated, energy dependent system (252,253) or as a process of passive diffusion with intracellular protein binding (67,249).

The fact that uptake competes with albumin binding of ligands is a consistent result of many studies (30,48,67,68, 179,246,248,249,251,252,254). If hepatic uptake of organic anions reflects an equilibrium between protein binding on both sides of the plasma membrane, then certain attributes of a carrier-mediated transport system could be accounted for by ligandin. The lower affinity of ligandin for various ligands with respect to albumin (167) weakens this argument, but the question of affinities is not clearly resolved, and if, as proposed by some workers (196), ligandin has a higher

affinity for bilirubin than has albumin, then ligandin may well be a major factor regulating the uptake process. The plasma membrane might aid the uptake process by promoting the dissociation of bilirubin from albumin (179), but there is at present little supportive evidence in favour of a carrier role for this structure. Preliminary studies have, however, indicated that binding sites for bile salts (250) and BSP (101,255,256) are present in the cell membrane, which may be shared with other organic anions. The role of these binding sites in the uptake process still remains to be determined.

iii) Gilbert's Disease

Constitutional hepatic dysfunction, or Gilbert's disease, has been widely studied as a means of gaining insight into the hepatic uptake process (2,3,21,22,61,90,91,187,257-263). This condition is characterised by mild unconjugated hyperbilirubinaemia, and although haemolysis (91) and diminished glucuronyl transferase activity (261) have been explored as possible causes of this syndrome, a defective uptake mechanism is clearly evident from radiobilirubin kinetic studies, and still remains unexplained (257,262). Contrary to the earlier belief that only bilirubin uptake is affected in this condition, it is now recognized that the uptake of BSP, ICG (258,260) and tolbutamide (187) may be impaired as well. None of these agents undergoes glucuronidation, but all three do bind to ligandin. It is therefore interesting that Frezza and Tiribelli (263) have reported that the

affinity of hepatic cytosol proteins for BSP is less than normal in Gilbert's disease. Phenobarbital treatment, which induces ligandin, also eliminates the hyperbilirubinaemia in this condition (259).

A deficiency or defect of ligandin in Gilbert's disease would clearly be strong evidence in favour of the role of ligandin in hepatic uptake. However, in four patients with this condition, ligandin concentration measured by immunodiffusion was normal (160) and is also apparently undiminished in the liver of the Southdown sheep (107), the laboratory analogue of Gilbert's disease. The fact still remains however, that nothing is known of the functional or structural characteristics of ligandin in these situations, and it is conceivable that these properties might be altered without demonstrable quantitative differences.

Recent studies have shown Gilbert's disease to be a heterogenous condition. Berk's group have distinguished 3 subgroups in patients with this condition (258,260). Group I have impaired uptake of bilirubin alone and constitute the majority of cases. Group II has in addition to impaired bilirubin uptake, a defect in BSP transport beyond the uptake process, while Group III have impaired uptake of bilirubin, BSP and ICG. Compartmental analysis studies also suggest that there may be a reduction of transport of bilirubin to the endoplasmic reticulum in all cases of Gilbert's disease (90,257). Thus the quantification and characterization of ligandin in Gilbert's disease needs to be assessed in relation to the various subtypes of this condition, and

also in relation to other rare conditions in which defective hepatic uptake and/or storage of organic anions have been described (264,265).

3. The Role of Ligandin in Intracellular Storage and Transport

As much of the evidence suggests, the binding of small molecules to ligandin does not necessarily indicate that this protein is the sole or even the most important determinant of uptake, but alternatively, that it functions as an "intracellular albumin" in the intracellular transport and storage of numerous small molecules (191). The capacity of the liver for storing the conjugates of bilirubin (74) and BSP (79) is less than that for the free compounds, and accords with the lower affinity of ligandin for these conjugates as opposed to free bilirubin and BSP (167,194). There is also some evidence to suggest that phenobarbital treatment increases the hepatic storage capacity of BSP (201), which is in keeping with ligandin induction. Ligandin may also be an essential factor in maintaining the intrahepatic store of GSH.

The induction properties of ligandin and the pattern of haem binding to this protein after ^{14}C-5 amino levulinic acid administration, have led Ketterer et al (183,184) to propose that ligandin is functionally linked to the endoplasmic reticulum, and that it may participate in the transport of haem from the mitochondria to the apo-enzymes of the endoplasmic reticulum. It may also facilitate the excretion of

bilirubin derived from cytochrome P-450 catabolism. Kirshenbaum et al (262) have alternatively suggested that ligandin may rather serve to maintain a compartment for incoming bilirubin separate from that produced in the liver, which may gain egress bound to newly synthesized albumin.

Recent studies have revealed that bilirubin is conjugated in 2 stages: to the monoglucuronide by a microsomal enzyme and then to the diglucuronide by a membrane bound enzyme (266). The order of affinities of the bile pigments for ligandin diminishes with the extent of conjugation (194). This may indicate that bilirubin is conjugated while bound to ligandin, and that conjugation in turn promotes the debinding and biliary excretion of bilirubin. It is not clear as yet whether binding to ligandin actively promotes the glucuronidation of bilirubin (see discussion ref. 8,9), but this remains an interesting question.

Evidence of the induction/competition type has led to speculation concerning the role of ligandin in the hepatic uptake of thyroid hormone (182). However, many different systems have been used to study thyroid hormone-binding proteins in the liver (182,267-269) and no clear resolution of the role of ligandin has emerged. It is possible that ligandin is one of a series of proteins constituting an intracellular chain, by which T_3 and T_4 traverse the cytoplasm to the nucleus. In this regard, ligandin may be analogous to the steroid hormone receptors, but the affinity of ligandin for T_3 is much lower than that reported for a putative receptor of this hormone (269). Similarly, ligan-

din is not thought to convey steroid hormones to the nucleus; this function belonging to a specific high affinity receptor (132,133). It is more likely that ligandin functions to transport sulphated steroids to the bile cannaliculi and in this manner serves to promote their excretion (13).

4. The Metabolic and Protective Role of Ligandin

The dual enzymatic and binding properties of ligandin ideally suit this protein for an important role in the biotransformation and elimination of many substances. Although only certain oestrogens appear to constitute "physiological" substrates for GSH conjugation (146), the GSH S-transferases appear to have evolved as a highly versatile detoxifying system, capable of neutralizing and promoting the excretion of a wide range of toxic xenobiotics, thus effectively protecting the cell and hence the organism against metabolic damage. A role for ligandin and the other transferases in the intermediary metabolism of prostaglandins (172) and steroid hormone synthesis (173) is also evident from preliminary studies and will need further exploration. Renal ligandin may be important in the biotransformation of diuretics in the proximal tubules (10,11,15), thus influencing their more distal effects.

Bilirubin and BSP are highly toxic to isolated mitochondria and there is experimental evidence to support the conclusion, that binding of bilirubin (270) and BSP (271) to ligandin effectively protects the mitochondria from damage by these organic anions. Induction of renal ligandin by

TCDD and thyroidectomy may protect the kidney against mercuric chloride ($HgCl_2$) induced tubular necrosis by providing sulphydryl groups for binding of mercury, thus shielding more vulnerable -SH containing proteins (10,11).

Ligandin is one of several carginogen-binding proteins isolated thus far from the rat and mouse (4,13,14,109,119, 219,220) which covalently bind the metabolites of DAB and 3-methylcholanthrene in vivo. Although a positive correlation between carcinogenesis and protein binding has been shown (108), the exact significance of carcinogen-protein interactions is not understood in terms of the promotion or prevention of carcinogenesis. When considered in the light of current hypotheses, binding of carcinogens to ligandin may imply:

(1) Alkylation of a cellular growth-control protein with subsequent deletion and initiation of carcinogenesis (116).

(2) Facilitation of transport of carcinogens to the nucleus (117), or

(3) sequestration of the carcinogen, coupled with detoxification and elimination (13).

The initial hypothesis remains untested. The second appears to be similar to the function of the steroid hormone receptor which, in fact, may bind 3-methylcholanthrene (272) and act as the "unintentional" means of carcinogen access to the nucleus. Ligandin has been found in the nucleus by Bannikov et al (211), but this has not been the experience of

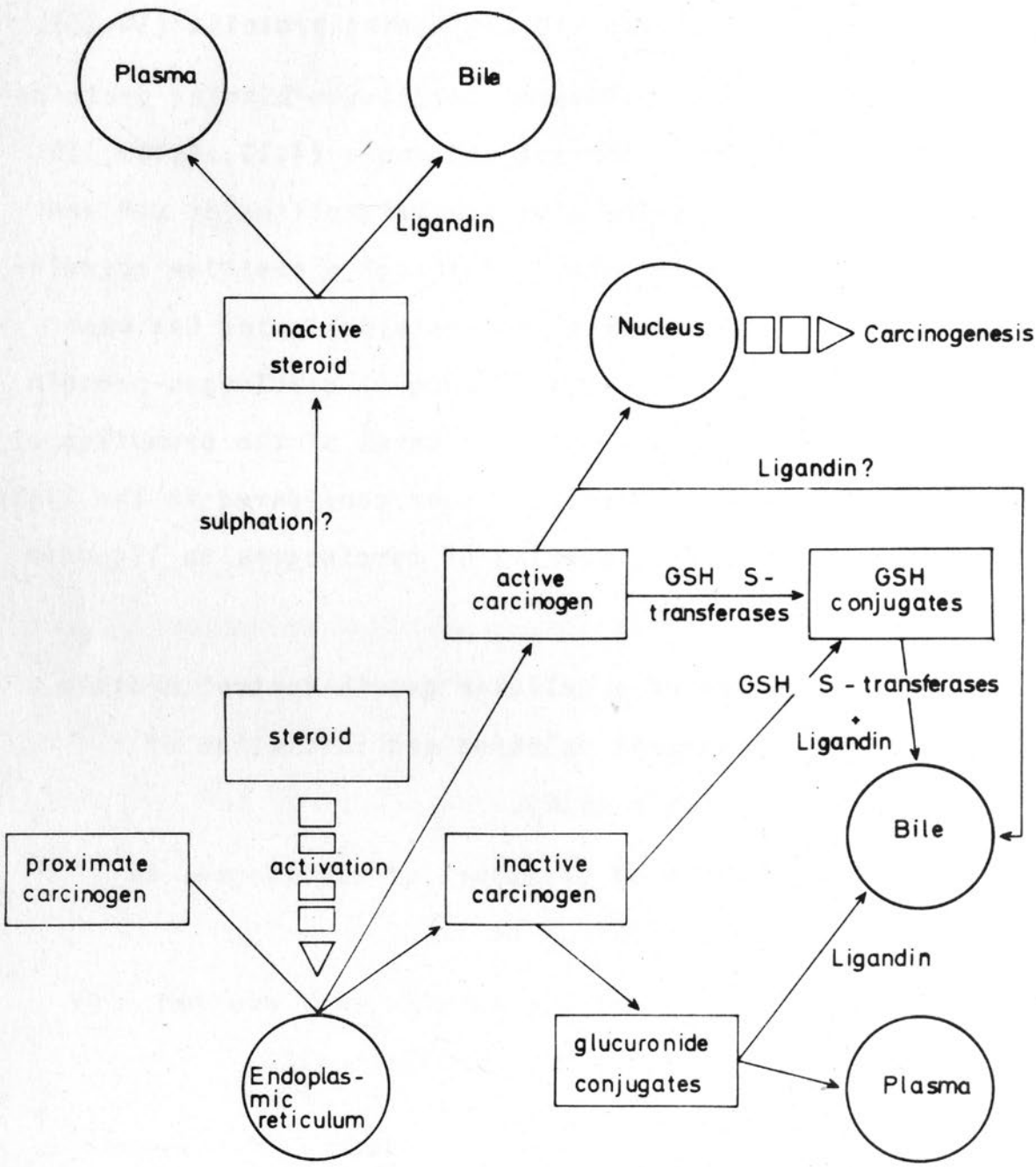

Fig. 1.10. The hypothetical protective role of ligandin and the other GSH S-transferases in carcinogenesis. (Reproduced from Smith et al (13)).

other workers (212). It is more likely that ligandin plays a protective role in keeping with hypothesis (3) above. The evidence in favour of this hypothesis has recently been reviewed by Litwack (133) and Smith et al (13), and is shown diagrammatically in Fig. 1.10. The argument presented by these authors supporting a protective role for ligandin in carcinogenesis, is largely based on the fact that the various hormonal and drug manipulations which increase hepatic ligandin are also associated with a decreased susceptibility of liver cells to carcinogens and neoplastic transformation. This apparent protective function of ligandin can be explained in three ways:

(1) Covalent and non-covalent binding of active carcinogens by ligandin may protect the genome from these agents i.e. a "buffering effect".

(2) Further protection by ligandin may result from the GSH conjugation of activated carcinogens, such as the azodyes and epoxide derivatives of polycyclic hydrocarbons, while ligandin transport of these conjugates to the bile cannaliculi may promote their elimination.

(3) The promotive effect of adrenal and gonadal hormones on carcinogenesis may be due to their stimulation of carcinogen activation reactions such as microsomal N-hydroxylation. Binding of these hormones and their metabolites by ligandin may effectively compete with their stimulation-activation function, and again promote their excretion in the bile.

A final point to be considered is the fact that the activated azodye carcinogen closely resembles steroid sulphates. Both these agents bind at the same site on ligandin (5,191), and it is possible that displacement of carcinogens from this protein by steroid metabolites, constitutes a mechanism whereby these hormones serve to promote carcinogenesis.

5. Ligandin as a Diagnostic Tool

One final role of ligandin remains to be considered; an essentially non-physiological, but nevertheless important role as an index of specific tissue necrosis. Preliminary studies (10,11,273,274) have revealed that following $HgCl_2$ administration to rats, ligandin is released into the urine where it may be detected by immunodiffusion and catalytic activity. Potassium dichromate ($K_2Cr_2O_7$) poisoning does not result in ligandinuria and from this it appears that ligandin may be confined to the pars recta of the proximal tubule - the site of $HgCl_2$, but not $K_2Cr_2O_7$ toxic action. In man, ligandinuria occurs following acute tubular necrosis. It is also detected following renal arteriography and in the pretransplantation "perfusate-urine" of donor kidneys, and may precede the development of frank tubular necrosis in these instances. The use of ligandinuria as a dianostic and prognostic indicator of acute tubular necrosis in man appears to be an important area worthy of further exploration. A similar diagnostic role for ligandin in hepatocellular necrosis might be feasible. However, the protein has not

been detected with available means in serum after acute liver injury (6,9).

6. Z Protein

A comprehensive review of Z protein is beyond the scope of this work, but it appears to be similar to ligandin in many respects. This ∿ 14,000 molecular weight protein is present in the liver, kidney, proximal small intestinal mucosa, myocardium and fat. It does not have GSH S-transferase activity, but may be important in the uptake and subsequent metabolism of fatty acids, sterols and organic anions. In addition, Z protein also binds carcinogens and in this regard, may have a function similar to that discussed for ligandin (7,182,201,229,230,275-283).

CHAPTER V

THE AIMS AND SCOPE OF THE PRESENT STUDY

Since the inception of the study of ligandin, the role of this protein in the cell has remained controversial. As discussed in the preceding chapter, the body of evidence concerning the function of ligandin in organic anion uptake and the intracellular transport of small molecules is indirect and dependent in most cases on reliable quantitative tissue data.

The assessment of ligandin concentration by means of ligand-binding and enzymatic techniques, is beset by the problem of overlapping substrate specificities and non-substrate binding affinities displayed by the entire group of rat GSH S-transferases, of which ligandin represents but a single member. These methods are thus far from ideal for use in the quantitative study of ligandin. Ligandin is, however, immunologically distinct from its fellow transferases, and the immunological methods for measuring this protein are the most definitive as regards specificity. However, the direct measurement of low concentrations of ligandin in the tissues and physiological fluids of the rat and in the tissues of new-born and developing animals has not been possible with available techniques. It was thus the need for a highly sensitive, as well as specific method for the quantification of ligandin that provided the impetus for this study.

The technique of radioimmunoassay (RIA), first described by Yalow and Berson (284) revolutionized the field of endo-

crinology by providing a means for measuring low concentrations of peptide hormones in physiological fluids. The use of this technique has subsequently been extended to the measurement of a large variety of biological and pharmacological substances (285-288) and has recently been applied to the measurement of enzymes (289-291) and other intracellular proteins (292-295) in tissues and in the plasma.

The primary undertakings of this study were thus:-

(1) To develop a sensitive and specific RIA for rat ligandin.

(2) To employ the RIA technique in a quantitative study of ligandin in the tissues of the adult and developing rat and to thus obtain further insight into the intracellular role of this protein.

(3) To apply the RIA technique to the measurement of ligandin in the plasma and urine under conditions of experimental hepatocellular and renal tubular necrosis, and by this means, to define the value of the measurement of this protein in physiological fluids as an index of specific tissue injury.

During the course of developing and applying the RIA of ligandin, certain observations came to light which made it evident that ligandin comprised two non-identical subunits, which further appeared to be the monomers of two distinct, yet closely related proteins. In view of the dual enzymatic and non-substrate binding activities of ligandin, the interesting question was thus raised as to whether these two func-

tions belong separately to two different proteins. The initial scope of this study was thus extended to incorporate:

(4) An attempt to define the nature of the two ligandin subunit species in relation to the enzymatic and non-substrate binding properties of this protein.

PART 2

EXPERIMENTAL

CHAPTER VI

GENERAL PRINCIPLES AND CONSIDERATIONS

1. General Principles of RIA

The principles and methodology of RIA have been exhaustively reviewed (285-288, 296, 297) and are broadly summarized by the set of competing reactions:

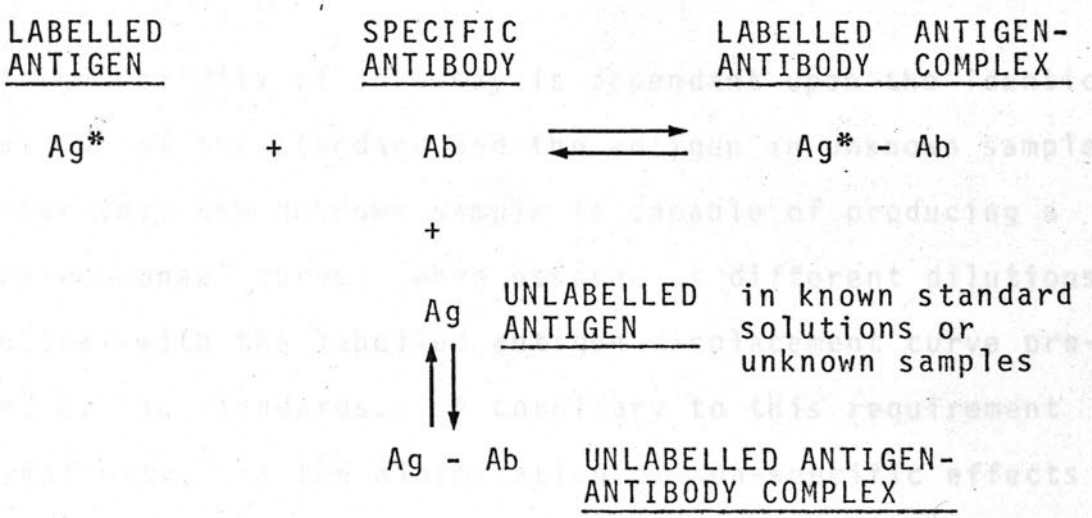

The technique of RIA exploits the ability of an unlabelled antigen in solution, to compete with its labelled counterpart ("tracer") for specific antibody binding. As a result of competitive inhibition, the ratio of antibody-bound to free labelled antigen (B/F) is diminished as the concentration of unlabelled antigen is increased. In order to determine the concentration of antigen in an unknown sample, the degree of competitive inhibition observed in the unknown is compared with that obtained in known standard solutions.

The essential requirements for setting up an RIA thus include:

(1) The availability or preparation of the individual reac-

tants, namely:

(a) Unlabelled antigen, for use as standards

(b) Labelled antigen, for use as "tracer", and

(c) Specific antibody.

(2) A technique for separating the antibody-bound from the free labelled antigen.

The validity of an assay is dependant upon the identical behaviour of the standard and the antigen in unknown samples, insofar that the unknown sample is capable of producing a "dose-response" curve, when assayed at different dilutions, identical with the labelled antigen displacement curve produced by the standards. A corollary to this requirement for validity, is the minimization of non-specific effects on the antigen-antibody reaction.

2. Presentation of Experimental Data

The chapters following the present one have been grouped into three broad sections, in accordance with the stated aims of this study, as well as the principles discussed above.

Section A is devoted to the "groundwork" of purifying and labelling ligandin, as well as the production of antiserum to this protein and the setting up and general characterization of the RIA.

Section B deals with the quantitative RIA of ligandin in the tissues of the rat and also integrates work dealing

with the characterization of the ligandin subunits.

Section C covers the quantitative RIA of ligandin in physiological fluids and explores the role of ligandin as a diagnostic tool.

Included in each chapter in this part of the thesis are the methods used, the results obtained as well as a discourse relevant to the particular findings reported.

3. General Considerations

In order to avoid repetition, certain general considerations pertaining to the experimental work of this thesis will be discussed at this point.

i) Animals

Unless otherwise stated, the animals used in this study were adult male rats of the Wistar strain (200-250g body weight), bred and housed under standard laboratory conditions. The animals were maintained on standard rat cubes and water ad libitum. Except in the instances where animals were bled from the tail veins, blood was obtained and tissues were removed while the rats were anaesthetized with 10% ether, 90% oxygen. Animals were sacrificed under anaesthesia by decapitation.

ii) Materials and Methods

A series of appendices will be found at the end of this thesis. A full list of all the materials used in this study, as well as their source of supply, is given in Appendix A.

Full details of established experimental, statistical, and computational methods used in this study have been recorded in Appendices B, C and D respectively. These methods will only be briefly mentioned or outlined in principle in this part of the thesis.

SECTION A

PURIFICATION OF LIGANDIN AND DEVELOPMENT OF THE RIA TECHNIQUE

CHAPTER VII

THE PURIFICATION OF HEPATIC LIGANDIN

1. Introduction

In order to provide a suitable antigen for developing a ligandin RIA, it was necessary to first purify ligandin from rat liver. A number of methods have been described to this end (see Chapter III.2) and the procedure of Kirsch et al (159) was employed in this study, as it offered the advantage of simplicity while apparently yielding a final product identical to that obtained by more complex and time-consuming methods (15). This method has been extensively employed in purifying ligandin from the liver (Fleischner, Kirsch, personal communications, see also refs. 2, 158, 167, 218), although it has only been reported in detail in relation to the purification of renal ligandin (159). This chapter therefore contains a detailed description of this method including some minor modifications, applied to the purification of rat hepatic ligandin. Ligandin was purified on several occasions during the course of this study and the ensuing description of methods and results is entirely representative.

2. Methods

General procedures:

The methods for preparation of cytosol (100,000 xg supernatant) (158, 159), quantitative determination of protein concentration (298), preparation of ion exchange and molecular sieve materials and columns (299), as well as

details concerning spectrophotometric methodology are given in Appendix B. Protein concentration in column fractions was determined spectrophotometrically (either manually or by means of an Isco model 6 recording UV-meter) at 280 nm, while BSP was similarly determined at 580 nm after alkalinization of 0.2 ml aliquots of fractions with 0.5 ml 0.1M NaOH, and correction of absorbance values for dilution.

Purification of ligandin:

All purification steps were carried out at 4°C. All concentration steps were performed using an Amicon model 202 ultrafiltration cell with a UM-10 membrane (molecular weight retention > 10,000 daltons).

Cytosol obtained from 100g rat liver was concentrated to 50 ml, dialysed against 0.01M Tris:HCl buffer pH 8.8 (I = 0.004M) and applied to a 35 x 6 cm column of triethylaminoethyl (TEAE) cellulose equilibrated with Tris dialysis buffer, and eluted by gravity flow at a rate of 60 ml/h. Fractions of 8 ml were collected. The single protein peak eluting from this column was pooled, concentrated to 5 ml and dialysed against 0.01M sodium phosphate buffer pH 7.4/ 0.1M NaCl. After incubation with 100 µl (5 mg) BSP for 30 min, this fraction was applied to an 88 x 2.5 cm column of Sephadex G-100 equilibrated with phosphate-saline dialysis buffer, and eluted using pump-driven upward flow (35 ml/h), with collection of 3 ml fractions. Fractions exhibiting maximum BSP binding were pooled, concentrated to 5 ml, dialysed against 0.01M Tris:HCl buffer pH 8.8, and loaded

onto a 38 x 2.5 cm column of QAE-Sephadex A-50 equilibrated with the Tris dialysis buffer. The column was developed by gravity flow, kept constant by means of a Mariotte flask reservoir (see Appendix B), at a rate of 45 ml/h, with collection of 3 ml fractions. The single protein peak eluting from this column was pooled and stored in sterile plastic tubes at $4^{o}C$.

The purity of ligandin was assessed by polyacrylamide gel electrophoresis (PAGE) in sodium dodecyl sulphate (SDS), isoelectric focusing and enzyme activity. The full details of these procedures are given in Appendix B but will be outlined in principle below. Homogeneity and BSP binding were also assessed by Sephadex G-100 chromatography performed as described above.

PAGE in SDS:

The separation of native proteins by PAGE is dependent not only on the charge, but very strongly on the size of the molecules. When this technique is performed in an environment of SDS, an anionic detergent, individual protein charge patterns are in essence eliminated and proteins become uniformly negatively charged and are separated according to their molecular sizes by the gel matrix.

PAGE in 0.1% SDS was performed by two methods:

(1) The discontinuous gel/buffer system described by Maizel (300), comprising:

(a) a 3% stacking gel in 0.0625 Tris:phosphate buffer

pH 6.7,

(b) a 7.5, 10, 12.5 or 15% resolving gel in 0.375M Tris:HCl buffer pH 8.9, and

(c) a 0.005M Tris:glycine pH 8.6 electrode buffer.

The gels were prepared and electrophoresis carried out either in 65 x 5 mm glass tubes (Shandon Apparatus) or in a specially designed 25 x 10 x 0.15 cm slab system.

(2) The continuous gel/buffer system described by Weber and Osborn (301) employing 10% gels in 0.1M sodium phosphate buffer pH 7.2 in a Shandon Apparatus.

Samples were prepared for electrophoresis by dissociation in 1% SDS with or without 1% 2-mercaptoethanol, a sulphydryl reducing agent. Gels were stained with Coomassie brilliant blue and densitometry of stained protein bands was achieved with a Vitatron flat bed scanning densitometer.

Isoelectric focusing:

Isoelectric focusing separates proteins according to their isoelectric points, along a pH gradient produced by a series of low molecular weight ampholytes. Isoelectric focusing in 10% polyacrylamide gel was performed according to the method of Wrigley (302), either in an MRA Apparatus, or in a Shandon Apparatus at $4^{o}C$ in both pH 3.5 - 10 and pH 7 - 10 ampholine ranges. Gels were stained with Coomassie brilliant blue by the method of Malik and Berrie (303), or by the method described by Ketterer et al (281).

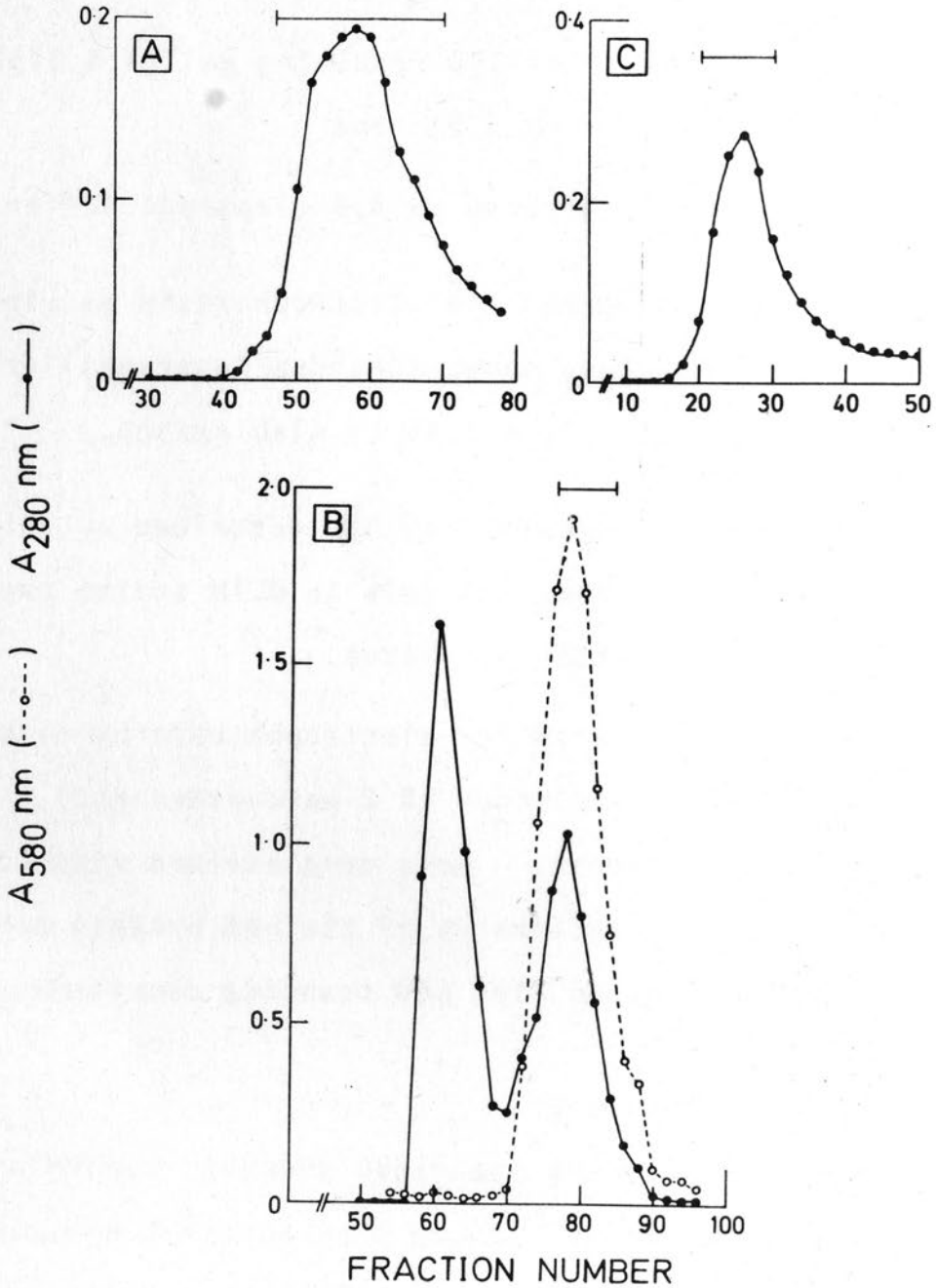

Fig. 2.1. Purification of ligandin from the 100,000 xg supernatant of rat liver. (A), Elution of protein from TEAE-cellulose in 0.01M Tris:HCl pH 8.8; (B), Elution of protein and BSP from Sephadex G-100 in 0.01M phosphate buffer pH 7.4/0.1M NaCl; (C), Purification of the BSP-binding peak on QAE-Sephadex in 0.01M Tris:HCl pH 8.8. Fractions pooled at each stage of purification are indicated by the horizontal bars. (See Methods and Results for details).

Enzyme assay :

GSH S-transferase activity was determined spectrophotometrically using 1-chloro-2,4-dinitrobenzene and 3,4-dichloronitrobenzene as substrates(155). A unit of activity is defined as the amount of enzyme catalysing the formation of 1 µmole of product per min under the conditions of the assay (see Appendix B). Specific activity is defined as the units of enzyme activity per mg of protein as measured by the method of Lowry et al (298).

Molecular size estimation:

Using appropriate protein standards, the molecular size of purified ligandin protomer was estimated by chromatography on a 40 x 2.5 cm column of Sephadex G-75 in 0.01M sodium phosphate buffer pH 7.4 / 0.1M NaCl (flow rate 40 ml/h), while the molecular size of ligandin subunits was determined by PAGE in SDS. R_f values were calculated as described in Appendix B. Straight line plots were obtained by the method of least squares (see Appendix C).

Y fraction analysis:

In order to compare purified ligandin with the proteins present in unpurified hepatic cytosol present in the Y peak of BSP-binding (see Fig. 1.5), 5 ml of hepatic cytosol mixed with 5 mg of BSP was separated by Sephadex G-100 chromatography under the same conditions described above for the purification of ligandin. 15 ml of the Y peak

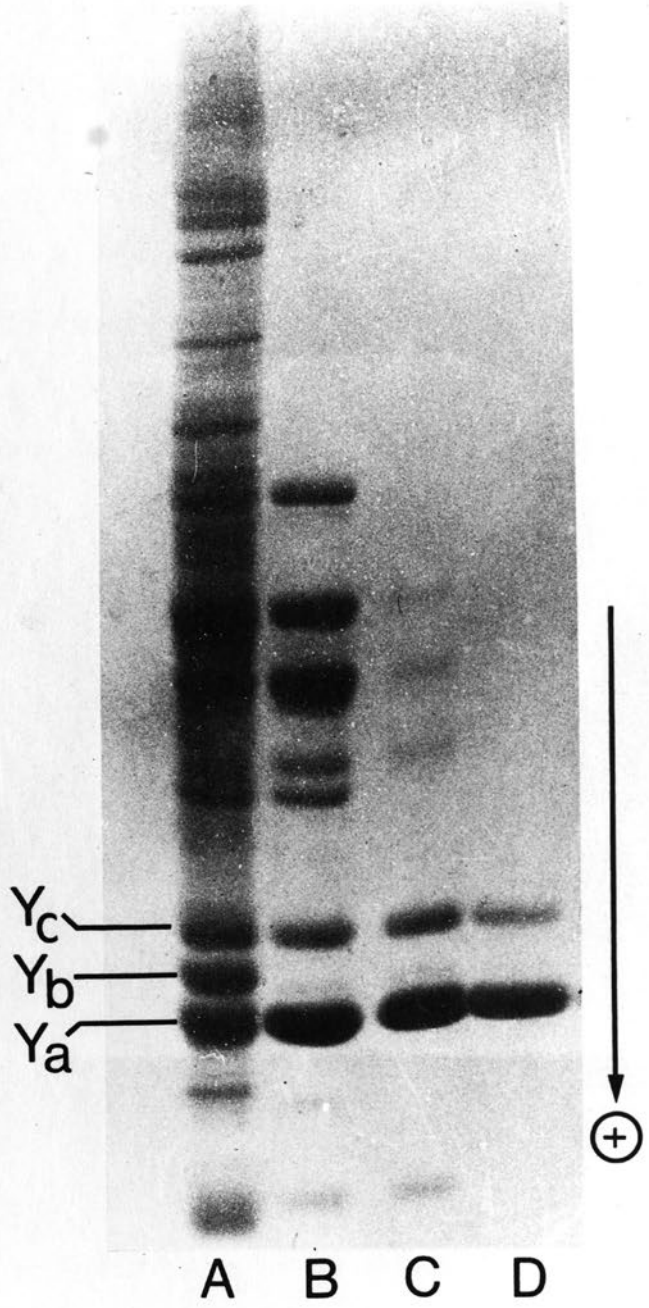

Fig. 2.2. Discontinuous slab PAGE in SDS (12.5% resolving gel) of (A), hepatic 100,000 xg supernatant; (B), pooled and concentrated protein peak from TEAE-cellulose; (C) pooled and concentrated BSP-binding peak from Sephadex G-100, and (D), pooled protein peak from QAE-Sephadex. Y_a, Y_b and Y_c represent the major subunit polypeptides found in the Y fraction of hepatic cytosol (see Fig. 2.3).

(fractions 70-74) were pooled, mixed, and a 5 ml aliquot concentrated 25 times in an Amicon B15 concentration cell and analysed by PAGE in SDS.

3. Results

The elution profiles from TEAE cellulose, Sephadex G-100 and QAE-Sephadex chromatography steps of ligandin purification are shown in Fig. 2.1. The patterns correspond generally to those obtained by Kirsch et al (159) for the purification of renal ligandin. After concentration of the single peak comprising basic cytosol proteins eluting from TEAE cellulose, and chromatography of these proteins on Sephadex G-100, two protein peaks eluted with BSP-binding almost entirely confined to the second peak, which eluted at 1.4 times the void volume. QAE-Sephadex chromatography of the proteins obtained from the second G-100 peak, yielded a total of 15 mg of protein, which showed the following properties:

(1) The protein eluted as a single, homogenous peak when chromatographed on Sephadex G-100 and further, showed symmetrical binding of BSP by this method.

(2) The specific activities of the protein with 1-chloro-2,4-dinitrobenzene and 3,4-dichloronitrobenzene as substrate, were in excellent agreement with those previously established for ligandin (Table 2.I).

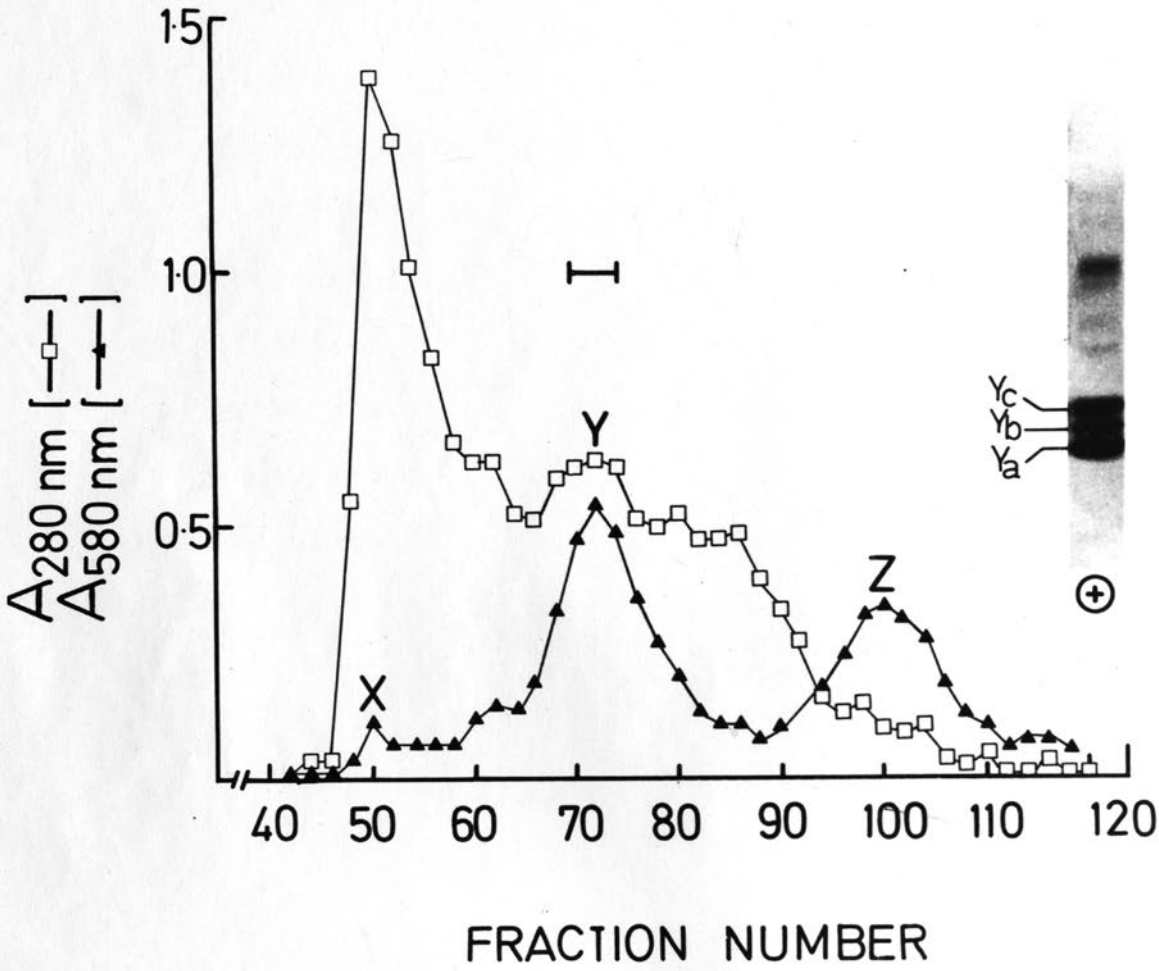

Fig. 2.3. Chromatography of hepatic cytosol (100,000 xg supernatant) and BSP on Sephadex G-100 in 0.01M phosphate buffer pH 7.4/0.1M NaCl, showing X, Y and Z BSP-binding fractions. The fractions indicated by the horizontal bars were pooled, concentrated and analysed by discontinuous slab PAGE in SDS (10% resolving gel, shown inset). Y_a, Y_b and Y_c represent the 3 major polypeptide subunits found in the Y fraction. (See Methods and Results for further details).

TABLE 2.I

GSH S-TRANSFERASE SPECIFIC ACTIVITIES OF LIGANDIN

Source of Data	Specific Activity (μmol/min/mg)	
	CDNB	DCNB
Present study	10	0.005
Habig et al (155,157)	11	0.003
Habig et al (15)	7.2*, 16.0	0.005*, 0.014
Hales and Niems (216)	11.82	0.005

CDNB: 1-chloro-2,4-dinitrobenzene; DCNB: 3,4-dichloro-nitrobenzene.
Values marked with an asterisk (*) were obtained with ligandin purified by the method used in the present study, while other values were obtained for ligandin isolated by a procedure used to separate several GSH S-transferases (see Discussion, this chapter). The difference in activities (*) was attributed to different methods used to store the purified protein.

Fractions from the various stages of purification of ligandin were analysed by discontinuous PAGE in SDS (Fig. 2.2). In Fig. 2.2, the designations Y_a, Y_b and Y_c refer to three major subunit species in unpurified cytosol in order of their relative mobilities on this system of analysis (Fig. 2.2A). This nomenclature was introduced, as these

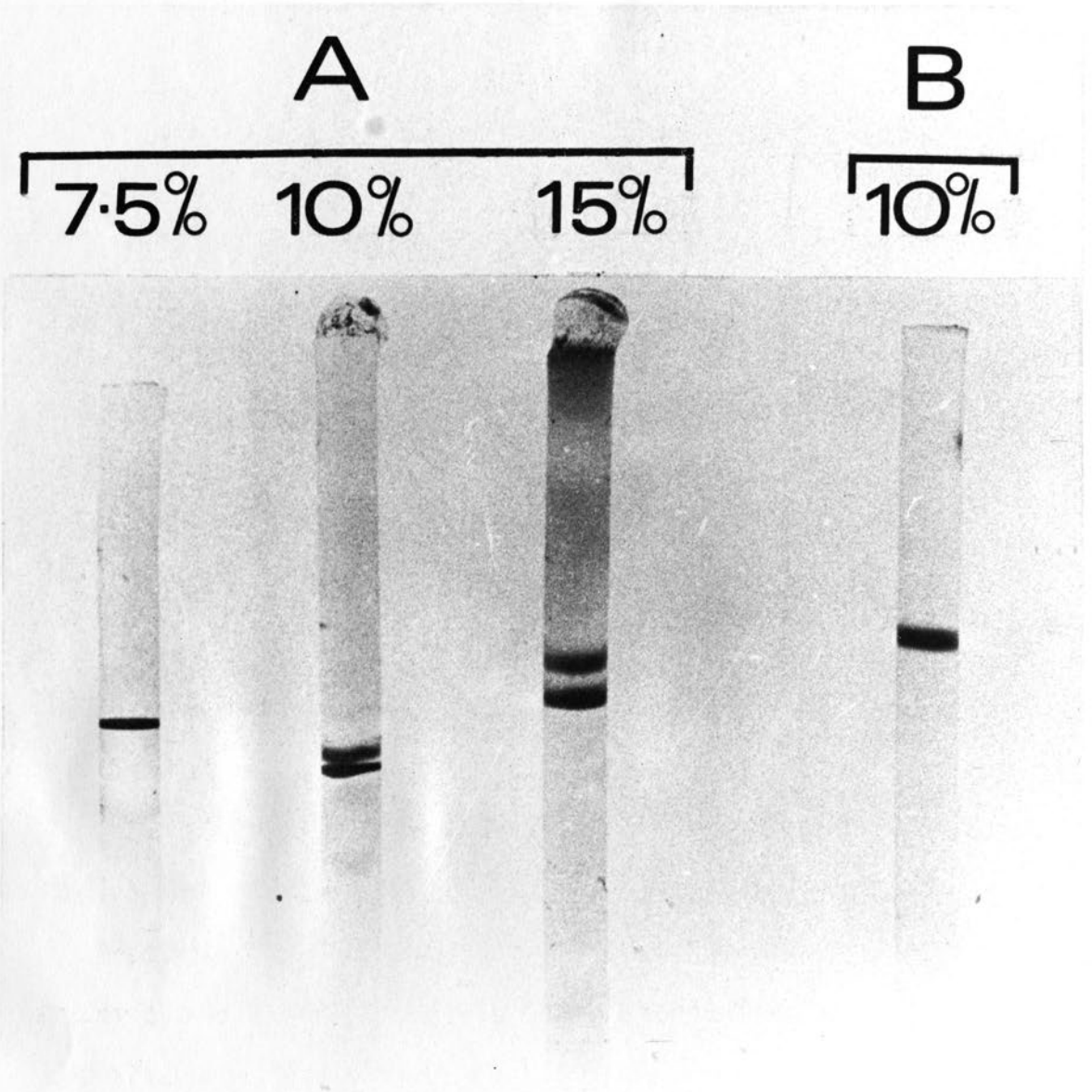

Fig. 2.4. Purified ligandin analysed by PAGE in SDS by the discontinuous system (7.5, 10 and 15% resolving gels) and the continuous system (10% gel in phosphate buffer). Approximately 10 µg of protein was loaded/gel. (Details of these procedures are given in Methods and Appendix B).

three peptide species were found to correspond to three major components present in the Y peak of BSP-binding of rat liver cytosol separated by Sephadex G-100 chromatography, when fractions from this peak were examined by discontinuous PAGE in SDS (Fig. 2.3). As illustrated in Fig. 2.2, the method of purification used resulted in a progressive enrichment of the Y_a and Y_c subunit species. The Y_b band was no longer detected after the first ion exchange step of the purification procedure (Fig. 2.2B) and thus probably represents a relatively acidic species in the "Y protein" fraction of hepatic cytosol.

The finding of two non-identical subunits in purified ligandin was intriguing, as previous reports had claimed identical sized subunits for this protein (1, 5, 131, 155, 159, 216). However, assessment of ligandin homogeneity in these studies had employed the continuous PAGE-SDS system (301), and indeed, when this method was used in the present study, it failed to reveal the dual subunit pattern evident from discontinuous PAGE in SDS analysis (Fig. 2.4). This system always gave a single protein band for ligandin, even when the amount of protein loaded was varied over a range of 1-20 µg/gel. If 2-mercaptoethanol was omitted from the ligandin sample preparation prior to PAGE in SDS, the Y_a and Y_c subunit bands migrated in identical fashion to the bands from samples which had been reduced by heating with 2-mercaptoethanol, suggesting a lack of disulphide bond linkage between these subunits.

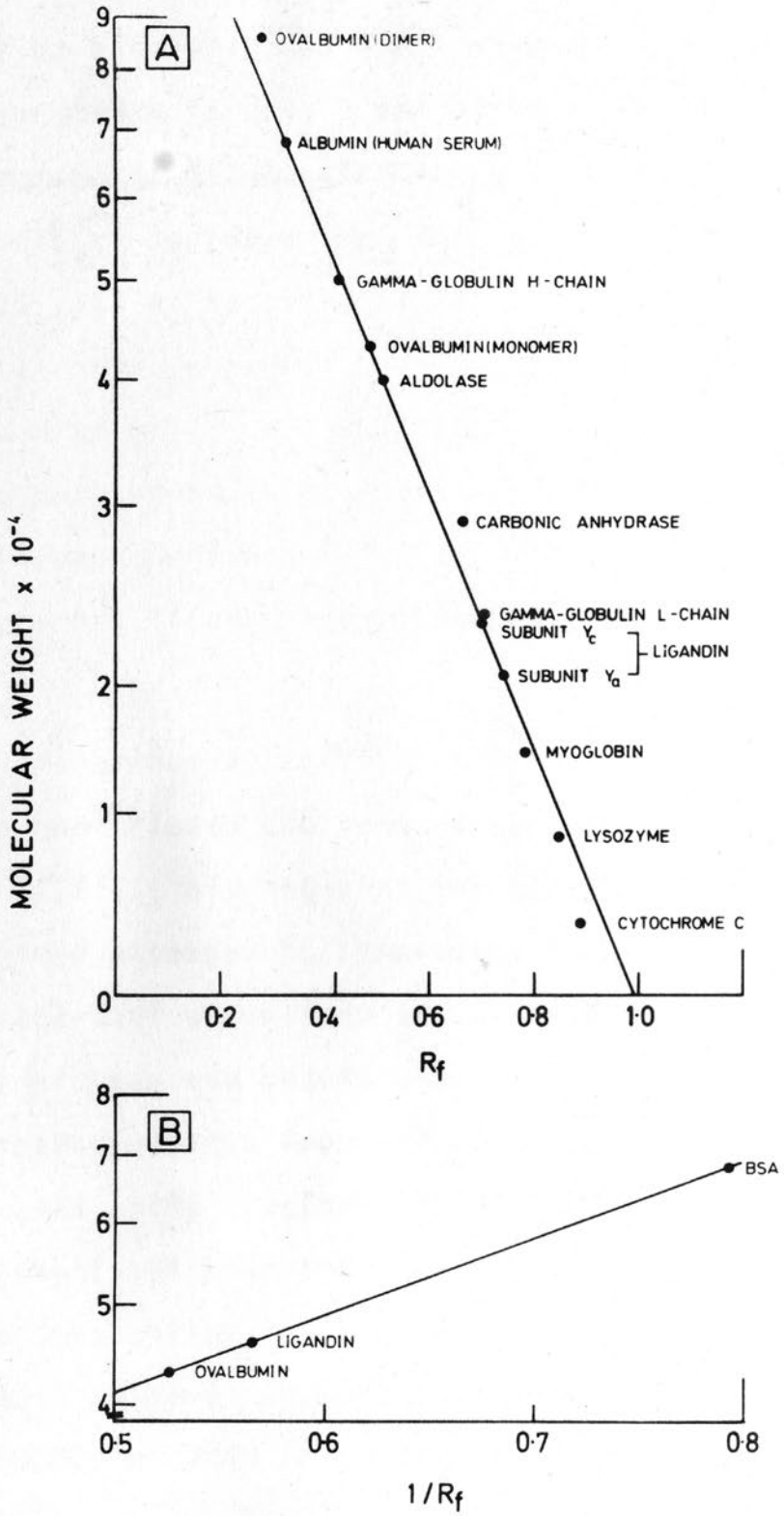

Fig. 2.5. Determination of comparative molecular weight of (A), ligandin Ya and Yc subunits by discontinuous PAGE in SDS, and (B), of ligandin protomer by Sephadex G-75 chromatography. (Details of these procedures as well as the assumed molecular weights of standard proteins are given in Appendix B).

Molecular size of ligandin:

The molecular size of the Y_a and Y_c subunits estimated by comparison with protein standards on discontinuous PAGE in SDS were ∿ 21,000 and ∿ 23,000 daltons respectively (Fig. 2.5A), while chromatography of purified ligandin on Sephadex G-75 resulted in a single symmetrical protein peak with a comparative molecular size of ∿ 46,000 daltons (Fig. 2.5B).

Isoelectric focusing:

Isoelectric focusing of purified ligandin in the pH 3.5-10 range resulted in a single protein band focusing in the 8-9.5 pH range (Fig. 2.6A). When this procedure was performed in the pH 7-10 range, two bands were consistently found (Fig. 2.6B). The approximate pI for each band was estimated (see Appendix B) as pH 8.7 and pH 9.1.

The non-artifactual nature of the hepatic Y peptides:

In order to exclude the possibility that the Y_a and Y_c ligandin subunits represented artifacts of proteolysis arising during cytosol preparation, the following studies were performed:

(1) Immediately after homogenization of rat liver performed at 4^oC in the presence of the trypsin inhibitor Trasylol, an aliquot of homogenate was subjected to PAGE in SDS analysis. The three major peptides Y_a, Y_b and Y_c (as seen in Fig. 2.2A) were found to be present.

(2) Aliquots of freshly prepared rat liver cytosol (pH 7.4)

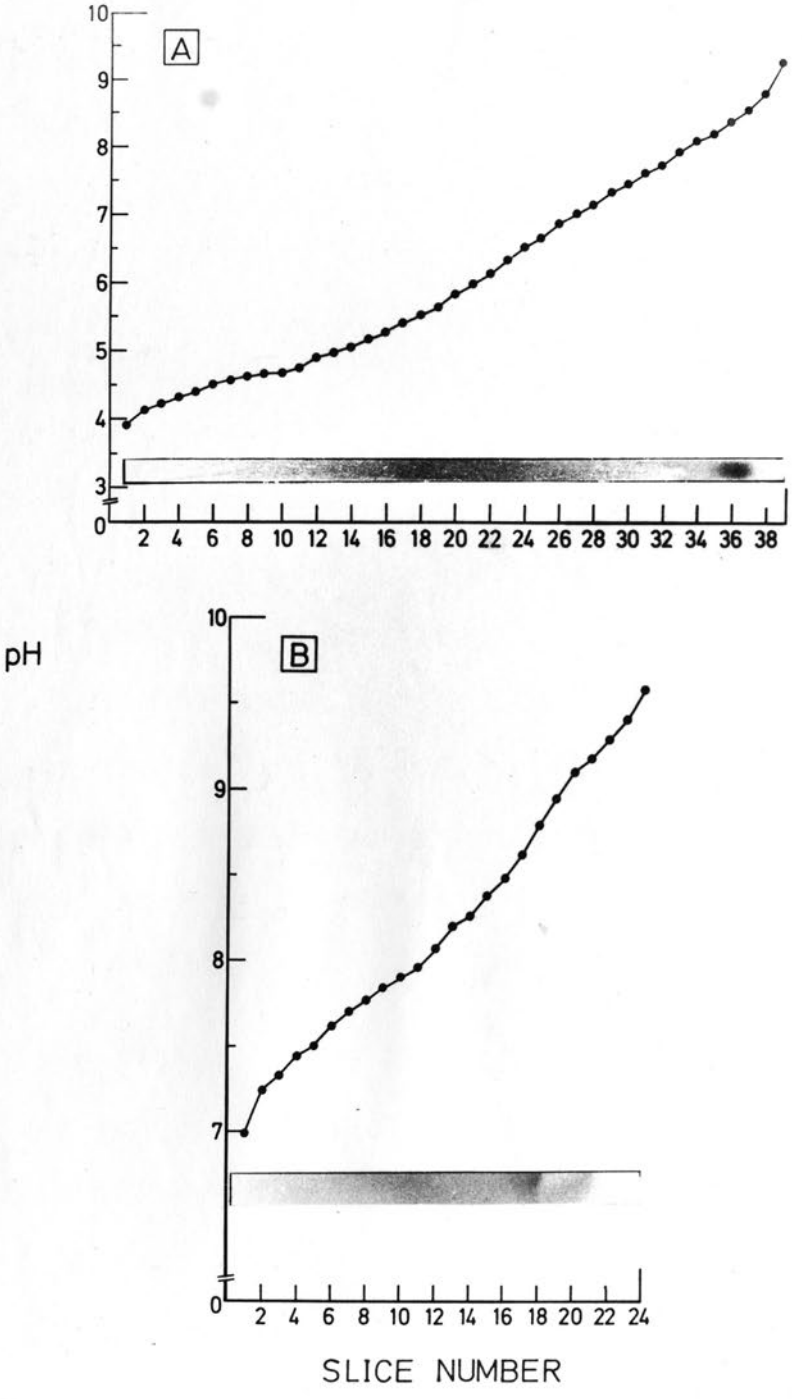

Fig. 2.6. Isoelectric focusing of ligandin in polyacrylamide gel. (A), Focusing in the pH 3.5-10 range, in an MRA apparatus, with staining of the gel according to Ketterer (281), and (B), focusing in the pH 7-10 range in a Shandon apparatus, with staining by the method of Malik and Berrie (303). (See Appendix B for details).

were incubated in sterile vials at 37°C for different intervals between 0 and 24h , and thereafter analysed by PAGE in SDS with densitometry of the protein bands. The result of this study is shown in Fig. 2.7. Incubation of cytosol up to 12h resulted in a gradual diminution of most of the cytosol proteins; by 24h the higher molecular weight proteins especially, were dramatically depleted. However, no increase in the Y_a band relative to the Y_c band was observed throughout this period, suggesting that the Y_a subunit does not obtain from proteolysis of Y_c.

These observations together, suggest that the Y_a and Y_c subunit species of ligandin exist in vivo. Furthermore, no time-dependent conversion of Y_a to Y_c subunit or decrease in either was observed on storage of purified ligandin for periods up to 6 months at 4°C.

4. Discussion

Of all the GSH S-transferases, ligandin (transferase B) is the most discriminatory between 1-chloro-2,4-dinitrobenzene and 3,4-dichloronitrobenzene as substrates (155, 216). Ligandin prepared in the present study exhibited a catalytic profile with these two substrates corresponding closely to those previously described for GSH S-transferase B (see Table 2.I). This is important, as it confirms the fact that the method used to purify ligandin in this study, essentially that described by Kirsch et al (159), yields the same product as that obtained by Habig et al (155) and

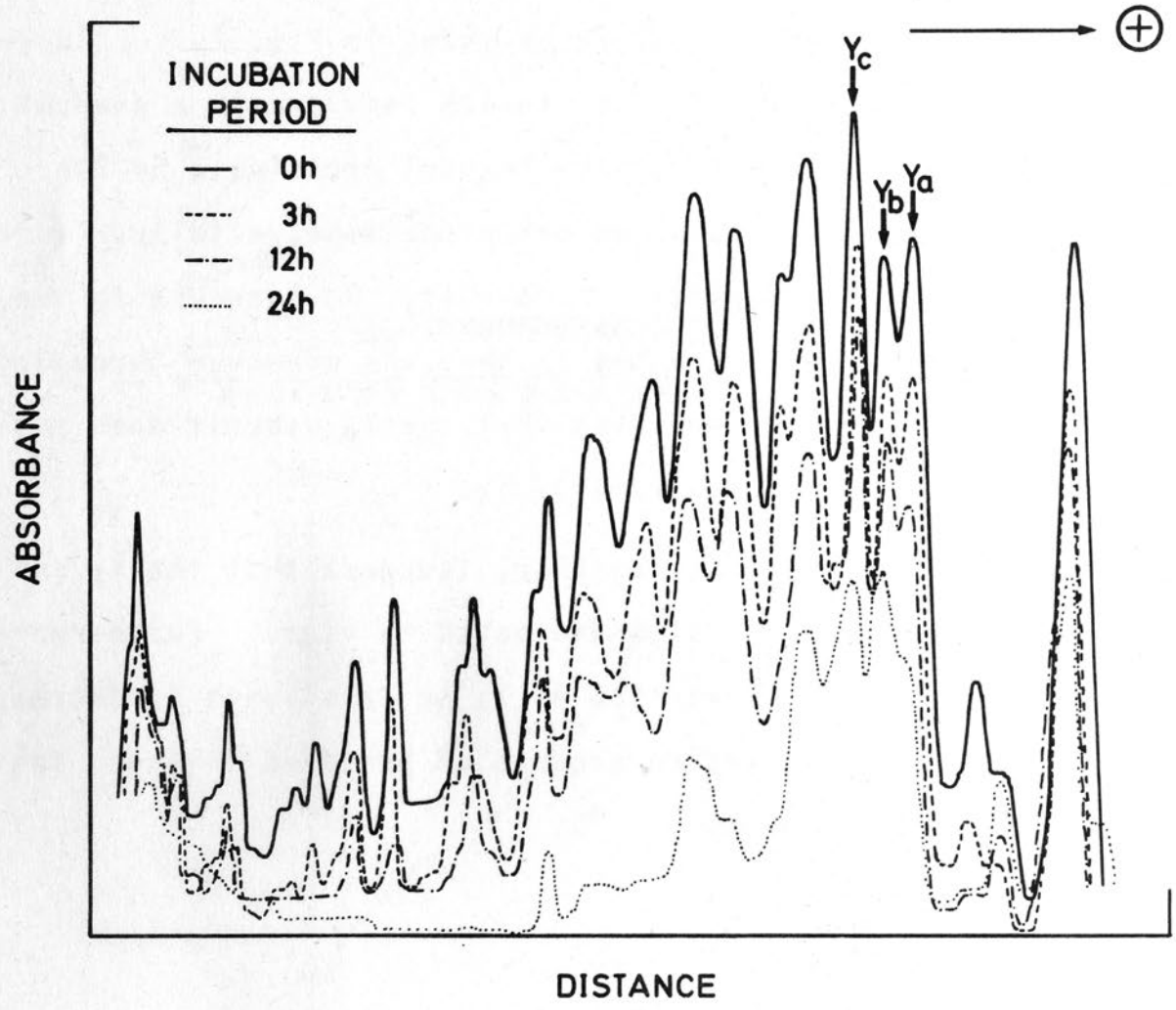

Fig. 2.7. Effect of incubation of hepatic cytosol at 37°C on the discontinuous PAGE-SDS polypeptide profile. After incubation of aliquots of hepatic cytosol at 37°C for the indicated periods, 10 µl of each aliquot was reduced in sample buffer (see Appendix B) and kept at 4°C until all incubations were completed. All samples were subjected to discontinuous PAGE in SDS on the same slab gel. Densitometry was performed using a Vitatron flat bed scanning densitometer on the gel stained with Coomassie blue. Ya, Yb and Yc indicate the peaks derived from the corresponding subunit bands in the gel.

Hales and Niems (216). In brief, the method used by these workers entails DEAE-cellulose chromatography of rat liver supernatant, followed by gradient elution from CM-cellulose, which largely separates the six basic GSH S-transferases (see Chapter II.5), and finally two hydroxylapatite chromatography steps.

Major differences in the resolving and separating properties between the discontinuous and continuous PAGE-SDS systems have been described (304), and although ligandin purified in this study gave a single protein band by continuous PAGE in SDS, thus fulfilling this widely used criterion of homogeneity, two unequal subunit bands were shown by the discontinuous system. It was thus edifying, that while this study was in progress, Listowsky et al (168) made light of the identical finding. Other workers in the field have subsequently also found that examination of ligandin by the discontinuous PAGE-SDS system reveals two non-identical subunits (Barghava, Ketterer, personal communications). It was also interesting to note that besides rat ligandin (GSH S-transferase B), human ligandin and rat GSH S-transferase A (prepared by Jakoby's group, see ref. 168) also displayed two non-identical subunits when reassessed by discontinuous PAGE in SDS.

A terminology was introduced in this study for the two non-identical ligandin subunits, based on the finding that they represented the highest and the lowest molecular weight components (Y_a and Y_c) of three major peptide species existent in the Y BSP-binding fraction of rat liver cytosol.

The nature of the Y_b subunit, which is intermediate in size of the three peptides, remains obscure, but it is clearly not a component of purified ligandin. The two non-identical subunits of ligandin found in this study and confirmed by others, could be viewed in two ways:

(1) On the basis of a single primary structure. This would suggest that the Y_a and Y_c subunit species share the same primary structure but that differences in electrophoretic mobility represent different disposition of intramolecular disulphide bridges. As both Y_a and Y_c subunits were observed in this study even after extensive reduction with 2-mercaptoethanol, while others have observed both subunits on PAGE in SDS after ligandin has been carboxymethylated and succinylated (Bhargava, personal communication), this does not seem a likely possibility.

(2) On the basis of two polypeptides of distinct primary structure. In accord with this consideration, is the possibility that the Y_a component might reflect proteolytic or chemical degradation of the Y_c subunit, consisting in other words, of the latter minus a $\sim$ 2,000 dalton length of its peptide sequence. Hayashi and Natori (305) have shown that proteases exist in the cytosol fraction of rat liver, which degrade the higher molecular weight cytosol proteins more rapidly than smaller ones at neutral pH. These findings were confirmed in the present study, while in addition, no time dependent conversion of the Y_c subunit to the Y_a subunit in cytosol could be demonstrated; nor was

such a conversion evident in purified ligandin preparations. These findings suggest that the Y_a and Y_c subunits occur as such in vivo. However, they do not rule out the possibility that Y_a subunit obtains from the Y_c subunit via a controlled proteolytic mechanism dependent upon cellular integrity. In the event of this not being the case, then it must be concluded that the non-identical ligandin subunits arise as separate gene products. Whatever the mechanism underlying the genesis of the non-identical ligandin subunits, their existence as two polypeptides of distinct primary structure would imply one of two things: either ligandin is composed of two non-identical subunits in vivo (Y_a-Y_c structure) or alternatively, the non-identical subunits represent the monomers of two distinct, although closely related proteins (Y_a-Y_a; Y_c-Y_c structure). These possibilities are further resolved in the chapters of Section B.

Analytical isoelectric focusing of ligandin in the pH 3.5-10 range gave a single band, while in the pH 7-10 range, two bands in equal proportion were obtained. These findings are identical to those described by several workers (155,159, 165, 216) and are similar to those reported by Listowsky et al (168), although these workers have observed several other minor components as well. If it were assumed that ligandin comprises two dimeric proteins Y_a-Y_a and Y_c-Y_c, then the two charge species thus defined by isoelectric focusing in the basic pH range, might represent these two proteins separately, although charge heterogeneity in a Y_a-Y_c combination might conceivably result in a similar pattern. It is

interesting, that two charge components have been found to characterize ligandin on starch gel electrophoresis (14) and also during purification of this protein from rat hepatic cytosol on CM-cellulose (163) and hydroxylapatite (155). CM-cellulose chromatography of mouse liver cytosol also reveals two "ligandin" peaks (basic proteins II and II, see Chapter III.6.ii). However none of these dual forms have been characterized as yet in terms of size heterogeneity.

CHAPTER VIII

ANTISERUM PRODUCTION

1. Introduction

Possibly the single most important factor in establishing an RIA is the production of a suitable antiserum. It has often been said that this is subject to the dictates of chance and good fortune, although a number of factors may influence the likelihood of success. One of the major factors determining the ease of production of antiserum is the immunogenicity of the antigen; i.e. its ability to invoke an immune response. The immunogenicity of a substance depends both on its size and chemical composition; and by the standards of RIA, most proteins with molecular weights in excess of 5,000 are usually good immunogens (306). Ligandin, which has a molecular weight of 46,000, appears to conform to this general rule, as judged by the number of studies in which antiserum has been successfully raised to this protein (1, 155, 158, 159, 209-212, 216). These studies however, examined the antiserum mainly by immunodiffusion. This method, while providing a suitable means of assessing the precipitin reaction and thus the valency and gross specificity of the interaction between antigen and its generated antibody, does not allow the quantitative assessment of the affinity of the antiserum nor the titre at which it should be employed in an RIA. These data are obtainable only from experiments employing antibody and labelled antigen with an incubation system identical to that intended for use in the final assay. These aspects of

antiserum characterization are covered in Chapter X. The present chapter confines itself to a description of the methods used to raise antiserum to ligandin and the testing of this reagent using the conventional methodology of visible immunoprecipitation in agar gel. The outcome of these experiments also provided a further means of assessing the purity of ligandin prepared as described in the previous chapter.

2. Methods

Immunization protocol:

Three month old male albino rabbits were immunized with either purified ligandin or hepatic cytosol proteins according to the following schedule:

(1) 50 µg of protein in 1 ml 0.01M sodium phosphate buffer pH 7.4 /0.15M NaCl was emulsified with 1.5 ml complete Freund's Adjuvant by expulsion via a 21 gauge syringe needle.

(2) The emulsion was injected bilaterally into the popliteal lymph nodes of rabbits anaesthetized with phenobarbital.

(3) Following the first inoculation, 50 µg of protein in adjuvant was injected into multiple subcutaneous sites at 3 week intervals.

(4) Animals were bled at 10 day intervals following each booster inoculation.

Processing of antisera:

Blood obtained from immunized rabbits was allowed to clot at room temperature for 1h and after further storage at 4°C for 24h, serum was separated by centrifugation at 4,000 xg for 30 min at 4°C in a Sorvall RC2-B centrifuge (158, 159). The separated sera were stored at 4°C with 0.1% sodium azide added as a preservative.

Testing of antisera:

Specific antibody production was assessed in harvested antisera by immunodiffusion (307) and immunoelectrophoresis (308) in agar gel against purified ligandin and rat liver cytosol. Immune precipitates were stained with amido-black (375). Details of these procedures are given in Appendix B. Non-immune rabbit sera (NIRS) were used as antiserum controls, while 0.9% saline and rat serum (see Chapter XV) served as antigen controls. Similar analyses were performed using goat anti-ligandin IgG (GAL-IgG) prepared against ligandin at the Albert Einstein College of Medicine Liver Research Centre in New York, and which was provided as a generous gift by Drs. G. Fleischner and I.M. Arias. Lyophilized GAL-IgG was dissolved in 0.01M sodium phosphate buffer pH 7.4 / 0.15M NaCl to a final concentration of 1 mg/ml prior to use.

Cross-absorption studies between rabbit anti-ligandin antiserum prepared in the present study and GAL-IgG, were performed as follows:

50 µl of rat liver cytosol was incubated at 4°C for 48h

with 400 µl of one of the following:

(1) Antiserum obtained from rabbits immunized with ligandin.

(2) NIRS.

(3) GAL-IgG.

(4) 0.9% Saline.

Thereafter, tubes were spun at 18,000 xg for 30 min (Sorvall HC-2B centrifuge) and the supernatants tested by immunodiffusion against (1) and (3).

Quantitative immunodiffusion:

Quantitative radial immunodiffusion (309, see Appendix B) was performed using rabbit anti-ligandin antiserum in order to assess the quantitative potency of the antiserum in an established system previously used to measure ligandin (158, 159) and to allow comparison between quantitative data derived by this method and that later obtained by RIA (see Chapter XI).

3. Results

Two rabbits were immunized with purified ligandin and both produced antisera evident from immunodiffusion studies. The following description of results however, is confined to the antiserum which was obtained after a second booster injection from one of these animals (antiserum no. 982/28/10) and which was subsequently used in the RIA (see Chapter X). Rabbit antiserum to ligandin generated a single precipitin

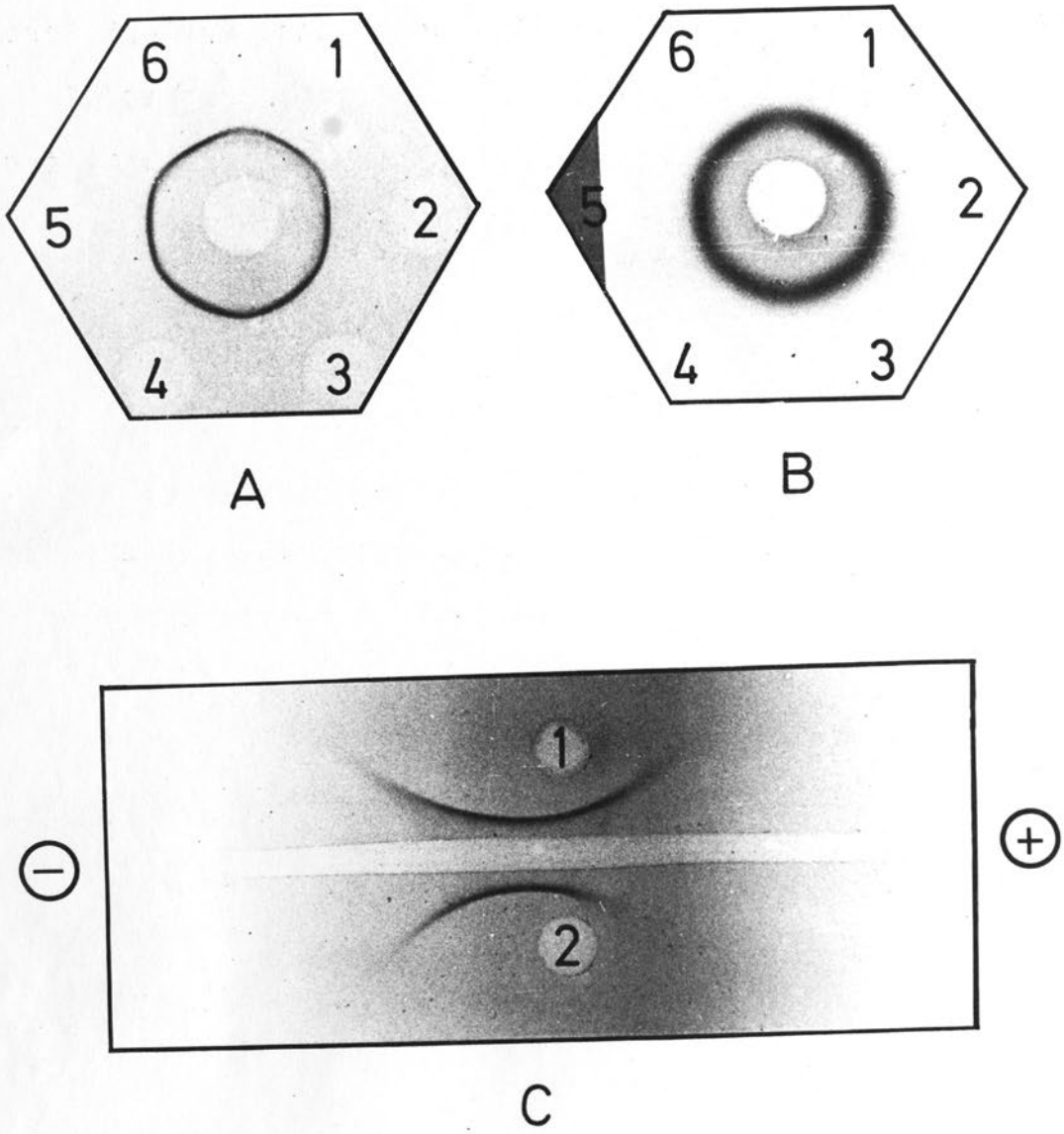

Fig. 2.8. Immunodiffusion and Immunoelectrophoresis in agar gel. (A and B): The centre wells contain: (A), rabbit anti-ligandin antiserum, and (B), GAL-IgG. Peripheral wells (A and B) contain: 1, 3 and 5, hepatic cytosol (1:4); 2,4 and 6, ligandin (1 µg). (C), Immunoelectrophoresis in agar gel. The trough contains rabbit anti-ligandin antiserum; the wells contain: 1, hepatic cytosol (1:4); and 2, ligandin (1 µg). Precipitates were stained with amidoblack. (Details of these procedures are given in Appendix B).

line on immunodiffusion (Fig. 2.8A) and immunoelectrophoresis (Fig. 2.8C) against purified ligandin and hepatic cytosol. Identical results were obtained in similar experiments using GAL-IgG (immunodiffusion shown in Fig. 2.8B), although a qualitatively different precipitin line was observed with this antibody. No precipitin lines were observed when immunodiffusion was performed with either NIRS in the centre well or when saline or rat serum replaced ligandin and hepatic cytosol in the peripheral antigen wells. In addition, purified ligandin gave a single precipitin line with multivalent rabbit antiserum prepared against rat hepatic cytosol proteins.

Neither rabbit antiserum to ligandin nor GAL-IgG produced a precipitin reaction with hepatic cytosol preadsorbed with either of these two antibody sources, but both formed precipitin lines with control cytosol incubated with either NIRS or saline (see Methods). The threshold of detection of the immunodiffusion system using antiserum 982/28/10 was $\sim$ 20 µg/ml of purified ligandin.

Table 2.II shows the results of quantitative immunodiffusion using rabbit anti-ligandin antiserum with hepatic and renal cytosol, as well as quantitative data reported by other workers for these tissues.

TABLE 2.II

LIGANDIN CONCENTRATION IN CYTOSOL OF RAT LIVER AND KIDNEY

Source of Data	Ligandin concentration (µg/mg)	
	Liver	Kidney
Present study	36.5 ± 2.3 (5)	15.2 ± 0.44 (5)
Fleischner et al (158,218)	44.7 ± 2.1 (10)	22.4 ± 2.7 (8)
Kirsch et al (159)	39.5 ± 2.3 (?)	31.2 ± 2.2 (?)
Hales and Niems (216)*	33 ± 2 (4)	nd

Data are for male rats only and are given as mean ± SEM in µg/mg supernatant protein. The number of rats used for each determination is given (where available) in parenthesis. Values were derived by quantitative immunodiffusion in all the studies except that marked with an asterisk (*), in which values were obtained by immunoprecipitation of 1-chloro-2,4-dinitrobenzene catalytic activity.

nd : not determined

4. Discussion

The monospecific nature of rabbit anti-ligandin antiserum raised in the present study, was evidenced by the fact that it gave single precipitin lines on immunodiffusion and immunoelectrophoresis with purified ligandin and hepatic cytosol. These observations as well as the finding of a single precipitin line with multivalent rabbit anti-rat hepatic cytosol and purified ligandin, also served as important confirmations of the homo-

geneity of ligandin prepared in this study. Furthermore, the cross-reaction of this protein with GAL-IgG served to establish its identity with ligandin prepared in the laboratory of Arias. Rabbit anti-ligandin antiserum and GAL-IgG further revealed complete congruency with respect to antigen recognition in hepatic cytosol by cross-adsorption analysis.

Quantitative immunodiffusion performed using rabbit anti-ligandin antiserum gave results for hepatic ligandin concentration in good agreement with those found by other workers (see Table 2.II). Renal ligandin concentration was found to be approximately half of that found in the liver, in accord with the findings of Fleischner et al (158, 218). Kirsch et al (159) however, have reported an absolute mean value for renal ligandin double that found in the present study. The fact that these workers used Sprague-Dawley rats while Wistar rats were used in the present study, may be invoked as an explanation of this discrepancy on the basis of strain variation. However, this would not account for the 40% higher values obtained by Kirsch et al (159) over those reported for renal ligandin by Fleischner et al (158) using the same strain of rats. Thus for the present, the reason for these absolute differences remains unknown.

CHAPTER IX

IODINATION

1. Introduction

Radioisotopes of iodine have become established tools in the creation of high specific activity (i.e. a high proportion of dpm per unit mass) labelled tracers for use in RIA procedures (287, 310, 311). Of these, the isotope ^{125}I has proven most popular. ^{125}I is a γ-ray emitter, which is counted with high efficiency, while its half-life of 60 days is of further advantage for compounds retaining their stability for periods in excess of a week. Several methods for iodinating protein and peptides have been described (311). One of the most widely used and probably the easiest to perform is the chloramine-T method (312), which results in the incorporation of iodine into the tyrosyl residues of the protein. This procedure almost universally results in a certain percentage of protein being damaged due to over-iodination or the effects of iodination reagents, leading to conformational changes which may adversely affect the affinity of the antigen-antibody interaction. This chapter describes the chloramine-T iodination of ligandin with ^{125}I and the subsequent purification of the labelled protein.

2. Methods

Counting of radioactivity:

All counting was performed in 12 x 75 mm plastic tubes as described in Chapter X.

Iodination:

A modification of the method of Greenwood et al (312) was used to prepare high specific activity ^{125}I-ligandin. Reactants were mixed in a small glass test tube using E-mil constriction pipettes at room temperature in the following order:-

Carrier free ^{125}I, 1 mCi:	10 µl
0.5M sodium phosphate buffer pH 7.4:	25 µl

The following reactants were then added (in the same phosphate buffer diluted 1:10) with mixing:-

Ligandin, 15 µg:	25 µl
Chloramine-T, 10 or 25 µg:	25 µl

To establish an optimum time for the iodination, the reaction was allowed to proceed for periods ranging from 1 to 30s. Thereafter the reaction was terminated by the addition of:-

Sodium metabisulphite, 50 µg:	100 µl
Potassium iodide, 2 mg:	200 µl
Total volume	385 µl

Purification of the reaction mixture:

Several procedures were examined in attempts to find a suitable means of isolating intact ^{125}I-ligandin from damaged protein, free ^{125}I and other components of the reaction mixture:-

(1) Adsorption chromatography: The reaction mixture was applied to a 2 x 0.4 cm column of Whatman CF II cellulose equilibrated with 0.01M sodium phosphate buffer, pH 7.4 /

0.15M NaCl. The column was washed 4 times with 1 ml of the phosphate-saline buffer, followed by 3 washes with 1 ml volumes of 2-15% bovine serum albumin (BSA) solution. Each wash effluent was collected separately.

(2) Gel filtration: The reaction mixture was loaded onto a 28 x 0.6 cm column of Sephadex G-100, prerun with 1 ml 5% BSA and eluted with phosphate-saline buffer at a flow rate of 6 ml/h with collection of 0.2 ml fractions.

(3) Ion exchange chromatography: The reaction mixture was applied to a 1 x 0.4 cm column of TEAE-cellulose, equilibrated and eluted with 0.03M Tris:HCl buffer, pH 8.8 (I = 0.01M). The flow rate was 30 ml/h and 0.25 ml fractions were collected.

(4) Combined gel filtration/ion exchange chromatography: The entire reaction mixture was mixed with 0.5 ml 0.1% BSA on 0.03M Tris:HCl buffer pH 8.8, and loaded onto a column comprising the following: a 30 x 0.7 glass Biorad disposable glass column packed to a height of 4 cm with TEAE-cellulose and packed to an additional height of 25 cm above the cellulose with Sephadex G-25 in the same buffer. The reaction mixture was eluted with the Tris buffer at a flow rate of 18-20 ml/h. Fractions of 0.6 ml were collected.

Assessment of iodination:

The iodination procedure was assessed for:

(a) Incorporation of ^{125}I into ligandin,

(b) Nature and extent of iodination damage,

(c) Efficacy of the procedures used to purify the label and

(d) Stability of ^{125}I-labelled ligandin by the following methods:

(1) Trichloroacetic acid (TCA) precipitation: 5 µl of reaction mixture or 20 µl of purification column fractions (see above) were added to 1 ml 0.05M sodium phosphate buffer pH 7.4 / 0.1% BSA, followed by addition of 1 ml 10% TCA with mixing. The mixture was incubated at 4°C for 30 min and then centrifuged (MSE centrifuge) for 30 min at 2,000 xg. Thereafter, radioactivity in the precipitate as well as in 0.5 ml of the supernatant was separately counted. The results of this procedure were expressed as the percentage of the total counts present in the precipitate.

(2) Chromatoelectrophoresis (313): Details of this procedure are given in Appendix B. Bromophenol blue was used as a marker for damaged products of iodination. The validity of this method for the assessment of ^{125}I-ligandin purification was explored as follows: 2.5 µg (200 µl) of ligandin was iodinated by the iodine monochloride method (314, see Appendix B) with 1 mCi ^{125}I yielding an incorporation of ^{125}I into ligandin of 13.6% (specific activity ∿ 0.05 µCi/µg protein). After dialysis, the resultant labelled protein was 99.9% precipitable with TCA. A 0.5 ml aliquot of the labelled ligandin was incubated with 0.5 ml trypsin (0.4 mg in

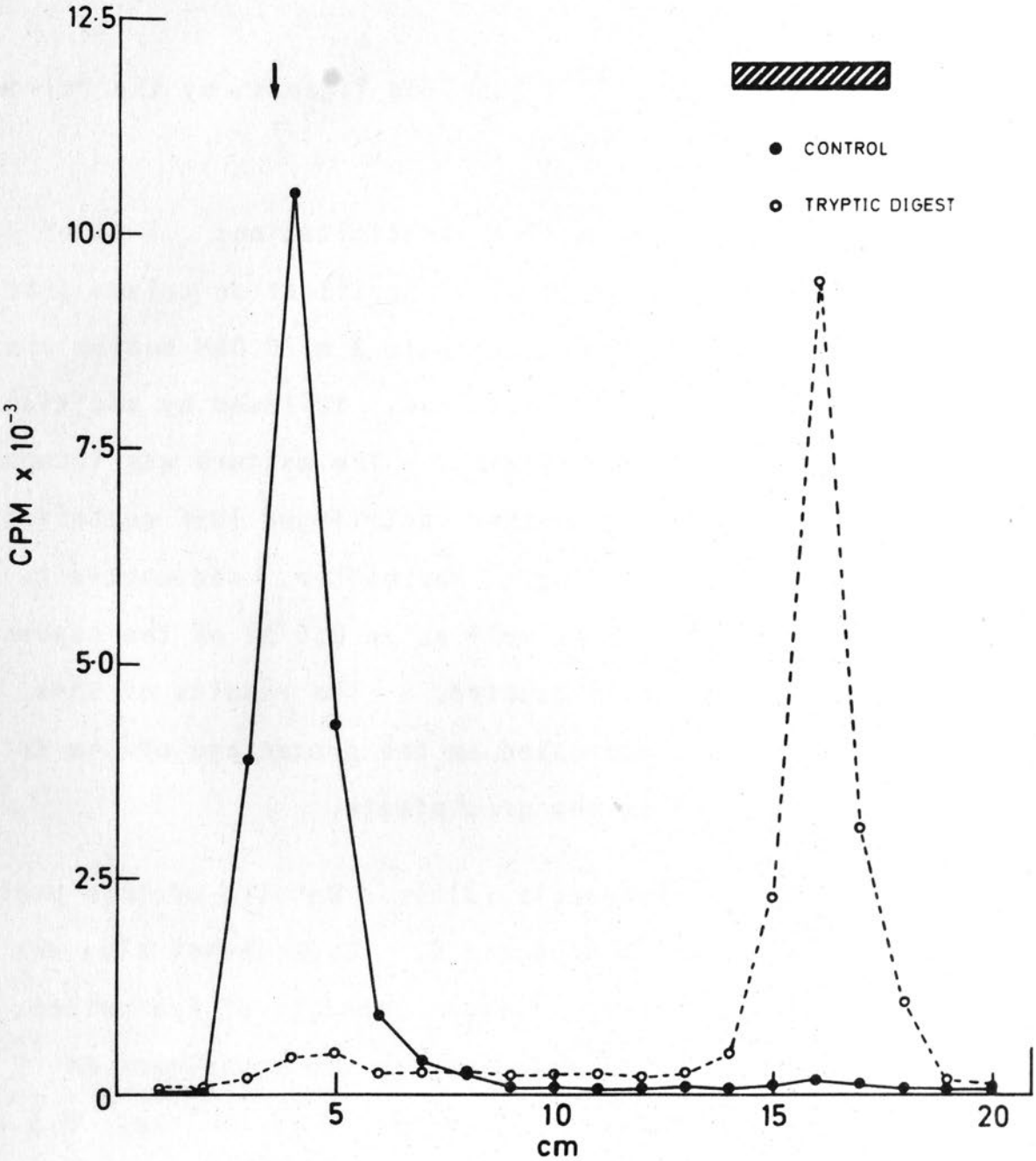

Fig. 2.9. Chromatoelectrophoretic profile of ^{125}I-ligandin, showing the effect of tryptic digestion on the migration of radioactivity. Ligandin labelled by the iodine monochloride method remained close to the origin (indicated by the arrow) whereas after tryptic digestion, most of the label migrated with the bromophenol blue front (shaded bar). Free ^{125}I migrated 1 cm ahead of the front (not shown). (Details of procedures are given in Methods and Appendix B).

0.5M sodium phosphate buffer pH 7.4) for 1h at room temperature. Another 0.5 ml aliquot of labelled ligandin was incubated with the phosphate buffer in the absence of trypsin at $4^{o}C$. Aliquots from both control and trypsin incubated ^{125}I-labelled ligandin were then assessed by chromatoelectrophoresis.

(3) PAGE in SDS with autoradiography: Samples of reaction mixture and peak fractions obtained from column purification of ^{125}I-ligandin were subjected to discontinuous slab PAGE-SDS analysis without reduction. Protein bands were detected by autoradiography using Kodak PE-4006 film (see Appendix B for details).

Storage of labelled ligandin:

^{125}I-ligandin was stored diluted in 0.05M sodium phosphate buffer pH 7.4 / 0.15M NaCl / 0.01M EDTA / 0.5% BSA / 0.1% sodium azide (assay diluent buffer - see Chapter X) at $4^{o}C$.

3. Results

Validation of chromatoelectrophoresis:

As shown in Fig. 2.9, ^{125}I-ligandin prepared by the iodine monochloride method, remained at the origin ("intact") on chromatoelectrophoresis, while tryptic digestion of the label resulted in radioactivity migrating with the bromphenol blue front ("damaged"). Free ^{125}I migrated ahead of the front.

Optimum iodination conditions:

The results of iodination of ligandin at different concentrations of chloramin-T with different periods of exposure, are shown in Table 2.III.

TABLE 2.III

EFFECT OF CHLORAMINE-T CONCENTRATION AND TIME ON IODINATION OF LIGANDIN

Chloramine-T(µg)	Time(s)	TCA%	Chromatoelectrophoresis(%)		
			Intact	Damaged	Free
10	1	0	0	0	0
10	10	1.6	2	1.5	96.5
25	15	13	11.6	6.4	82
25	30	43	31.4	14.4	54.2

The incorporation of ^{125}I into ligandin is represented by the percentage of total counts precipitated by TCA (TCA%) and alternatively, by the sum of the percentage intact and damaged chromatoelectrophoresis fractions.

Except where stated to the contrary, conditions yielding between 40-50% incorporation of ^{125}I into ligandin i.e. 25 µg chloramine-T with 30s exposure, were selected for all subsequent iodinations.

Purification of ^{125}I-ligandin:

Both Whatman cellulose and Sephadex G-100 chromatography proved unsuitable as means for obtaining purified ^{125}I-ligandin. In the former case, the intact label could not be desorbed from the cellulose by protein solutions of up to 15% strength. In the latter case, radioactivity eluted in an irregular pattern showing up to 11 discernable peaks, none of which contained more than 70% intact label. The results of TEAE-cellulose purification were far more promising. The first 10 fractions eluting from this column contained approximately equal amounts of radioactivity. Analysis of the reaction mixture and the initial TEAE column fractions is shown in Table 2.IV.

TABLE 2.IV

PURIFICATION OF IODINATION REACTION MIXTURE BY TEAE-CELLULOSE

Fraction	TCA %	Chromatoelectrophoresis(%)		
		Intact	Damaged	Free
Reaction mixture*	11.4	11	8	81
1	88	85	12	3
2	49	45	42	13
3	5	1	9	90

* 25 µg chloramine-T, 15s exposure time. Fractions following no. 3 contained mainly free ^{125}I.

The data in Table 2.IV reflects the pronounced ability of

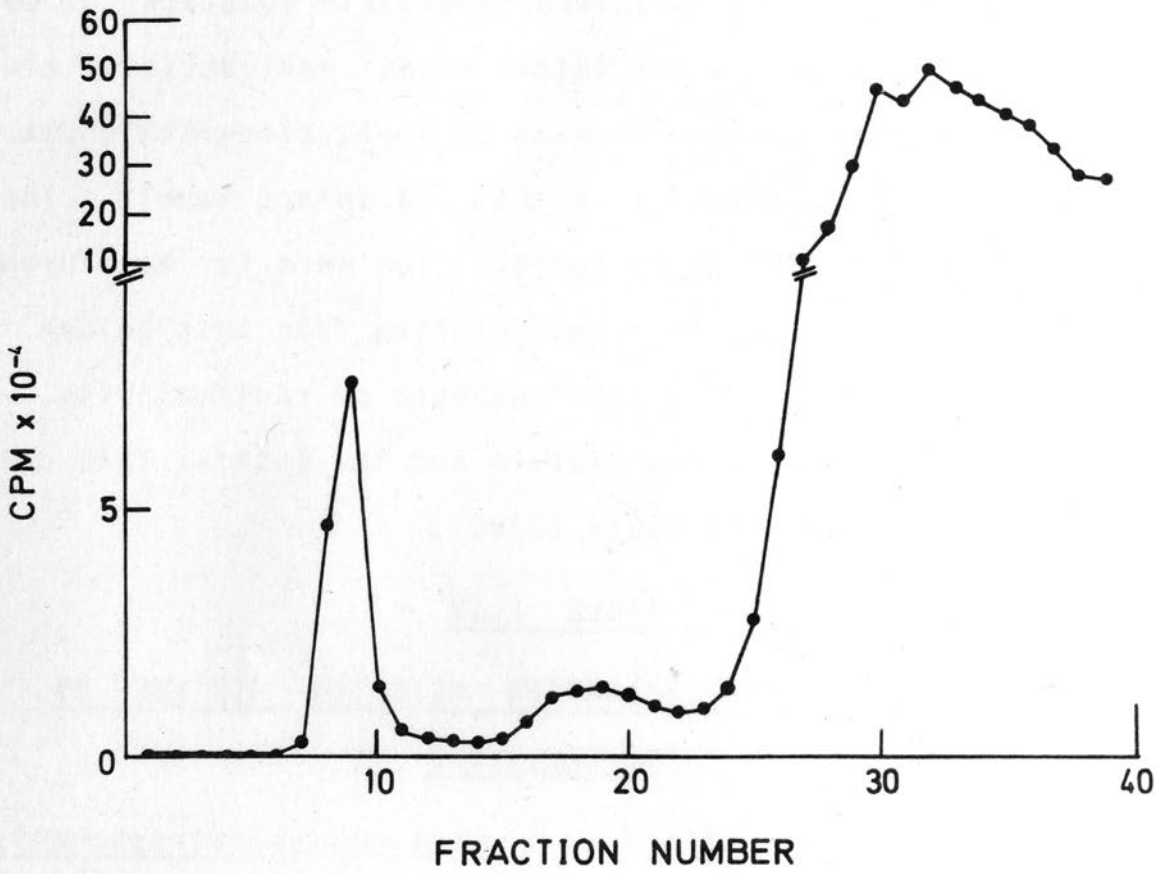

Fig. 2.10. Purification of ^{125}I-ligandin by Sephadex G-25/ TEAE-cellulose chromatography. After mixing with 0.5 ml 0.1% BSA in column buffer (0.03 Tris:HCl pH 8.8), the reaction mixture was loaded onto the purification column (see Methods for details). Fractions of 0.6 ml were collected, and after dilution with 1 ml of assay diluent, 5 µl aliquots were counted in an autogamma spectrometer.

TEAE-cellulose to resolve intact labelled ligandin from damaged components and free ^{125}I. In order to enhance the separation of low molecular weight reactants and peptides from intact ^{125}I-ligandin, prior to final TEAE-cellulose purification, a combined, sequential Sephadex-TEAE column was devised (see Methods). A typical purification of the iodination reaction mixture by this method is illustrated in Fig. 2.10. Three peaks of radioactivity eluted. Assessment of aliquots from each peak by TCA precipitation and chromatoelectrophoresis (Table 2.V) revealed the first peak to contain the purified label, the second peak to consist of mainly damaged protein, while the third peak represented free ^{125}I.

TABLE 2.V

PURIFICATION OF IODINATION REACTION MIXTURE BY SEPHADEX-TEAE CHROMATOGRAPHY (see Fig. 2.10)

Fraction	TCA %	Chromatoelectrophoresis(%)		
		Intact	Damaged	Free
Reaction mixture	34	26	40	34
9	100	98.5	1	0.5
19	9	5	80	15
29	2	0.2	2	97.8

The chromatoelectrophoretic profiles of the reaction mixture and column fractions listed in Table 2.V are illustrated in Fig. 2.11. The efficiency of the Sephadex-TEAE puri-

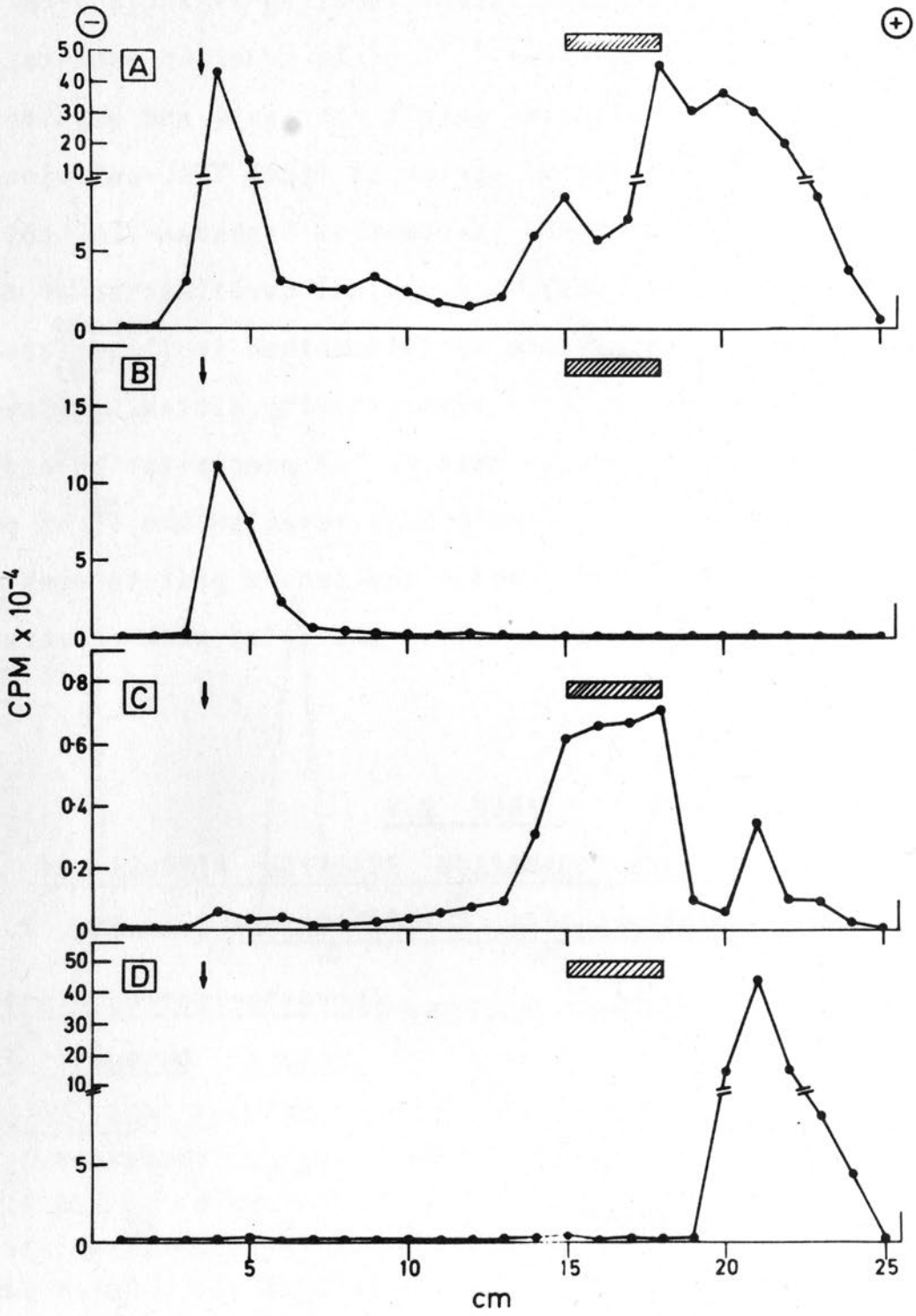

Fig. 2.11. Chromatoelectrophoresis of (A) the iodination reaction mixture, and fractions (B), 9; (C), 19 and (D), 29 from the purification column (see Fig. 2.10). Intact labelled protein remained near the origin (arrow), damaged products of iodination migrated with the bromophenol blue front (shaded bar), while free ^{125}I migrated ahead of the front. (See Appendix B for details of procedure).

fication method is clearly evident from the data in Table 2.V and the profiles in Fig. 2.11. The chromatoelectrophoretic profile of the reaction mixture (Fig. 2.11A) also revealed a degree of heterogeneity in the protein damage resulting from iodination. Furthermore, only a small portion of the damaged material was precipitable with TCA (fraction 19, see Table 2.V).

PAGE-SDS analysis was performed on aliquots of the reaction mixture and peak fractions obtained from the purification column. Autoradiography of the gel revealed the presence of only Y_a and Y_c ligandin bands in both the reaction mixture and first column peak. No bands were seen in the damaged protein and free ^{125}I peaks.

Reproducibility of iodination and label purification:

The mean values obtained from 20 consecutive iodination/purification procedures performed over a period of 12 months are given in Table 2.VI.

TABLE 2.VI

MEAN DATA FOR IODINATION AND PURIFICATION OF ^{125}I-LIGANDIN

	TCA %	Chromatoelectrophoresis (%)		
		Intact	Damaged	Free ^{125}I
Reaction mixture:	42.27±1.78	31.40±1.33	16.50±2.11	52.10±2.10
First column peak:	98.53±0.30	96.66±0.33	2.21±0.306	1.13±0.135

Results are given as Mean ± SEM for 20 procedures

Specific activity of ^{125}I-ligandin:

The average incorporation of ^{125}I into ligandin (derived from both TCA and chromatoelectrophoresis data in Table 2.VI) was 45%. The approximate specific activity of the labelled protein was calculated from the formula:

$$\text{Specific Activity} = \frac{\text{incorporation of } ^{125}\text{I} \times 1000\ \mu\text{Ci}}{\text{mass of protein iodinated}}$$

$$= 30\ \mu\text{Ci}/\mu\text{g ligandin}$$

The number of iodine atoms per molecule of ligandin was derived from the formula:

$$\mu\text{mol } ^{125}\text{I}/\mu\text{mol ligandin} = \frac{\text{Ligandin specific activity} \times \text{molecular weight ligandin}}{\text{Atomic weight } ^{125}\text{I} \times ^{125}\text{I specific activity}}$$

The specific activity of ^{125}I quoted by the suppliers was 11-17 mCi/µg I (100% isotopic abundance), and assuming a molecular weight of 46,000 for ligandin, the range obtained from the formula was 1.00 - 0.650 µmol ^{125}I/µmol ligandin (atoms of Iodine per molecule ligandin). It should be noted that the extrapolation of the specific activity data thus derived for ^{125}I-ligandin to the purified labelled protein subsequently used in the RIA, rests on the assumption that the purification procedure did not enhance or diminish the calculated specific activity of labelled ligandin, i.e. it did not differentially separate labelled from unlabelled or monoiodinated from polyiodinated intact ligandin.

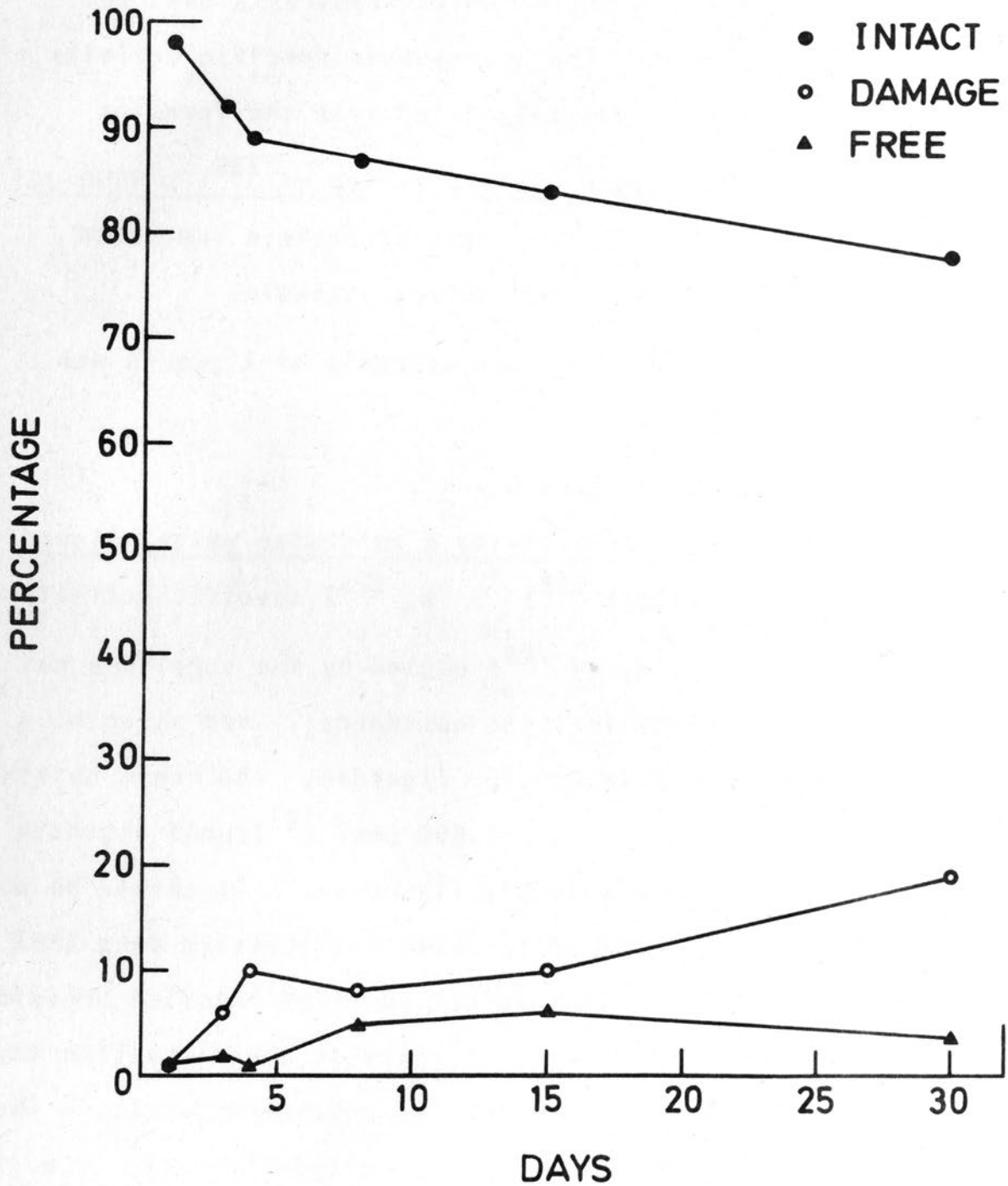

Fig. 2.12. Change in the percentage intact, damaged and free ^{125}I chromatoelectrophoretic fractions in purified ^{125}I-ligandin as a funtion of time.

Stability of ^{125}I-ligandin:

A decline in intact ^{125}I ligandin occurred most rapidly during the first 4 days of storage following iodination (Fig. 2.12). Thereafter a slow, uniform decrease in intact label occurred - reaching 78% in 30 days post-iodination - accounted for mainly by an increase in the damaged component.

4. Discussion

Iodination of ligandin was successfully achieved using the chloramine-T method, and a purification method was developed which yielded over 95% chromatoelectrophoretically intact labelled protein from the reaction mixture. It is noteworthy, that the purification method in effect reproduces a step of the method used to purify ligandin from rat liver viz. TEAE-cellulose anion exchange chromatography. The proportions of labelled and damaged ligandin to free ^{125}I eluting from the column (see Fig. 2.10) were markedly less than expected from chromatoelectrophoretic analysis of the reaction mixture (Table 2.V and Fig. 2.11), and it would thus appear that a considerable amount of the intact and damaged label remained adsorbed to the column. Nevertheless, the yield of purified ^{125}I-ligandin from a single iodination was entirely adequate for the running of several assays (see Chapter X).

In view of the high tyrosine content of ligandin (see Table 1.I) overiodination might conceivably have presented a problem. Loss of immunoreactivity has been associated with iodination resulting in a ratio of iodine atoms:protein

molecules in excess of an ideal 1:1 maximum ratio (311). The iodination protocol adopted for labelling ligandin appears satisfactory in this regard, as it engenders a high specific activity label without exceeding a 1:1 ratio of iodine atoms:ligandin molecules.

Over one third of the labelled ligandin was damaged by the iodination process, of which a variable portion in reaction mixtures was not precipitable with TCA. The major portion of the second ("damage") peak eluting from the purification column was unprecipitable and furthermore, did not give rise to an autoradiographically detectable protein band on PAGE-SDS. These findings suggest that the damaged fraction eluting in the second column peak comprised mainly small peptide and possibly amino acid fragments, while larger (TCA precipitable) damaged peptides preferentially - and advantageously - adsorbed to the column. No stable aggregates were detected on PAGE-SDS of the reaction mixture, suggesting that this form of iodination damage did not occur during the labelling of ligandin by the chloramine-T method.

The rapid initial decay of intact labelled ligandin followed by a slower decay phase might reflect the more rapid and early breakdown of more heavily iodinated molecules, followed by the more gradual degradation of lightly labelled molecules. It is important to note that the characteristics of the RIA (see Chapter X) were not unduly affected by the degree of label breakdown observed on chromatoelectrophoresis for up to 3 weeks following preparation of the label. Nevertheless, preparation of fresh labelled ligandin for use

in the assay was undertaken at least every second week.

Far more important than chromatoelectrophoresis as a criterion of the success of iodination and label purification, is the binding affinity between the labelled antigen and specific antibody. This is dealt with in the following chapter.

CHAPTER X

THE RADIOIMMUNOASSAY

1. Introduction

The preceding three chapters have dealt with the acquisition of the "essential reagents" for the RIA technique, i.e. the isolation and iodination of ligandin, as well as the production of antiserum to this protein. The present chapter describes the institution and general characterization of the ligandin RIA.

2. Methods

RIA Procedure:

(1) General protocol:

(a) All determinations were performed in 12 x 75 mm plastic tubes (Falcon plastics, no. 2052).

(b) All dilutions of tracer, standards, unknowns, NIRS and antisera were made in standard assay diluent buffer comprising 0.05M sodium phosphate buffer pH 7.4 / 0.15M NaCl / 0.01M EDTA /0.5% BSA / 0.1% sodium azide using an LKB model 2075 automatic diluter.

(c) Separation of antibody-bound from free labelled antigen was accomplished using a modification of the double antibody system of Morgan and Lazarow (315).

(2) Tube protocol:

Components in appropriate dilutions were added using Oxford pipettes to each standard and unknown sample tube as follows:

	Volume (µl)
Diluent buffer	200
Standard/unknown	200
Rabbit anti-ligandin antiserum (First antibody)	200
NIRS	100
^{125}I-ligandin (approximately 10,000 cpm/tube)	200
Total 1st incubation volume:	900

Whenever a particular component was omitted (see below), the volume deficit was made up with diluent buffer. Tubes were then incubated for 24h at 4°C followed by addition of:

Donkey anti-rabbit globulin (DARG)	100
Final incubation volume	1000

This was followed by a further incubation for 24h at 4°C. Thereafter, tubes were centrifuged at 2,000 xg for 30 min at 4°C in an MSE centrifuge. Supernatants were decanted, and after drainage for 5 min onto absorbant paper towelling, the tubes were swabbed to within 1 cm of the precipitates with cotton wool swabs.

(3) Assay protocol:

Each assay comprised the following:

(a) 4 tubes containing total counts only (T tubes).

(b) 4 tubes with no standards or unknowns added (B_o tubes).

(c) 4 tubes with no first antibody added (non-specific binding (NSB) tubes).

(d) 24-28 tubes (12-14 duplicates) containing standard concentrations of unlabelled ligandin from 0.3-2,400 ng/tube.

(e) Up to 200 tubes containing unknown samples - including internal standards - in duplicate. At least 2 dilutions of each unknown sample were assayed in order to allow determinations to be made in the steep (sensitive) region of the assay standard curve. Whenever appropriate, several serial dilutions of unknown samples were also assayed in order to compare the dose-response behaviour of unknowns with the standard curve.

Preparation of standards for the assay:

Protein concentration was determined (see Appendix B) in triplicate in two dilutions of a stock solution of purified ligandin. Thereafter, serial dilutions were made to provide a range of standards for use in the assay. An internal standard for the assay was provided by a sample of hepatic cytosol from a single rat. This was stored in aliquots at

-20°C and thawed as required.

Optimization of second antibody precipitation conditions:

In order to obtain the optimum proportions of DARG and NIRS for use in the assay, serial dilutions from a large pooled stock of DARG were incubated with serial dilutions of NIRS in the presence of a constant amount of ^{125}I-ligandin and a 1:1,000 initial dilution of first antibody, according to the assay protocol outlined above.

Determination of first antibody titre:

In general terms, the dilution (titre) of specific antiserum used in an RIA is that which demonstrates binding of 50% of the tracer in the absence of unlabelled antigen. This optimum was determined by incubation of serial dilutions of rabbit anti-ligandin antiserum (see Chapter VIII) with constant amounts of ^{125}I-ligandin according to the standard assay protocol.

Optimization of incubation times:

The incubation conditions for the assay (24h at 4°C for both first and second antibodies) were initially chosen as probably representing adequate, besides convenient, conditions for the attainment of equilibrium. This assumption was tested by monitoring the binding of tracer by antibody at assay titre under the following conditions:

(1) Keeping the first incubation time constant at 24h and varying the second incubation time between 8-48h.

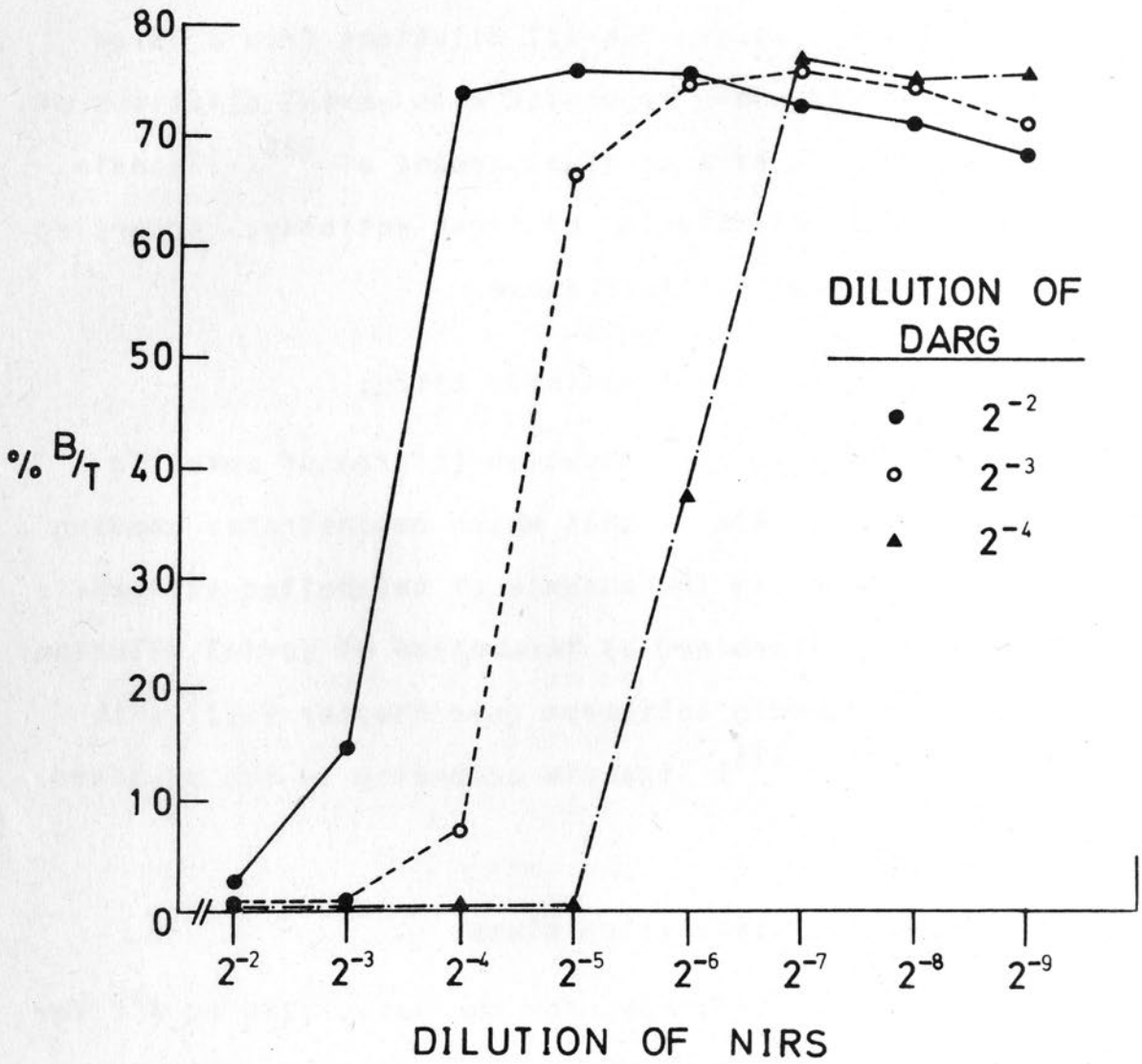

Fig. 2.13. Optimization of conditions for second antibody precipitation. The precipitation (% B/T) of ^{125}I-ligandin (in the presence of a 1:1000 initial dilution of first antibody) by different amounts of DARG in the presence of various dilutions of NIRS, was measured under standard assay conditions. (See Methods for details).

(2) Keeping the second incubation time constant at 24h and varying the first incubation time between 2-48h.

The temperature of 4°C was maintained for all incubations. The effect of 24h delayed addition of ^{125}I-ligandin to the assay was also explored.

Counting of radioactivity:

Precipitates were counted in a Beckman autogamma spectrometer with an ^{125}I isoset window for a minimum of 10,000 counts/tube. Background radioactivity was subtracted automatically from all assay counts. Counts were recorded on paper tape by a Packard teletype printer, and by this means raw data was transferred to a computer file (see below).

Calculation of binding data:

Binding data were calculated by means of an adaptation of the RIARUN Fortran IV-G programme devised by Rodbard and Lewald (316, see also ref. 297) run on the University of Cape Town Univac 1106 digital computer. An annotated specimen of a computed assay printout is displayed in Appendix D. In essence, this programme fits the standard curve of the assay to a linear function from which the values or "potency estimates" of unknowns can be derived. The linearization of the standard curve employs the "logit-log" method, using the relationship:

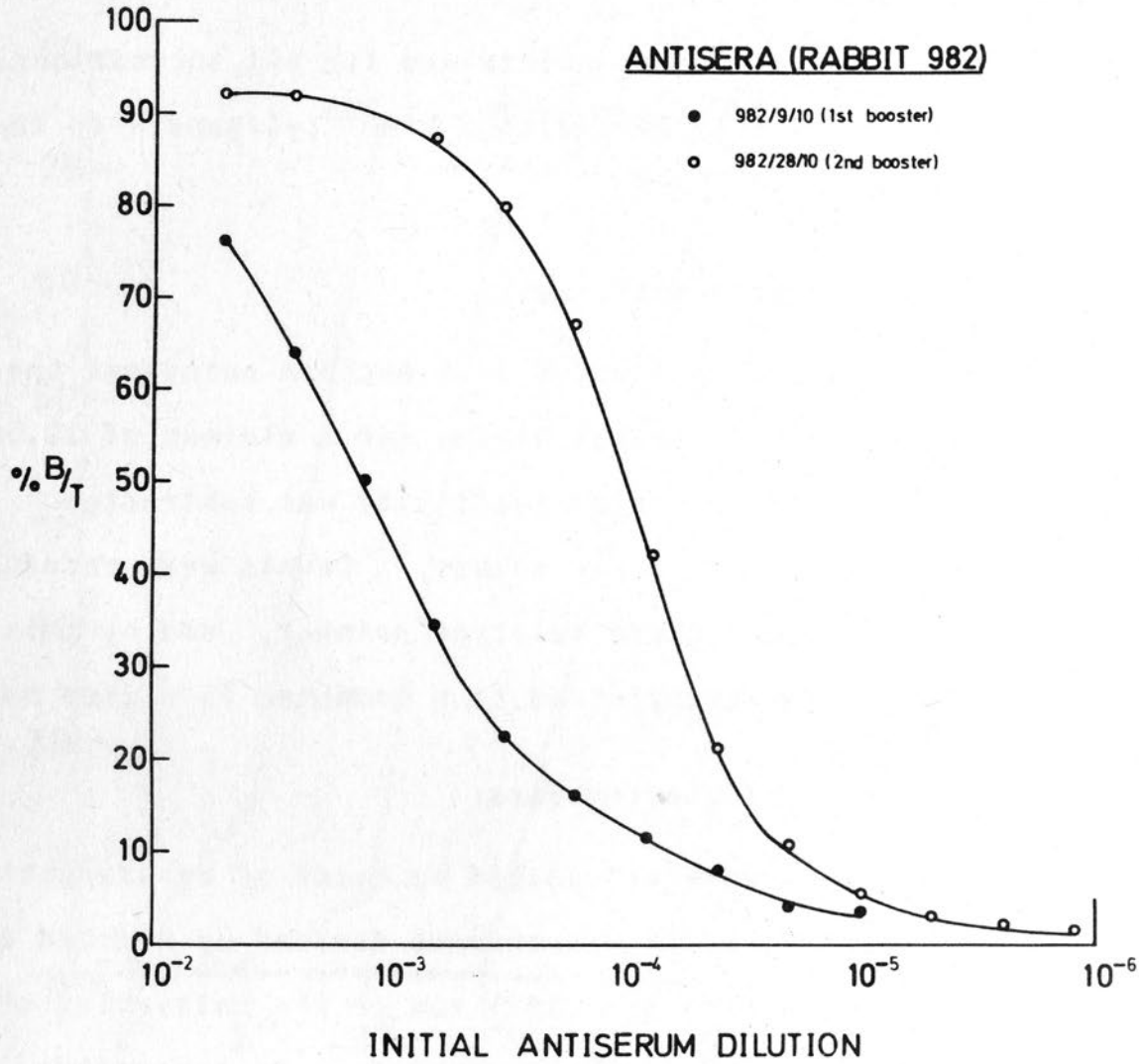

Fig. 2.14. Antiserum dilution curves of rabbit anti-ligandin antiserum. Serial dilutions of antisera harvested from rabbit 982 following the first and second booster inoculations, were incubated with constant amounts of ^{125}I-labelled ligandin according to the standard assay protocol (see Methods for details). The "titre" of antiserum is that demonstrating binding of 50% of the tracer.

$$\text{logit } (Y) = \alpha + \beta \log_e (X)$$

where $Y = B/B_o$, the ratio of bound counts (B) to counts bound in the absence of unlabelled antigen (B_o), with both numerator and denominator corrected for NSB counts;

$\text{logit } (Y) = \log_e (Y/1 - Y)$;

X is the dose of unlabelled antigen;

α, β are the intercept and slope respectively, of the linearized curve.

The derivation of antiserum affinity data by means of Scatchard plot analysis (317), as well as derivation of part of the data relevant to the proficiency testing and quality control (287, 297) of the assay, were also executed by the RIARUN programme (see Appendix D). When appropriate, e.g. in the case of antiserum dilution curves, binding data were calculated as the percentage ratio of bound to total counts (% B/T, corrected for NSB counts) using an Olivetti P203 computer. Plots of % B/B_o or % B/T vs dose or dilution (log scale) have been used to represent binding data in graphic form.

3. Results

Optimum conditions for second antibody precipitation:

The precipitation of antibody-bound ^{125}I-ligandin by different amounts of DARG and NIRS is shown in Fig. 2.13. These reagents were subsequently used at dilutions of 1:8 (DARG) and 1:128 (NIRS) as they gave maximal precipitation of the antibody-bound tracer, and were also within a decidedly

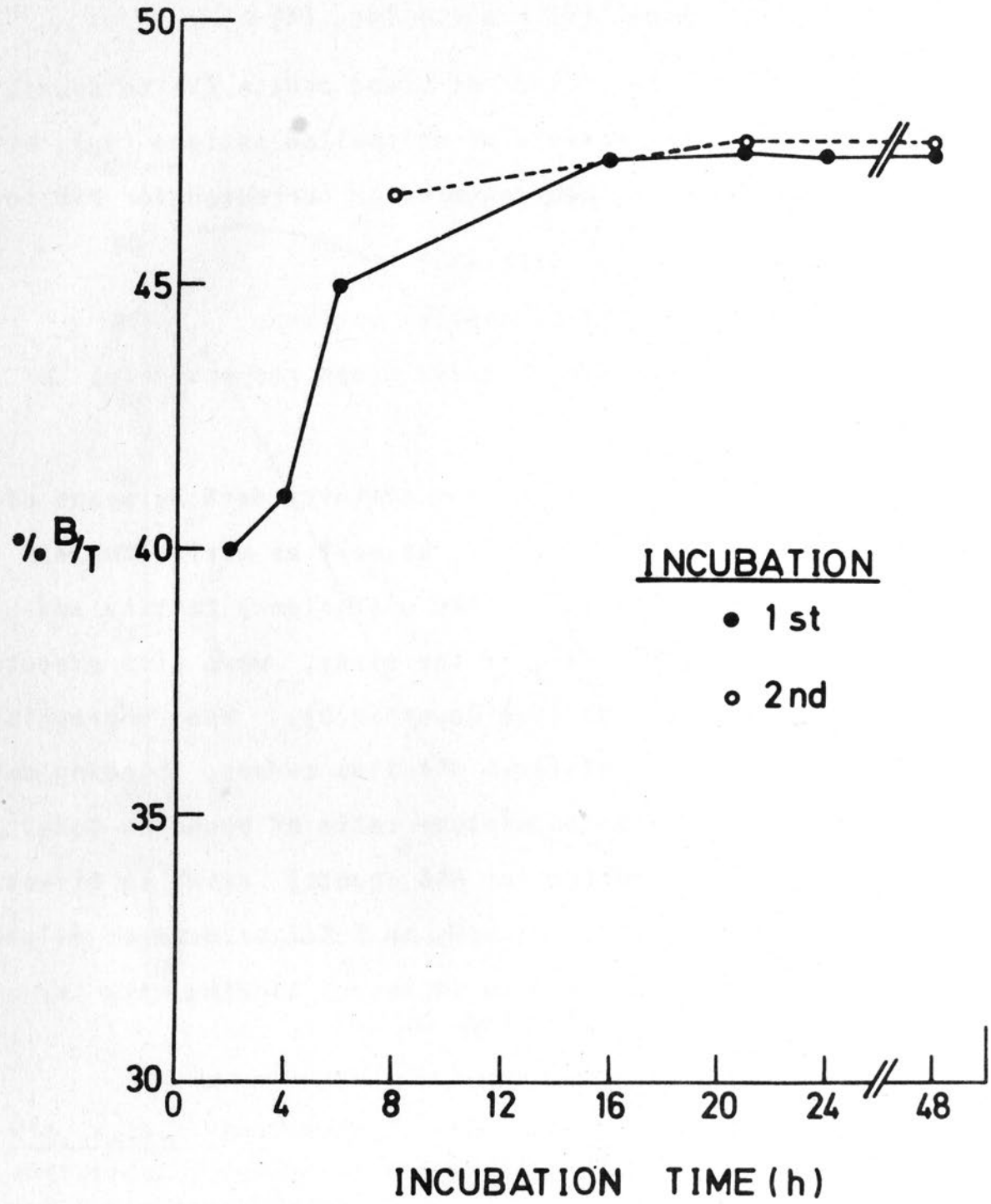

Fig. 2.15. Optimization of assay incubation times. The precipitation of ^{125}I-ligandin (% B/T) in the absence of unlabelled ligandin was determined for the first incubation (24h constant second incubation) and for the second incubation (24h constant first incubation). Attainment of equilibrium is indicated by the plateau in % B/T with time.

safe precipitation zone i.e. where small errors in pipetting either DARG or NIRS would have little effect on maximum precipitation.

First antibody titre:

The binding of a constant amount of ^{125}I-ligandin by serial dilutions of rabbit anti-ligandin antiserum after the first and second booster injections (982/9/10 and 982/28/10) are shown in Fig. 2.14. Antiserum 982/28/10 bound 50% of the tracer at an initial dilution of 1:8,000 (= final dilution of 1:40,000) and was used at this concentration in all subsequent assays. At initial dilutions between 1:200 and 1:500, antiserum 982/28/10 bound 97-100% of freshly prepared ^{125}I-ligandin. Five days after preparation of label, maximum binding fell to 88-93%, while after 20 days 75-78% binding of tracer by excess antibody was observed. Thus the immunoreactivity of ^{125}I-ligandin declined on storage in an almost parallel fashion to the chromatoelectrophoretic integrity of the label (see Fig.2.12).

Incubation periods required for equilibrium:

Both the first and second antibody stages of binding reached equilibrium by 24h at 4^{o}C (Fig. 2.15). No increase in % B/T was found when either incubation step was prolonged to 48h.

The standard curve:

A typical standard curve obtained by the addition of increasing amounts of unlabelled ligandin to tubes containing

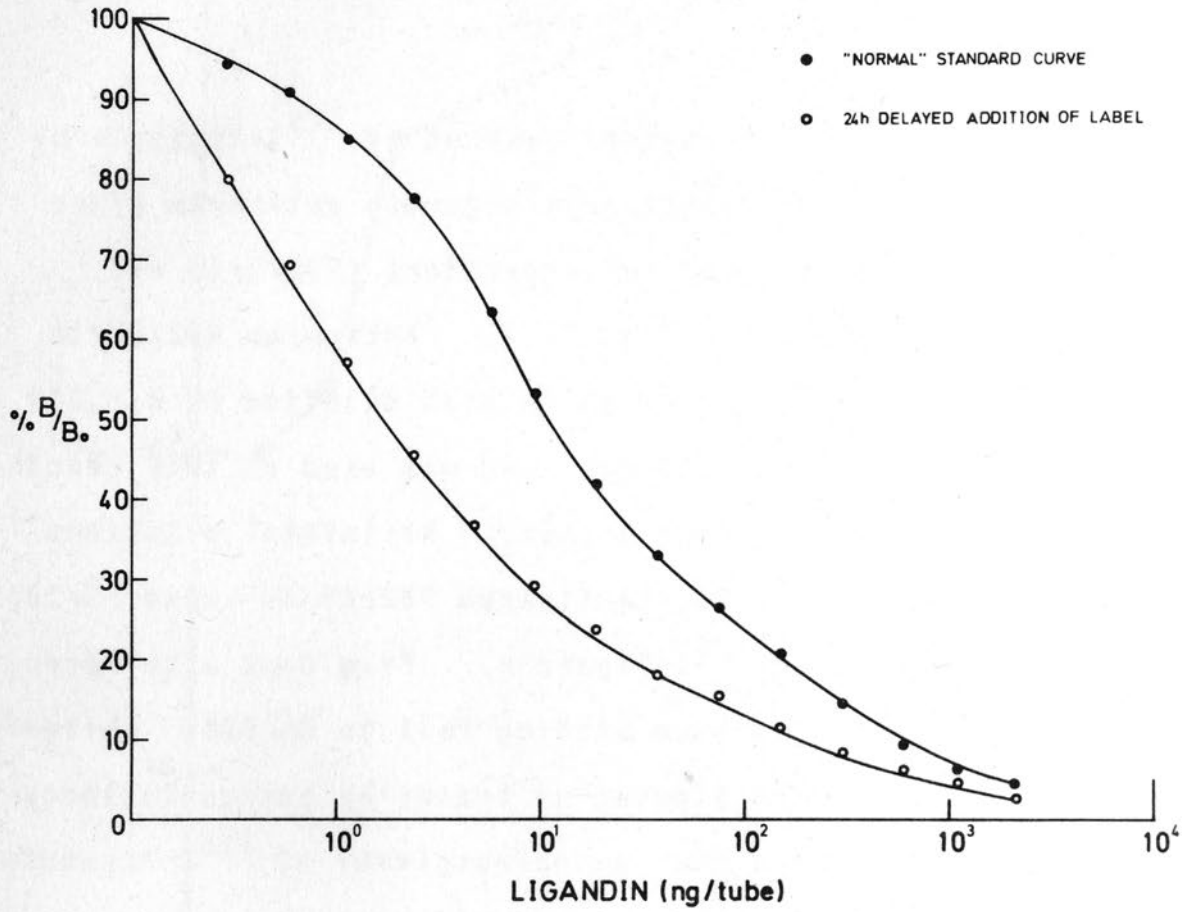

Fig. 2.16. Ligandin RIA standard curve. The "normal" curve was obtained under standard assay incubation conditions, while the left-hand curve was obtained after addition of ^{125}I-ligandin 24h after pre-incubation of the other reagents, followed by a further 24h first incubation.

constant amounts of anti-ligandin antiserum and ^{125}I-labelled ligandin is shown in Fig. 2.16. Also illustrated in Fig. 2.16 is the curve obtained when ^{125}I-ligandin was added 24h after the other reagents, with a further period of incubation for 24h prior to addition of the second antibody. The "normal" standard curve fell throughout the nanogram range, while late addition of label resulted in a pronounced curve shift-to-the-left with a resultant increase in sensitivity and precision in the upper picogram and low nanogram range.

Characteristics and proficiency of the assay:

Fig. 2.17 shows the variation in seven parameters of the RIA over 20 assays (quality control chart). The average values for total cpm (T), the fraction of labelled antigen bound at zero dose (% B_o/T) and the percentage of total counts bound in the absence of specific (first) antibody (% NSB/T) were derived from input data by the RIARUN programme, while the slope, 50% intercept and minimum detectable dose (see Fig. 2.17) were derived from the computer-calculated weighted least-squares regression line of logit(Y) vs $\log_e$(X) (see Appendix D). These latter three parameters, amongst others, provide means for assessing the proficiency criteria of an RIA viz:

(1) Precision

"Precision" may be used to describe the ability of an assay system to distinguish between two antigen concentrations at any point on the response curve (287). In

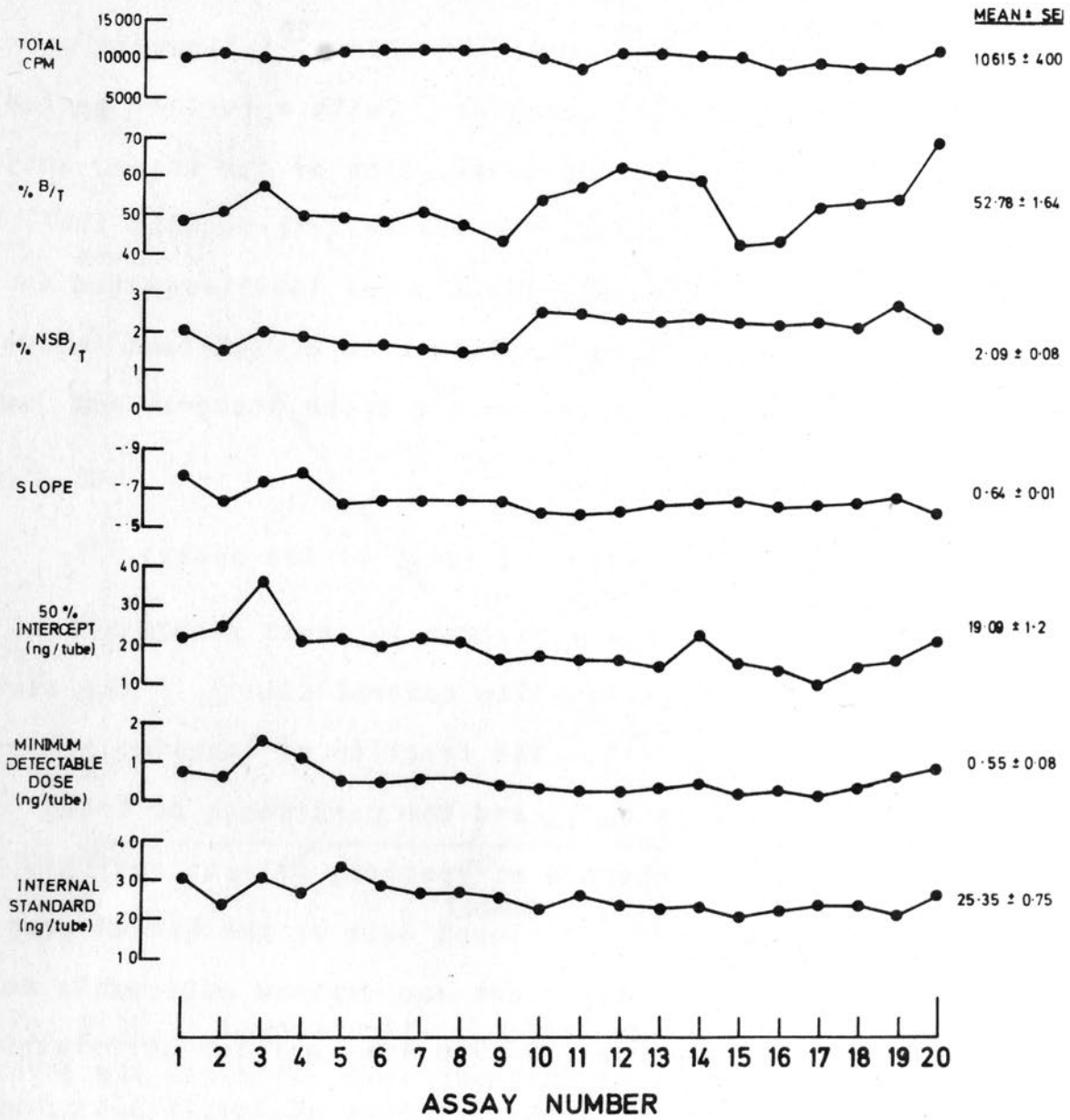

Fig. 2.17. Quality control chart of ligandin RIA. The variation in total cpm, the percentage counts bound in the absence of unlabelled antigen (% B/T), the percentage non-specific bound counts (% NSB/T), the slope and midpoint (50%) intercept of the logit curve, the minimum detectable dose, and internal standard value over 20 consecutive assays are shown.

the RIA system, precision is dependant on the extent of change in Y with fractional changes in unlabelled antigen (X) concentration. The slope of the regression of logit (Y) vs $\log_e$ (X) affords a reasonable estimate of precision, and under "ideal" circumstances i.e. circumstances of greatest precision, is equal to -1.0 (297). The average slope of the ligandin RIA curve (Mean $\pm$ SEM, see Fig. 2.17) for 20 assays was -0.64 $\pm$ 0.012. The 50% binding intercept i.e. that dose of unlabelled antigen which lowers Y to half its initial value (% Y = 50%; logit Y = 0) falls on the portion of the assay curve with the steepest slope and provides a measure of the midrange, and thus the most sensitive (see below) region of the curve. This factor averaged (Mean $\pm$ SEM, see Fig. 2.17) 19.09 $\pm$ 1.20 ng/tube for the ligandin RIA.

(2) Sensitivity

"Sensitivity" is, in effect, a special case of precision (287, 297) and is defined as "the smallest amount of unlabelled antigen which when added to a solution containing no unlabelled antigen, results in a significant change in the response variable (B/B_o)". In essence therefore, sensitivity is equal to the minimum detectable dose (see Fig. 2.17) which averaged (Mean $\pm$ SEM) 0.55 $\pm$ 0.076 ng/tube over 20 assays.

(3) Reproducibility

Reproducibility is best assessed by the duplication of values within or between assays. The results of 20 determinations of two dilutions of a sample of rat liver cytosol (see Chapter XI) in a single assay are shown in Table 2.VI. The coefficient of variation (CV, see Appendix C) ranged between 4.6 - 6.8%.

TABLE 2.VI

WITHIN-ASSAY VARIATION FOR LIGANDIN RIA

Replicate No.	Sample values (ng/tube)	
	1:5,000 ← Dilutions →	1:10,000
1	25	11
2	26	12
3	24	12
4	25	11
5	25	11
6	23	12
7	25	12
8	26	13
9	26	12
10	24	12
11	27	14
12	26	12
13	25	12
14	22	12
15	24	13
16	24	12
17	24	12
18	25	12
19	25	13
20	25	14
Mean ± SEM	24.8 ± 0.26	12.2 ± 0.83
CV (%)	4.6	6.8

The sample used was rat hepatic cytosol

The average value obtained for the measurement of a sample of liver supernatant (1:5,000 dilution) in 20 consecutive assays (internal standard, Fig. 2.17) was 25.35 ± 0.75 ng/tube (Mean ± SEM) yielding an overall coefficient of variation of 13.2%. The between-assay variation improved with repeated performance as evidenced by the fact that the variation encountered in the first ten assays (Mean ± SEM: 27.4 ± 1.07 ng/tube; CV: 12.3%), was reduced in the next ten assays (Mean ± SEM: 25.35 ± 0.75 ng/tube; CV: 7.6%). The validation of hepatic cytosol ligandin measurement is dealt with in Chapter XI.

(4) Specificity

Specificity has been defined as "the extent of freedom from interference by substances other than the one intended to be measured" (287). The specificity of antibody for antigen is influenced by 3 main factors:-

(a) Heterogeneity:

A particular antigen will virtually always induce the formation of several populations of antibodies. The antigen will combine with the heterogenous antibodies to various degrees, depending on the respective affinity constants (K) generated (287). The Scatchard plot analysis of ^{125}I-ligandin binding to its antiserum (see Appendix D) revealed the presence of at least 2 populations of antibodies (a 3 parameter model): one of high and one of considerably lower affinity. It must be borne in mind however, that the validity of the data

from the Scatchard plot is based upon several major assumptions (319), not the least of which is that the mass of labelled antigen be known with considerable accuracy. Based on the estimated specific activity of ^{125}I-ligandin (see Chapter IX), an approximate mass of 0.1 ng/tube was calculated for the tracer, which generated mean values of $K = 0.23 \pm 0.028 \times 10^{11}\ M^{-1}$ and antibody binding capacity, $Q = 0.58 \pm 0.09 \times 10^{-10}$ M. It is stressed that these data must be considered in the light of the error in estimating the mass of tracer ^{125}I-ligandin.

(b) Cross-reactivity

Two different antigens from the same or different species may cross-react as a result of sharing one or more antigenic determinants. The broad specificity of the assay was explored by assaying several intracellular proteins at 1 mg/ml concentration (Table 2.VII). The values obtained reflect a very low (< 0.001%) degree of cross-reactivity by these species with the assay and confirm the specificity of the antiserum used.

TABLE 2.VII

CROSS-REACTION OF INTRACELLULAR PROTEINS WITH LIGANDIN RIA

Protein	Immunoreactivity (ng/ml)
Myoglobin	2
Cytochrome c	2
Ferritin	3
Carbonic anhydrase	11
Alcohol dehydrogenase	<1

Protein solutions were assayed in distilled water at 1 mg/ml concentration

(c) Non-specific interference:

Non-specific factors in biological fluids may modify the antigen-antibody association. These include amongst other factors, ionic strength, pH, heparin, urea and bilirubin. Consideration of interference by these extraneous factors will be given in subsequent chapters. It is important in this regard to note that EDTA was included in the assay buffer medium in order to eliminate possible inhibition of the antigen-antibody reaction by serum complement which is a frequently encountered cause of non-specific interference (287).

The ligandin RIA was characterized by a very low non-specific binding of labelled antigen in the absence of specific antibody (% NSB/T, see Fig. 2.17; Mean $\pm$ SEM: 2.09 $\pm$ 0.084%), which was not increased by the presence of standards, tissue supernatants or physiological fluids and could be lowered to less than 1% by increasing the concentration of BSA in the assay diluent buffer. Other aspects relating to the specificity of the assay are dealt with in subsequent chapters.

(5) Accuracy

This final criterion of assay proficiency is often the most difficult to evaluate. It refers to the extent to which a given measurement or measurements of a substance agrees with the standard measured value of that substance. Usually, it is only possible to establish relative accuracy of an RIA firstly, by comparison of

assay values with those obtained by another "reference" method and secondly, by quantitative recovery experiments using pure antigen. Details of these procedures appear in later chapters.

4. Discussion

A highly sensitive and reproducible RIA was developed for rat ligandin, employing ^{125}I-labelled rat hepatic ligandin and rabbit anti-ligandin antiserum. The double antibody method used in establishing the assay is probably the most generally applicable and technically simple separation technique used in RIA and gives excellent separation of bound from free antigen (318). Addition of increasing amounts of unlabelled purified ligandin displaced antibody-bound ^{125}I-ligandin to yield an assay standard curve which combined features of adequate precision, a wide working range and a sensitivity readily capable of detecting 1 ng/tube. Even greater sensitivity was obtainable through manipulation of the time of tracer addition. The kinetics of this phenomenon, attributable to non-equilibrium conditions, have been discussed by Feldman and Rodbard (319).

The general specificity of the assay was attested to by the negligible cross-reaction with various intracellular proteins. Data fulfilling more rigorous criteria of specificity are presented later in this work. The assay was characterized by a very low non-specific binding of ^{125}I-ligandin, attributable in part to the presence of BSA in the assay diluent and probably also indicative of the lack of signifi-

cant adherence of ^{125}I-ligandin to plastic tubes or plasma proteins. This is an advantageous feature, as high non-specific binding has been regarded as one of the major problems in RIA procedures (287).

A high affinity was computed for the antiserum (982/28/10) used in the assay, although it must be appreciated that the estimate of K, the affinity (equilibrium) constant, is at best only an approximation. The heterogeneity of the antiserum evident from Scatchard plot analysis must be viewed in the light of the fact that the production of "homologous" antiserum consisting of antibodies entirely specific for a particular antigen, has not been reported (287). Antibodies directed against a single antigenic determinant may vary considerably in terms of number and location of binding sites, and thus generate a series of K. Moreover, the relatively large size of ligandin would be in keeping with the presence of several antigenic determinants on its surface, each giving rise to a distinct, heterogenous population of antibodies. In this regard, peptides of ligandin obtained by cyanogen bromide cleavage, have revealed three antigenic reactants on immunodiffusion and immunoelectrophoresis (Bhargava, personal communication).

SECTION B

LIGANDIN IN THE TISSUES OF THE RAT

CHAPTER XI

QUANTITATIVE TISSUE DISTRIBUTION OF LIGANDIN IN THE ADULT RAT

1. Introduction

A number of diverse methods have been employed in the past to measure ligandin in rat tissues (see Chapter III.6.i). The aim of this study was to establish the quantitative tissue distribution of ligandin in the adult rat by RIA. To this end, it was necessary to establish the validity of the RIA measurement of ligandin in the cytosol of rat tissues, by examining the immunochemical displacement behaviour and the molecular size of immunoreactive material in tissue extracts. The relative accuracy of the RIA (see Chapter X) was assessed by examining the recovery of ligandin from standard and modified tissue extraction techniques and also by performing qualitative immunodiffusion studies on tissue cytosol extracts. Levels of immunoreactive ligandin were also compared with the GSH S-transferase activities of a limited number of tissues.

2. Methods

Preparation of tissues for assay

As ligandin is a cytoplasmic protein, only the 100,000 xg supernatants (cytosol fraction) of tissues were assayed. These were prepared from 5-25% homogenates of different tissues (see Appendix B) obtained from 56 male and 6 female rats, as well as from liver obtained from guinea pig, Long-Evans rat, albino mouse, albino rabbit and human being. The latter was a 20 year old male "cadaver" renal transplant donor with fatal head injuries from whom

liver was obtained after full legal consent had been granted, at the time of kidney removal. In order to assess the effect of different homogenization buffers on the behaviour of cytosol in the assay, a single rat liver was divided into 3 portions. Each portion was individually homogenized and centrifuged in one of the following media:

(1) 0.01M sodium phosphate buffer pH 7.4 / 0.25M sucrose (standard homogenization buffer)

(2) 0.05M sodium phosphate buffer pH 7.4 / 0.15M NaCl (phosphate-saline buffer)

(3) Phosphate-saline buffer with 2 mM Dithiothreitol (DTT).

Each extract was then assayed at several dilutions. All cytosol extracts were either used on the day of preparation or stored at -20^{o}C for no longer than seven days prior to usage. Protein concentration (298) was determined as outlined in Appendix B. Supernatants were assayed for ligandin as described in Chapter X.

Enzyme activity

GSH S-transferase activity of cytosol and column fractions was assayed with 1-chloro-2,4-dinitrobenzene as outlined in Appendix B. The correlation coefficient (r) was derived from the least-squares analysis of data (see Appendix C).

Immunodiffusion and immunoelectrophoresis

These techniques were performed as described in Appendix B using rabbit anti-rat ligandin antiserum.

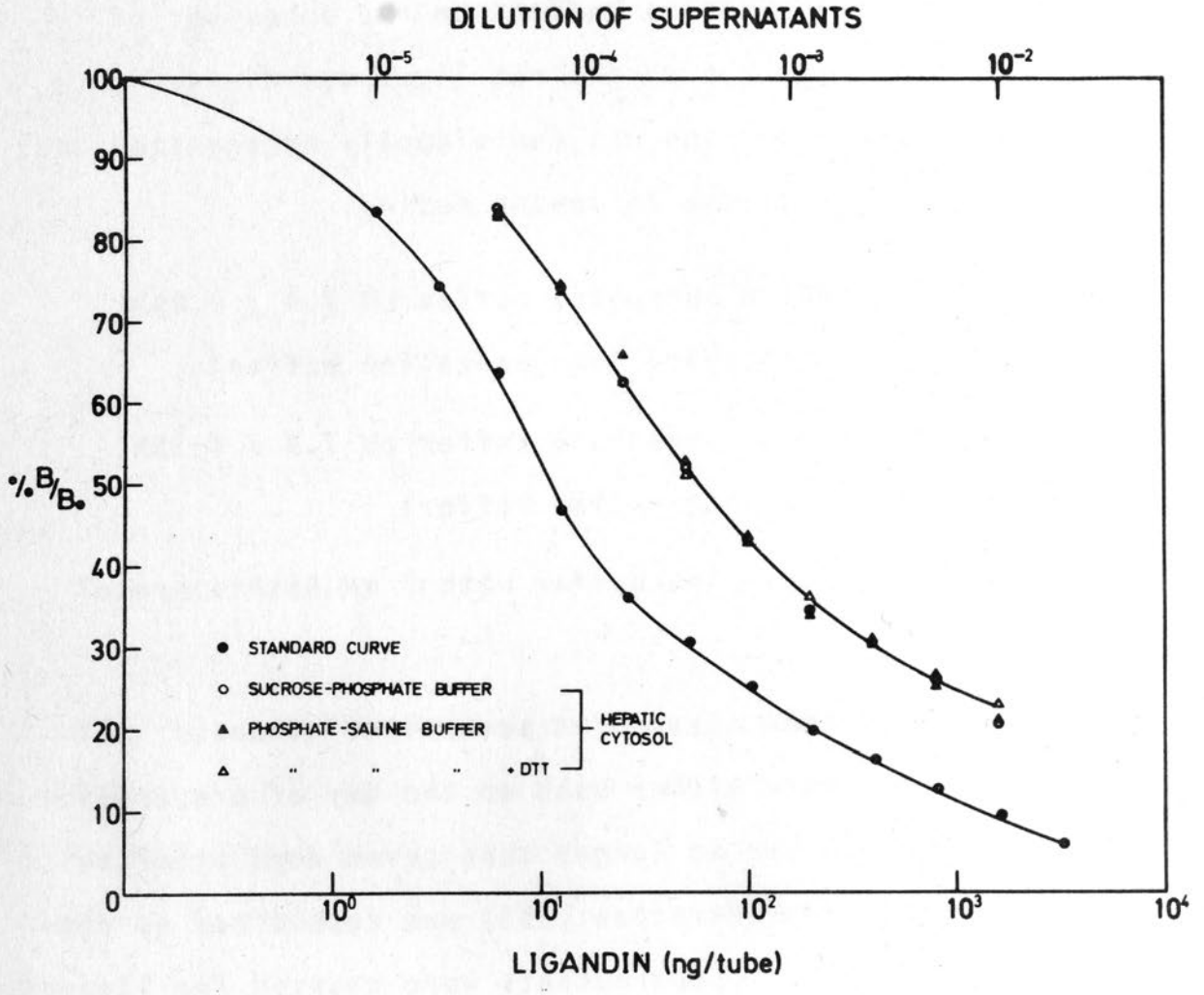

Fig. 2.18. Effect of different homogenization buffers on the immunochemical displacement curve of hepatic cytosol. On the ordinate is the percentage ratio of antibody-bound radioactivity to radioactivity bound in the absence of unlabelled ligandin (% B/Bo) and on the abscissa (log scale), the amount of unlabelled ligandin and the dilutions of hepatic cytosol.

Gel filtration

The molecular size of immunoreactive ligandin in the liver, kidney, intestinal mucosa, testis and myocardium was determined by chromatography of 5 ml of cytosol from each of these tissues mixed with 5 mg BSP on a 100 x 2.5 cm calibrated column of Sephadex G-100 in 0.01M sodium phosphate buffer pH 7.4 / 0.1M NaCl. The column was eluted by pump-driven upward flow at 40 ml/h with collection of 3.5 ml fractions. Protein and BSP concentrations were determined spectrophotometrically (see Chapter VII), while ligandin was measured by RIA.

PAGE-SDS of immunoreactive peaks

In order to assess the relative molecular sizes of peptides present in immunoreactive ligandin peaks observed on gel fitration of tissue cytosol fractions, immunoreactive peaks were separately pooled, concentrated 25 times (see Chapter VII.2, Y fraction analysis) and analysed by discontinuous slab PAGE in SDS (see Appendix B).

3. Results

Tissue extraction methodology

The recovery from 100,000 xg supernatants of ^{125}I-ligandin (TCA precipitable) added to tissues prior to homogenization was between 85 and 93%. The effect of different homogenization buffers on the assay behaviour of liver cytosol is shown in Fig. 2.18. No differences were apparent in the immunochemical displacement curves of cytosol prepared in

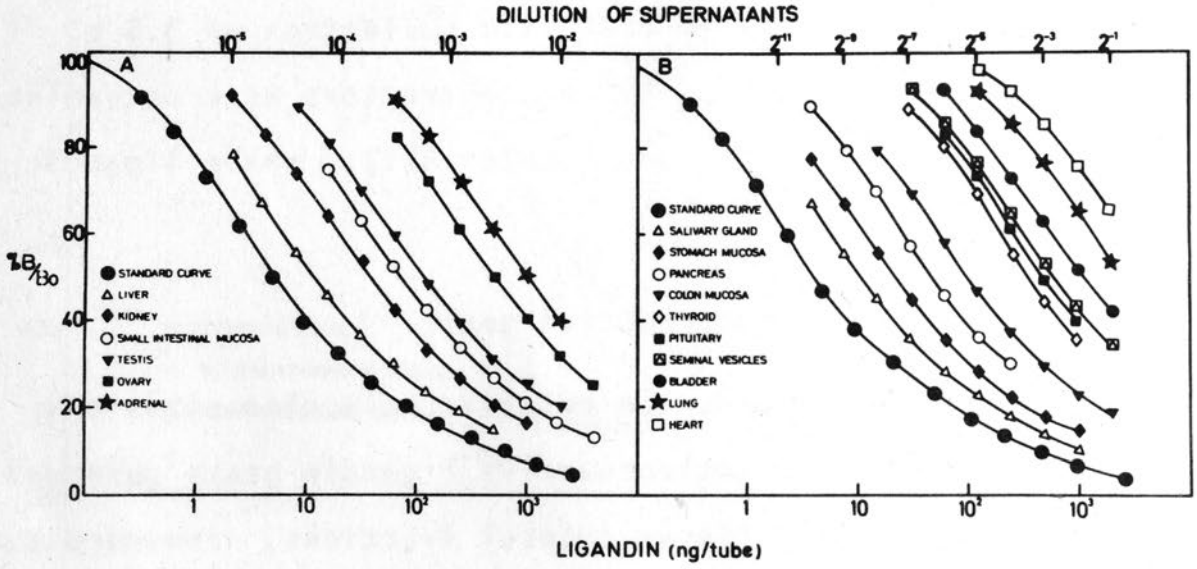

Fig. 2.19. RIA of ligandin in rat tissues. (A and B), Standard curves and immunochemical displacement curves of different tissue 100,000 xg supernatants. Ordinate and abscissa are as described in legend to Fig. 2.18.

either sucrose-phosphate or phosphate-saline buffer with and without the sulphydryl reagent DTT. Homogenization buffer alone had no effect on the assay.

The initial strength of the homogenate had no apparent effect upon the assay of ligandin, as evidenced by the fact that cytosol prepared from 25, 10 and 5% homogenates of portions obtained from a single liver, gave values for immunoreactive ligandin of 40, 46 and 44 µg/mg supernatant protein respectively. Almost identical values were obtained for immunoreactive ligandin concentration in cytosol samples before and after freezing at -20°C. In addition, cytosol samples maintained stable levels of immunoreactive ligandin when stored at -20°C for up to three months.

Quantitative tissue distribution of ligandin

Immunoreactive ligandin was measured in the cytosol of 21 different rat tissues. Serial dilutions of cytosol prepared from these tissues gave immunochemical displacement curves identical to the standard curve obtained with pure ligandin (Fig. 2.19), indicating the presence of an immunochemically similar protein in the 100,000 xg supernatants of these tissues. The mean values obtained for immunoreactive ligandin in the cytosol of tissues assayed, are shown in Table 2.VIII (cf Table 2.II). Immunoreactive ligandin shows a widespread tissue distribution, the highest concentrations (above 1 µg/mg supernatant protein) occuring in liver, kidney, small intestinal mucosa, testis, ovary

TABLE 2.VIII

IMMUNOREACTIVE LIGANDIN CONCENTRATION IN THE TISSUES OF THE RAT

Tissue	Ligandin (µg/mg protein)
Liver	45.08 ± 3.52
Kidney	16.02 ± 0.92
Proximal small intestinal mucosa	9.22 ± 0.87
Distal small intestinal mucosa	2.49 ± 0.19
Testis	6.07 ± 0.73
Ovary	2.16 ± 0.32
Adrenal gland	1.76 ± 0.13
Salivary gland	0.50 ± 0.07
Stomach mucosa	0.42 ± 0.06
Pancreas	0.20 ± 0.04
Colon mucosa	0.13 ± 0.011
Pituitary	0.11 ± 0.025
Lung	0.056 ± 0.007
Thyroid	0.054 ± 0.002
Bladder	0.039 ± 0.004
Heart	0.025 ± 0.003
Seminal vesicles	0.017 ± 0.001
Brain, spleen, skeletal muscle, uterus	< 0.001

Results are expressed as Mean ± SEM in µg/mg supernatant protein. Tissues from 6 animals were used for each determination except in the case of thyroid and pituitary where tissues from 6 animals were pooled and 2 pools estimated.

and adrenal gland, with smaller amounts assayed in other tissues. Minute amounts of immunoreactive ligandin were also detected in brain, spleen, skeletal muscle and uterus. These tissues were not perfused free of blood prior to homogenization, and thus the presence of immunoreactivity in these tissues possibly reflects the presence of blood, which was later shown to contain small amounts of immunoreactive ligandin (see Chapter XV).

If the specific activity of ligandin with 1-chloro-2,4-dinitrobenzene is taken as 10.0 μmol/min/mg (see Table 2.I), then using the values for immunoreactive ligandin concentrations shown in Table 2.VIII, it is possible to estimate the 1-chloro-2,4-dinitrobenzene conjugating activity attributable to ligandin ("L_C") within different tissues, from the simple formula:

$$L_C = \text{ligandin (mg/mg)} \times 10.0 \text{ (μmol/min/mg)}$$

A limited number of tissues were assayed for total GSH S-transferase activity with 1-chloro-2,4-dinitrobenzene as substrate in order to ascertain the correlation between GSH S-transferase specific activity and immunoreactive ligandin concentration in these tissues. These enzyme activities are shown in Table 2.IX. Included in this table are the values of L_C expressed in the case of each tissue as a percentage of the total 1-chloro-2,4-dinitrobenzene conjugating activity.

TABLE 2.IX

GSH S-TRANSFERASE ACTIVITIES OF RAT TISSUES

Tissue	Specific Activities (S) (μmol/min/mg)	%L_C/S
Liver	1.95 ± 0.34	23
Kidney	0.233 ± 0.007	69
Proximal small intestinal mucosa	0.327 ± 0.026	28
Distal small intestinal mucosa	0.150 ± 0.005	17
Testis	1.5 ± 0.07	4
Lung	0.115 ± 0.024	0.5
Heart	0.091 ± 0.002	0.3

Values of S are expressed as Mean ± SEM μmoles 1-chloro-2,4-dinitrobenzene conjugated/min/mg supernatant protein. Tissues from 3 animals were used for each determination. L_C represents the conjugating activity of each tissue with 1-chloro-2,4-dinitrobenzene attributable to ligandin alone (see text for details).

As shown in Table 2.IX, it is evident that ligandin accounts for an extremely variable percentage of the total 1-chloro-2,4-dinitrobenzene conjugating activity in different tissues. Thus it is not surprising, that no significant correlation ($r = 0.747$, $P > 0.05$) was obtained between the GSH S-transferase activities of the tissues in Table 2.IX (which reflect the total 1-chloro-2,4-dinitrobenzene conjugating activity of all the combined GSH S-transferases,

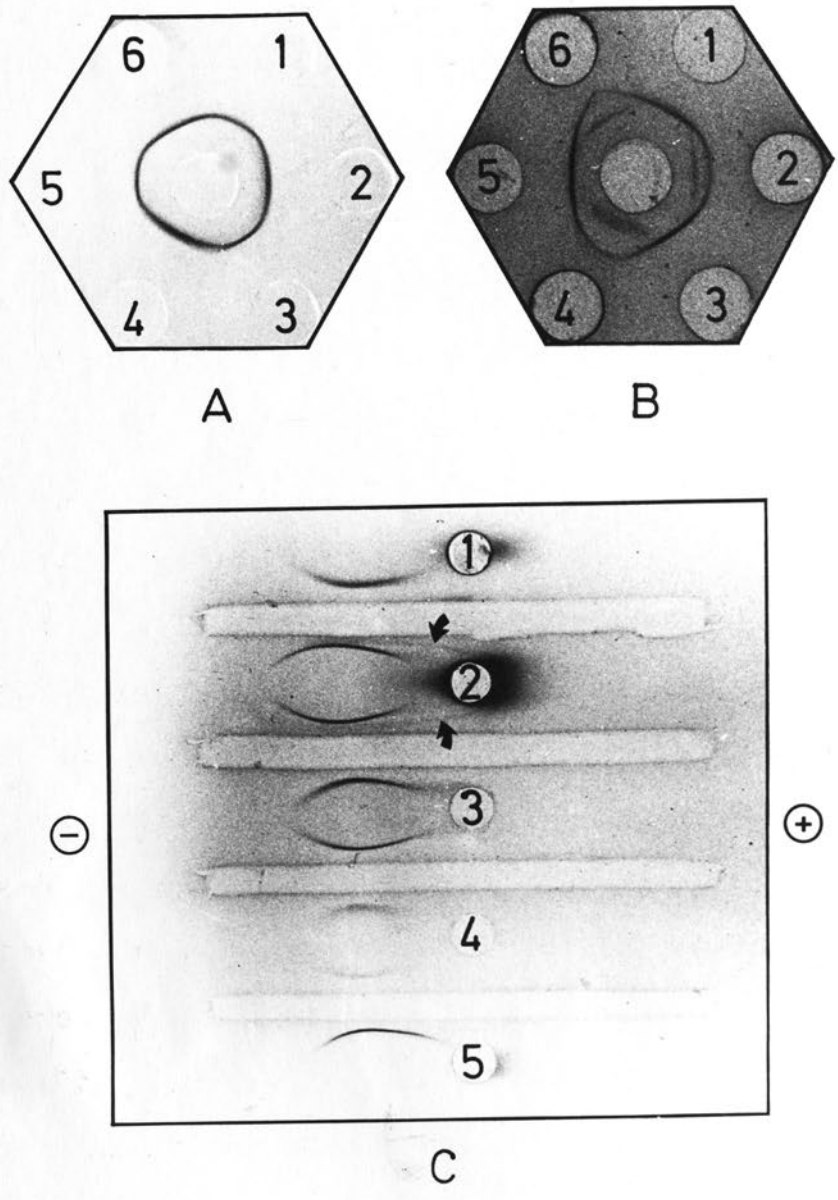

Fig. 2.20. Immunodiffusion and immunoelectrophoresis in agar gel. (A and B), the centre wells contain rabbit anti-ligandin antiserum. Peripheral wells contain: (A), 1, 3 and 5, 1 µg ligandin; cytosol from: 2, liver (1:4); 4, kidney (1:2) and 6, small intestinal mucosa; (B), 1, 3 and 5, ligandin (1 µg); cytosol from 2, testis; 4, ovary and 6, adrenal. No precipitin lines were obtained with cytosol from other tissues listed in Table 2.VIII. (C), Immuno-electrophoresis in agar gel. The wells contain cytosol from 1, liver (1:4); 2, testis; 4, small intestinal mucosa and 5, kidney (1:2) with ligandin (1 µg) in well 3. The troughs contain rabbit anti-ligandin antiserum. Precipitates were stained with amidoblack. (See Appendix B for details of procedures).

including ligandin) and their corresponding values for immunoreactive ligandin (Table 2.VIII).

Immunodiffusion and immunoelectrophoresis were performed in order to obtain a relative assessment of the sensitivity and accuracy of the RIA compared with these techniques. Antiserum to purified rat ligandin gave a single line of complete identity on immunodiffusion with purified ligandin and cytosol fractions from rat liver, kidney and small intestinal mucosa (Fig. 2.20A). Besides the cytosol fractions of these latter three tissues, only supernatants from the testis, ovary and adrenal gland gave precipitin lines with the ligandin antiserum (Fig. 2.20B). However, the cytosol fractions from these latter three tissues gave rise to 2 separate precipitin lines; a line of partial identity (Ouchterlony type 3 reaction (307)) and a line of identity with purified ligandin. This phenomenon was also observed when GAL-IgG were used instead of the rabbit anti-ligandin antiserum in these studies. On immunoelectrophoresis, cytosol of liver, kidney and small intestinal mucosa as well as purified ligandin gave rise to single precipitin arcs with anti-ligandin antiserum (Fig. 2.20C). Cytosol from testis gave rise to two distinct arcs migrating in fairly close proximity to one another. Continuation of electrophoresis for a minimum period of 2h was required in order to reveal this latter feature.

Gel filtration and PAGE in SDS

Fractionation of cytosol from liver, kidney, small

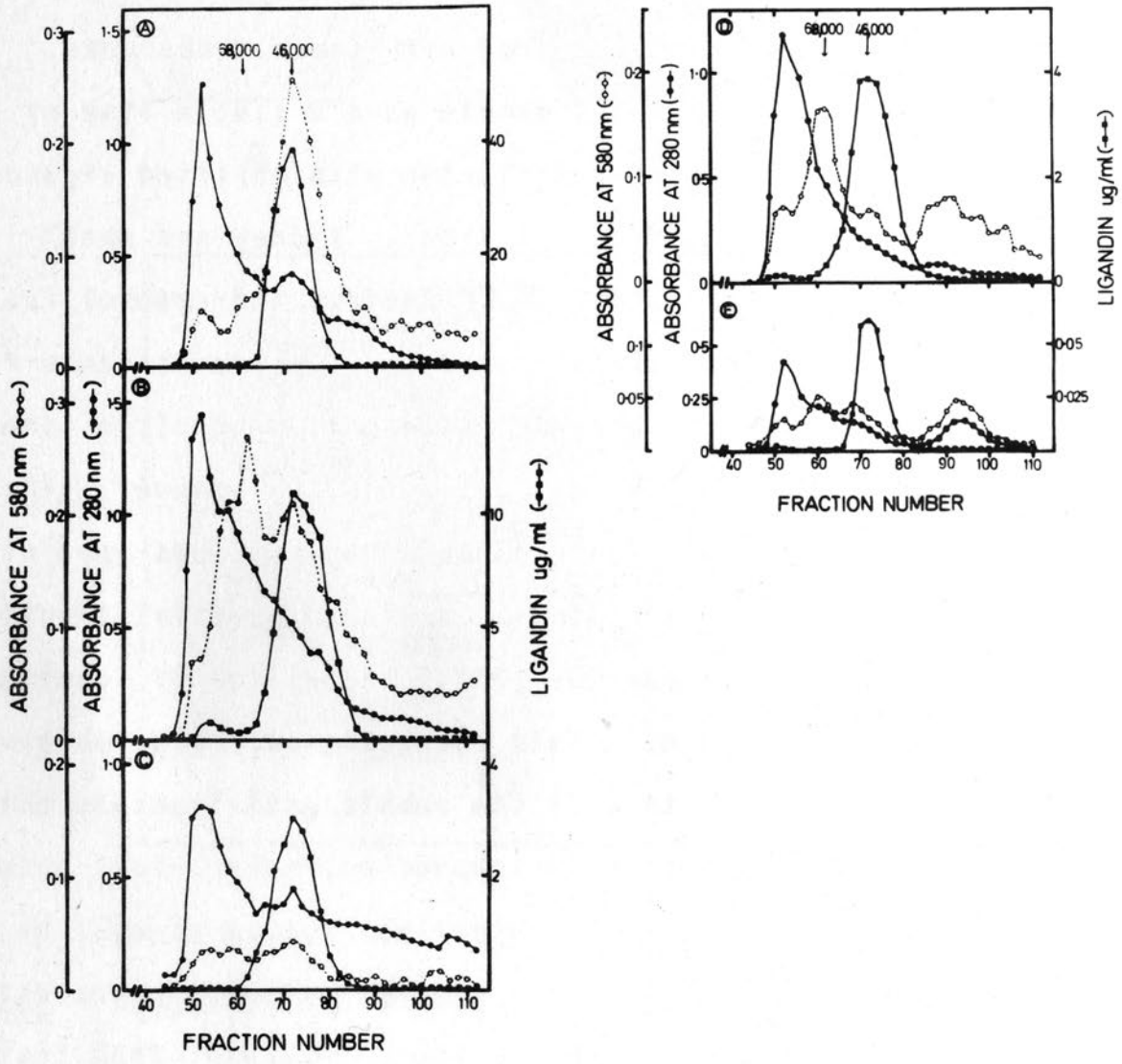

Fig. 2.21. Immunoreactive ligandin and BSP-binding in tissue supernatants chromatographed on Sephadex G-100. 5 ml of cytosol from (A), liver; (B), kidney; (C), small intestinal mucosa; (D) testis and (E), myocardium were each mixed with 5 mg BSP and chromatographed on Sephadex G-100 as described in Methods. Protein and BSP were measured spectrophotometrically while ligandin was determined by RIA.

intestinal mucosa, testis and myocardium was carried out on Sephadex G-100 with BSP as a marker for ligandin, and assayed for specific ligandin immunoreactivity (Fig. 2.21). Identical results were obtained for immunoreactivity when BSP was omitted, while 10 times the concentration of the dye present in the column fractions caused no interference with the assay. In the case of each tissue studied by this means, a major peak of immunoreactivity was revealed in the 44,000 molecular weight region, corresponding to the elution volume of pure ligandin (V_e/V_o = 1.4). This immunoreactive peak was also found to coincide with:

(1) Peak GSH S-transferase activity with 1-chloro-2,4-dinitrobenzene as substrate (all 5 tissues tested).

(2) All immunoreactivity detected on immunodiffusion in the case of liver, kidney, small intestinal mucosa and testis.

A small amount of immunoreactivity was detected by RIA in the region of proteins eluting in the void volume in effluent fractions of kidney, testis and myocardium (Fig. 2.21B, D and E). It is not known whether this represents ligandin in aggregated form, or cross-reaction with high molecular weight proteins bearing an immunochemical similarity to ligandin. However, this fraction constituted less than 1% of the total eluted immunoreactivity in each case and is thus thought not to contribute significantly to the values of ligandin obtained in tissue supernatants. BSP-binding to a protein in the fraction containing immunoreactive ligandin was most prominent in the liver and kidney

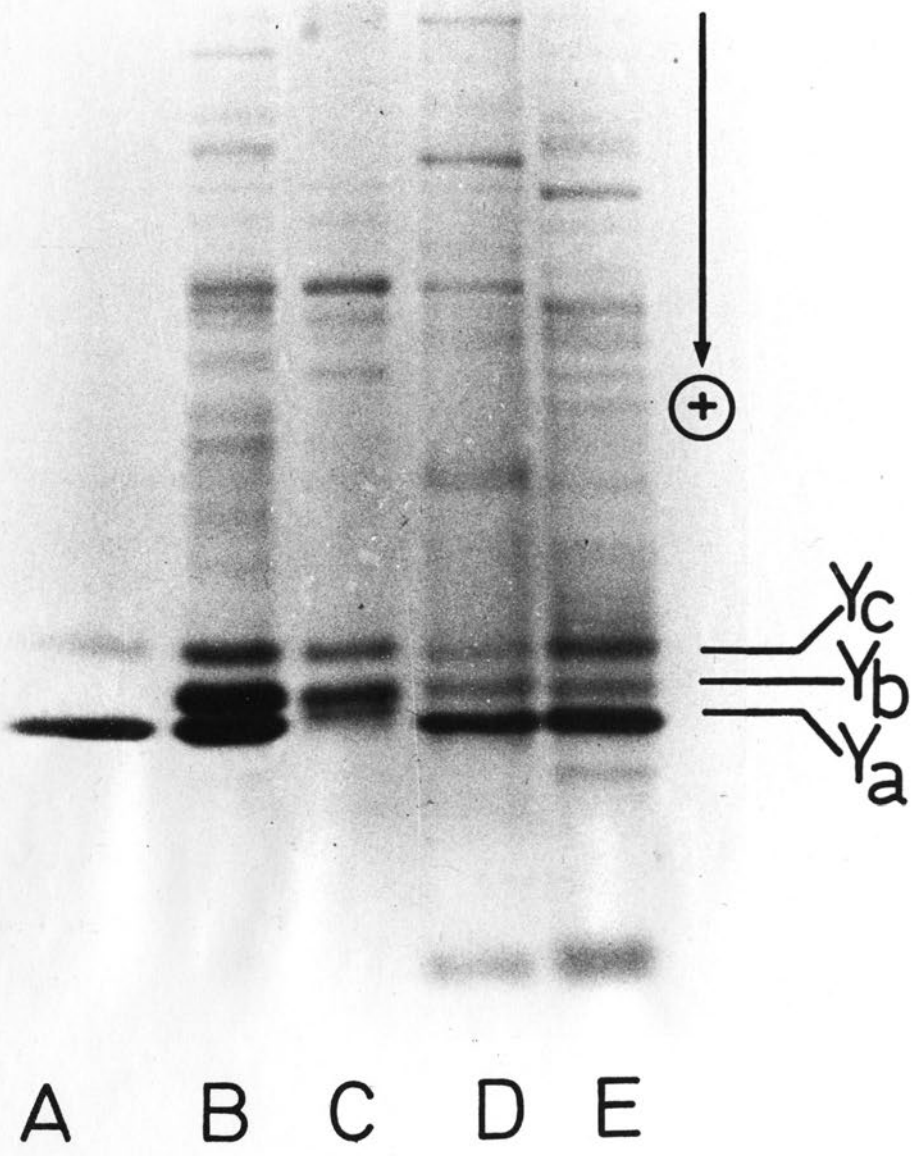

Fig. 2.22. Discontinuous slab PAGE in SDS of (A), ligandin, and the Sephadex G-100 immunoreactive ligandin peaks of (B), liver; (C), testis, (D), small intestinal mucosa and (E), kidney (12.5% resolving gel). Details are given in Methods. Y_a, Y_b and Y_c indicate the subunit species corresponding in size to the 3 major subunit polypeptides of the hepatic Y fraction.

(Fig. 2.21A and B), while being much less marked in the ligandin containing fractions of the other tissue supernatants. An earlier peak of BSP binding corresponding to the elution volume of albumin (V_e/V_o = 1.2) was often more pronounced.

Aliquots from the pooled and concentrated immunoreactive ligandin peaks (Fractions 70-73) of liver, kidney, small intestinal mucosa and testis were analysed comparatively by discontinuous slab PAGE in SDS. The results are shown in Fig. 2.22). Three major "Y peptide" bands (Y_a, Y_b and Y_c; see Chapter VII) were found with identical migrations in the immunoreactive ligandin peaks of liver, kidney and small intestinal mucosa. The immunoreactive peak of testis cytosol revealed major bands corresponding to the Y_b and Y_c subunits, with a minor component migrating just ahead of the Y_b peptide band. Significantly, a band corresponding to the ligandin Y_a subunit was not seen; and thus if Y_a is present in the testis, its concentration must be too small to be detected by this method.

Cross-reaction with different species

Supernatants of liver from guinea pig, mouse, human being and rabbit cross-reacted with the assay, but immunochemical displacement curves showed marked deviation from parallelism with the standard curve (Fig. 2.23). The hepatic cytosol of rabbit, the species in which the assay antiserum was raised, showed the least degree of cross-reaction of all the species tested. Long-Evans rat liver, on the other hand,

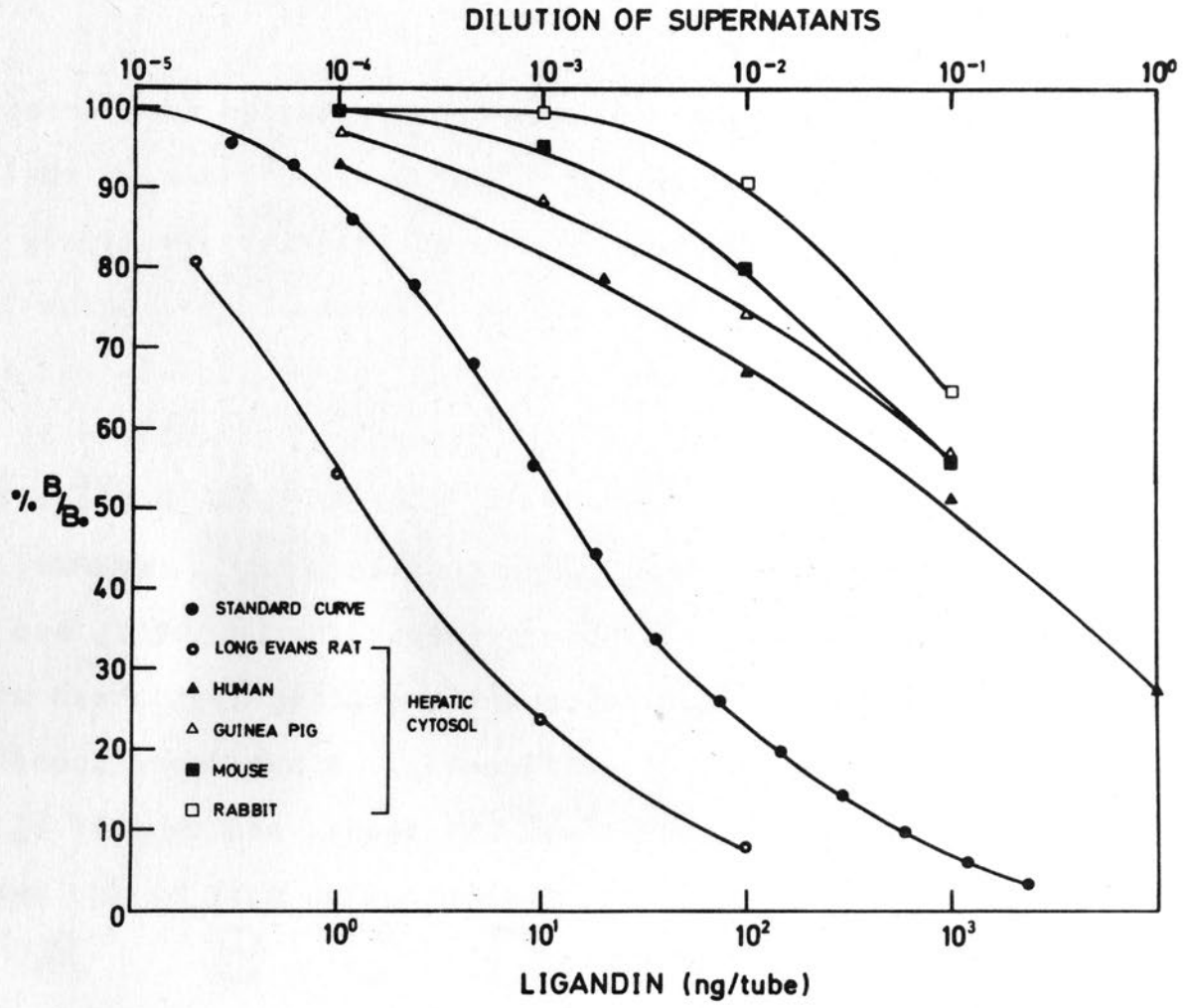

Fig. 2.23. Comparison between immunochemical displacement curves of hepatic cytosol from various species and the standard curve of ligandin RIA. Ordinate and abscissa are as described in legend to Fig. 2.18.

gave results comparable with Wistar rat liver and showed an immunochemical displacement curve completely superimposable on the RIA standard curve (Fig. 2.23).

4. Discussion

Quantitative data for ligandin have been previously reported for liver, kidney and small intestinal mucosa, and the values obtained for these tissues by RIA are in good agreement with those derived by quantitative immunodiffusion (see Chapter VIII, Table 2.II). Furthermore, the sensitivity of the RIA method, which is capable of measuring ligandin in the nanogram range, allowed for the first time the direct measurement of ligandin in other tissues as well. RIA measurements revealed a widespread tissue distribution of ligandin in the rat, although concentrations above 1 µg/mg supernatant protein were found only in the liver, kidney, small intestinal mucosa, testis, ovary and adrenal gland. In addition, only supernatants from these six tissues gave detectable precipitin reactions on immunodiffusion with rabbit anti-ligandin antiserum. Other workers employing immunodiffusion and immunofluorescence techniques have reported the presence of ligandin in liver, kidney (158, 209-212), small intestinal mucosa (158, 210-212), testis and ovary (210, 211). Ketterer has also demonstrated the presence of ligandin by immunological means in concentrated supernatants of rat lung, bladder and skin (Ketterer, personal communication). Fleischner et al (212) noted more intense ligandin-specific immunofluorescence in the proximal than in the distal

small intestinal mucosa. In accord with these findings, a higher concentration of ligandin in proximal relative to distal small intestinal mucosa was measured in the present study by RIA.

The pattern of immunoreactive ligandin distribution in the tissues holds several implications. It is interesting to note that in certain respects, the distribution of ligandin is similar to that of glucuronyl-transferase, which occurs mainly in the liver, but has also been found in kidney, ovary, testis, adrenal gland, skin and synovial membrane (320). It is possible that a common factor is responsible for the de-repression of the separate genes coding the synthesis of ligandin and glucuronyl-transferase in certain tissues. The high concentration of ligandin in liver, kidney and small intestinal mucosa may correlate with the major role of these tissues in organic anion uptake. This matter has been extensively discussed and debated in terms of the role of ligandin in hepatic and renal uptake of organic anions (see Chapter IV). The role of ligandin in organic anion uptake by the gut has not been explored, although Tidball (321) has demonstrated that passive absorption of BSP occurs from the small intestine, and a role might be proposed for intestinal ligandin in this process. Unfortunately, this hypothesis is not supported by the fact that this worker (321) found no difference in BSP absorption between proximal and distal small bowel, which do, however, differ considerably in ligandin content. It has been frequently demonstrated, that the extrahepatic

tissues are capable of removing significant amounts of BSP from the circulation (40, 41, 322). The presence of ligandin, albeit in small quantities, in a large number of extrahepatic tissues might be important as regards this phenomenon. The finding of relatively high concentrations of ligandin in the testis, ovary and adrenal gland is of considerable interest. Ligandin has been shown to bind steroid hormones as well as their metabolites (see Chapter III.5), and its presence in the steroid producing endocrine tissues may indicate a role in the intracellular transport of these substances. Furthermore, the recently proven identity between ligandin and Δ^5-3-ketosteroid isomerase (173) adds a highly significant functional dimension to the presence of ligandin in the steroid producing tissues, where its primary role may be the conversion of Δ^5-3-keto-steroids to the corresponding α, β-unsaturated Δ^4-3-keto-steroids.

Although the major portion of GSH S-transferase activity with several substrates is found in the liver (223), GSH S-transferase activity has also been detected in kidney, lung, heart, spleen, intestine, brain, skeletal muscle and adrenal gland (142, 145, 147). However, the relative activities of these tissues differ considerably with different substrates. This phenomenon has been particularly well illustrated by the studies of Kaplowitz et al (213, 215) and Clifton et al (214). These workers have shown that GSH S-transferase specific activities in kidney relative to liver for aryl, aralkyl, epoxide, alkyl and alkene sub-

strates are 2, 17, 68, 92 and 109% respectively. In the present study, an extremely variable and often very small percentage of the GSH S-transferase activity of various tissues (see Table 2.IX) with 1-chloro-2,4-dinitrobenzene as substrate, could be accounted for by the ligandin (GSH S-transferase B) content of these tissues estimated by RIA (see Table 2.VIII). It would seem reasonable, on the basis of these findings, to propose that the different GSH S-transferases (AA, A, B, C, D, E and M) do not maintain constant proportions relative to one another, but rather manifest in widely varying proportions in different tissues. This might well account for the different substrate-defined activities shown for different tissues evident from the studies discussed above. The findings of the present study further serve to emphasize that whatever substrate is used, GSH S-transferase activity reflects the cumulative activity of the several distinct transferases, and as such, cannot be equated with ligandin content.

The RIA appears highly specific for ligandin, as evidenced by the following:

(1) Immunoreactive ligandin in tissue extracts (cytosol) gave immunochemical displacement curves parallel with the standard curve.

(2) There was negligible cross-reaction with other intracellular proteins (see Chapter X).

(3) There was a lack of correlation between 1-chloro-2,4-dinitrobenzene conjugating activity and immunoreactive

ligandin content in a number of tissues. This suggests, although indirectly, that no significant cross-reaction occurred between the assay and the other GSH S-transferases in tissue extracts. For example, the 1-chloro-2,4-dinitrobenzene conjugating activity of testis was found to be surprisingly high (77% of hepatic activity), whereas the ligandin concentration of this tissue was only 14% of the hepatic value. This suggests that ligandin does not make the major contribution towards 1-chloro-2,4-dinitrobenzene conjugating activity in the testis (approximately 4%), but rather transferases AA, A and C which were not detected by the assay.

(4) The immunoreactivity in tissue extracts separated by gel filtration appeared in the same elution position as pure ligandin. Matsushita et al (207) recently reported that the peak of BSP-binding to rat ligandin (the Y BSP-binding peak) on gel filtration of renal cytosol, elutes later than the corresponding peaks in hepatic and small intestinal mucosa cytosol. Contrary to these findings, the present study demonstrated complete correspondence between peaks of immunoreactive ligandin and Y BSP-binding in renal and hepatic supernatants. Kaplowitz et al (215) have also shown identical elution volumes of several GSH S-transferase activities in kidney and liver cytosol on Sephadex G-100 chromatography. The discrepant findings of Matsushita et al (207) might be explained by the fact that BSP-binding to renal cytosol ligandin affords a less accurate means

of locating this protein in column eluates compared with specific immunoreactivity or GSH S-transferase activity. Indeed, the early study of Levi et al (107) failed to locate the presence of ligandin in the kidney (or any other extrahepatic tissue) by means of BSP-binding on gel filtration. Certainly, in the case of renal cytosol, displacement of BSP from ligandin may occur as a result of the presence of haem (159), which is known to bind with a relatively higher affinity to ligandin (see Chapter III and Table 1.III).

Discontinuous PAGE-SDS analysis of the immunoreactive ligandin peaks of liver, kidney, small intestinal mucosa and testis revealed an extremely interesting feature. The presence of the three Y peptide bands (Y_a, Y_b and Y_c; see Chapter VII) was revealed in each tissue with the exception of the testis, in which the Y_a band was absent. The Y_a and Y_c bands correspond in size to the non-identical subunits of ligandin, and thus the absence of a Y_a band in the testis strongly suggests that the Y_a and Y_c subunits of ligandin are not in fact the non-identical subunits of a single dimeric protein (Y_a-Y_c combination), but rather the monomers of two distinct dimeric proteins (Y_a-Y_a and Y_c-Y_c combinations). Concerning the nature of the Y_b peptide present in the immunoreactive ligandin peaks of all the tissues examined by PAGE-SDS, it would be logical to propose that this species represents the monomer of yet another dimeric 40-50,000 dalton protein:Y_b-Y_b; although beyond this, the relationship of Y_b subunit species to ligandin (which

by definition, would comprise Y_a-Y_a and Y_c-Y_c dimers) is by no means clear.

A definite antigenic structural similarity between the Y_a and Y_c subunit species of ligandin could be inferred from the fact that rabbit anti-ligandin antiserum reacts in a monospecific fashion against purified ligandin, as well as supernatants from liver, kidney and small intestinal mucosa - all of which contain both Y_a and Y_c subunit species - on immunodiffusion and immunoelectrophoresis. The reason for the heterogeneity evident in the antiserum reaction in agar gel with supernatants of testis, ovary and adrenal gland is not clear, but the finding that of the two ligandin subunit species, only the Y_c subunit is unequivocally present in the testis, may be significant in this regard. It is also interesting to note, that the RIA did not differentiate between immunoreactive ligandin in the testis - which contains only the Y_c-Y_c species - and immunoreactivity in cytosol of liver, kidney and small intestinal mucosa, all of which appear to contain both Y_a-Y_a and Y_c-Y_c dimeric species. This might be taken as further evidence for the close immunochemical relationship between the subunit Y_a and subunit Y_c ligandin components.

The concept of ligandin consisting of two related dimeric proteins also raises the important question: to what extent does each of these species contribute towards the non-substrate binding and GSH S-transferase catalytic activity of ligandin? The presence of both GSH S-transferase catalytic activity and immunoreactive ligandin in the

testis (both confined to the 40-50,000 molecular weight zone on gel filtration), which further only contains the Y_c subunit representative of the ligandin peptides, might be indicative of the presence of catalytic activity in the Y_c-Y_c dimeric species. However, the question is not conclusively resolved by these findings, as purified GSH S-transferase A has also been shown to consist of unequal subunits corresponding in size to the Y_a and Y_c species of ligandin (168). The results of the present study certainly indicate that the bulk of GSH S-transferase activity in the testis is due to transferases other than ligandin. It is thus important to consider the feasibility that the Y_c subunit species of ligandin and that of transferase A - which should theoretically differ in charge, antigenicity and amino acid composition (155) - might differ considerably in catalytic activity or even in the possession thereof. The difficulty in drawing finite conclusions concerning catalytic activity from the size-class of Y peptides occurring in different tissue supernatants, can be further appreciated if it were postulated that all the multiple GSH S-transferases possess size heterogeneity similar to that of ligandin and transferase A; although this has not been established as yet.

Species-specificity of ligandin was evident from the studies of Fleischner et al (218). These workers only found cross-reaction between goat antiserum to rat ligandin and hamster tissues. No cross-reaction with mouse liver was observed by these workers, although Bannikov et al (211) have reported cross-reaction between mouse tissues and rabbit

antiserum to rat ligandin. The immunochemical displacement curves of liver cytosol from different species in the rat ligandin RIA provide a novel means of assessing the antigenic relationships between ligandin obtained from different species. Liver cytosol of rabbit, mouse, guinea pig and human being all cross-reacted poorly with the assay, as evidenced from the high concentrations of cytosol required in each case to effect displacement of ^{125}-ligandin and also from the lack of parallelism of immunochemical displacement curves with the standard curve. On the other hand, no strain-specificity of ligandin is apparent from the behaviour of Long-Evans rat hepatic cytosol in the assay. Strictly speaking however, an assessment of the relative degrees of cross-reaction shown by the hepatic cytosol of different species in Fig. 2.23 is not entirely valid, as no normalization of the data was made for protein concentration.

CHAPTER XII

THE EFFECT OF PHENOBARBITAL ON LIGANDIN

1. Introduction

The GSH S-transferases are amongst the few cytoplasmic enzymes which are induced in a manner similar to the microsomal drug-metabolizing enzymes by phenobarbital and polycyclic hydrocarbons (213). A number of reports have been made on the inducing effects of xenobiotics on GSH S-transferase activity, "Y peak" ligand-binding capacity and immunologically determined ligandin concentration in the liver and kidney of the rat (see Chapter III.6.vii). The development of an RIA for ligandin introduced an entirely new means for the quantification of this protein, and thus a study was undertaken using this technique to explore the effect of phenobarbital administration on the levels of ligandin in several tissues of the adult rat. Furthermore, in view of the evidence favouring the existence of the non-identical subunits of ligandin as the monomers of two distinct dimeric proteins: Y_a-Y_a and Y_c-Y_c (see Chapter XI), the present study also incorporated an attempt to ascertain the effect of phenobarbital treatment on the hepatic Y peptides.

2. Methods

Experimental protocol:

Eight rats were given daily subcutaneous injection of 8 mg/100g body weight of phenobarbital sodium (40 mg/ml in 0.9% saline) for 14 days. An identical number of control

animals received equivalent volumes of saline for the same period of time. Animals were sacrificed 24h after the final injection and cytosol was prepared from the liver, kidneys and small intestinal mucosa of each animal as well as from the testes of 4 of the phenobarbital-treated rats and each control animal (see Appendix B). Ligandin content of supernatants was determined by RIA; protein concentration was measured as described in Appendix B. In order to eliminate spurious effects which might have been introduced by interassay variation, each specific tissue from the phenobarbital-treated group was assayed together with its respective controls en bloc in a single assay. Student's t test was used for statistical comparison of data (see Appendix C).

Aliquots of hepatic cytosol (∿ 50 µg of protein) from phenobarbital-treated and control animals were analysed by slab discontinuous PAGE in SDS (see Appendix B) using pure ligandin as a positional marker for the Y peptide protein bands. Densitometry of stained protein bands in gels was performed with a Joyce Loebl Chromoscan apparatus, using a no. 5022 green filter.

3. Results

Phenobarbital treatment resulted in an increase in liver weight compared with that in control animals (Table 2.X). There were no differences in body weight or in the weight of kidneys, small intestinal mucosa and testes between phenobarbital-treated and control animals.

TABLE 2.X

EFFECT OF PHENOBARBITAL ON BODY AND TISSUE WEIGHT

Tissue	Phenobarbital-treated (g)	Controls (g)	P
Whole body	233.67 ± 7.91	239.37 ± 6.81	ns
Liver	16.78 ± 0.33	12.48 ± 0.72	<0.001
Kidney	1.80 ± 0.04	1.7 ± 0.09	ns
Small intestinal mucosa	2.45 ± 0.08	2.33 ± 0.13	ns
Testes	2.86 ± 0.04*	2.86 ± 0.09	ns

Results are expressed as Mean weight in grams ± SEM. Tissues from 8 animals were used for each determination, except in the case marked with an asterisk (*) where 4 animals were used. ns = no significant difference ($P > 0.05$).

The effect of phenobarbital treatment on immunoreactive ligandin concentration in liver, kidney, small intestinal mucosa and testis in shown in Table 2.XI. A significant increase in hepatic ligandin of 108% above control levels was associated with phenobarbital treatment. Lesser, but significant increases in ligandin above control levels were also observed in the kidney (26%) and small intestinal mucosa (51%) of phenobarbital-treated animals, while testicular ligandin concentration showed no change.

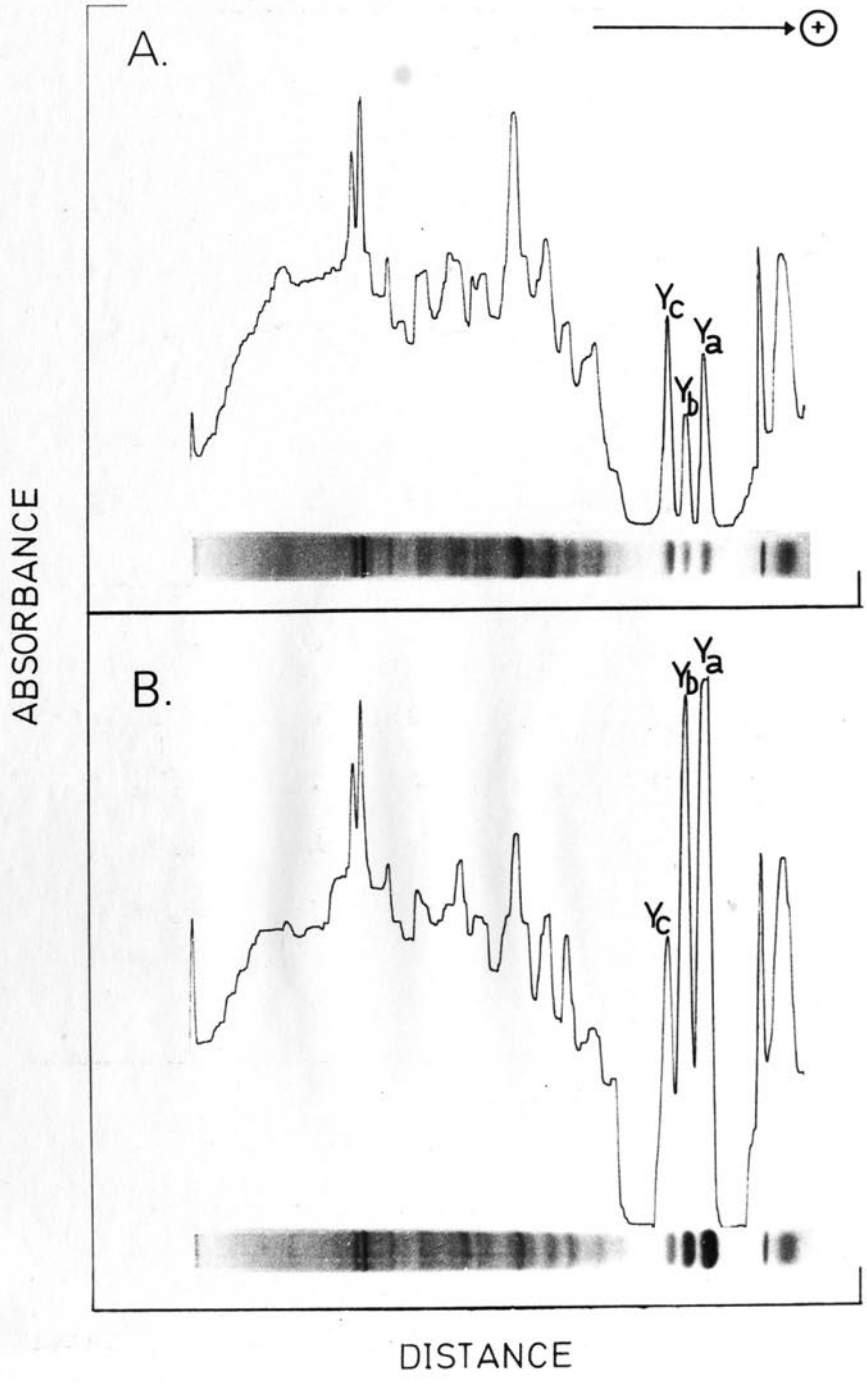

Fig. 2.24. Discontinuous slab PAGE in SDS of 50 µg of hepatic cytosol from (A), saline - and (B), phenobarbital-treated rats (12.5% resolving gel). After staining with Coomassie blue, gel strips containing protein bands were cut out and densitometry performed with a Joyce Loebl Chromoscan. Y_a, Y_b and Y_c indicate the peaks derived from the corresponding subunit bands in the gel.

TABLE 2.XI

EFFECT OF PHENOBARBITAL ON IMMUNOREACTIVE LIGANDIN CONCENTRATION

Tissue	Phenobarbital-treated (µg/mg)	Controls (µg/mg)	P
Liver	82.86 ± 2.47	39.93 ± 3.07	<0.001
Kidney	22.84 ± 1.81	18.19 ± 1.16	<0.05
Small intestinal mucosa †	10.16 ± 0.48	6.73 ± 0.41	<0.001
Testis	5.72 ± 0.42*	6.53 ± 0.45	ns

Results are expressed as Mean ± SEM in µg/mg supernatant protein. Tissues from 8 animals were used for each determination except in the case marked with an asterisk (*) where 4 animals were used. †: mucosa from the entire length of small intestine was used. ns: no significant difference ($P > 0.05$).

When whole hepatic cytosol from phenobarbital-treated rats was compared with that obtained from saline-treated controls by discontinuous PAGE in SDS, a marked incremental effect was consistently noted on the Y_a and Y_b subunit bands. A typical example of this effect is illustrated in Fig. 2.24. The increments in the Y peptides in the supernatant of phenobarbital-treated rat liver, relative to the corresponding components of control supernatant in Fig. 2.24 were estimated by densitometry as: subunit Y_a, 130%; subunit Y_b, 240% and subunit Y_c, 5%.

4. Discussion

The induction of hepatic ligandin by phenobarbital administration has been reported by workers using quantitative immunodiffusion (158, 159) and immunoprecipitation of GSH S-transferase B activity (217), and was confirmed in the present study by RIA. However, previous studies using quantitative immunodiffusion found no effect on renal (158, 159) or small intestinal mucosal (158) concentrations of ligandin following phenobarbital treatment. Indeed, Kirsch et al (159) could only induce renal ligandin with TCDD treatment. The differences obtained in renal and intestinal ligandin between phenobarbital-treated and control animals in the present study, might be attributable to the greater sensitivity and precision of the RIA method. It is noteworthy, that with one exception, phenobarbital induction of rat kidney enzymes has not been reported. The exception in this case was the finding of Clifton et al (214) of an exclusive increase in GSH S-aralkyltransferase (p-nitrobenzyl chloride) conjugating activity in the kidneys of rats treated with phenobarbital. However, these data are difficult to interpret in terms of ligandin, which in the purified state appears to have little activity towards this substrate (155).

The present study demonstrated an increase in the ligandin concentration of small intestinal mucosa with phenobarbital treatment. It is interesting to note in this connection, that Thomas et al (323) have shown that phenobarbital treatment stimulates the absorption of both haem and non-haem iron by rat duodenum. As one of the highest affinities reported

for ligandin is that for haem (see Chapter III.5 and Table 1.III), the role of ligandin in the intestinal transport of this substance merits consideration.

The hepatic subunit Y_a and subunit Y_c species showed clearly unequal responses to phenobarbital treatment. This phenomenon provides further evidence to support the hypothesis that ligandin comprises two dimeric proteins (Y_a-Y_a and Y_c-Y_c combinations) and that the Y_a-Y_c combination does not occur in vivo. Induction of hepatic GSH S-transferase activity towards several substrates (213) as well as Y fraction ligand-binding capacity (185, 201) have been shown to result from phenobarbital treatment. Thus the conclusion may be drawn from the findings of the present study (i.e. that subunit Y_a but not subunit Y_c increases significantly in response to phenobarbital treatment), that both catalytic activity and non-substrate binding activity reside in the Y_a-Y_a component of ligandin. These findings do not, however, exclude the possibility that the Y_c-Y_c component also possesses binding and catalytic properties. Strange et al (190) performed equilibrium dialysis studies on the hepatic Y fraction, which revealed the presence of both low and high affinity binding proteins for cholic acid. Phenobarbital treatment increased the amount of the low affinity but not of the high affinity binder in the rat hepatic Y fraction; and the question must be raised of whether and how these binding proteins of differing affinity and phenobarbital response relate to the subunit Y_a, subunit Y_b and subunit Y_c protein species defined in the present study.

As discussed in Chapter XI, the Y_b subunit species appears to represent the monomer of a major dimeric protein, Y_b-Y_b, in the Y fraction of hepatic and other tissue cytosols. Subunit Y_b, similarly to subunit Y_a, is increased in hepatic cytosol by phenobarbital treatment and thus although subunit Y_b is not a component of purified ligandin, the possibility exists that the dimeric proteins Y_a-Y_a, Y_b-Y_b and Y_c-Y_c form a structurally and functionally related group of proteins in vivo. However, the exact nature of the interrelationship between these Y peptide dimers is not clear. Certainly, the existence of the Y peptides in terms of a precursor-product series is an interesting possibility, although their unequal responses to phenobarbital treatment as well as the lack of apparent transition from one form to another on incubation of cytosol (see Chapter VII), would seem more in keeping with the hypothesis that each of the Y peptides represents a separate gene product.

It is attractive to envisage the lack of phenobarbital effect on the hepatic Y_c subunit as the reason for the lack of induction of immunoreactive ligandin in the testis, where only the subunit Y_c size component of ligandin is manifestly present. However, other general factors may be important as regards the refractory nature of the testis to phenobarbital treatment, as it has been shown that chronic phenobarbital treatment which induces hepatic cytochrome P-450, has no effect on cytochrome P-450 activity in the testis (324).

CHAPTER XIII

THE DEVELOPMENT OF LIGANDIN IN RAT LIVER AND KIDNEY

1. Introduction

The perinatal maturation of enzyme systems has been the subject of considerable investigation (for reviews see refs. 240 and 325). The development of ligandin in neonatal animals is important in relation to the development of drug-metabolising capacity at this stage of life, inasmuch as it is a member of the GSH S-transferases, a group of detoxifying enzymes of broad specificity towards a large range of xenobiotics. However, it is important to note that ligandin has a relatively narrow range of activities towards a large range of substrates (155), while on the other hand, its affinity for non-substrate ligands is greater than that of the other transferases (175). Thus specific measurement of ligandin is clearly desirable in relation to the study of organic anion clearance by the liver and kidney, and the development of these functions in neonatal animals. The developmental pattern of ligand-binding capacity and GSH S-transferase activity in rat liver and kidney have been described in several studies (185,188,203,225,226,244), but these measurements reflect contributions from each of the several GSH S-transferases, and no direct measurement of ligandin in the newborn and developing rat has been achieved. The present study aimed to provide for the first time, the specific developmental pattern of immunoreactive ligandin in the liver and kidney of the neonatal rat.

2. Methods

Experimental protocol:

The young rats of various ages used in this study were born in the laboratory and were the offspring of four female Wistar rats. Where animals were less than 20 days old, both sexes were used, while only males were studied beyond this age. Rats less than 40 days old were sacrificed by decapitation and allowed to exsanguinate, while older animals were sacrificed under ether anaesthesia (see Chapter VI.3.i). The liver and kidneys were removed, and in the case of animals less than 20 days old, sliced in several places and washed with ice-cold 0.9% saline to remove entrapped blood. Livers and kidneys of older animals were perfused as described in Appendix B. Six animals (2 from each of 3 litters) were used for estimations of renal and hepatic ligandin on the day of birth and on days 5, 9, 16, 25 and 37 following birth. Three animals (one from each of the 3 litters) were used for estimations on days 60 and 90 post-partum. Individual preparations of cytosol were made from the liver and both kidneys of each animal used in this study (see Appendix B) and assayed for ligandin by RIA. Protein concentration of cytosol was determined as described in Appendix B.

3. Results

The developmental patterns of hepatic and renal ligandin from birth to 90 days of age are illustrated in Fig. 2.25. On the day of birth, hepatic ligandin levels were about 4%

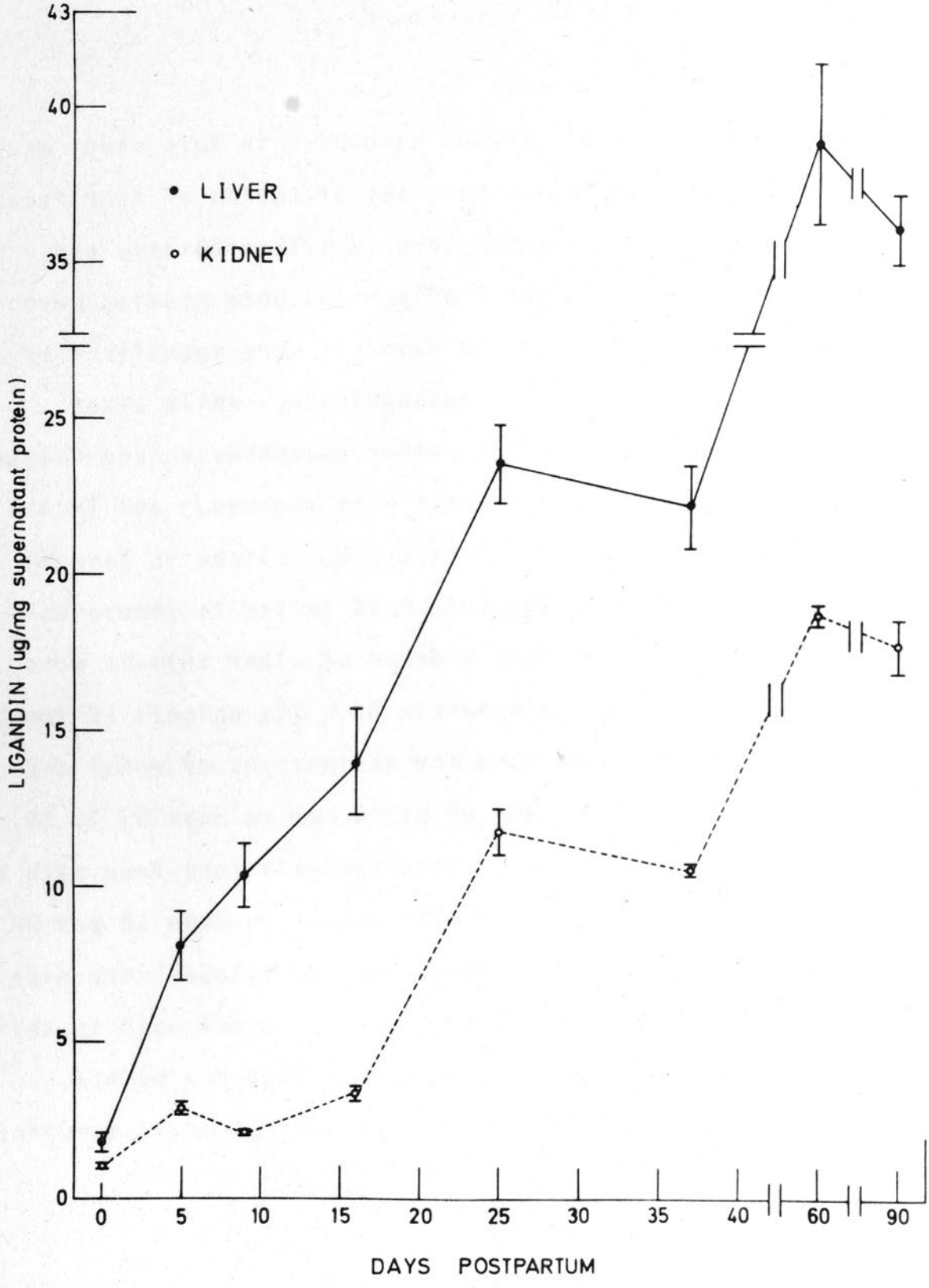

Fig. 2.25. Development of ligandin in the liver and kidney of the rat. Each point represents the mean ± SEM of six individual determinations up to 37 days, and thereafter 3 individual determinations.

of adult values. By the fifth day of life, hepatic ligandin increased to five times the level at birth and thereafter increased progressively to the fourth week post-partum, after which development plateaued till the seventh week. By day 60 of life, hepatic ligandin had attained adult levels and showed no change at 90 days post-partum.

Renal ligandin showed a decidedly different early developmental pattern from its hepatic counterpart. At birth, renal ligandin levels were approximately 6% of adult values and trebled during the first five days of life. No significant change occurred thereafter until the third week of life, during which time a dramatic increase in renal ligandin concentration occurred, reaching a peak by the fourth week post-partum ($\sim$ 70% of adult values). In a manner similar to hepatic ligandin development, a plateau occurred in renal ligandin development between the fourth and seventh weeks of life with attainment of adult levels by the sixtieth day post-partum.

4. Discussion

The ontogeny of ligandin has been studied in a number of species (see Chapter III.6.v), but the present discussion will be confined to available data concerning the rat. GSH S-transferase activity has been measured in the developing rat by Combes and Stakelum (225) and Bell and Echobicon (226) using BSP as substrate. The former workers observed a rapid development in the activity of "BSP-GSH conjugating enzyme" to 50% of adult values in the first 3 days post-partum, and

thereafter a more gradual rise in activity which reached adult levels by the seventh post-partum week. The study of the latter workers yielded a decidedly different pattern for the same enzyme activity. They found that the apparent Vmax of "BSP-GSH conjugating enzyme" did not alter significantly for the first 14 days of life, but increased sharply thereafter to a level three-fold higher than both levels by day 35. Furthermore, they were also able to demonstrate a change in the apparent Km of this enzyme activity after the third week of life. The marked lack of agreement in the reported developmental patterns of BSP conjugation, the great difficulty in interpreting changes in apparent Km and the poor BSP-conjugating activity of ligandin make the above data unsuitable for consideration in direct relation to the question of ligandin development and its correlation with the maturation of hepatic uptake.

The development of BSP-binding capacity should theoretically relate more effectively than BSP-conjugating activity to ligandin maturation, although BSP-binding is also complicated by the contributory effects of all the GSH S-transferases. The development of organic anion-binding capacity of whole hepatic cytosol in the rat was studied by Grodsky et al (188), while more specific data on the development of hepatic Y peak BSP-binding in the rat have been reported in two studies (185,203). Furthermore, while the present study was in progress, Hales and Niems (217) described the developmental patterns of both GSH S-transferase activity towards 1-chloro-2,4-dinitrobenzene and 3,4-dichloronitrobenzene in the rat, as well as the specific developmental pattern of

ligandin measured by immunoprecipitation of enzyme activity by specific antiserum to GSH S-transferase B. It is important to note that these workers clearly showed that the early developmental rate of conjugating activity was distinctly different for the two enzyme substrates studied. These workers' findings further suggest that during the first week of life, transferase B (ligandin) matures more rapidly than the other transferases collectively.

Some of the essential differences and similarities between the results of the present and of comparable studies are summarized in Table 2.XII. The similarity between the results of Foliot et al (203) and the present study is readily seen, while obvious differences are apparent between these two studies and those of Klaasen (185) and Hales and Niems (217). A possible explanation for these differences may be the fact that Wistar rats were employed in the present study and that of Foliot et al (203) while rats of the Sprague-Dawley strain were used in the other two studies. This however, does not reconcile the differences between the two studies using the latter strain (see Table 2.XII). The existence of qualitative differences between the different studies on ligandin development might also reflect the different techniques used to measure ligandin and to some extent, the differences in the post-partum days sampled in the different studies. The importance of establishing the developmental pattern of ligandin with accuracy must be stressed, especially as regards correlation with the maturation of uptake parameters. Unfortunately, no study of the development of isolated hepatic uptake has been per-

TABLE 2.XII

COMPARISON OF DATA ON THE DEVELOPMENT OF LIGANDIN IN RAT LIVER

Source of data	Strain of rats	Attainment of adult levels (day)	% Adult levels at birth	% Adult levels at 5 days	Early pattern
Present study	W	60	4	20	Rapid: days 1-25 Plateau: days 25-37
Foliot et al (203)	W	60	nd	17	Rapid: days 5-30 Plateau: not observed
Klaasen (185)	SD	35*	nd	10	Gradual: days 5-15 Rapid: days 15-35 Plateau: days 35-40
Hales & Niems (217)	SD	45	20 (day 1)	nd	Rapid: days 1- 8 Plateau: days 8-16 Rapid: days 16-30 Gradual: days 30-45

W: Wistar

SD: Sprague-Dawley

nd: Not determined

*: Values were less than comparable adult values reported in the same paper, but no developmental data later than 35 days were given.

formed in the rat, and it is thus not possible at this stage to correlate rat ligandin developmental data described in the present and previous studies with related uptake data.

Hales and Niems (217) have suggested that the GSH S-transferases follow a pattern of development which would include them in the group of liver enzymes accumulating in the third postnatal week, known collectively as the "late suckling cluster" (325). The emergence of this cluster of enzymatic activities coincides with several hormonal and dietary events. The early surge in hepatic ligandin development noted in the present study, and of GSH S-transferase B relative to the other transferases observed by Hales and Niems (217) would seemingly be more consistent with the classification of ligandin development along with the "neonatal cluster" of enzymes. This group of enzymes, which also includes glucuronyl transferase (325, 326), probably emerges in response to numerous factors arising from the separation of the foetus from the placental circulation. In the case of ligandin, an important factor governing its emergence may be the need to dispose of bilirubin. Indeed, the observation of Foliot et al (203) of a more rapid development of BSP-binding in Gunn rats than in normal Wistar rats, may be taken as evidence in favour of this hypothesis.

Pegg and Hook (244) compared the development of PAH transport and GSH S-transferase activity in the kidneys of newborn and week-old rats. These authors concluded that no correlation existed between these two parameters, as renal

GSH S-transferase activity in week-old rats was not significantly different from adult kidney levels, whereas PAH transport capacity in week-old rats was clearly less than that in adult rats. However, the developmental pattern of immunoreactive renal ligandin observed in the present study was considerably different from the pattern of renal GSH S-transferase maturation found by Pegg and Hook (244). The development of immunoreactive ligandin in the kidney is different from that in the liver, while in common with the majority of renal enzymes, displays the phenomenon of a late (14-19 days) precipitous rise (325). It is nevertheless not easy to see a distinct correlation between the developmental pattern of immunoreactive rat kidney ligandin and the detailed maturation profile of in vitro rat kidney transport of PAH. This latter process, according to Kim et al (327), was inefficient at birth (∿ 30% adult values), doubled at 10 days of life, then declined until day 14 with a subsequent gradual increase to adult levels. A simultaneous study of both the development of PAH uptake and ligandin in the kidney would probably be of more conclusive value in deciding the role of ligandin in the renal transport of organic anions.

CHAPTER XIV

PURIFICATION AND CHARACTERIZATION OF SUBUNIT Ya - LIGANDIN

1. Introduction

During the course of the present study, several observations were made (see Chapters XI and XII) which led to the conclusion that ligandin comprises two separate dimeric proteins: a species composed of two 21,000 dalton subunits (subunit Y_a species) and a species composed of two 23,000 dalton subunits (subunit Y_c species). These two "size heteromers" of ligandin differ in tissue distribution and response to phenobarbital treatment, but appear to be closely related in terms of size, charge and antigenic properties. Two main questions are posed concerning the two subunit variants of ligandin:

(1) Are they precursor-product related i.e. does subunit Y_a derive from subunit Y_c, or are they the products of separate genes?

Evidence presented and discussed thus far (Chapter XII) appears to be in favour of the latter possibility but does not entirely rule out the former from being the case.

(2) In what manner do the subunit Y_a and subunit Y_c proteins contribute to the functional properties of ligandin viz. GSH S-transferase activity and non-substrate binding affinity?

The likelihood of both of these properties residing in the subunit Y_a species has been discussed (see Chapter XII),

but a direct answer to this question would only be provided by studying the binding and catalytic properties of homogenous forms of both the subunit Y_a and subunit Y_c proteins. Towards this end, several methods were used in attempts to isolate both these species in pure form. These attempts were unfortunately only partially fruitful, in that only the subunit Y_a species was eventually isolated in a form suitable for the study of its individual properties.

This chapter deals mainly with the successful purification of the subunit Y_a component of hepatic ligandin (Y_a - ligandin) and its characterization, while giving a brief account of the unsuccessful manoeuvres employed in attempts to achieve isolation of both subunit Y_a and subunit Y_c species.

2. Methods

Isolation procedures:

Ligandin containing both subunit Y_a and subunit Y_c components was purified as described in Chapter VII. The isolation of subunit Y_a and subunit Y_c from purified ligandin was attempted using the following procedures:

(1) Renaturation from PAGE-SDS

This was performed as described by Weber and Kuter (328). In brief, ligandin was separated into peptide components by slab discontinuous PAGE in SDS (see Appendix B). A strip was cut off the gel lengthwise so as to contain half of a set of protein bands and rapidly stained with

Coomassie brilliant blue. This permitted location across the gel of the protein bands from samples loaded in each bay. The areas containing the Y_a and Y_c peptides were carefully excised and eluted separately in 0.1% SDS. Electrophoretic elution of entrapped protein from gel slices into small dialysis bags was also employed on occasions. Staining of the remaining gel revealed no residual protein bands. Y_a and Y_c eluates were separately pooled, dialysed against Tris:acetate/urea/2-mercaptoethanol buffer (328) and passed through small columns of Dowex AG 1-X2 resin to remove SDS. Urea was removed from eluates by dilution in Tris:acetate/2-mercaptoethanol/EDTA buffer followed by concentration and dialysis against the same buffer.

(2) 1 ml of purified ligandin was made 1% in SDS and chromatographed on a 1.6 x 90 cm column of Sephadex G-50 in 0.01M sodium phosphate buffer pH 7.4 / 1% SDS. The flow rate was 20 ml/h and 1 ml fractions were collected.

(3) Purified ligandin was dialysed against 0.01M Tris:HCl buffer pH 9.1 (I = 0.002M), and chromatographed on a 38 x 2.5 cm column of QAE-Sephadex in the same buffer at a flow rate of 45 ml/h with collection of 3 ml fractions. This procedure was also performed with 0.01M Tris:HCl buffer pH 9.2, using a linear 500 ml gradient of 0 to 0.01M NaCl in the same buffer to elute protein from the column.

(4) Ligandin was purified from 100g of rat liver by a modification of the method described in Chapter VII. The two essential departures from the standard method were:

(1) the rats used were first treated with phenobarbital according to the schedule outlined in Chapter XII, and

(2) both anion-exchange chromatography steps and prior dialyses were carried out using pH 9.1 Tris buffer (see (3) above).

General analytical procedures:

Estimation of protein and BSP in column eluates as well as molecular weight estimation of undissociated Y_a-ligandin by Sephadex G-75 chromatography was performed as described in Chapter VII. Quantitative estimation of protein concentration, discontinuous slab PAGE-SDS and isoelectric focusing in the pH 7-9 range was performed as described in Appendix B.

Enzyme assay:

GSH S-transferase activity was measured spectrophotometrically with 1-chloro-2,4-dinitrobenzene, 3,4-dichloronitrobenzene, BSP and p-nitrobenzyl chloride as substrates (155). Details of these assays are given in Appendix B.

Amino acid analysis:

Amino acid analysis of purified Y_a-ligandin was performed

in collaboration with the Department of Biochemistry, University of Cape Town. 1 mg aliquots of the protein were hydrolysed for 27, 49 and 73h and analysed on a Beckman Model 120C amino acid analyser, according to the procedure of Moore and Stein (329). Tryptophan was determined spectrophotometrically (330). Details of these procedures are given in Appendix B.

Binding studies:

For the purpose of these experiments, a molecular weight of 46,000 was assumed for Y_a-ligandin dimer. Bilirubin was recrystallized from chloroform/methanol as described by Ostrowet al (331). The εmM of recrystallized bilirubin at 437 nm in 0.01M NaOH was 52 mM^{-1} cm^{-1}, a figure in complete agreement with that determined by Blauer and King (25). The binding of bilirubin to Y_a-ligandin was determined by the difference spectrophotometry method described by Tipping et al (164) in 0.05M Tris:HCl buffer pH 8.2/0.1M KCl at a protein concentration of 5 µM. Changes in absorbance with increasing amounts of bilirubin added to ligandin were monitored at 474 nm (the maximum in the difference spectrum of the bilirubin-ligandin complex). The $\Delta\varepsilon$mM for bilirubin-ligandin complexes at the lowest bilirubin:protein ratio was 20.7 mM^{-1} cm^{-1}, a value similar to that of 20.4 mM^{-1} cm^{-1} reported by Tipping et al (164).

The binding of (^{35}S) BSP to Y_a-ligandin was determined by equilibrium dialysis according to the method of Kamisaka et al (167) in 0.01M sodium phosphate buffer pH 7.4 for 72h

at room temperature. The glass dialysis chambers utilized 1.5 ml of protein solution (4 μM) on one side of the membrane and protein-free buffer on the other side. The recovery of counts from (^{35}S) BSP added to dialysis chambers after incubation was approximately 98%, while no adsorption of protein was detected. Detailed descriptions of all binding study methodology are given in Appendix B.

The results of binding experiments were analysed by the method of Scatchard (317). From the mass action law, the equation for the binding of small ligands to macromolecules can be expressed as:

$$\bar{\nu}/L = (N - \bar{\nu})K_a$$

where $\bar{\nu}$ is the molar ratio of ligand to protein;

L is the concentration of unbound ligand;

N is the number of binding sites in a single class;

K_a is the association constant.

Linear plots of $\bar{\nu}$ against $\bar{\nu}/L$ were calculated by the method of least squares (see Appendix C).

Immunology:

RIA was performed as described in Chapter X. Antiserum to Y_a-ligandin was raised in rabbits according to the protocol given in Chapter VIII. Immunodiffusion and immunoelectrophoresis were carried out as described in Appendix B.

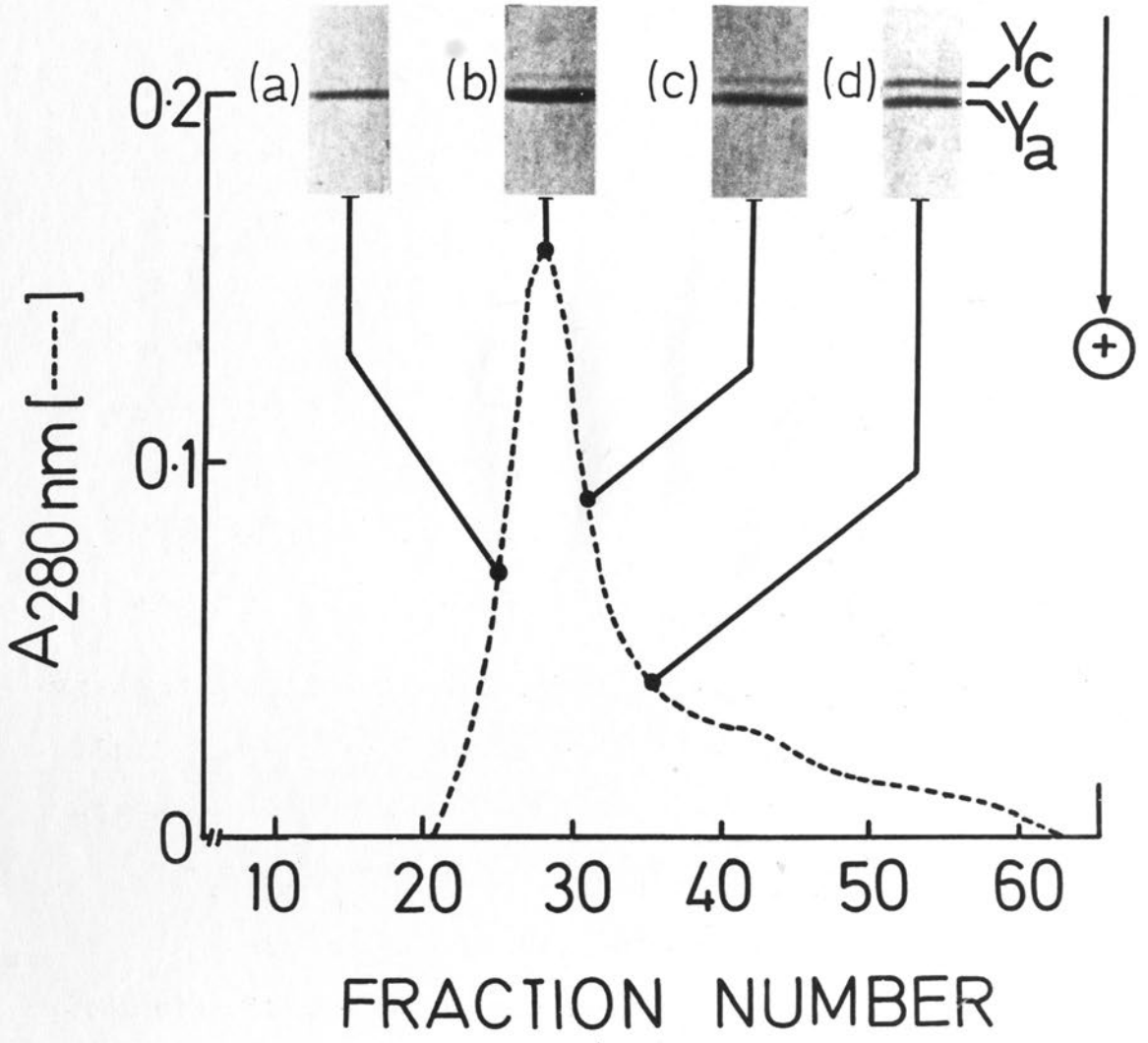

Fig. 2.26. Chromatography of ligandin on QAE-Sephadex in 0.01M Tris:HCl pH 9.1. Approximately 5 mg of ligandin in 5 ml was chromatographed on QAE-Sephadex as described in Methods. Aliquots of 25 µl from fractions (a), 25; (b), 28; (c), 32 and (d), 35 were analysed by discontinuous slab PAGE in SDS (10% resolving gel). Y_a and Y_c represent the ligandin subunit species.

3. Results

Purification of Y_a-ligandin:

An attempt was made to recover Y_a and Y_c peptides from discontinuous PAGE-SDS, as this technique had shown excellent separation of these two components of ligandin. However, all attempts to renature protein bands from the gels led to complete loss of detectable protein and immunoreactivity. Separation of Y_a and Y_c peptides by molecular sieve chromatography in SDS was thus tried, but only a single, symmetrical peak eluted in the 20-30,000 dalton zone, which on PAGE in SDS revealed the presence of both Y_a and Y_c bands.

The effect of QAE-Sephadex anion exchange chromatography on separating the Y_a and Y_c components of ligandin was explored at pH 9.1. Protein eluted from this column as a single major peak with a fairly prominent amount of "tailing" (see Fig. 2.26). The early peak fractions appeared to contain only subunit Y_a species uncontaminated with subunit Y_c, but this latter species increased progressively in all subsequent fractions containing protein, and was present in equal proportion to subunit Y_a in the later fractions of the peak. This retardation effect of anion exchange chromatography on the subunit Y_c component of ligandin suggested a less basic pI for this species relative to the subunit Y_a component. Although partial separation of subunit Y_a-ligandin from a mixture of subunit Y_a and subunit Y_c components was achieved by this method, the yield of pure Y_a-ligandin was inadequate for further study. When ligandin was chromatographed on QAE-Sephadex at pH 9.2, no protein eluted from

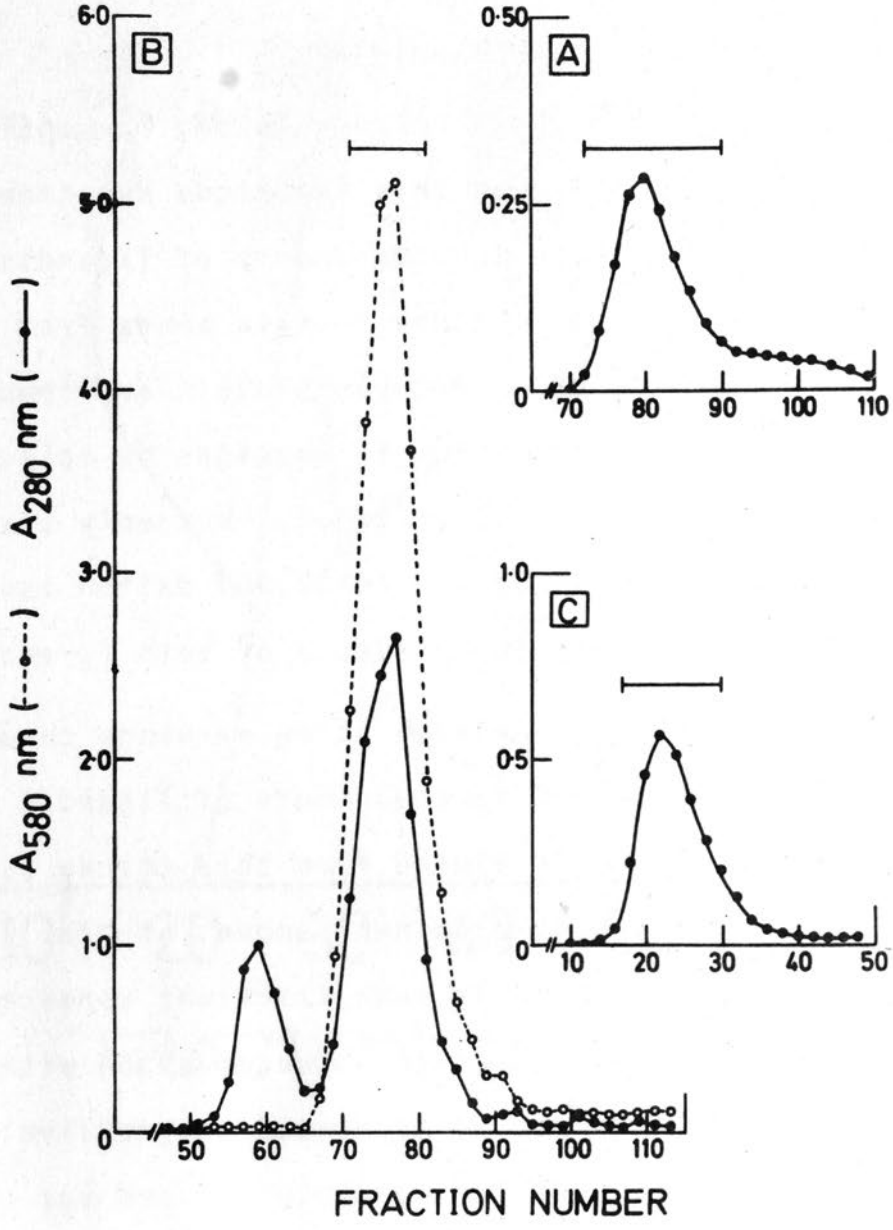

Fig. 2.27. Purification of Ya-ligandin from the 100,000 xg supernatant of phenobarbital-treated rat liver. (A), Elution of protein from TEAE-cellulose in 0.01M Tris:HCl buffer pH 9.1. (B), Elution of protein and BSP from Sephadex G-100 in 0.01M phosphate buffer pH 7.4/0.1M NaCl. (C), Purification of the BSP-binding peak on QAE-Sephadex in 0.01M Tris:HCl buffer pH 9.1. Fractions pooled at each stage of purification are indicated by the horizontal bars. (See Methods and Results for details).

the column. Elution by means of a salt gradient resulted in recovery of a single protein peak without separation of the two ligandin components.

Y_a-ligandin was purified from the livers of rats treated with phenobarbital using anion exchange chromatography at pH 9.1. It was hoped that this approach would give a high yield of pure Y_a-ligandin, firstly, by the selective effect of phenobarbital treatment on Y_a-ligandin (see Chapter XII), and secondly, by availing itself of the relatively less basic pI of Y_c-ligandin in eliminating this species during the ion exchange steps of purification. The elution profiles of protein from TEAE-cellulose and QAE-Sephadex and of protein and BSP from Sephadex G-100 obtained during the purification of Y_a-ligandin are shown in Fig. 2.27 (cf Fig. 2.1). Fractions from each stage of purification were analysed by discontinuous slab PAGE-SDS as shown in Fig. 2.28 (cf Fig. 2.2). The Y_c subunit band was no longer detectable after the first anion exchange step (Fig. 2.28B). At this stage of purification, only two major bands were evident on PAGE SDS analysis: a band corresponding to subunit Y_a and a relatively higher molecular size band which was found to obtain from the leading protein peak eluting from Sephadex G-100 (Fig. 2.27B). The effect of phenobarbital was clearly evident from the considerable increase in the BSP-binding peak eluting from this column. This peak, as well as the peak eluting from QAE-Sephadex (Fig. 2.27C), was found to contain only subunit Y_a bands without any detectable subunit Y_c contamination (Fig. 2.28C and D).

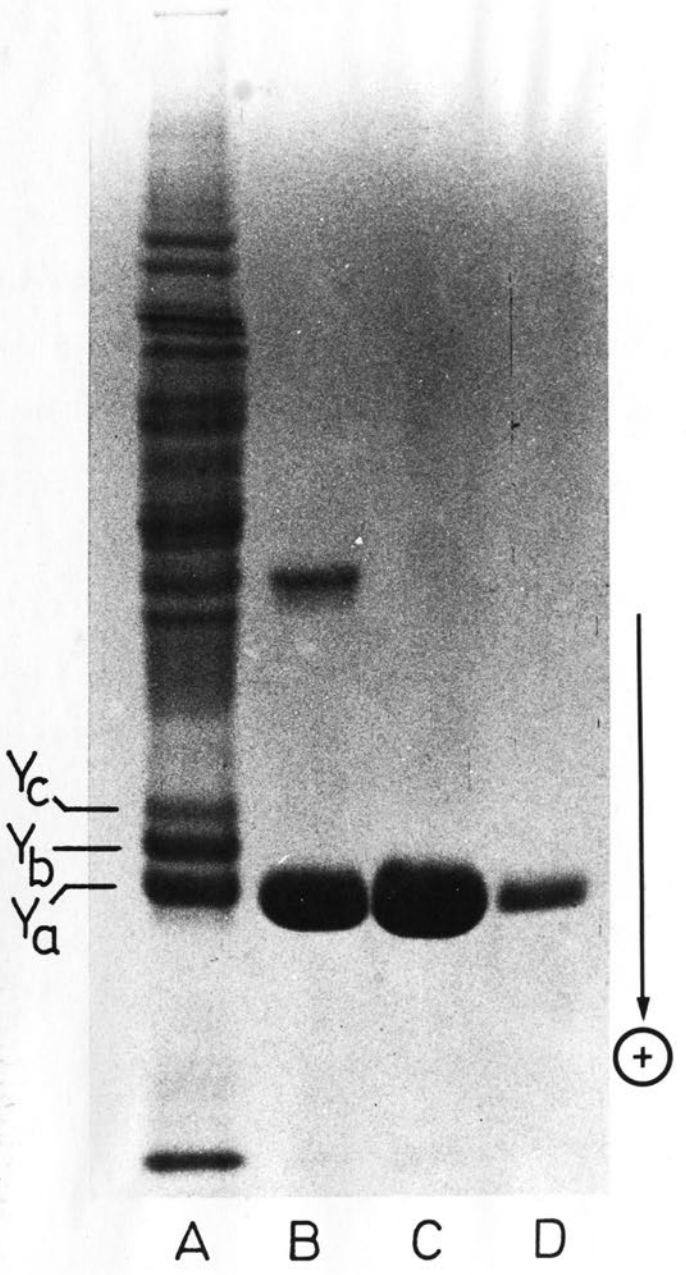

Fig. 2.28. Discontinuous slab PAGE in SDS (12.5% resolving gel) of (A), hepatic 100,000 xg supernatant from phenobarbital-treated rats; (B), pooled and concentrated protein peak from TEAE-cellulose; (C), pooled and concentrated BSP-binding peak from Sephadex G-100, and (D), pooled protein peak from QAE-Sephadex. Y_a, Y_b and Y_c represent the major subunit polypeptides found in the Y fraction of hepatic cytosol (cf Figs. 2.2 and 2.3).

TABLE 2.XIII

SUMMARY OF PURIFICATION OF Y_a-LIGANDIN FROM PHENOBARBITAL TREATED RATS

Purification Step	Volume (ml)	Total Protein (mg)	Total Activity* (µmol/min)	Specific Activity* (µmol/min/mg)
1. Homogenate	350	21,000	24,780	1.18
2. 27,000 xg supernatant	200	6,800	14,212	2.09
3. 100,000 xg supernatant (concentrated)	30	2,577	11,403	4.42
4. TEAE-cellulose (concentrated)	9.6	120	2,638	22.0
5. Sephadex G-100 (concentrated)	7.9	68	†	†
6. QAE-Sephadex (concentrated)	46	50.8	1,289	25.2

* Determined with 1-chloro-2,4-dinitrobenzene as substrate

† The presence of BSP interference invalidates enzyme assay results at this step of purification.

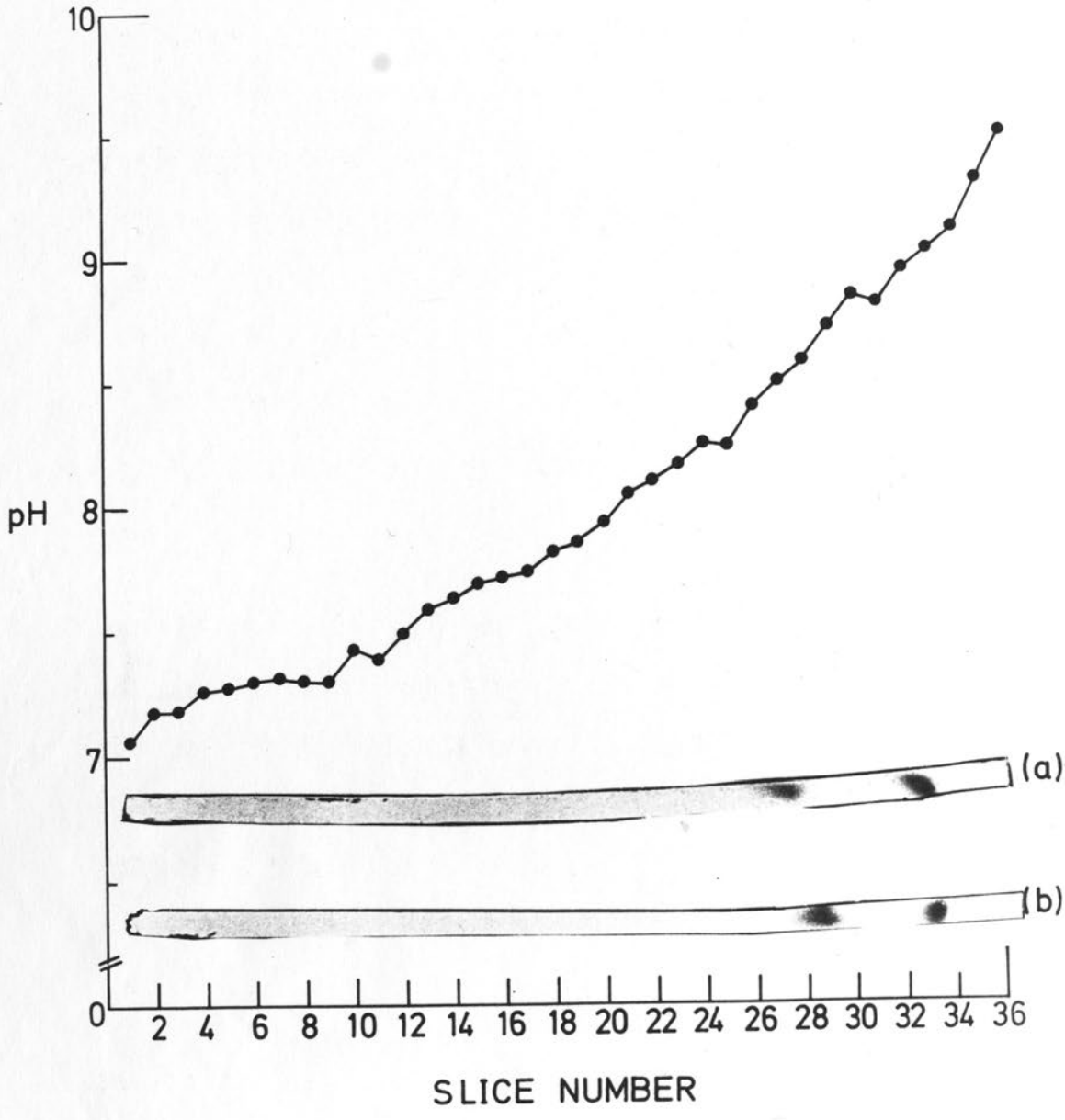

Fig. 2.29. Isoelectric focusing in polyacrylamide gel in the pH 7-10 range of (a), Y_a-ligandin and (b), Y_a/Y_c ligandin. Isoelectric focusing was performed in an MRA apparatus, and gels were stained by the method of Ketterer (281). (See Appendix B for details of procedure).

The conjugation of 1-chloro-2,4-dinitrobenzene with GSH was used to monitor the course of Y_a-ligandin purification (Table 2.XIII). Purification of Y_a-ligandin resulted in a recovery of 5% of the total 1-chloro-2,4-dinitrobenzene conjugating activity from liver homogenate, while a 20-fold purification of Y_a-ligandin from homogenate was obtained. The effect of phenobarbital treatment is again evident from the high specific activity of the 100,000 xg supernatant given in Table 2.XIII (cf Table 2.IX).

Molecular size:

Y_a-ligandin migrated on discontinuous PAGE in SDS as a single band (see Fig. 2.28D) of molecular size 21,000 daltons by comparison with standard proteins. On Sephadex G-75 chromatography, Y_a-ligandin eluted as a single, symmetrical protein peak with a comparative molecular size of 46,000 daltons.

Isoelectric focusing:

When Y_a-ligandin was focused in the pH 7-10 ampholine range in polyacrylamide gel, two bands of protein in equal proportion were evident on staining, corresponding exactly to those observed when ligandin (subunit Y_a and subunit Y_c components) was analysed by this technique (Fig. 2.29, cf Fig. 2.6B).

Amino acid analysis:

The amino acid composition of Y_a-ligandin is presented in Table 2.XIV together with the range of values quoted by

several workers for ligandin (both subunit Y_a and subunit Y_c components). As shown in Table 2.XIV, there was little apparent difference between the amino acid profile of Y_a-ligandin and the analyses previously described for ligandin.

TABLE 2.XIV

AMINO ACID ANALYSIS

Moles of amino acid/mole of protein*

Amino Acid	Y_a-ligandin	Ligandin (Refs: 1,14,155,159,163)
Lysine	35	33-36
Histidine	4	5-6
Arginine	20	21-22
Aspartic acid	31	34-37
Threonine †	12	11-12
Serine †	14	13-18
Glutamic Acid	40	39-46
Proline	17	16-20
Glycine	16	18-21
Alanine	26	26-31
Cysteine	nd	2-4
Valine	17	16-25
Methionine	12	8-15
Isoleucine	18	18-19
Leucine	46	46-50
Tyrosine	12	12-15
Phenylalanine	15	17
Tryptophan ‡	1	2-9
Amide $-NH_3$	21	nd

* All analyses based on a protein molecular weight of 45,000

† Determined by extrapolation to zero hydrolysis time (see Appendix B)

‡ Determined spectrophotometrically in 0.1M NaOH (see Appendix B)

nd Not determined

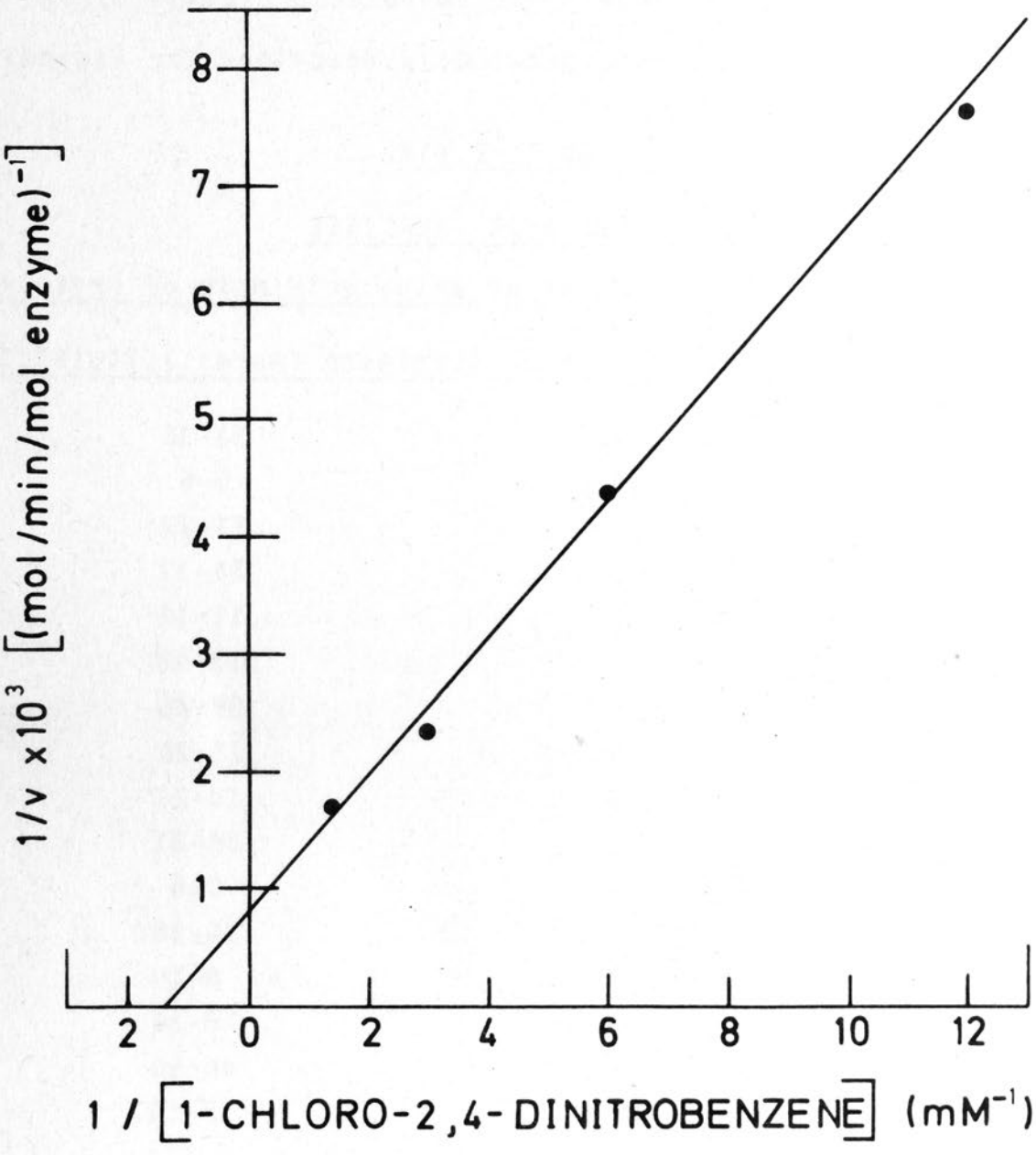

Fig. 2.30. Double-reciprocal plot of reaction velocity (v) as a function of substrate concentration for the conjugation of 1-chloro-2,4-dinitrobenzene with GSH by Ya-ligandin. $1/V_{max}$ is represented by the ordinate intercept, $1/Km$ by the abscissa intercept. Each point represents the mean of duplicate determinations.

GSH S-transferase activity:

The activity of Y_a-ligandin with several substrates is shown in Table 2.XV.

TABLE 2.XV

GSH S-TRANSFERASE ACTIVITY OF Y_a-LIGANDIN

Substrate	Specific Activity (μmol/min/mg)
1-Chloro-2,4-dinitrobenzene	25.2
3,4-Dichloronitrobenzene	0.027
BSP	0*
p-Nitrobenzyl chloride	0.70

Specific activities were determined under the standard assay conditions described by Habig et al (155; see Appendix B for details). * No activity observed at the highest enzyme concentration used.

The specific activity of Y_a-ligandin with 1-chloro-2,4-dinitrobenzene was twice the value previously reported for transferase B, while activities with 3,4-dichloronitrobenzene and p-nitrobenzyl chloride were nine and seven times higher respectively (see Table 1.II). Fig. 2.30 shows the double-reciprocal plot of v versus {S} obtained for Y_a-ligandin conjugation of 1-chloro-2,4-dinitrobenzene. The Km obtained with this substrate was 0.73 mM, a value similar to that of ligandin (GSH S-transferase B) while the Vmax was 1,280 moles/

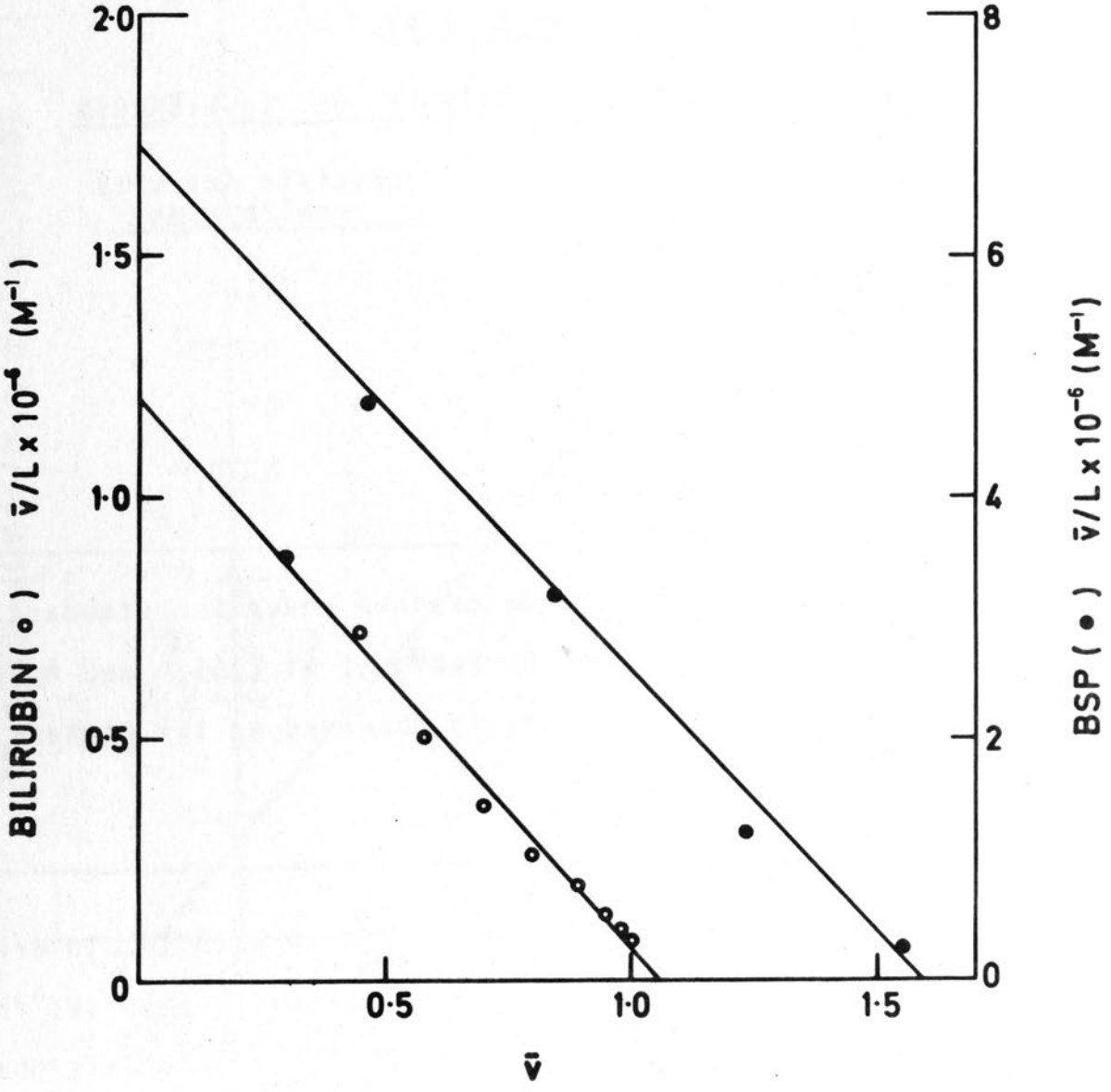

Fig. 2.31. Scatchard plot for the binding of bilirubin (difference spectrophotometry) and BSP (equilibrium dialysis) to Ya-ligandin. Each point represents the mean of duplicate determinations.

min/mole enzyme, a value 50% greater than the corresponding value reported for transferase B (see Table 1.II).

Binding properties:

The Scatchard plots for the binding of BSP and bilirubin to Y_a-ligandin are shown in Fig. 2.31. Bilirubin was bound to Y_a-ligandin at a single primary binding site. Although a linear plot for BSP binding was obtained, implying interaction at a single class of binding sites, the value of N for BSP of 1.5 might conceivably reflect binding at a single primary site with effects due to interaction at lower affinity secondary site(s). Under the given experimental conditions, the association constants (K_a) obtained for the two ligands were 4.5×10^6 M^{-1} for BSP and 1.1×10^6 M^{-1} for bilirubin. The value of K_a for bilirubin interaction with Y_a-ligandin is the same as that obtained by Tipping et al (164) for ligandin using the same method (1×10^6 M^{-1}), while K_a for BSP-binding compares favourably with the value of 6×10^6 M^{-1} for ligandin estimated by Kamisaka et al (167) under conditions essentially the same as those employed in the present study. Tipping et al (191) obtained a higher value for the association constant of BSP-binding to ligandin by equilibrium dialysis (1.1×10^7 M^{-1}), but experimental conditions differed with respect to volumes of incubation, pH and ionic strength from those of Kamisaka et al (167) and the present study.

Immunological properties:

Y_a-ligandin generated a single precipitin line on

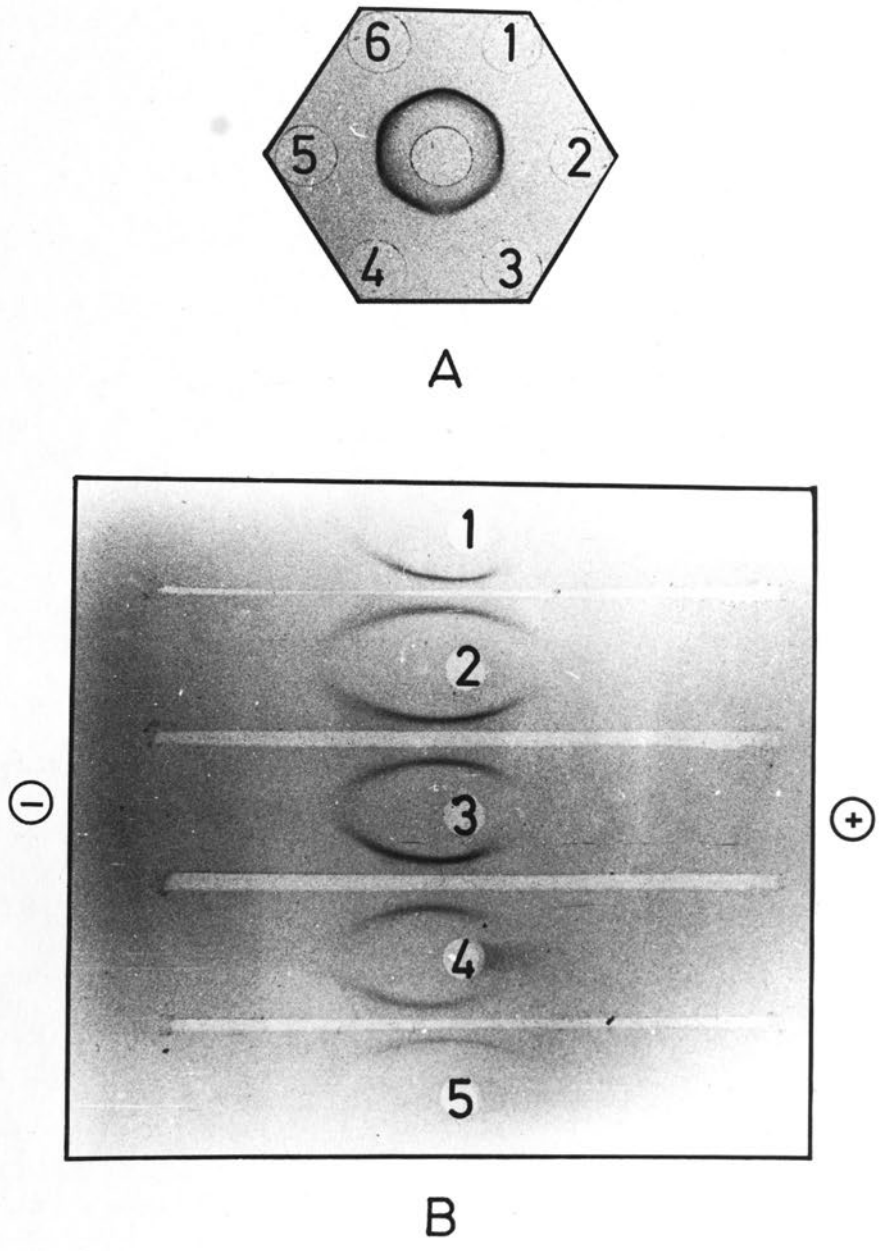

Fig. 2.32. Immunodiffusion and immunoelectrophoresis in agar gel. (A), The centre well contains rabbit anti-(Y_a-ligandin) antiserum. Peripheral wells contain: 1 and 5, 1 µg Y_a-ligandin; and cytosol from 2, liver (1:4); 3, kidney (1:2); 4, testis and 6, small intestinal mucosa. (B), Immunoelectrophoresis in agar gel. The wells contain cytosol from 1, small intestinal mucosa; 2, liver (1:4); 4, testis and 5, kidney (1:2) with Y_a-ligandin (1 µg) in well 3. The troughs contain rabbit anti-(Y_a-ligandin) antiserum. Precipitates were stained with amidoblack. (See Appendix B for details of procedures).

immunodiffusion and immunoelectrophoresis with rabbit anti-ligandin antiserum and GAL-IgG and further, gave a dose response curve identical both qualitatively and quantitatively with the standard curve of the RIA for ligandin. Antiserum raised in rabbits against Y_a-ligandin gave a single precipitin line on immunodiffusion against supernatants of liver, kidney, small intestinal mucose and testis (Fig. 2.32A). Interestingly, no line of partial identity similar to that seen on immunodiffusion of testis cytosol against antiserum to ligandin (Y_a and Y_c components), was evident with testis cytosol and antiserum to Y_a-ligandin. The same antiserum also gave a single precipitin arc with Y_a-ligandin and the abovementioned tissue supernatants on immunoelectrophoresis (Fig. 2.32B).

4. Discussion

The results of the present study afford conclusive evidence that the subunit Y_a component of hepatic ligandin constitutes the monomer of a 46,000 dalton dimeric protein, which possesses both binding and GSH S-transferase catalytic properties. Y_a-ligandin showed higher specific activities than those reported for ligandin with several substrates (155). This raises the possibility that the Y_a-ligandin prepared from phenobarbital-treated rats was contaminated to some extent by the presence of other transferases, notably A and C. These members of the GSH S-transferase family have much higher activity with substrates such as 1-chloro-2,4-dinitrobenzene (transferase A), p-nitrobenzyl chloride and

3,4-dichloronitrobenzene (both transferases A and C), than those reported for transferase B (155). The possibility of contamination also bears the implication that phenobarbital treatment markedly enriches a "subunit Y_a" size component of transferases A and/or C in rat liver. Indeed, in this regard it has been shown that transferase A has two different components of the same size as the Y_a and Y_c components of ligandin (168), although the analogous subunit properties of transferase C are, as yet, unknown. However, several points emerged which suggest that significant contamination of Y_a-ligandin with identical sized components of other transferases was not, in fact, the case:

(1) Y_a-ligandin showed no activity with BSP. This substrate is conjugated 30 to 90 times more efficiently by transferases C and A respectively than by transferase B (155). It is therefore important to consider the possibility, that the difference in catalytic profile between Y_a-ligandin and that established for transferase B reflects freedom from as yet undefinable effects induced by the presence of the subunit Y_c component.

(2) On isoelectric focusing of Y_a-ligandin, two protein bands were observed which corresponded to those observed in the present study and that of Habig et al (155) for ligandin. No bands of apparently lower pI, attributable to transferases A or C (155), were evident. From this finding it is also apparent, that the two bands observed on electrofocusing of ligandin (Y_a and Y_c components)

cannot be attributed on a one-to-one basis to the subunit Y_a and subunit Y_c component of ligandin. The finding in the present study of a less basic pI for Y_c-ligandin relative to Y_a-ligandin on QAE-Sephadex separation, might have supported this speculation; however, it is obvious that the subunit Y_a component alone can give rise to both charge species observed on isoelectric focusing. At this stage it is not clear whether these charge species arise as a result of purification, or reflect in vivo microheterogeneity.

(3) The amino acid analysis of Y_a-ligandin bears a marked proximity to the published analyses of ligandin, while differing sufficiently from those of the other transferases (155,157) to exclude the possibility of significant contamination by these species. It should also be noted that the low content of tryptophan present in Y_a-ligandin, although not matching the high content of 9 residues/molecule determined for transferase B by Habig et al (155), corresponds with the data of several other workers who have found only 2 residues of tryptophan/molecule of ligandin (1, 14, 131, 163; see also Chapter III.3). The great similarity between the amino acid analysis of Y_a-ligandin and those of ligandin (Y_a and Y_c components) would also imply a definite structural relationship between the subunit Y_a and subunit Y_c components of ligandin, although some preliminary studies (Bhargava, personal communication) employing peptide mapping and chemical substitution of ligandin suggest

that the two components differ in primary structure.

(4) Transferases A and C are immunologically distinct from transferase B (ligandin), and the lack of heterogenous effects in the immunological reactions of Y_a-ligandin both in the ligandin (Y_a and Y_c component) RIA, and also on immunodiffusion and immunoelectrophoresis with specific anti- (Y_a-ligandin) antiserum, could be taken as evidence against the presence of significant quantities of other transferase components in Y_a-ligandin purified in the present study. The cross-reaction of testis cytosol, which contains a subunit Y_c but not a subunit Y_a size component, with antiserum to Y_a-ligandin, provides strong evidence of an antigenic similarity between the Y_a component of liver and the Y_c component of testis (and inferrentially, of liver). The lack of a reaction of partial identity in this instance is interesting, as it suggests that this phenomenon, observed with testis cytosol and antiserum to both hepatic Y_a and Y_c components (see Chapter XI), is due to the presence of antibodies directed against an antigenic determinant of the Y_c component of hepatic ligandin interacting with one of the Y-fraction (40-50,000 dalton class) proteins of the testis.

GSH S-transferase AA has a catalytic profile closely similar to ligandin and gives a single band on isoelectric focusing identical to the more basic of the two ligandin bands (157). However, the arguments against transferase A

and C contamination of Y_a-ligandin, based on amino acid analysis and immunological behaviour ((3) and (4) above), are equally valid against transferase AA contamination. A further point in this regard is that transferase AA inexplicably, but consistently, exhibits two protein bands of 44,000 and 23,000 molecular size on PAGE in SDS (157). The definite absence of a 44,000 molecular size component on PAGE-SDS analysis of Y_a-ligandin also excludes the significant presence of transferase AA in this preparation.

The results of binding studies performed with Y_a-ligandin indicate that ligands are bound at a single site on this protein. Y_a-ligandin is composed of two Y_a subunits, and it is possible that both subunits co-operate in forming the ligand-binding site of this protein. Experiments in which substituted derivatives of ligandin (Y_a and Y_c components) were studied for non-substrate binding and catalytic activity, have concluded that the binding and catalytic sites of ligandin are chemically distinct (Bhargava, personal communication). The present study has clearly shown that these findings do not necessarily relate to separate properties of the Y_a and Y_c components of hepatic ligandin, but that both properties do reside on the Y_a component alone; although it is possible that these properties reside at different sites on this protein. The observations made in the present study do not exclude the possibility that the subunit Y_c component of hepatic ligandin also has binding and catalytic properties, or that it may in some way act to modify these properties of Y_a-ligandin. This complex question can only be answered

satisfactorily when the isolation of the subunit Y_c component of hepatic ligandin has been successfully achieved.

SECTION C

LIGANDIN IN PHYSIOLOGICAL FLUIDS: IMPLICATIONS FOR USE AS A DIAGNOSTIC TOOL

CHAPTER XV

LIGANDINAEMIA AS AN INDEX OF HEPATOCELLULAR NECROSIS

1. Introduction

The release of enzymes into the circulation following tissue necrosis was first appreciated seventy years ago, but only became recognized as a phenomenon of clinical importance in the mid-1950's. The observations made at this time concerning the release of transaminases into the plasma following myocardial infarction and viral hepatitis, gave birth to the ever-expanding field of clinical enzymology, a discipline concerned mainly with the diagnostic applications of intracellular enzymes released into the circulation from damaged tissues (for reviews see refs. 332-335). The liver contains a large variety of enzymes in great abundance, many of which show increased plasma activities in liver disease. Probably the most useful and certainly the most widely estimated of these enzymes are the transaminases (332, 333), which often show massively raised activity in the serum of patients and experimental animals with hepatocellular necrosis.

The usefulness of a particular serum enzyme measurement in the diagnosis of tissue necrosis is dependent upon a number of factors, but is largely decided by the organ-specificity of that enzyme and its sensitivity. For example, the enzyme glutamic-oxalacetic transaminase (GOT) is a sensitive indicator of liver cell damage but is richly distributed in other tissues as well, while "liver-specific" enzymes

such as sorbitol dehydrogenase, are insensitive and generally not of much use in diagnosis (333). The sensitivity or degree of elevation of a particular serum enzyme estimation in relation to tissue necrosis is again dependent on many factors influencing its release, extracellular distribution and elimination. The release of an enzyme from damaged cells is of prime importance in this regard. This is not a well understood mechanism, but is dependent, amongst other things, upon the intracellular distribution, molecular size and, most important, the concentration gradient of the enzyme between the intra- and extracellular space (333, 335). Ligandin is present in considerable abundance within the liver, and a large potential gradient for this protein must exist between the liver cells and the plasma. The aim of the present study, therefore, was to measure the release of immunoreactive ligandin into the plasma under conditions of experimentally induced hepatocellular necrosis, and to compare "ligandinaemia" in this situation with the plasma GOT (abbreviated herein as the SGOT). As a prerequisite to this study, the validity of plasma ligandin measurement by RIA was first established and is dealt with as an integral part of this chapter. For the larger part of this study, hepatocellular necrosis was produced by feeding rats with carbon tetrachloride (CCl_4). The hepatotoxic effects of this agent are well recognized and have been exhaustively reviewed (336). A limited study of the effect of acute bile duct ligation on ligandinaemia and the SGOT is also presented.

2. Methods

Experimental protocol:

Rats were fasted for 12h before and during the period following administration of CCl_4. Water was given ad libitum. CCl_4 was administered in doses of 0.05, 0.125, 0.25 and 0.5 ml/100g body weight. These amounts of CCl_4 were diluted in equal volumes of vegetable oil and administered intragastrically via a soft polyethylene tube on the tip of an 18 guage needle. Control animals were also fasted, and received equivalent volumes of mineral oil alone. "Normal" rats used in this study were not fasted. Rats were bled in groups of six at 24h after administration of different doses of CCl_4 and at intervals of 3, 6, 15, 24 and 30h following the 0.25 ml/100g body weight dose. Cytosol (see Appendix B) was prepared from the livers and kidneys of rats given 0.25 ml CCl_4/100g body weight, 24h after the dose was administered. Protein concentration was determined as outlined in Appendix B. Acute bile duct obstruction was effected in six animals by tying the common bile duct with two silk ligatures 3 mm apart. These animals were bled in groups of 3 at intervals 12 and 24h after the operation. Sham-operated animals underwent laparotomy alone and were bled in groups of 2 at both intervals. SGOT was determined in plasma samples by the method of Karmen (337, see Appendix B), while ligandin concentration in plasma and cytosol was measured by RIA (see Chapter X). Immunodiffusion was performed as outlined in Appendix B. Statistical comparison of data employed Student's t test (see Appendix C).

Blood samples:

Blood was collected from the abdominal aorta using a 21 guage "butterfly" needle into heparinized plastic tubes. The amount of heparin (Pularin) in these tubes was sufficient to allow a final concentration of heparin of approximately 15 units/ml of blood. Blood was centrifuged at 2,000 xg for 30 min at 4°C in an M.S.E. centrifuge. The plasma was separated and kept unfrozen on ice for no longer than 12h prior to assay. No haemolysis of blood was observed during routine collections. In order to assess the effect of haemolysis on the assay, some blood samples were divided into two aliquots and haemolysis produced in one of these by forceful injection of the blood via a 26 guage needle prior to separation of plasma. In some instances, blood was collected into tubes containing no heparin and rapidly divided into two aliquots. One of these was heparinized, while the other (unheparinized) was permitted to clot at 0°C. Serum was separated as outlined above. Blood from human subjects was obtained by venepuncture and plasma separated as outlined above. The pooled samples used in this study were comprised of combined equal volumes of plasma or serum obtained from 3 animals. Pooled plasma from CCl_4 treated rats was obtained 24h after administration of a dose of 0.25 ml/100g body weight of the toxin. TCA precipitation of ^{125}I-ligandin in plasma was performed as described in Chapter IX.

Recovery experiments:

Two pools of normal rat plasma were each divided into five aliquots. One aliquot from each pool was assayed for

endogenous ligandin concentration, while the remaining four were assayed after addition of pure ligandin to final concentrations of 100, 500, 5,000 and 10,000 ng/ml. These final values were predicted on the basis of the protein concentration of pure ligandin measured by the method of Lowry et al (298, see Appendix B).

Gel filtration:

2.5 ml of rat plasma samples were mixed with equal volumes of 0.01M sodium phosphate buffer pH 7.4 / 0.1M NaCl and chromatographed in the same buffer on a 97 x 2.5 cm calibrated column of Sephadex G-100, using pump-driven upward flow of 43 ml/min with collection of 3.8 ml fractions. Protein was determined spectrophotometrically (see Chapter VII) while ligandin was measured by RIA. Immunoreactive peaks were also examined by discontinuous slab PAGE in SDS (see Appendix B). Samples studied were: normal rat plasma, normal rat plasma with pure ligandin added to a final concentration of 12 µg/ml and plasma from a rat 6h after CCl_4 administration (0.25 ml/100g body weight).

3. Results

Characterization of RIA of ligandin in plasma

Tracer quantities of ^{125}I-ligandin incubated in 1 ml volumes of normal rat plasma at temperatures of -20, 4 and 25^{o}C for 4h, were 95, 96 and 95% precipitable with TCA respectively. ^{125}I-ligandin in assay tubes containing plasma from normal and CCl_4-treated rats were 97-98% precipi-

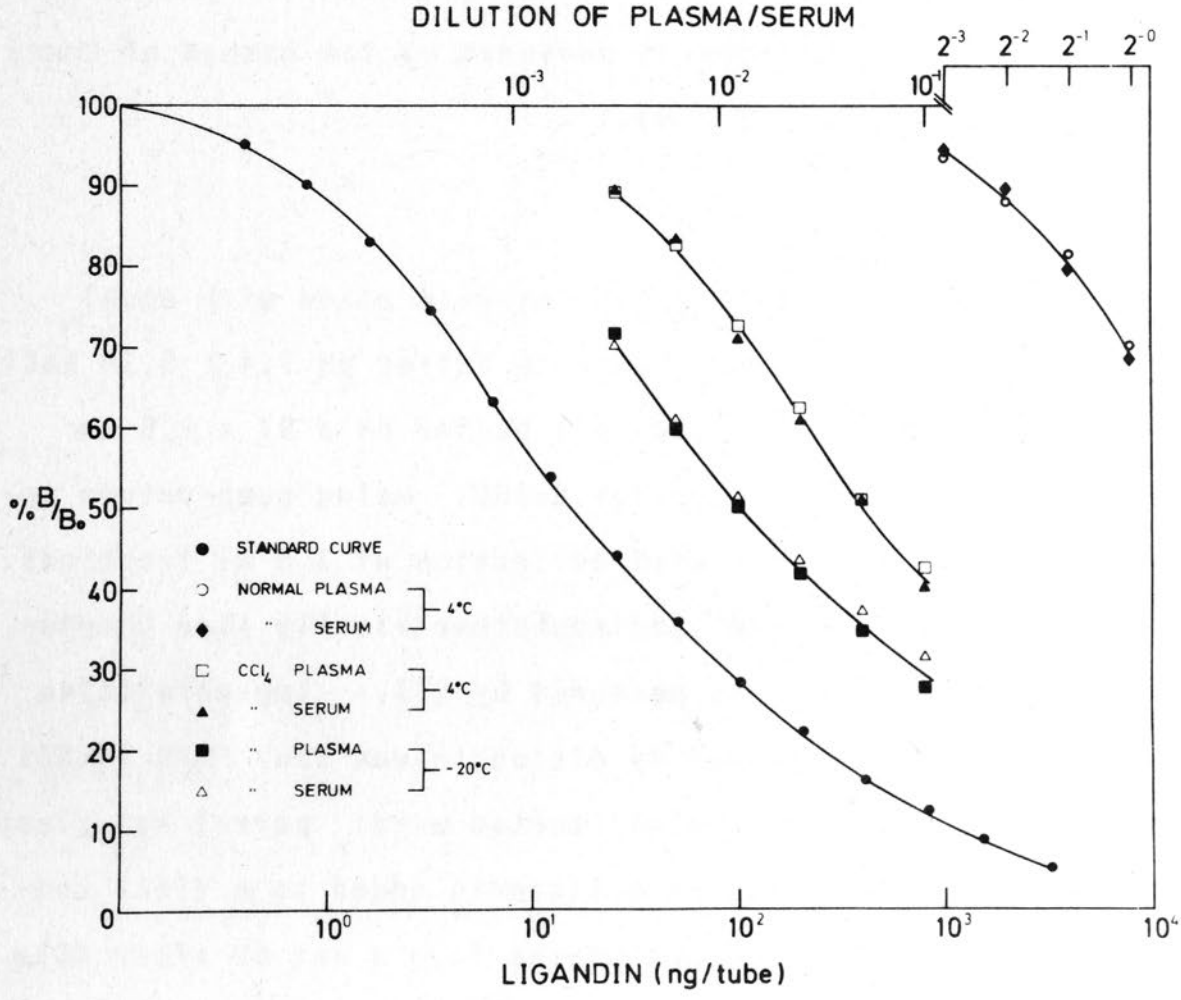

Fig. 2.33. Comparison between immunochemical displacement curves of plasma and serum from normal and CCl_4-treated rats and the ligandin RIA standard curve. The effect of freezing at -20°C on the curve of serum and plasma from CCl_4-treated rats is also shown. Ordinate and abscissa are as described in legend to Fig. 2.18.

table with TCA after 48h incubation at 4°C. These findings are consistent with a lack of a degradative effect of plasma on ^{125}I-labelled ligandin.

Human plasma from 10 normal individuals, as well as plasma from 2 patients with obstructive jaundice and 3 patients with acute viral hepatitis, did not displace antibody-bound ^{125}I-ligandin in the assay. Neither rat nor human plasma had any significant effect on the non-specific binding of ^{125}I-ligandin in the RIA.

No difference was found between the values obtained using plasma or serum from normal or CCl_4-treated rats. Pooled plasma and serum obtained from the same animals gave identical immunochemical displacement curves, which were parallel with the RIA standard curve (Fig. 2.33).

The results of RIA of pure ligandin added to normal rat plasma are summarized in Table 2.XVI. As shown in Table 2.XVI, the RIA recovery of ligandin from plasma over a wide range of concentrations was between 90-113%. When single pools of plasma from CCl_4-treated rats were incubated at 4 and 25°C for 4h, the values obtained by RIA were 94 and 97% respectively, of the values obtained for each pool prior to any incubation. A similar pool of plasma stored at 0°C for 24h returned a value of 93% of that obtained prior to incubation. Freezing of plasma or serum resulted in a consistent increase in the values of immunoreactive ligandin. After being frozen for 2h at -20°C, immunoreactive ligandin levels in 4 pools of plasma and serum from

TABLE 2.XVI

RECOVERY OF PURE LIGANDIN FROM NORMAL RAT PLASMA

Pool no.	Endogenous (A) (ng/ml)	Predicted (B) (ng/ml)	Assayed (C) (ng/ml)	C - A (ng/ml)	% Recovery % (C-A/B)
1	36	100	139	103	103
		500	485	449	90
		5,000	4,758	4,722	94
		10,000	9,242	9,206	92
2	50	100	149	99	99
		500	616	566	113
		5,000	4,566	4,516	90
		10,000	9,466	9,416	94

Each pool comprised equal volumes of plasma obtained from 3 rats. Predicted (B) values were based on the addition of known amounts of pure ligandin (see Methods for details).

CCl_4-treated rats were elevated to between 153-173% of the values obtained for these pools prior to freezing. Continued freezing of these same pools for a week at -20°C resulted in no further increase; and values obtained at this stage were between 78 and 101% of those measured after 2h at this temperature. The cause of this phenomenon was not found. However, freezing did not affect the parallel dose response of plasma or serum in the assay, but created a "shift downwards" in these curves consistent with the observed increase in immunoreactivity (Fig. 2.33). Thus for the purpose of this study, plasma was either assayed immediately or kept at 0°C before assay. No difference in the values of immunoreactive ligandin was apparent between unhaemolysed and haemolysed plasma aliquots derived from the same blood samples.

The normal range of values:

The means and ranges of values obtained in several normal rats for plasma immunoreactive ligandin and SGOT are given in Table 2.XVII.

TABLE 2.XVII

NORMAL VALUES OF PLASMA LIGANDIN AND SGOT IN THE RAT

	No. rats	Mean + SEM	Range
Plasma ligandin (ng/ml)	22	25.77 ± 2.83	6 - 57
SGOT (mU/ml)	14	37.36 ± 2.32	25 - 51

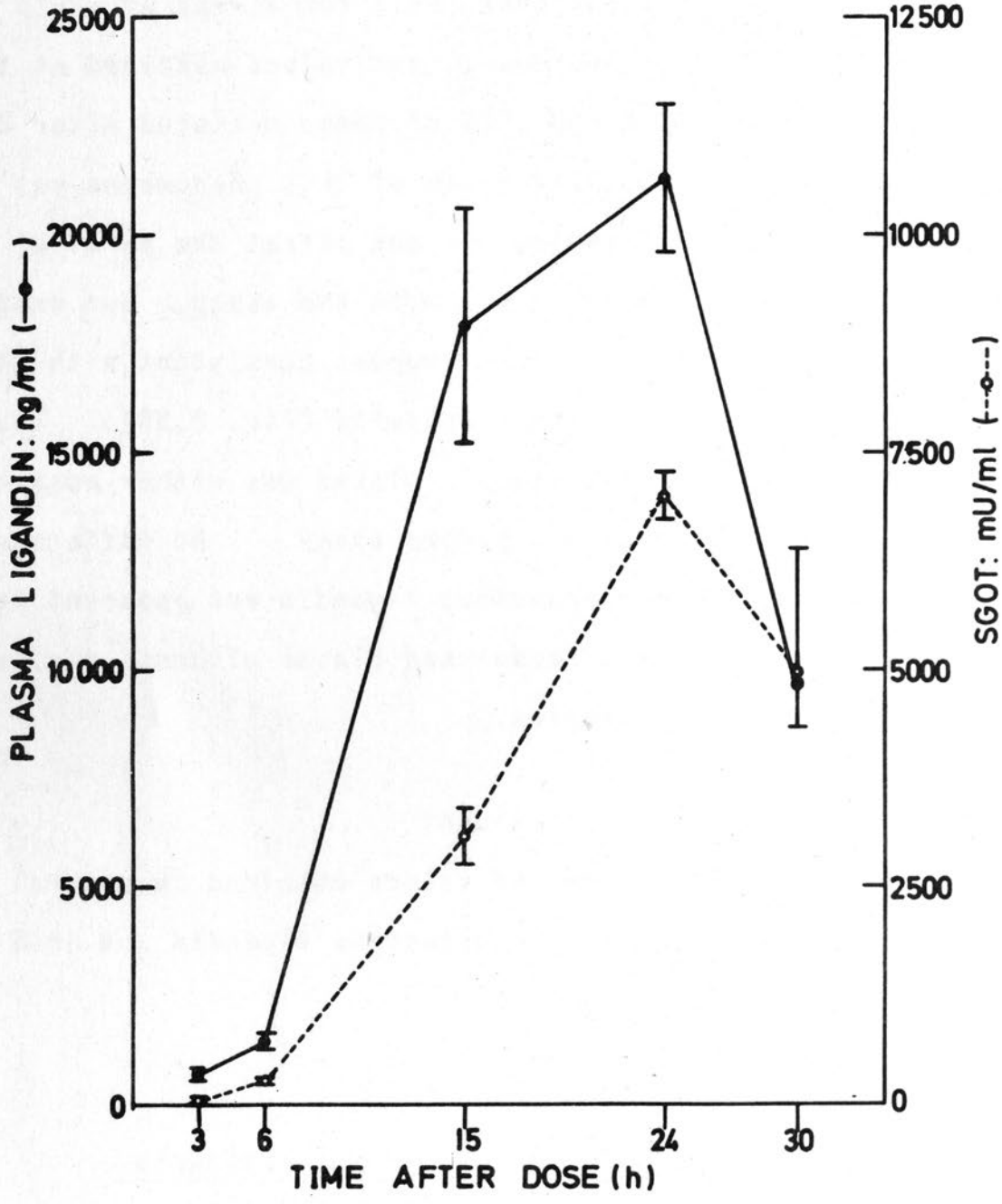

Fig. 2.34. The release of ligandin and GOT into the circulation following CCl_4 administration. Animals received 0.25 ml CCl_4/100g body weight. Each point represents the Mean ± SEM of six individual determinations.

Immunoreactive ligandin in normal rat plasma gave an immunochemical displacement curve parallel with the standard curve of the RIA (Fig. 2.33).

Plasma ligandin and SGOT responses to CCl_4 intoxication:

The responses of plasma ligandin and SGOT at 3, 6, 15, 24 and 30h after a dose of 0.25 ml/100g body weight of CCl_4 are illustrated in Fig. 2.34. Values are given in Table 2.XVIII. The responses of plasma ligandin and SGOT were similar, both reaching a maximum 24h after the dose and then declining. The rate of increase of ligandin in the plasma was greater than that of the SGOT. From as early as 3h after the dose, the mean plasma ligandin level was 12 times the upper limit of normal, while the SGOT had only risen to 1.3 times normal. By 24h, ligandin had risen to 374 times normal compared with 137 times normal for the SGOT. Control animals fed vegetable oil alone, showed no increase above normal for either plasma ligandin or SGOT values.

When doses of CCl_4 ranging from 0.05 to 0.5 ml/100g body weight were given to rats, the responses of ligandin and SGOT 24h after dosing were both curvilinear (Fig. 2.35, Table 2.XVIII), although the ligandin response was linear over a greater part of the range prior to plateauing between the highest doses. Of the six animals receiving the highest dose (0.5 ml/100g body weight), only four survived for 24h. Levels of plasma ligandin above 20,000 ng/ml were readily detected on immunodiffusion. Fig. 2.36 shows the single precipitin line of identity obtained between the plasma of 2

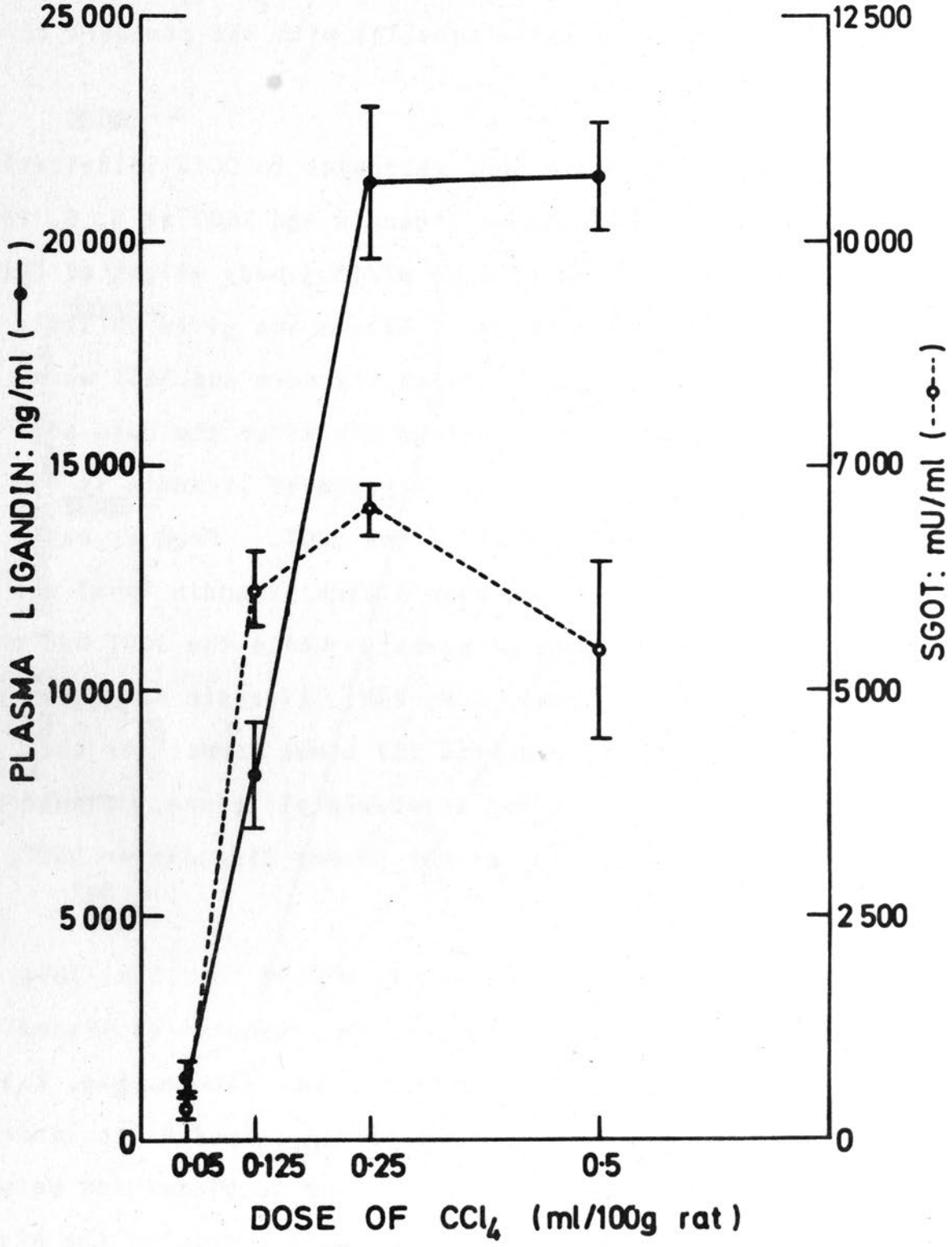

Fig. 2.35. Response of plasma ligandin and SGOT 24h after various doses of CCl_4. Each point represents the Mean ± SEM of six individual determinations excepting the highest dose, where only four determinations were possible.

TABLE 2.XVIII

PLASMA LIGANDIN AND SGOT LEVELS AFTER CCl_4 ADMINISTRATION AND ACUTE BILE DUCT LIGANDIN

Time (h)	Dose of CCl_4 (ml)	No. of rats	Ligandin (ng/ml)	SGOT (mU/ml)
After CCl_4 administration				
3	0.25	6	677 ± 133 (12)	64 ± 13 (1.3)
6	0.25	6	1,466 ± 162 (26)	271 ± 40 (5.3)
15	0.25	6	17,904 ± 2,682 (314)	3,077 ± 325 (60)
24	0.05	6	1,413 ± 345 (25)	373 ± 124 (7)
	0.125	6	8,119 ± 1,178 (143)	6,114 ± 414 (120)
	0.25	6	21,320 ± 1,704 (374)	7,009 ± 265 (137)
	0.5	4	21,425 ± 1,202 (376)	5,453 ± 957 (107)
30	0.25	6	9,696 ± 1,059 (170)	4,948 ± 1,441 (97)
After acute bile duct ligation				
12		3	202 ± 8.6 (3.5)	419 ± 31 (8.2)
24		3	39 ± 3.2 (N)	354 ± 37 (7)

Values are given as Mean ± SEM. Elevations of mean values above the upper limit of normal (see Table 2.XVII) are given in parentheses.

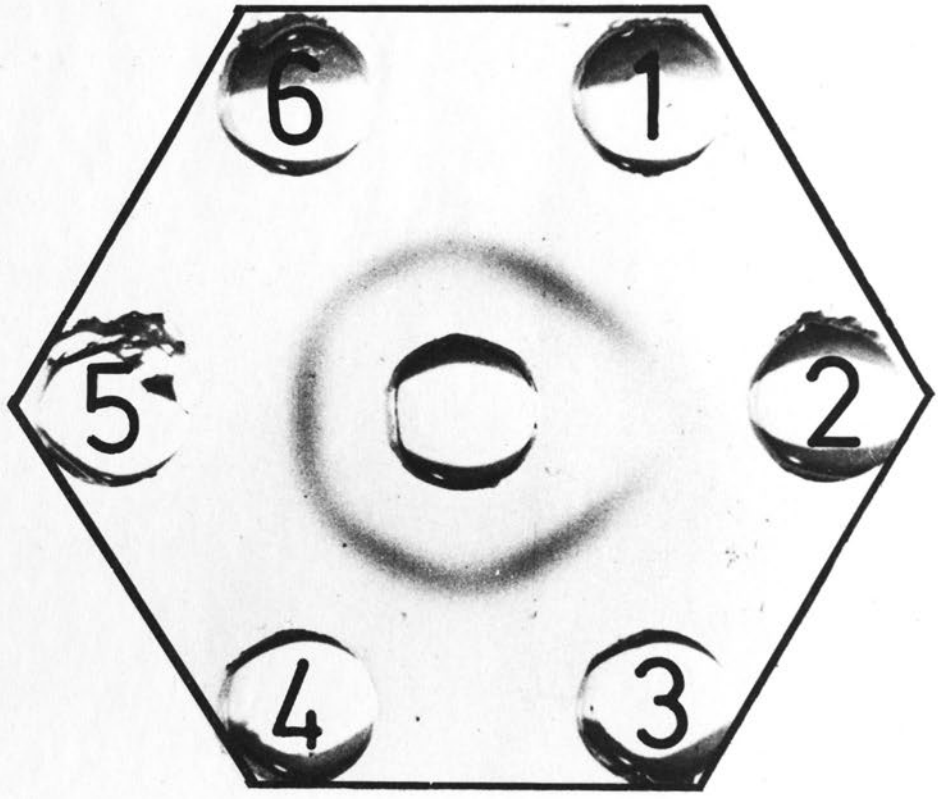

Fig. 2.36. Immunodiffusion in agar gel. The centre well contains rabbit anti-ligandin antiserum; the peripheral wells contain: 1 and 3, plasma from CCl_4-treated rats; 2, normal rat plasma; cytosol from 4, liver (1:4) and 6, kidney (1:2) with ligandin (1 µg) in well 5. Precipitates were stained with amidoblack. (See Appendix B for details of procedure).

CCl_4-treated rats with immunoreactive plasma ligandin values above 20,000 ng/ml, cytosol of liver, kidney and pure ligandin, on immunodiffusion against anti-ligandin antiserum. No precipitin line was observed with normal rat plasma.

The effect of CCl_4 administration on hepatic and renal ligandin levels:

The levels of ligandin in the livers and kidneys of rats 24h after receiving either 0.25 ml of CCl_4/100g body weight or equivalent volumes of vegetable oil (controls) are given in Table 2.XIX. Extreme fatty change was evident in the livers of all the CCl_4-treated rats at 24h, while the kidneys of these animals were swollen and pale. The organs of control animals were normal in appearance at 24h.

TABLE 2.XIX

HEPATIC AND RENAL LIGANDIN LEVELS AFTER CCl_4 ADMINISTRATION

Tissue	CCl_4 treated (µg/mg)	Controls (µg/mg)	P
Liver	18.02 ± 1.47	34.16 ± 2.63	<0.005
Kidney	12.37 ± 0.99	15.80 ± 1.17	ns

Results are expressed as Mean ± SEM in µg/mg supernatant protein. Six animals were used for each determination.

ns: not significant ($P > 0.05$).

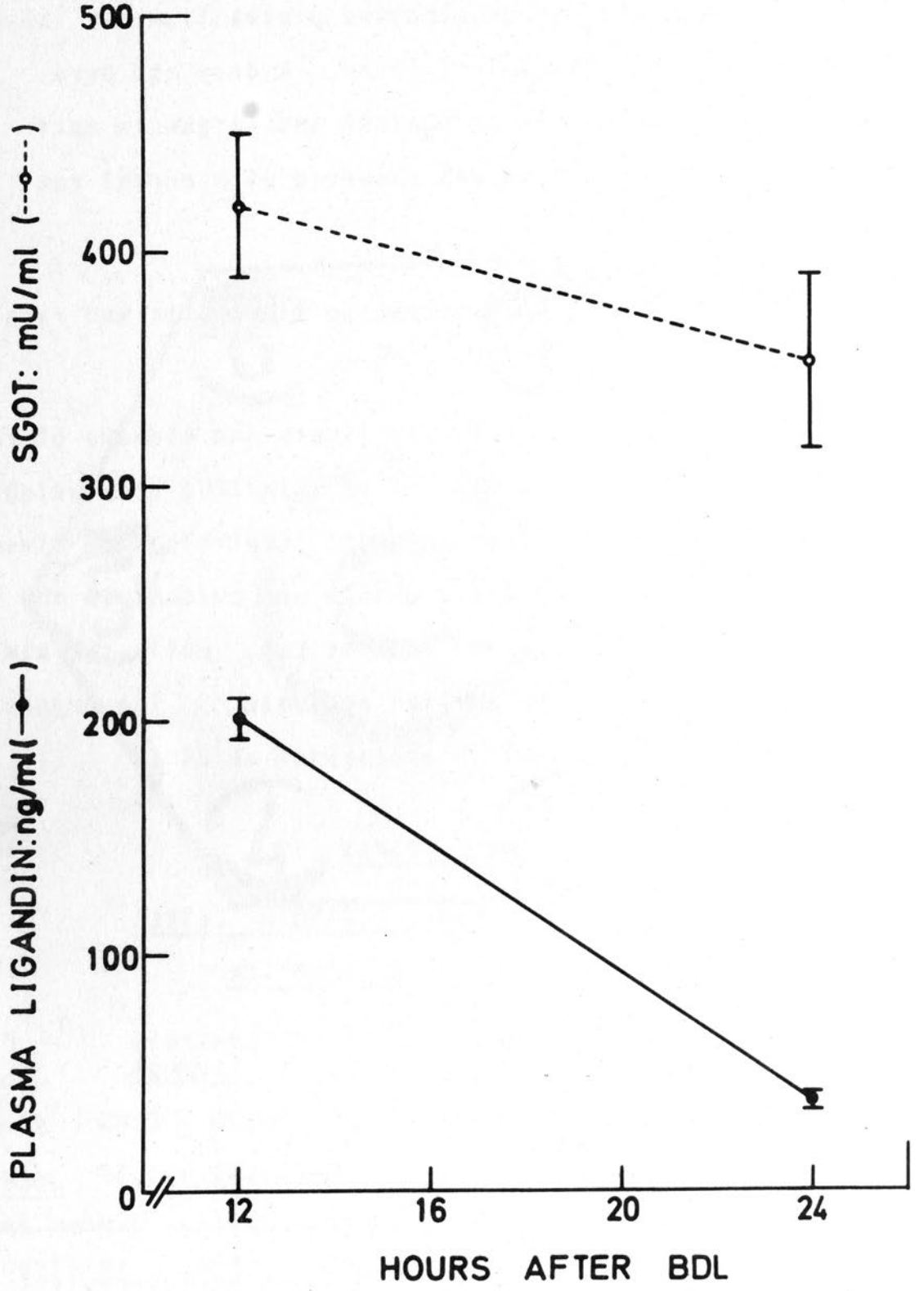

Fig. 2.37. Plasma ligandin and SGOT levels 12 and 24h following acute bile duct ligation. Each point represents the Mean ± SEM of three individual determinations.

Hepatic ligandin levels 24h after CCl_4 administration were depleted to 53% of control values. Renal values were diminished to 78% of controls, but this difference was not significant on statistical testing.

The effect of acute bile duct ligation on plasma ligandin and SGOT:

The results of this experiment are illustrated in Fig. 2.37; values are given in Table 2.XVIII. Acute bile duct ligation produced comparatively moderate elevations of both ligandin (3.5 x normal) and SGOT (8.2 x normal) after 12h. By 24h, ligandin levels were normal, whereas the SGOT remained elevated 7 times above normal levels. Ligandin and SGOT levels were normal in sham-operated controls at both 12 and 24h.

The molecular size of immunoreactive plasma ligandin:

The results of gel filtration and RIA of normal rat plasma with and without added pure ligandin, and of CCl_4-treated rat plasma, are shown in Fig. 2.38. No immunoreactivity was detected in the elution profile of normal rat plasma alone (Fig. 2.38A), probably due to the dilution of the small amount of ligandin present in normal plasma below the limit of detection of the assay. Adsorption of ligandin by Sephadex was also suggested by the finding that the estimated recovery of ligandin (calculated by triangulation) after gel filtration of normal plasma with added ligandin (Fig. 2.38B), was only 20% of the quantity initially added. CCl_4-treated rat plasma showed an immunoreactive peak (Fig.

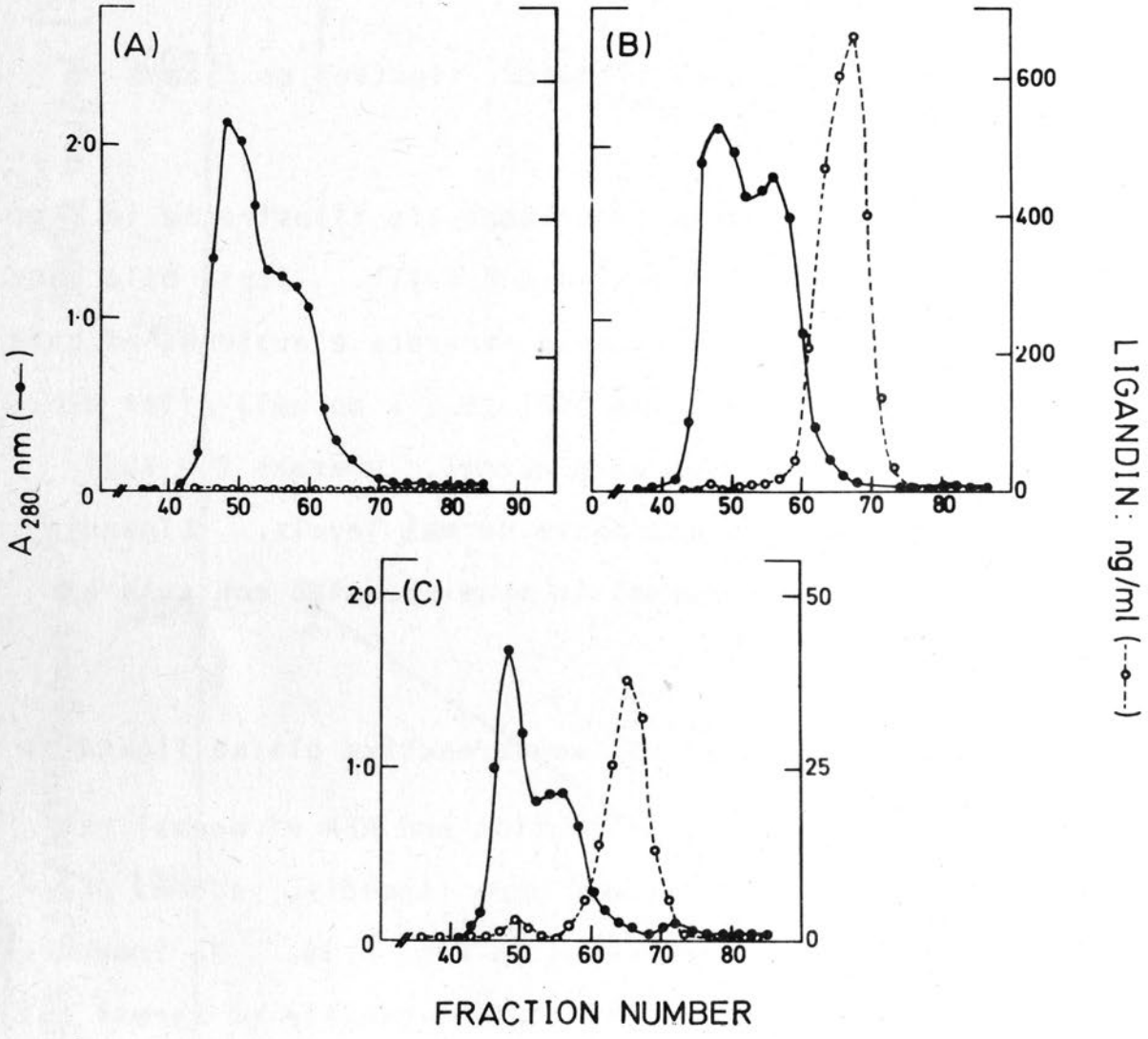

Fig. 2.38. Immunoreactive ligandin in rat plasma chromatographed on Sephadex G-100. (A), Normal rat plasma; (B), normal rat plasma with ligandin added to a concentration of 12 µg/ml and (C) plasma from a rat 6h after CCl_4 administration (0.25 ml/100g body weight). Protein was determined spectrophotometrically, while ligandin was measured by RIA.

2.38C) corresponding in elution volume to the immunoreactive peak obtained on gel filtration of normal rat plasma to which pure ligandin had been added (Fig. 2.38B). A small amount of immunoreactivity was evident in the high molecular weight region in both these cases (Fig. 2.38B and C). This feature was not evident on gel filtration and RIA of ligandin in the absence of plasma, and may have resulted either from an aggregating effect of plasma on ligandin, or binding of ligandin to plasma proteins of high molecular weight. Discontinuous PAGE in SDS analysis of the immunoreactive peak from CCl_4-treated rat plasma, revealed the presence of 3 very faint bands corresponding in size to the Y_a, Y_b and Y_c peptide bands of hepatic cytosol. These bands were not detected in the corresponding elution volume of normal rat plasma.

4. Discussion

The use of the RIA technique for measuring the release of structural components from damaged or diseased tissue is a recent concept. RIA of circulating myoglobin has proved to be of value in the diagnosis of myocardial infarction (294). RIA of plasma trypsin provides a sensitive means of diagnosing acute pancreatitis (290), while the value of RIA's of circulating procollagen in diagnosing Paget's disease (295) and of acid phosphatase in detecting prostatic carcinoma (291), have also been proposed. Liver-specific antigens have been demonstrated by immunodiffusion methods in the serum of animals with experimentally induced hepato-

cellular necrosis, and in human beings with liver disease (338-340). Except in the case of the highly liver-specific F-antigen (340), little characterization of these antigens has been performed and no liver antigens have been directly measured in the circulation by RIA.. There are definite advantages in using RIA as opposed to enzyme determinations for diagnostic use. Firstly, RIA may provide a degree of sensitivity several orders of magnitude greater than enzyme assay of the same protein (341). Secondly, RIA provides a means of direct measurement of the mass of a particular protein, utilizing its antigenic properties as opposed to its functional properties as an enzyme. Enzyme activity is highly dependent upon assay conditions, and factors such as the presence of inhibitors which may affect enzyme activity, do not affect the RIA measurement of enzyme proteins (290, 335). In the present study, the presence of factors such as bilirubin and haemolysis had no effect on the RIA of ligandin in plasma. Haemolysis, however, may seriously affect the determination of SGOT (332).

In the present study, plasma ligandin appeared more sensitive to CCl_4-induced hepatocellular necrosis than did the SGOT. Factors responsible for the greater sensitivity of plasma ligandin may include the high concentration of ligandin in the liver, as well as its comparatively low molecular size. It is theoretically sound to propose that this latter factor promotes the egress of ligandin from the liver cell with respect to the larger, and thus less readily released, molecules of GOT (342). From the point of view of

comparative assessment between RIA and enzyme activity, it would be interesting to assess the release of ligandin from injured liver using both RIA and GSH S-transferase activity, even though the latter is not specific for ligandin alone. Plasma GSH S-transferase activity was not measured in the present study, but Javitt (343) and Datta et al (344) have both reported increased levels of GSH S-aryltransferase (BSP-conjugating) activity in the plasma of rats after CCl_4 administration. It is interesting to note that this particular catalytic activity appeared less sensitive than the direct measurement of ligandin used in the present study. Datta et al (344) found no BSP-conjugating activity in plasma 3h after CCl_4 administration (0.5 ml/100g body weight), while Javitt (343) reported a peak elevation of this activity at 24h of 6 times normal, after a dose of CCl_4 (0.05 ml/100g body weight) which in the present study, produced a 25-fold rise in plasma ligandin at 24h. The lesser sensitivity of the enzyme assay used by these workers (343, 344), compared with the RIA of plasma ligandin, may reflect amongst other factors, the insensitivity of BSP as a substrate for the GSH S-transferases. Further exploration of the use of plasma GSH S-transferase activity as an index of hepatocellular necrosis, would therefore be served best by using a sensitive substrate such as 1-chloro-2,4-dinitrobenzene. The presence of small quantities of immunoreactive ligandin in normal rat plasma is probably analogous to the low levels of many enzymes (333, 334) and structural tissue proteins (293-295) normally occurring in plasma, presumably as a result

of leakage from various tissues.

A comprehensive study of hepatic enzyme release following CCl_4 administration to rats, was performed by Zimmerman et al (345). The considerable variability of response of plasma ligandin levels (indicated by the large SEM's) is a phenomenon observed for all hepatic enzymes released into the plasma following CCl_4 administration. The pattern of ligandin release following CCl_4 administration is very similar to those of a number of hepatic enzymes distributed in the cytoplasm alone (e.g. phosphohexose isomerase and lactate dehydrogenase), and in both cytoplasm and mitochondria (e.g. GOT and malate dehydrogenase). Plasma ligandin also showed a more linear incremental response to increasing doses of CCl_4 than did the SGOT. In this respect, ligandin displayed behaviour similar to the cytoplasmic enzymes studied by Zimmerman et al (345), while the curvilinear response of SGOT found in the present study confirms these workers' findings for this enzyme. It was proposed (345) that the curvilinear response of the SGOT might reflect progressive "exhaustion" of the intracellular store of this enzyme. It should be noted, however, that the 24h response of ligandin between the dose levels of 0.25 and 0.5 ml/100g body weight showed no further increase; yet at this time, the livers of animals treated with CCl_4: 0.25 ml/100g body weight, still contained appreciable quantities of ligandin. Thus some other mechanism besides "exhaustion" of intracellular ligandin must operate in limiting the linear dose response of this protein at high CCl_4

dose levels.

Hepatic ligandin levels were markedly depleted by CCl_4 administration, and it appears that the high circulating levels of ligandin in CCl_4 treated rats obtain largely from the liver. Although renal ligandin levels were not significantly reduced, it is still feasible that the nephrotoxic action of CCl_4 (336) led to some escape of ligandin from the kidneys into the plasma. In this event, the comparison of plasma ligandin sensitivity vs the SGOT is still valid, as the concentration of GOT in the kidney of the rat is almost the same as that in the liver (346), and could thus be expected to contribute to the SGOT in a manner analogous to the release of renal ligandin. It should be noted that the levels of hepatic ligandin in control animals were lower than the mean range previously obtained in normal rats (see Chapter XI). This may well reflect the effect of fasting, which has been shown to reduce hepatic levels of ligandin (229).

Plasma retention of BSP occurs in animals treated with CCl_4 (41, 347), and the question is raised whether depletion of hepatic ligandin is an important factor in the pathogenesis of this dye retention. Brauer and Pessoti (67) and Brauer et al (41) concluded that CCl_4 poisoning did not affect BSP uptake by rat liver slices or by isolated perfused rat livers, nor did it affect hepatic storage of BSP in dogs. The mechanism of BSP retention after CCl_4 administration appeared rather, to involve the biliary excretion of the dye (41). Klaasen and Plaa (347) reached the same conclusion after

studying rats treated with CCl_4; and although BSP-conjugating activity was significantly depleted in these animals, storage of the dye was not affected. It is difficult to reconcile the results of these studies and the marked depletion of hepatic ligandin observed in the present study with a proposed role for ligandin in the hepatic storage of BSP. Also, in the light of the present findings, the uptake of organic anions in CCl_4-treated animals should be re-evaluated in relation to hepatic ligandin levels.

Moderate elevation of SGOT is known to occur following acute bile duct obstruction (332, 348) and probably reflects hepatocellular necrosis consequent to increased cannalicular pressure and bile reflux. Plasma ligandin was moderately elevated in rats 12h after acute bile duct obstruction, and the mechanism is probably the same as that effecting the raised SGOT. The return of ligandin levels to normal after 24h is perplexing in the light of the findings of Trams and Symeonidis (349), who noted microscopic evidence of necrosis persisting up to 14 days in rats after bile duct ligation. It is possible that only the initial trauma to liver cells, occurring within the first 12h after obstruction of the bile duct, is sufficiently severe to promote a sustained release of both ligandin and SGOT; and that a much faster rate of removal of ligandin than SGOT accounts for the difference observed at 24h, at which time the rate of release of intracellular proteins may have subsided considerably. The question of ligandin removal from the plasma is considered in the following chapter.

CHAPTER XVI

THE DISAPPEARANCE OF LIGANDIN FROM THE PLASMA

1. Introduction

The concentration of any plasma constituent at any given time depends on many variables, including the rate of its delivery into the intravascular compartment, the volume of this compartment, the rate of entry from the intravascular to the extravascular compartment(s) and vice versa, and the metabolic breakdown and excretion of the substance under investigation. Enzymes released into the circulation have characteristic rates of disappearance from the blood (335, 350), although in most cases, the exact mechanisms responsible for their removal are not understood. Owing to the high molecular weight of most enzymes, urinary excretion is not an important factor in their elimination from the circulation. However, in the case of ligandin, which has the comparatively low molecular size of 46,000, excretion in the urine might be important as a route of elimination. This chapter describes a preliminary study which was undertaken in order to answer the questions:

(1) At what rate is ligandin removed from the plasma?

(2) Is ligandin excreted from the plasma into the urine?

2. Methods

Experimental protocol:

Pure ligandin was freshly prepared (see Chapter VII) prior to use. ^{125}I-ligandin was prepared by the iodine mono-

chloride method (see Appendix B). The final preparation of labelled protein contained 0.71% free ^{125}I and had an estimated specific activity of 0.2 µCi/µg. Hepatic cytosol was prepared as described in Appendix B. Unlabelled and labelled pure ligandin, and hepatic cytosol, were each dialysed against 20 volumes of 0.01M sodium phosphate buffer pH 7.4 / 0.15M NaCl and centrifuged to remove flocculated material prior to injection. The concentration of pure ligandin (labelled and unlabelled) was determined by the method of Lowry et al (298, see Appendix B), while the concentration of ligandin in cytosol was determined by RIA. All injections were given intravenously via the tail vein in volumes of 0.5 ml. Animals were injected and bled from the tail vein according to the schedule summarized in Table 2.XX.

TABLE 2.XX

INJECTION AND BLEEDING SCHEDULE FOR LIGANDIN DISAPPEARANCE STUDIES

Test substance	No. of rats	Ligandin dose (µg/100g body wt)	Sampling times after injection*	
			min.	h
Pure ligandin	3	100	30	1,2,4,8,12,24
Hepatic cytosol	4	100	5,30	1,2,3,4,6,8,12,14,24
^{125}I-ligandin	4 †	30	5,30	1,2,4,8,12,24

* Each animal was bled at each time interval

† Animals receiving ^{125}I-ligandin were maintained on water containing 0.12% sodium iodide for 2 days prior to injection.

In a separate experiment, urine was collected from four rats housed in individual stainless steel metabolic cages over urine-faeces separator funnels. Urine was collected in graduated glass centrifuge tubes kept on crushed ice chips. These animals were denied food but allowed water ad libitum during the experiment. After a basal 24h period of urine collection, 2 of the rats were injected intravenously with pure ligandin (250 µg/100g body weight in 0.5 ml 0.9% saline), while the remaining 2 received equivalent volumes of 0.9% saline. Urine was collected over an initial period of 2h and a second period of 5h after the injections.

Blood and urine samples:

Blood obtained from the tail veins of animals was collected into plastic microfuge tubes and spun at 12,000 xg for 2 min in a Beckman Model 150 microfuge at room temperature. In the case of samples from animals injected with either unlabelled ligandin or hepatic cytosol, 50 µl aliquots of serum were diluted to 1 ml with cold ($4^{o}C$) assay diluent buffer, and assayed for ligandin by RIA. Only serum ligandin levels of greater than 30 ng/ml could be measured when serum was assayed in this manner. In the case of animals injected with ^{125}I-ligandin, 10 µl aliquots of serum were diluted to 1 ml with 0.5 ml phosphate buffer pH 7.4 / 0.1% BSA and counted for radioactivity as described in Chapter X. Thereafter, protein was precipitated in each tube with 10% TCA (see Chapter IX), followed by separate determination of counts in precipitates and supernatants.

Urine samples were spun at 2,000 xg for 30 min in a Sorval RC2-B centrifuge at 4°C to remove particulate matter, and stored at -20°C prior to determination of ligandin concentration by RIA. The validation of urine ligandin measurement by RIA is covered in Chapter XVII.

Gel filtration:

0.5 ml of urine from a sample obtained from one rat during the 2h period following injection of pure unlabelled ligandin, was chromatographed on a 30 x 0.7 cm calibrated column of Sephadex G-75. The column was eluted with 0.01M sodium phosphate buffer pH 7.4 / 0.1M NaCl at a flow rate of 18 ml/h with collection of 3 ml fractions. Ligandin was measured in column fractions by RIA.

Mathematical treatment of data:

One of two models were used to describe the disappearance of ligandin from plasma:

(1) A model in which the protein is irreversibly cleared from a single compartment (the plasma pool)

(2) A model in which the protein in the plasma pool (compartment 1) is in dynamic equilibrium with a second pool (compartment 2), with irreversible removal of the protein occurring from either or both compartments.

The general exponential equations describing the dissappearance curves for each model are:

$$X(t) = C_o e^{-Kt} \qquad \text{(for model 1)}$$

and

$$X(t) = C_1 e^{-K_1 t} + C_2 e^{-K_2 t} \qquad \text{(for model 2)}$$

where $X(t)$ is the concentration of ligandin in the serum at time t;

C_o is the concentration of ligandin in the plasma at t = 0;

K is the slope of the single exponential curve of model 1;

C_1, K_1 are the y-intercept and slope respectively of the first exponential component, and C_2, K_2 are the y-intercept and slope of the second exponential component of the bi-exponential curve of model 2 (in which case $C_o = C_1 + C_2$).

Individual disappearance curves were assessed as behaving either according to model 1 (single exponential) or 2 (two exponential) from inspection of semilogarithmic plots of serum ligandin concentration vs time. The goodness-of-fit of each curve to a specific model was confirmed by computer analysis on a Hewlett-Packard Model 9830A computer, using a programme based on the non-linear least squares curve-fitting method of Tyson et al (351), which also derived the values for C_o and K (for single exponential curves), and C_1, K_1, C_2 and K_2 (for bi-exponential curves). The fraction of the circulating ligandin pool irreversibly

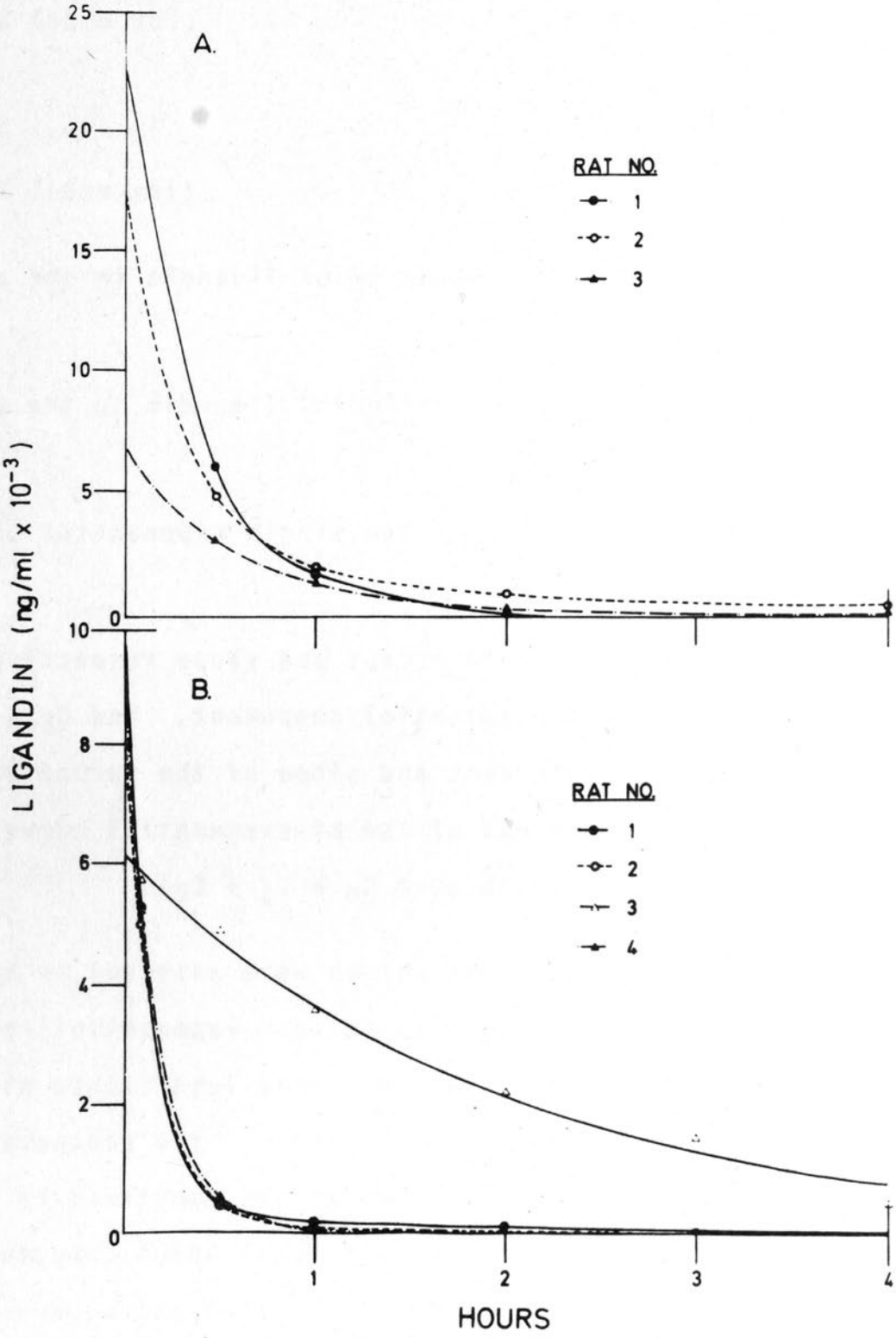

Fig. 2.39. Disappearance of immunoreactive ligandin from the circulation of the rat following intravenous administration of (A), pure ligandin, and (B), hepatic cytosol. The points are experimental results for individual animals; the curves were "best fit" regressions calculated by computer. (See Methods and Results for details).

cleared/h (K_e) is, in the case of single exponential (model 1) disappearance curves, equal to the slope (K) of the curve. In the case of curves requiring two exponentials to fit the data, K_e was derived from the relationship:

$$K_e = \left(\frac{A}{K_1} + \frac{B}{K_2} \right)^{-1}$$

where $A = \frac{C_1}{C_o}$ and $B = \frac{C_2}{C_o}$;

i.e. $A + B = 1$.

3. Results

Removal of ligandin from the circulation:

The curves of ligandin disappearance from the serum following intravenous administration of either pure, unlabelled ligandin or hepatic cytosol, are shown in Fig. 2.39. Normal values (see Chapter XV) were attained in individual rats at different times, varying between 2 and 8h; and the curves shown in Fig. 2.39 were calculated from the full range of data in each case up till the point where values became normal. The appearance of curves for the first 4h only are shown in Fig. 2.39, in order to facilitate comparison of curves within and between each group. The model to which each of these curves conforms, as well as the computer-fitted parameters and estimated value of K_e in each case are given in Table 2.XXI. In most cases, the sum of two exponentials was required to fit the disappearance curves of ligandin from the circulation of rats injected with either

TABLE 2.XXI

PARAMETERS OF LIGANDIN DISAPPEARANCE FROM THE PLASMA

Injectate/Rat No.	Model	C_1 (ng/ml)*	C_2 (ng/ml)*	K_1 (hr^{-1})*	K_2 (hr^{-1})	K_e (hr^{-1})
Pure Ligandin						
1	1	22,900	-	2.59	-	2.59
2	2	15,584	1,884	3.01	0.381	1.73
3	2	6,789	104	1.57	0.056	1.12
Hepatic Cytosol						
1	2	9,342	347	7.28	0.584	5.15
2	2	8,327	174	6.28	0.817	5.54
3	1	6,246	-	0.512	-	0.512
4	2	8,408	282	5.90	1.469	5.38

* In the case of model 1 curves, $C_1 = C_o$ and $K_1 = K$, while in the case of model 2 curves, $C_o = C_1 + C_2$.

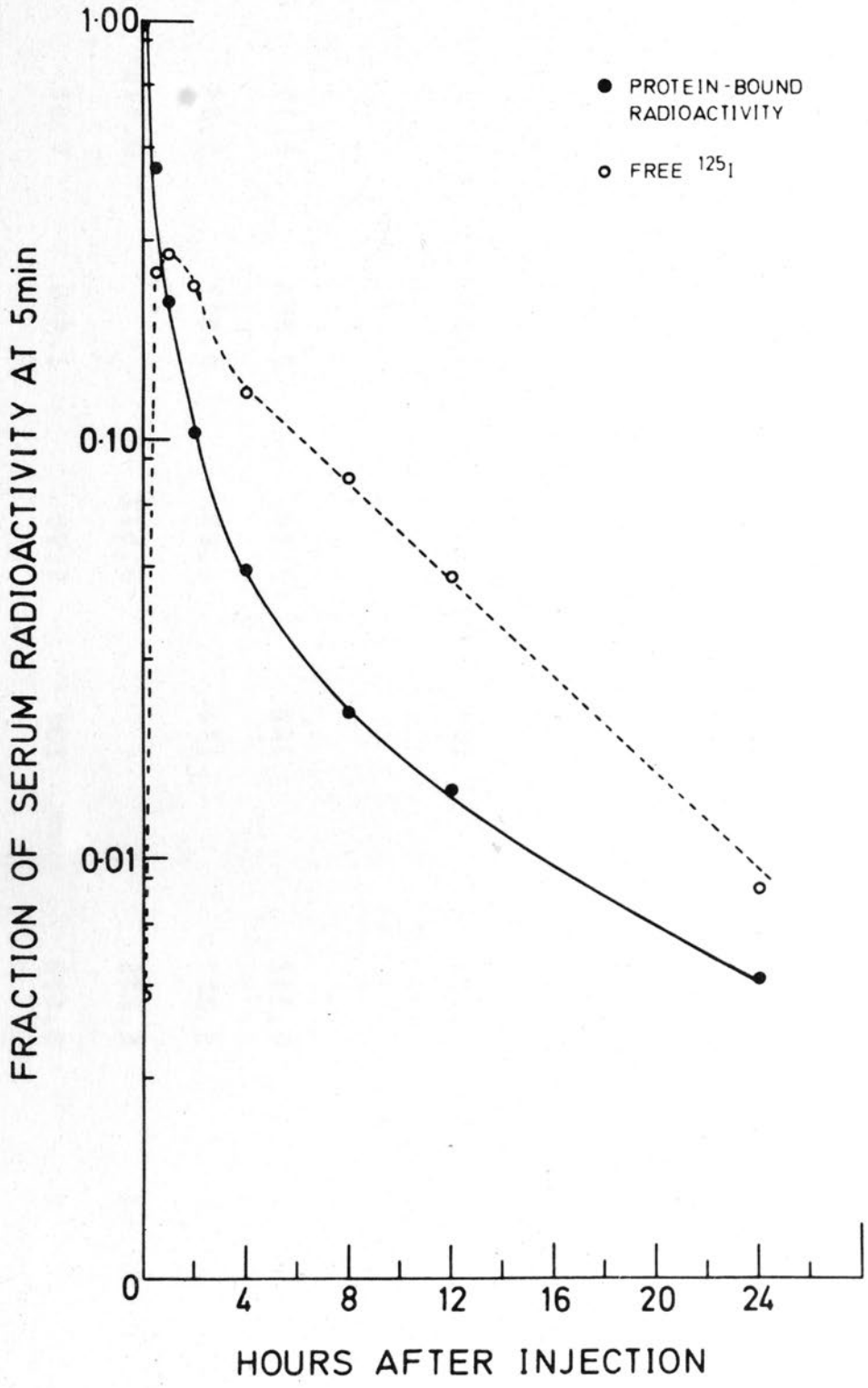

Fig. 2.40. Serum "protein bound" and free ^{125}I radioactivity (log scale) as a function of time, following intravenous administration of ^{125}I-ligandin. Ligandin was labelled by the iodine monochloride method. Data shown are for a typical experiment involving one rat. (See Methods and Results for details).

pure ligandin or hepatic cytosol. Thus in most cases, the disappearance of ligandin was characterized by an initial rapid followed by a slower process of removal. Two exceptions were rat no. 1 injected with pure ligandin, and rat no. 3 injected with hepatic cytosol. In these cases, the disappearance of ligandin was characterized by only a single exponential function which appeared to derive from a rapid removal process in rat no. 1 injected with pure ligandin, and a relatively slow process in rat no. 3 injected with hepatic cytosol. Unfortunately, rats injected with pure ligandin were not sampled prior to 30 min, and this probably accounts for the large variance in C_o obtained in this group.

In the 4 rats injected with ^{125}I-ligandin, 95-99% of the plasma counts were protein bound 5 min following the injection. This was reduced to 42-63% by 30 min, indicating a rapid liberation of ^{125}I from labelled ligandin. A typical profile of protein-bound and free radioactivity obtained from one animal over the course of 24h is shown in Fig. 2.40. It should be noted that the form of the protein-bound radioactive curve is probably not representative of ligandin removal after 2h, as beyond this stage, the TCA precipitable radioactivity remained constant between 10-15% of total serum counts and could be largely attributable to free ^{125}I trapped in the carrier-protein precipitate. That this was indeed the case, seems borne out by the fact that the late "protein-bound" curve ran roughly parallel to the free ^{125}I disappearance curve. In view of the uncertainty introduced by this factor into the estimation of the true

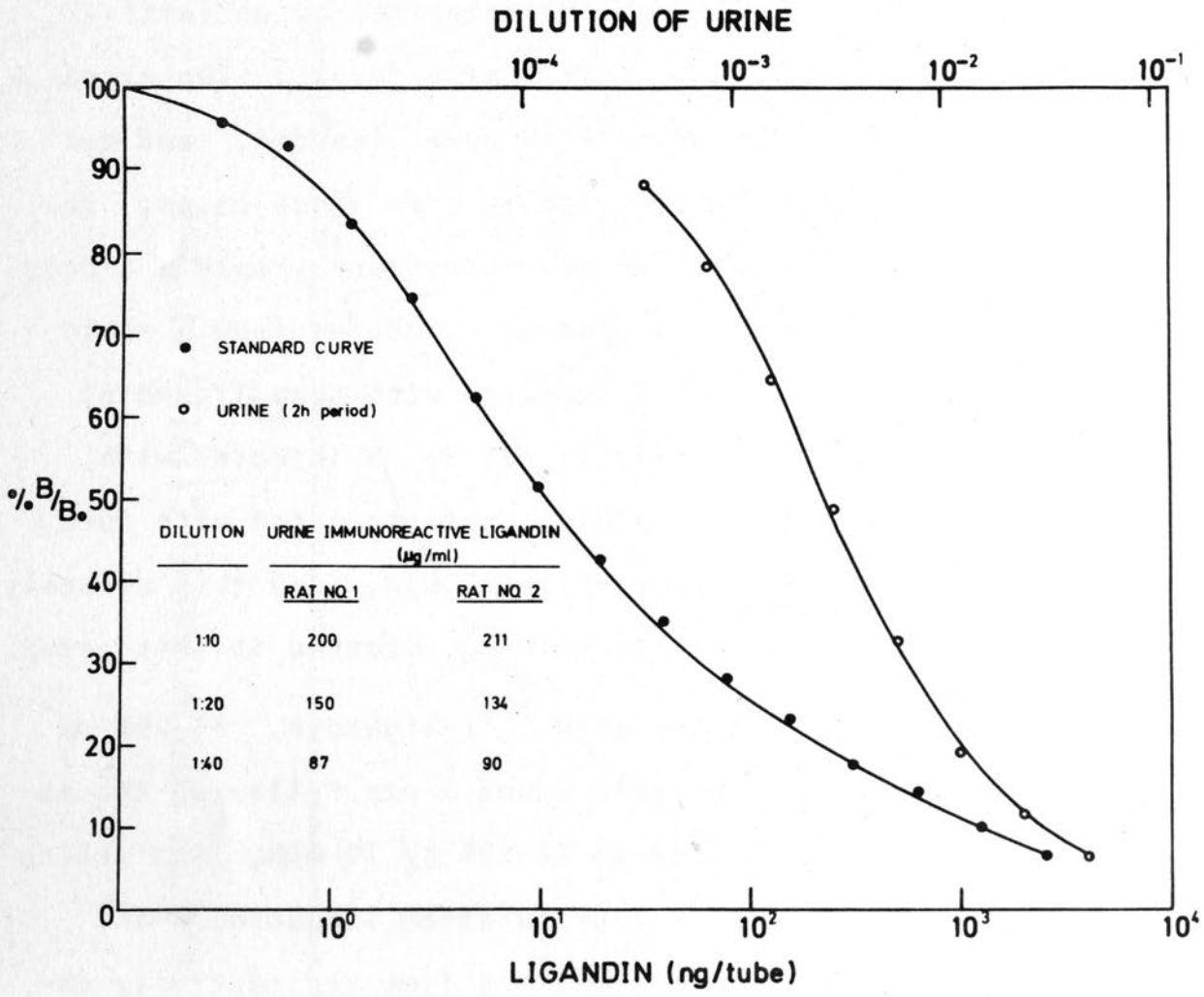

Fig. 2.41. Comparison between immunochemical displacement curve of urinary immunoreactive ligandin following intravenous administration of ligandin and the ligandin RIA standard curve. The loss of parallelism displayed by the urine curve was reflected in a progressive drop in ligandin values obtained with increasing dilution (inset table). Ordinate and abscissa are as described in legend to Fig. 2.18.

protein-bound fraction of radioactivity at any time, these curves were not analysed further for removal data.

Excretion of ligandin in the urine:

Prior to intravenous injection of ligandin or saline, urinary ligandin excretion was less than the normal limit of 46 ng/h in all six animals (see Chapter XVII). During both the 2h and subsequent 5h period following administration of either substance, the urine of control animals showed no rise above normal levels of ligandin excretion, while a marked increase in immunoreactivity was evident in the urine of ligandin injected rats. However, this immunoreactivity showed a loss of dilutional parallelism with the assay standard curve (Fig. 2.41), which manifested as a progressive drop in the values obtained with increasing dilution (see inset table, Fig. 2.41). This was in marked contrast to the parallel immunochemical displacement curves obtained with the urine of normal and nephrotoxin treated animals (see Chapter XVII). Thus valid measurements and recovery estimates of urinary ligandin excretion were not possible in this instance. The possibility that this loss of parallelism was due to the excretion of ligandin in the form of immunoreactive fragments derived from partial catabolism was explored by examining the molecular size of immunoreactivity in the urine of an animal 2h after receiving ligandin intravenously. Contrary to this expectation, immunoreactivity was located in a peak appearing in the void volume on Sephadex G-75 chromatography as shown in Fig. 2.42. This was again in contrast to the findings made with the urine of nephrotoxin

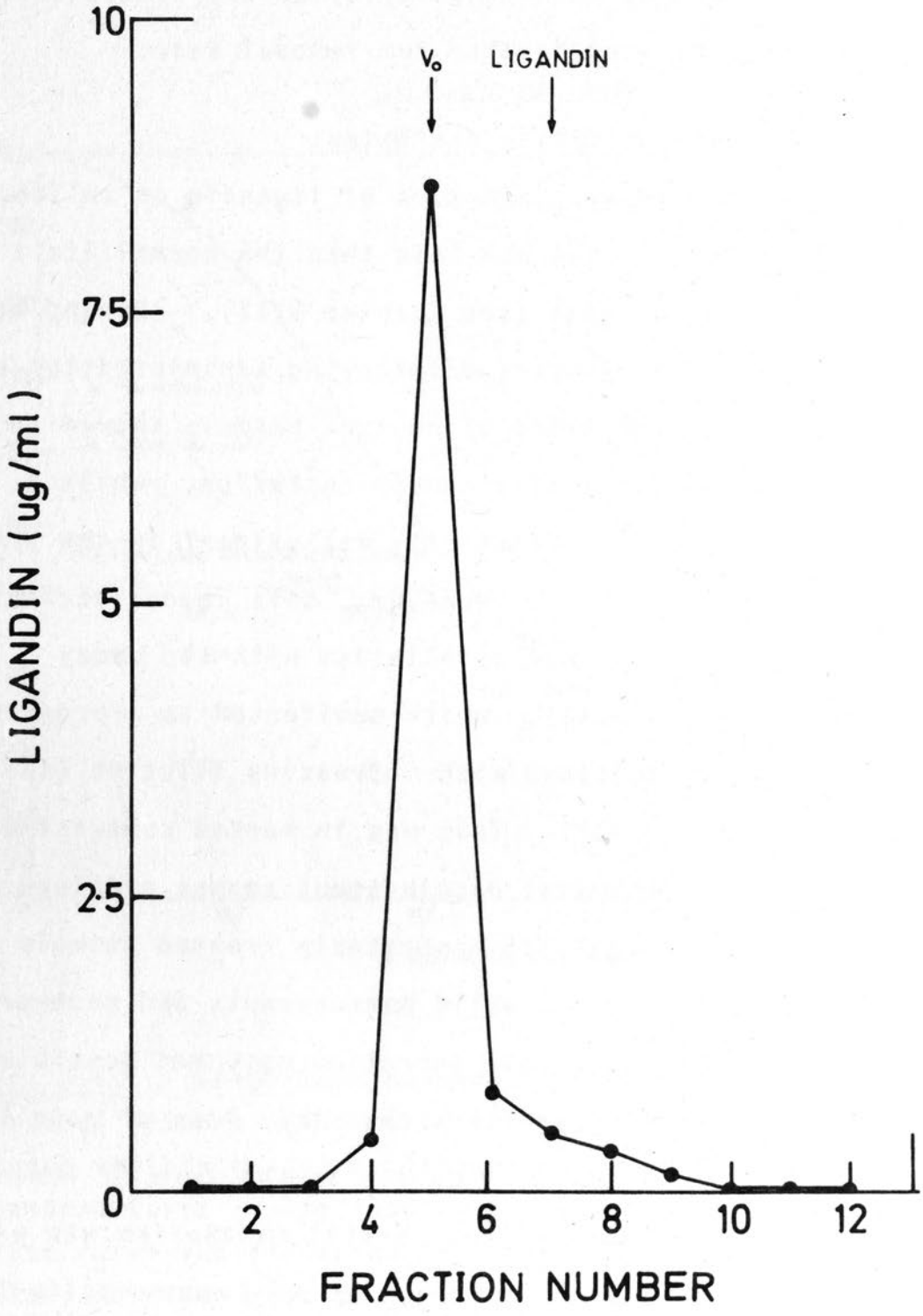

Fig. 2.42. The molecular size of immunoreactive ligandin excreted in the urine following intravenous administration of ligandin. An aliquot from urine collected for 2h following the intravenous administration of pure ligandin to a rat was chromatographed on a calibrated column of Sephadex G-75. Ligandin was determined by RIA. (See Methods and Results for details).

treated animals, in which the major peak of urinary immunoreactive ligandin emerged in the expected elution volume for ligandin (see Chapter XVII, Fig. 2.47).

4. Discussion

In the case of most enzymes studied, disappearance from the plasma is characterized by at least two exponential decay components, and frequently by more than two. These reflect, amongst other things, the three major processes which are active in the removal of proteins (and enzymes) from the circulation (350), viz:

(1) Rapid binding of a portion of the material at sites closely adjacent to the intravascular compartment. This occurs particularly with denatured protein.

(2) A phase of mixing, during which time equilibration between intravascular and extravascular compartments takes place. This is more accurately seen as a redistribution rather than a true removal process.

(3) Irreversible catabolism of circulating and bound protein at sites and by mechanisms which are, as yet, not completely defined.

A fourth factor, that of urinary excretion, is not considered to be of importance in the elimination of the vast majority of released tissue enzymes for which removal data are available. However, urinary excretion of liver-specific

antigens following induced liver-injury in rats as well as in human liver disease, has been clearly demonstrated (352, 353), and the possibility of these antigens being enzymes or fragments thereof, has been raised. The results of the present study have shown that ligandin, when injected in large quantities, is rapidly removed from the circulation, and that elimination of ligandin in the urine represents at least one pathway of its removal. In this regard, ligandin is similar to amylase which also, by virtue of its low molecular weight, undergoes elimination to some extent via the urine (354). The disappearance of ligandin in most of the animals injected with either the pure protein or hepatic cytosol, was characterized by the sum of two exponential decay processes. These, at the risk of some oversimplification, may be regarded as indicating the simultaneous operation of both a rapid and a relatively slow process removing ligandin from the circulation, of which one is equilibrative, and the other irreversible. Although it was shown that ligandin appears in the urine within the 2h period following injection, in most cases, the bulk of circulating protein had disappeared by 1h. Thus the lack of earlier urine sampling (which would have required catheterization of animals), coupled with the alteration of excreted ligandin to a form which invalidated quantitative recovery estimation from the urine, make it difficult to resolve whether the rapid component of ligandin disappearance from the circulation is attributable to urinary loss, or whether this is due to mixing between intra- and extravascular compartments, adsorption

and catabolism of a portion of the injected material - possibly denatured ligandin - near the intravascular space, or other factors; under these circumstances, the slow component of ligandin disappearance could reflect urinary loss of the protein. The reason for the monoexponential clearance of ligandin observed in two of the animals is also not clear. Measurements of urinary ligandin immunoreactivity in these animals might have been valuable in resolving the uncertainties discussed above.

^{125}I-labelled ligandin was readily de-iodinated after introduction into the circulation. This seems unlikely to be due to the action of the plasma alone, in which ^{125}I-ligandin appears relatively stable (see Chapter XV), and may thus be indicative of a rapid uptake and partial catabolism of ligandin at some site close to the intravascular compartment. However, this may only be true in the case of labelled ligandin in which a denaturing effect of iodination causes it to be handled in a different manner to unlabelled protein (350). Nevertheless, support for the hypothesis that ligandin is catabolised in some manner prior to any urinary excretion, is lent by the finding that ligandin, which has passed from the circulation into the urine, takes the form of polymolecular aggregates of high molecular weight. As this is not observed to a significant degree in the case of ligandin lost into the urine directly from the renal tubules (see Chapter XVII), it may indicate that circulating ligandin is altered by some catabolic process prior

to its loss in the urine in a manner which promotes the later formation of ligandin aggregates in the urine.

The disappearance ratesof specific enzymes following the intravenous injection of purified material, or of impure tissue extracts, may differ significantly (350). For this reason, the disappearance of ligandin following injection of both purified protein and hepatic cytosol were followed. In both cases, ligandin was removed rapidly from the circulation, although more subtle differences between the disappearance of this protein after injection of pure material and hepatic cytosol were evident. The confirmation of these differences, as well as resolution of some of the other questions raised by this preliminary study, will no doubt obtain from experiments employing larger numbers of animals, with more elaborate simultaneous sampling of plasma and urine.

CHAPTER XVII

LIGANDINURIA IN ACUTE TUBULAR NECROSIS

1. Introduction

It is well recognized that acute renal failure may be produced by the administration of a large variety of nephrotoxic compounds (for review, see ref. 355). The majority of these compounds exert their toxic effects in the general region of the proximal tubular segment of the nephron, although a few are known to produce even more highly circumscribed lesions within this anatomical zone. Such is the case with the extensively studied nephrotoxin $HgCl_2$ (356), which produces acute epithelial necrosis of the pars recta of the proximal tubule, while sparing the remaining parts of the nephron (357-360); and also $K_2Cr_2O_7$, which selectively damages the pars convoluta of the proximal tubule when administered in sublethal doses (359). The selective anatomical sites of necrosis produced by these agents has prompted their use in a number of experimental studies aimed at elucidating the pathophysiology of acute renal failure, with particular attention paid to the correlation between specific structural tubular lesions and functional renal impairment (359, 360). The tubular lesions produced by specific compounds have in most cases been defined by detailed histological examination of kidney sections (357, 358, 360) and isolated nephrons (359), while the sequence of disruption of subcellular structures by nephrotoxins has been explored by histochemical techniques (355, 361, 362) as well as by the measurement of the urinary excretion of enzymes of

known subcellular organelle distribution (363). However, although the activities of several enzymes have been shown to vary in relation to different anatomical regions of the nephron (364), the patterns of urinary enzyme excretion following the administration of different nephrotoxins do not provide information regarding the different areas of the nephron damaged by different nephrotoxic agents (363, 365). It was thus of much interest when Kirsch et al (273) and Feinfeld et al (274) reported that ligandin was excreted in the urine of rats given $HgCl_2$ but did not appear in the urine of animals treated with $K_2Cr_2O_7$. These findings suggested that renal ligandin is preferentially located in the pars recta of the proximal tubule and that measurement of ligandinuria may provide a highly specific means of locating damage to this anatomical region of the nephron. Evidence that measurement of ligandinuria may be of value in the clinical detection and prediction of acute tubular necrosis in man has also been presented (see Chapter IV.5).

Ligandinuria has previously been detected by immunodiffusion methods as well as by the measurement of GSH S-transferase activity. The RIA technique provides an extremely sensitive and specific means of measuring ligandin directly, and it was thus of importance to examine the value of this method in the quantification of ligandinuria in both normal and nephrotoxin-treated animals. This chapter describes the validation and results of ligandin measurement in normal rat urine, and in the urine of nephrotoxin treated animals by RIA. A further study was also performed in order to discover

whether ligandinaemia accompanies ligandinuria in rats with $HgCl_2$ induced tubular necrosis, and to assess the relationship between the time of onset of these events and the development of renal failure in this animal model.

2. Methods

Experimental protocol:

Urine was collected from rats housed in metabolic cages as described in Chapter XVI. Rats were allowed food and water during the experiments. Food was accessible to animals in a small compartment away from the collection funnel, while water bottle spouts contained ball-valves. These measures effectively prevented contamination of urine with food or drinking water. Fresh solutions of $HgCl_2$ and $K_2Cr_2O_7$ (1% in distilled water) were prepared prior to use. These substances as well as 0.9% saline, were administered to rats by subcutaneous injection. At the end of each collection period, the collection funnels of the metabolic cages were cleaned with distilled water. Two groups of rats were studied:

Group 1

After a basal urine collection period of 24h, six animals received $HgCl_2$ (0.5 mg/100g body weight), another six received $K_2Cr_2O_7$ (0.7 mg/100g body weight) (359), while a further three received equivalent volumes of saline and served as controls. Following the injections, urine was collected from each animal over periods of 0-6, 6-12,

12-24, 24-36, 36-48 and 48-72h.

Group 2

After a basal urine collection period of 24h, six animals received $HgCl_2$ (1 mg/100g body weight). Urine was collected from each animal over periods 0-6, 6-12 and 12-24h following the injections. Blood samples were obtained from the tail veins at the end of the basal and each post-injection collection period. At 24h, four of the six rats were sacrificed, the livers and kidneys removed, and cytosol prepared from these tissues for ligandin determination (see Appendix B). For control estimations of tissue ligandin levels, cytosol was also prepared from the livers and kidneys of another four rats injected with saline 24h prior to sacrifice. Urine and blood were not collected from these animals.

Analysis of samples:

Ligandin was measured in urine, serum and cytosol by RIA (see Chapter X). Neither $HgCl_2$ nor $K_2Cr_2O_7$ at concentrations of 0.4M caused any displacement of antibody-bound ligandin in the RIA. Protein concentration of cytosol was determined as described in Appendix B. After measurement of volumes, urine samples were centrifuged (see Chapter XVI). and assayed either immediately or after storage at $-20^{o}C$. Protein and glucose in urine were measured qualitatively by means of Ames Labstix. Several samples of urine obtained during basal collection periods as well as during the periods following $HgCl_2$ administration were each divided into 4

aliquots. In the case of each sample, one aliquot was assayed immediately after the collection, while the remaining three were assayed after incubation at -20, 4 and 25°C for 24h respectively. In order to compensate for variation in ligandin concentration produced by fluctuation in urine flow, ligandin excretion in the urine was expressed as:

$$\text{Urinary ligandin excretion (ng/h)} = \frac{\text{Urine ligandin concentration (ng/ml)}}{\text{Duration of collection period (h)}} \times \text{Total sample volume (ml)}$$

Serum was separated from blood samples and 50 µl of each sample diluted with cold assay diluent, as described in Chapter XVI, for ligandin determination. Blood urea nitrogen (BUN) was estimated in duplicate on 10 µl aliquots of each serum sample by means of a Beckman BUN autoanalyser. The operating instructions supplied by the manufacturer were followed in performing these estimations, and details are not given in the Appendix. BUN values were multiplied by the factor 2.142 to convert to urea (mg%). Immunodiffusion was performed as described in Chapter VIII and Appendix B.

Statistical comparison of data employed Student's paired t test (for parametric paired data), the Wilcoxon paired signed-ranks test (for non-parametric paired data) and Student's unpaired t test (for parametric unpaired data). The correlation coefficient (r) was derived from least squares analysis of data (see Appendix C).

Recovery experiments:

The estimation of quantitative recovery of pure ligandin added to urine was performed according to the same protocol outlined for plasma in Chapter XV. The "predicted" values in this case were 100, 500, 10,000 and 20,000 ng/ml. Each pool comprised equal volumes of urine obtained from 3 rats during basal urine collection periods.

Gel filtration:

2.5 ml of pooled urine samples from rats in Group 2 were chromatographed on Sephadex G-100 as described in Chapter XV. Ligandin was measured in column fractions by RIA. Samples studied were:

(1) normal rat urine - comprising 3 pooled aliquots from basal collection samples,

(2) a similar pool of urine collected from rats 6-12h after $HgCl_2$ administration.

3. Results

Characterization of RIA of ligandin in urine:

Immunoreactive ligandin was detected in all urine samples assayed. Twenty-one normal (basal) urine samples yielded a range of concentrations for immunoreactive ligandin of between 1.0-189 ng/ml, while values in some $HgCl_2$-treated animals were as high as 80,000 ng/ml. Normal urine as well as urine containing high concentrations of immunoreactive ligandin following nephrotoxin administration, gave immuno-

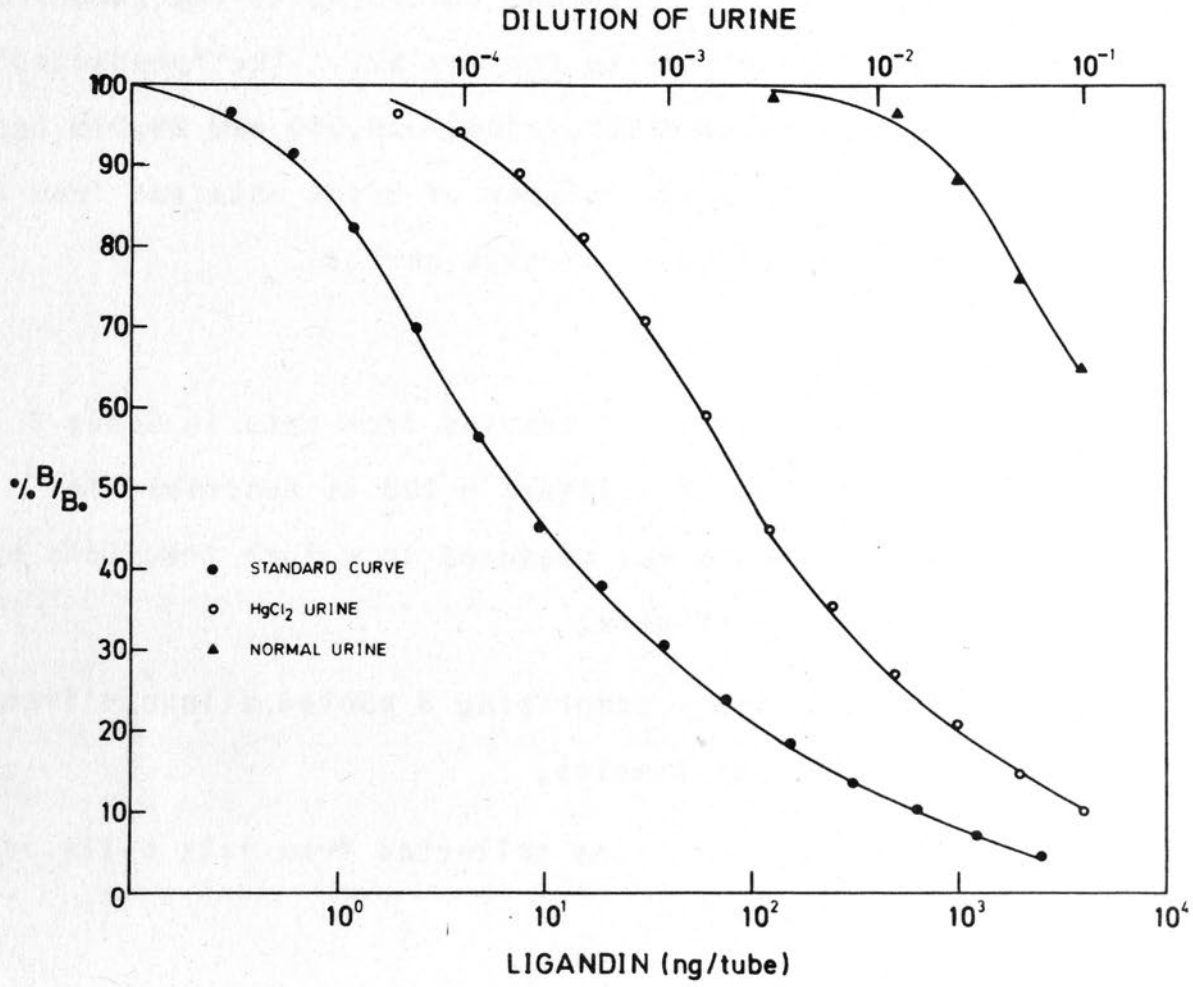

Fig. 2.43. Comparison between immunochemical displacement curves of normal and $HgCl_2$-treated rat urine and the ligandin RIA standard curve. Ordinate and abscissa are as described in legend to Fig. 2.18.

chemical displacement curves which ran parallel with the standard curve of the assay (Fig. 2.43). It was found however, that when some urine samples were assayed without prior dilution, values were obtained which were anomalously low in comparison with the consistent values obtained for the same samples assayed over a wide range of dilutions. The non-specific interference of factors in urine, such as urea and high salt concentration, with RIA's are well recognized (286, 287), and it thus seemed likely that the anomalous values obtained when urine was assayed undiluted were due to these and possibly other factors present in high concentration. This problem was overcome simply by assaying all urine samples at initial dilutions of 1:5 and greater.

RIA measured recoveries of pure ligandin added to normal rat urine are shown in Table 2.XXII.

Aliquots from four samples of normal (basal) urine and from four samples of urine containing high levels of immunoreactive ligandin following $HgCl_2$ administration were assayed immediately after collection as well as after incubation at different temperatures for a 24h period (see Methods). The values obtained for these samples after incubation expressed as percentages of the values obtained after immediate assay, were between 83-104% (-20°C), 74-89% (4°C) and 48-54% (25°C). Thus the apparent "enhancement" effect of freezing on immunoreactive ligandin in plasma (see Chapter XV) was not observed with urine. The loss of immunoreactive ligandin in urine kept at 25°C could be due to several factors, the most

TABLE 2.XXII

RECOVERY OF PURE LIGANDIN FROM NORMAL RAT URINE

Pool no.	Endogenous (A) (ng/ml)	Predicted (B) (ng/ml)	Assayed (C) (ng/ml)	C - A (ng/ml)	% Recovery % (C-A/B)
1	52	100	132	80	80
		500	518	466	93
		10,000	9,628	9,576	96
		20,000	19,852	19,800	99
2	91	100	190	99	99
		500	500	409	82
		10,000	9,410	9,319	93
		20,000	19,980	19,889	99

Each pool comprised equal volumes of urine obtained from 3 rats during basal period collections. Predicted (B) values were based on the addition of known amounts of pure ligandin (see Methods for details).

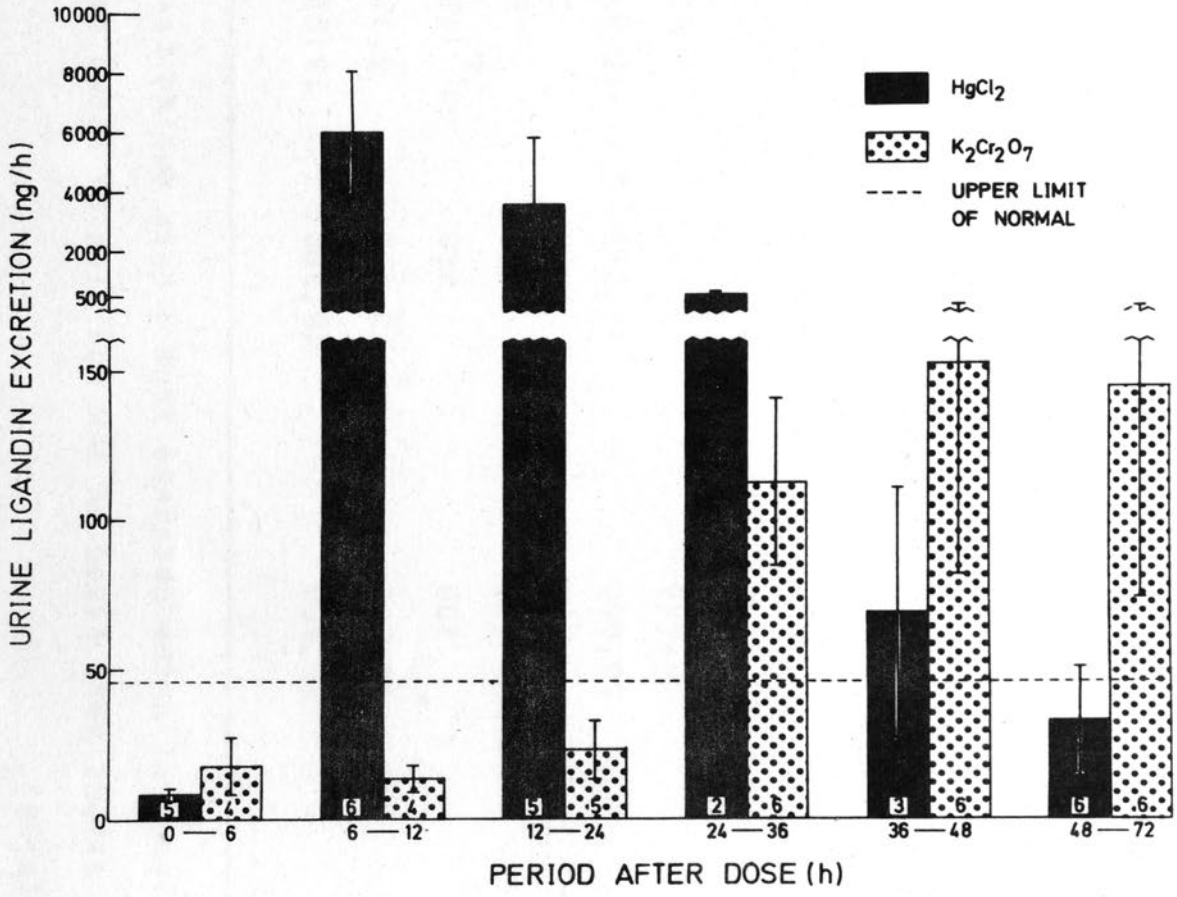

Fig. 2.44. Ligandinuria in rats following administration of either $HgCl_2$ (0.5 mg/100g body weight) or $K_2Cr_2O_7$ (0.7 mg/100g body weight). Each bar shows ligandin excretion as Mean ± SEM for the number of animals (given at the bottom of each bar) passing sufficient urine for assay during each sampling period.

likely being degradation of the protein by bacterial and other proteases present in the urine. However, loss of immunoreactivity in these specimens was not accompanied by a loss of immunochemical displacement curve parallelism.

Basal excretion of ligandin in the urine:

Although a wide range of immunoreactive ligandin concentrations were encountered in basal urine samples (see above), when compensation was made for variations in urine flow by taking the factors of time and urinary volume into consideration, the range of values obtained for ligandin excretion in 21 rats calculated from 24h basal urine collections was 2-46 ng/h (Mean $\pm$ SEM: 14.86 $\pm$ 2.81 ng/h). Thus for the purpose of this study, an excretion of 46 ng/h of ligandin in the urine was taken as the upper limit of normal.

Ligandinuria following $HgCl_2$ and $K_2Cr_2O_7$ administration:

The mean excretion of ligandin in the urine of rats up to 72h following administration of either $HgCl_2$ or $K_2Cr_2O_7$ is illustrated in Fig. 2.44. During the basal collection period, urine volumes sufficient for assay purposes were obtained from all rats. However, as shown in Fig. 2.44, several rats did not pass sufficient urine for assay during the sampling period following nephrotoxin administration. This was particularly the case with $HgCl_2$-treated animals 24-48h following administration of the toxin. In animals treated with either $HgCl_2$ or $K_2Cr_2O_7$, ligandin excretion remained normal during the first 6h of urine collection

following administration of these toxins. A dramatic increase in ligandin excretion was shown by the $HgCl_2$-treated rats over the 6-12h period following injection. Over subsequent urine collection periods, mean ligandinuria declined in these animals and reached normal limits between 48-72h following injection. A different pattern of ligandinuria was evident in $K_2Cr_2O_7$-treated rats. Mean ligandin excretion in these animals remained normal up till 24h after injection. Thereafter, for the remaining three collection periods, $K_2Cr_2O_7$-treated rats (excepting for one during the 24-36h, and two during the 48-72h collection period) showed abnormally elevated ligandin excretion. It should be noted however, that the extent of abnormal ligandinuria developed by $K_2Cr_2O_7$-treated animals was at least an order of magnitude less than the maximum seen in $HgCl_2$-treated rats. Basal urine samples contained no glucose, while most showed traces of protein. The $HgCl_2$-treated rats developed glycosuria from 6h, and this persisted for the duration of the experiment. Glycosuria was only evident in the $K_2Cr_2O_7$-treated animals after 36h, lasting up till the final collection period. Proteinuria (1+) was observed in most of the $HgCl_2$- and $K_2Cr_2O_7$-treated rat urines from 0-6h after injection. Thereafter, all urines collected showed 2-3+ proteinuria. When rats were sacrificed at the termination of this experiment, the kidneys of both $HgCl_2$ and $K_2Cr_2O_7$-treated animals showed swelling and discolouration. None of the control rats showed glycosuria or excretion of ligandin above the upper limit of normal during any of the

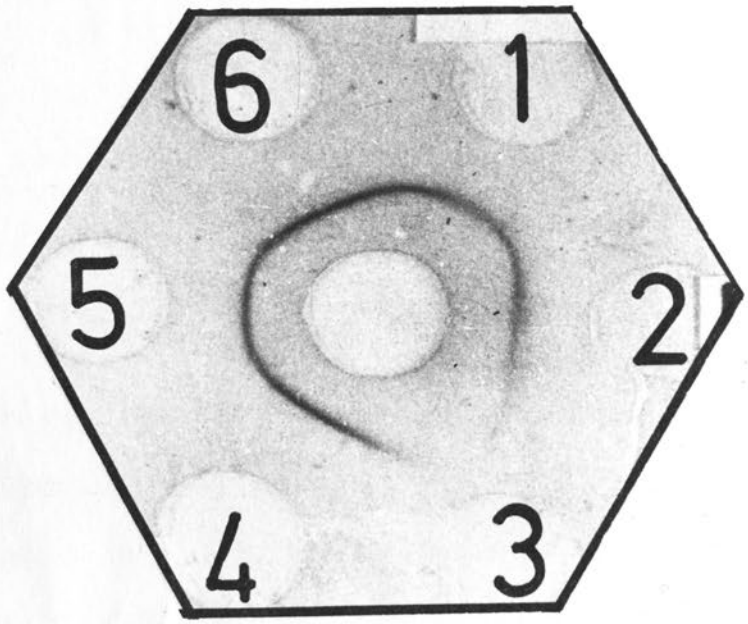

Fig. 2.45. Immunodiffusion in agar gel. The centre well contains rabbit anti-ligandin antiserum; the peripheral wells contain: 1 and 5, urine from $HgCl_2$-treated rats; 3, normal rat urine; cytosol from 4, liver (1:4) and 6, kidney (1:2) with ligandin (1 µg) in well 2. Precipitates were stained with amidoblack. (See Appendix B for details of procedure).

collection periods.

When unconcentrated urine specimens were tested by immunodiffusion with rabbit antiserum to pure ligandin, precipitin lines were only observed with specimens of urine obtained from $HgCl_2$-treated rats 6-24h after injection, in which concentrations of immunoreactive ligandin were greater than 20,000 ng/ml. A single precipitin line of complete identity was obtained between these urine samples, cytosol from liver and kidney, and pure ligandin on immunodiffusion (Fig. 2.45). Normal (basal) rat urine showed no precipitin line on immunodiffusion.

Ligandinuria, ligandinaemia and renal failure following $HgCl_2$ treatment:

The individual levels of urinary ligandin excretion, serum ligandin and serum urea obtained in six rats before and after $HgCl_2$ administration (1 mg/100g body weight) are illustrated in Fig. 2.46. No urine was obtained at any time from rat no. 1 following the administration of the nephrotoxin, or from the other five animals during the 12-24h period following injection. During the 0-6h collection period, ligandin excretion in four of the five rats passing urine was greater than the upper limit of normal, and for the five animals as a group, ligandin excretion was significantly greater during this period than during the basal collection period ($P < 0.01$). During the 6-12h collection period, ligandin excretion in all five animals was markedly increased and coincided in each case with the onset of glucosuria. Proteinuria (3+) was found in all the

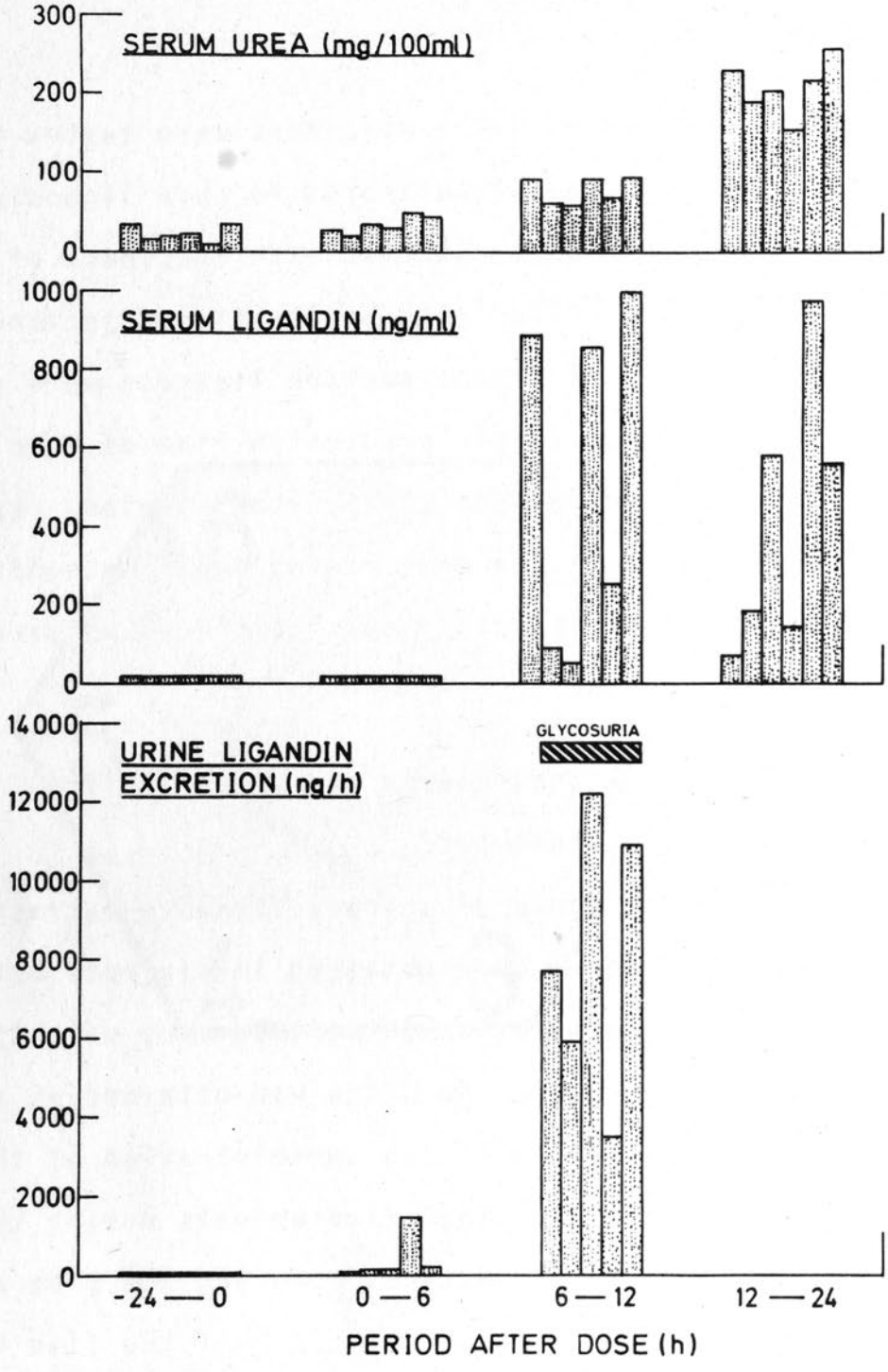

Fig. 2.46. Ligandinuria, ligandinaemia and azotaemia in rats following $HgCl_2$ administration. Rats received 1 mg $HgCl_2$/100g body weight. Six animals were used; bars represent individual values. Urine was not obtained from rat no. 1 after injection, nor from any of the remaining animals after 12h.

urine specimens obtained after injection of HgCl2.

Serum ligandin levels were undetectable (< 30 ng/ml) in all six animals at the end of the basal period, and remained thus at 6h after $HgCl_2$ administration. By 12h, serum ligandin levels were measurable in all the rats and were greater than normal in all except rat no. 3. On statistical analysis (rat no. 1 excluded), there was no significant correlation between 6-12h ligandin excretion and 12h serum ligandin levels ($r = 0.77$, $P > 0.05$). At 24h after $HgCl_2$ injection, serum ligandin levels were abnormally elevated in all six rats.

6h after $HgCl_2$ administration, serum urea levels were higher than 0h levels in 5 out of the 6 rats. However, for the group as a whole, urea levels were not significantly greater at 6h than at 0h ($P > 0.05$). Nevertheless, it is interesting to note that a five-fold increase in serum urea occurred from 0-6h in the rat (no. 5) which showed the greatest ligandin excretion during this period. Serum urea levels were significantly raised in the rats by 12h ($P < 0.01$), and showed a further significant increase by 24h.

The kidneys of $HgCl_2$-treated rats at 24h appeared swollen and pale; but the livers were normal in appearance. Ligandin concentration in the kidneys of $HgCl_2$-treated rats was significantly reduced to about 30% of control values (Table 2.XXIII). There was no difference in mean heaptic ligandin concentration between $HgCl_2$-treated and control animals.

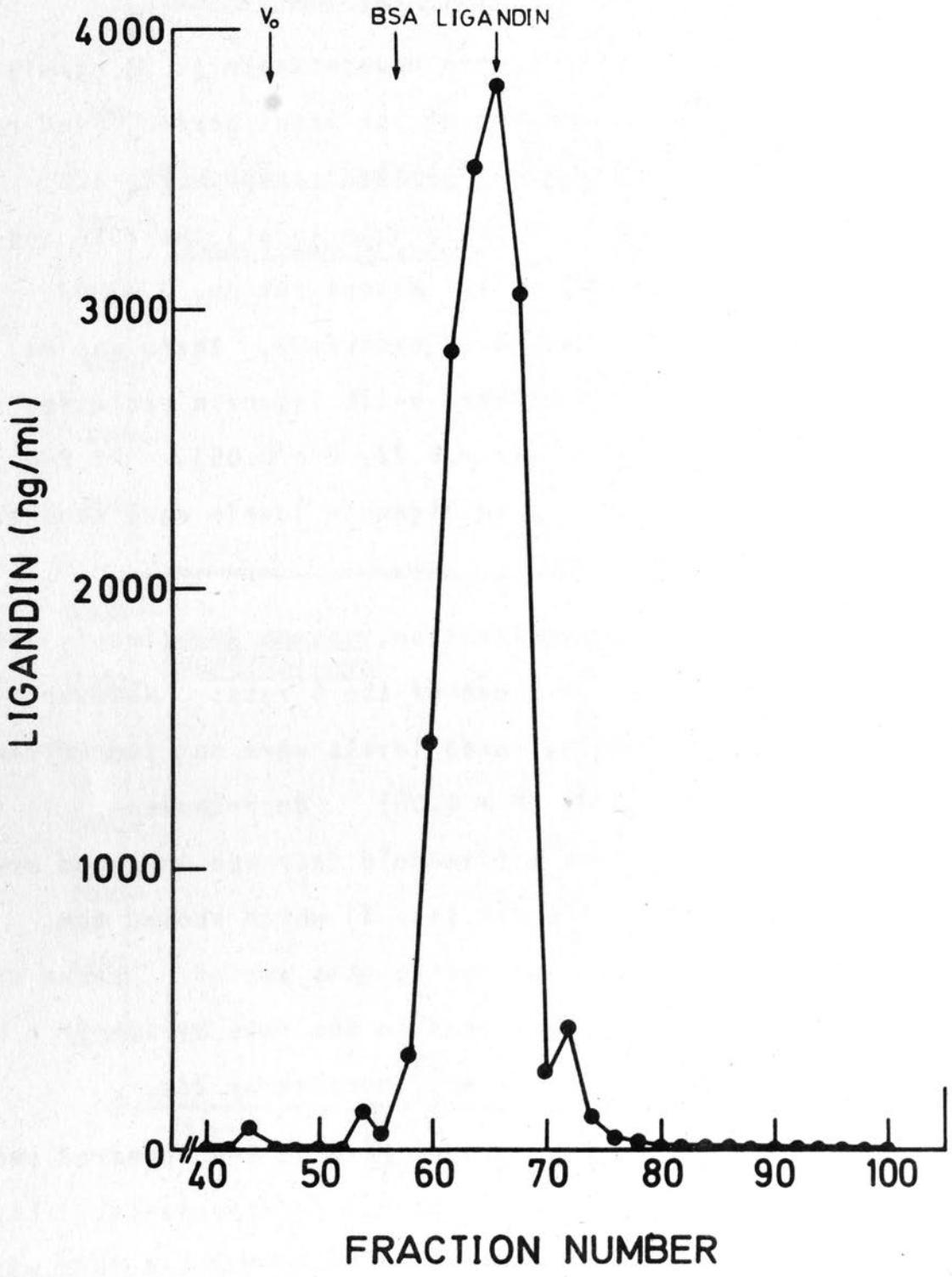

Fig. 2.47. Immunoreactive ligandin in $HgCl_2$-treated rat urine chromatographed on Sephadex G-100. Pooled urine obtained from 3 rats 6-12h following $HgCl_2$ administration (1 mg/100g body weight) was chromatographed on Sephadex G-100 as determined in Methods. Ligandin was measured by RIA.

TABLE 2.XXIII

HEPATIC AND RENAL LIGANDIN LEVELS 24h AFTER $HgCl_2$ ADMINISTRATION

Tissue	$HgCl_2$-treated (µg/mg)	Controls (µg/mg)	P
Liver	44.3 ± 4.69	36.76 ± 2.85	ns
Kidney	6.26± 1.28	18.24 ± 1.55	< 0.001

Results are expressed as Mean ± SEM in µg/mg supernatant protein. 4 Animals were used for each determination.
ns: not signigicant ($p \geq 0.05$)

Molecular size of urinary immunoreactive ligandin:

When pooled urine from $HgCl_2$-treated rats was chromatographed on Sephadex G-100 and fractions assayed for ligandin, a major peak of immunoreactivity was found in the expected elution volume of ligandin (Fig. 2.47). Three minor peaks of immunoreactivity were also evident, eluting in the void volume and just before and after the main peak respectively. These minor immunoreactive peaks may have indicated cross-reaction of other proteins excreted in the urine of $HgCl_2$-treated rats with the RIA, or else may have arisen from denatured ligandin eluting in aggregated and fragmented form. On gel filtration of normal rat urine, no immunoreactive ligandin could be detected in column fractions, probably for the same reason that no immunoreactive peak was observed

in normal rat serum (see Chapter XV) i.e. dilution of the small quantity of ligandin in normal urine below the limit of RIA sensitivity and adsorption of ligandin by the Sephadex matrix.

4. Discussion

A large number of proteins and enzymes are detectable in the urine under normal circumstances, and many of the enzymes have found diagnostic applications because of variation in the amounts excreted under pathological conditions (334, 363, 365, 366). These variations may arise from serum enzymes by glomerular leakage or by cellular breakdown in the kidney or other parts of the genitourinary tract and also from the presence of bacteria in the urine. Rosenmann et al (367), using immunodiffusion, have also detected a kidney-specific antigen in the urine of animals with experimental tubular necrosis but not in normal rat urine. In the present study, immunoreactive ligandin was detected in normal rat urine by RIA, and this most probably arises from the renal tubular epithelial cells although other parts of the genitourinary tract e.g. the bladder (see Chapter XI) may also contribute. Another possibility to be borne in mind is that some of the ligandin detected in normal urine may arise from the glomerular filtration of this protein from the plasma. However, the fact that immunoreactive ligandin in normal rat urine demonstrated parallelism with the RIA standard curve, while ligandin excreted from the plasma into the urine showed deviation from

parallelism (see Chapter XVI), suggests that under normal circumstances, the bulk of detectable urinary ligandin derives from the genitourinary tract in an immunologically intact form.

A large number of enzymes are excreted in the urine as a result of renal tubular damage (334, 363, 365), although only a few, such as the glycosidases, appear to be specific for tubular necrosis per se (365, 368). These enzymes are excreted in large amounts following the administration of several nephrotoxins including $HgCl_2$ and $K_2Cr_2O_7$ (365). In contrast, Feinfeld et al (274) reported transient ligandinuria occurring in $HgCl_2$-treated rats 12-24h following administration of the toxin, whereas $K_2Cr_2O_7$ poisoning did not result in detectable ligandinuria. In view of the fact that $HgCl_2$ and $K_2Cr_2O_7$ in low dosages (359) produce discrete necrosis of the pars recta and convoluted portions of the proximal tubule respectively, it appeared from these findings that ligandin is confined to a very limited portion of the nephron, viz. the pars recta of the proximal tubule. The present study largely confirms the findings of Feinfeld et al (274), in that massive ligandinuria was only obtained in $HgCl_2$-treated rats, although peak excretion of ligandin was found 6-12h after administration of the toxin at both 0.5 and 1 mg/100g body weight doses. Furthermore, the sensitivity of the RIA permitted detection of abnormal ligandinuria occurring within 6h in rats receiving the higher dose of the toxin, and also revealed abnormal ligandin excretion occurring in $K_2Cr_2O_7$-treated animals.

Following the administration of $HgCl_2$ to rats, both the time at which tubular lesions appear and also the extent of these lesions have been shown to be highly dose dependent (357, 358). Following the administration of $HgCl_2$ in low doses, similar to that given to Group 1 rats in the present study, electron microscopy has revealed subtle changes throughout the proximal tubule from as early as 15 min, while severe changes in the proximal pars recta have been observed at 6h (360). By 12h, the plasma membranes of the pars recta show distortion and rupture (358), while at 24h, complete necrosis of the pars recta is seen with minimal changes elsewhere in the tubule (358, 360). The appearance of the lesion produced by low-dose $HgCl_2$ does not change up to 72h after administration (359). Thus the time of onset and progression of ligandinuria shown by $HgCl_2$-treated Group 1 rats in the present study, would appear to coincide with the onset and progression of microscopic changes observed following $HgCl_2$ poisoning. The earlier onset of abnormal ligandinuria in Group 2 rats could also be explained as resulting from the higher dose of $HgCl_2$ given to these animals precipitating earlier necrosis of the pars recta (357, 358). The uniform anuria developed by these animals after 12h, has been noted by several workers studying $HgCl_2$-induced renal failure in rats (369-371) and several hypotheses have been advanced to explain the pathogenesis of this phenomenon, but are beyond the scope of this discussion.

It is interesting to note that a significant increase in ligandin excretion occurred prior to development of signifi-

cant azotaemia in Group 2 rats, thus suggesting that necrotic changes in the pars recta precede significant azotaemia in this model of acute renal failure. However, an apparent causal relationship between necrosis of the pars recta and the early pathogenesis of renal failure after $HgCl_2$ poisoning must be considered in the light of the observations of McDowel et al (360) and Zalme et al (362). These workers have clearly shown that considerable histochemical changes occur throughout the entire proximal tubule in $HgCl_2$-treated rats, which precede by several hours any evidence of necrosis in the pars recta. Furthermore, the rats studied by these workers developed significant azotaemia 6h after a 0.4 mg/100g body weight dose of $HgCl_2$, while glomerular filtration rate and tubular reabsorption of sodium and potassium were significantly reduced at this stage. The hypothesis was thus presented (362), that $HgCl_2$ given to rats interacts with the brush border of the entire proximal tubule, leading to greatly diminished reabsorption of sodium mainly due to sublethal injury to the pars convoluta. This in turn results in increased release of renin from the macula densa, which leads to haemodynamic alterations, a decreased glomerular filtration rate and other functional disturbances associated with renal failure. Development of necrosis in the pars recta would thus appear to be a relatively late event occurring as a result of further accumulation of Hg^{++} in this region, and this is probably important in the perpetuation of functional renal disturbance (359, 362). The early significant increase in ligandinuria

prior to the development of significant azotaemia in Group 2 rats may thus indicate a slightly different pathogenesis of early renal dysfunction from that discussed above, occurring as a result of the relatively high dose of $HgCl_2$ given to Group 2 rats. Under these conditions, necrosis of the pars recta - leading to increased excretion of ligandin - may occur sooner after administration of the toxin, and thus play a more important role in the initial stages of acute renal failure. Further study will be required to clarify this question.

The relationship observed in the present study between glycosuria and ligandinuria in both $HgCl_2$- and $K_2Cr_2O_7$-treated rats was interesting. Glycosuria is often seen in rats after administration of several nephrotoxins (359, 363) and was encountered in all urine samples of $K_2Cr_2O_7$ and $HgCl_2$ treated rats by Biber et al (359) 3 days (the earliest period these workers studied) after injection of doses of these toxins similar to those employed in the present study for Group 1 rats. Glycosuria under these conditions is thought to result from diminished glucose reabsorption from the proximal tubule - mainly from the pars convoluta. Thus, even though $K_2Cr_2O_7$-treated rats showed marked proteinuria prior to developing glycosuria, the absence of glucose from the urine of these rats up till the time of established abnormal ligandinuria is difficult to explain. If marked necrosis of the pars convoluta had occurred in these animals prior to the onset of increased ligandinuria at 24-36h, then it would be reasonable to expect them to have also shown

marked glycosuria. This in essence raises the question of the time sequence of $K_2Cr_2O_7$-induced necrosis of the pars convoluta. Established necrosis of this region of the nephron has been clearly shown to be present from 48-72h following $K_2Cr_2O_7$ administration to rats (359, 372), but early time studies, similar to those undertaken in the case of $HgCl_2$, are not available. Thus it is necessary to raise the possibility that necrosis of the pars convoluta following a small dose (0.7 mg/100g body weight) of $K_2Cr_2O_7$ only becomes established 24h after injection. In this case, the increased excretion of ligandin seen in $K_2Cr_2O_7$-treated rats after 24h may indicate the presence of ligandin in the pars convoluta, although in considerably smaller concentration than that occurring in the pars recta of the proximal tubule. Support for this hypothesis is lent by the study of Fleischner et al (212), in which ligandin-specific immunofluorescence was seen in all segments of the proximal renal tubule.

Abnormal ligandinaemia was also demonstrated in the present study following $HgCl_2$ administration. It seems most likely, that increased serum ligandin in this situation obtains from the necrotic pars recta of the renal tubules. Indeed, many enzymes which are excreted in the urine in increased amounts following tubular necrosis are also raised in the serum (334). However, the possibility also exists that ligandinaemia following $HgCl_2$-induced renal failure could result from diminished excretion of this protein from the plasma, especially as urinary excretion appears to be

important as regards the elimination of this protein from the circulation (see Chapter XVI). An examination of ligandinaemia and ligandin removal from the plasma in nephrectomized animals should be helpful in solving this problem. Following poisoning with $HgCl_2$, a small fraction of the dose is accumulated in the liver and excreted in the bile (356), although evidence for a direct toxic effect of $HgCl_2$ on the liver has not been documented. Thus it seems unlikely that the ligandinaemia observed in $HgCl_2$-treated rats in the present study might have resulted as a manifestation of toxic hepatocellular necrosis - especially as the livers of these animals were of normal appearance and contained normal levels of ligandin.

In conclusion, the results of the present study indicate that the measurement of ligandinuria by RIA provides a highly sensitive index of tubular necrosis, especially when the pars recta is involved. The RIA technique for measuring ligandin should thus provide a valuable tool for the experimental study of acute renal failure, and may be of use in screening tests for potentially nephrotoxic compounds administered to rats. The application of a ligandin RIA in the diagnosis of renal tubular disease in man is an exciting and worthwhile prospect which should soon lead to the development of a suitable RIA for human ligandin.

PART 3

SUMMARY AND CONCLUSIONS

CHAPTER XVIII

AN OVERVIEW OF THE PRESENT STUDY

1. Introduction

In the wake of the experimental work presented and discussed in Part 2 of this thesis, all that remains is to provide a concise synthesis of the new data that has emerged from the present study, and to examine its contribution to the established framework of knowledge concerning ligandin.

The work presented in this thesis has centred mainly on the development and applications of an RIA technique for measuring ligandin, whilst also delving into the morphological and functional properties of this protein. The scope of this study has thus included aspects of methodology, "basic research" into the properties, distribution and development of ligandin, as well as an exploration of the diagnostic potential of ligandin measurement in physiological fluids. The discussion that follows is contained under three headings appropriate to the abovementioned aspects of the work of this thesis. Thereafter, follows a consideration of the broader implications of the ligandin RIA, with special reference to its place in future research and clinical investigation.

2. RIA of Ligandin - A New Technique

An RIA for rat ligandin was successfully instituted and characterized along the lines of established principles of RIA. The essentials of the RIA methodology were: iodination

of ligandin with ^{125}I by the chloramine-T method, purification of the labelled protein by combined Sephadex G-25/TEAE-cellulose chromatography, and separation of antibody-bound from free labelled protein by a double antibody method. A high titre antiserum to ligandin was raised in rabbits by means of a conventional immunization protocol. The RIA constitutes an entirely new and thus far the most sensitive means for measuring ligandin. The RIA was found to be applicable to the measurement of ligandin in tissue supernatants, plasma, serum and urine, and showed relative freedom from non-specific interference effects. In addition, the RIA appeared specific for ligandin (GSH S-transferase B), although the evidence obtained for lack of cross-reaction with the other rat GSH S-transferases was indirect; and it would be interesting to assess this level of assay specificity directly with homogenous preparations of the several rat GSH S-transferases. The RIA for rat ligandin is easily performed and highly reproducible, and provides a new research tool for the quantitative study of ligandin in the rat. Furthermore, this technique offers the advantage of enabling numerous samples to be measured within a single assay, while consuming only minute quantities of specific antiserum and pure ligandin.

Although demonstrating cross-reaction with hepatic supernatants from several species, the present assay is only valid for quantifying ligandin in the rat. It is hoped, however, that the methodology developed in this study for RIA of ligandin in the rat will be of practical value in establishing similar assays for ligandin in other species, including man.

3. Ligandin - Towards a Better Understanding

The discovery of ligandin emerged as an exciting and dramatic event which held the promise of yielding much to the understanding of the basic molecular events underlying hepatic transport of small molecules and carcinogenesis. Subsequently, ligandin grew in stature with the acquisition of an additional, enzymatic identity. However, as discussed at length in Chapter IV, the intracellular role of ligandin - and more specifically, its non-enzymatic role - still lacks clear definition. The present study has confirmed and extended knowledge concerning the distribution, development and properties of ligandin, and in doing so has aimed at extending the insight into the role of this protein in the cell.

Immunoreactive ligandin was shown to be widely distributed throughout the tissues of the rat, although in accord with other workers (see Chapter III.6.ii), the highest concentrations were found in the liver, kidney and small intestinal mucosa. The only other tissues with ligandin levels > 1 µg/mg supernatant protein were the testis, ovary and adrenal gland. All tissue supernatants containing immunoreactive ligandin generated immunochemical displacement curves which were parallel with the ligandin RIA standard curve, while in addition, immunoreactivity was essentially confined to the appropriate size class of proteins on Sephadex G-100 chromatography of five different tissue supernatants. It was also evident that the proportion of ligandin to the other GSH S-transferases varies to a large degree in different

tissues. The established effect of phenobarbital treatment on hepatic ligandin concentration was confirmed in the present study, while smaller increases of the protein in kidney and small intestinal mucosa were also found in response to phenobarbital treatment. Testicular ligandin concentration did not change on treatment with this drug.

The neonatal development of ligandin was measured directly by RIA, and different patterns were obtained in liver and kidney. In both tissues, ligandin levels were < 10% of adult levels at birth. Hepatic ligandin concentration increased rapidly and progressively after birth; renal ligandin concentration increased up till day 5 after birth, thereafter remaining unchanged until a marked rise in the third week of life. The different patterns of development shown by ligandin in the liver and kidney may relate to differences in the development of specific transport functions in these tissues, and further work is required to test this hypothesis.

When ligandin was purified from rat liver, the protein was found to consist of two non-identical subunits which corresponded in size to the smallest (subunit Y_a) and the largest (subunit Y_b) of the three major subunit species (Y_a, Y_b and Y_c) present in the hepatic BSP-binding Y peak (which corresponds to the immunoreactive ligandin peak). The immunoreactive ligandin peaks of kidney and small intestinal mucosa also revealed the presence of subunits corresponding in size to the Y_a, Y_b and Y_c subunits of hepatic cytosol, whereas in the testis, no Y_a subunit was evident although subunits

corresponding in size to the Y_b and Y_c species were present. Furthermore, phenobarbital treatment led to a marked increase in the hepatic Y_a and Y_b subunits, but not the Y_c subunit. It is concluded from these findings, that the hepatic Y fraction contains 3 separate 40-50,000 dalton dimeric protein size classes: Y_a-Y_a, Y_b-Y_b and Y_c-Y_c in ascending order of size, and that purified ligandin consists of two distinct dimeric proteins corresponding in size to the Y_a-Y_a class (Y_a-ligandin) and the Y_c-Y_c class (Y_c-ligandin). From the behaviour of the different sized Y proteins on anion exchange chromatography, a different order in terms of charge may be proposed from most to least basic: Y_a-Y_a > Y_c-Y_c >> Y_b-Y_b. The subunits of these dimers are not disulphide linked, while incubation studies with cytosol suggest that all 3 forms are present in vivo with no interconversion from the larger to the smaller species in vitro. The selective effect of phenobarbital on Y_a-ligandin, as well as the more basic pI of this protein relative to Y_c-ligandin were subsequently used to purify Y_a-ligandin free of contamination from Y_c-ligandin. Y_a-ligandin possessed catalytic activity with several of the GSH S-transferase substrates, showing higher specific activities with all the substrates - excepting BSP, with which no activity was found - than the activities previously reported for mixtures of Y_a- and Y_c-ligandin (Y_a/Y_c-ligandin). The K_m of Y_a-ligandin with 1-chloro-2,4-dinitrobenzene as substrate was similar to that previously reported for GSH S-transferase B (see Chapter XIV.4), while V_{max} was 50% higher. Y_a-ligandin

also bound BSP and bilirubin, both at a single site, with affinities closely similar to those previously reported for Y_a/Y_c-ligandin. Other points which were established concerning Y_a-ligandin were: an amino acid analysis corresponding closely to the established analyses for Y_a/Y_c-ligandin, parallel cross-reaction in the ligandin RIA and generation of an antiserum which showed a single precipitin line of identity on immunodiffusion and immunoelectrophoresis with cytosol from liver, kidney, small intestinal mucosa and testis. This latter behaviour contrasted with the behaviour of antiserum to Y_a/Y_c-ligandin, which gave reactions of both complete and partial identity with testis cytosol (as well as cytosol from ovary and adrenal gland). This antiserum also gave only a single line with cytosol from the other tissues mentioned above. It is thus concluded, that a close structural relationship exists between the Y_a and Y_c species of ligandin, and that although no conversion from Y_c- to Y_a-ligandin was evident in vitro, an in vivo precursor-product relationship between these forms remains a possibility. However, assuming this hypothesis is correct, it is not easy to explain the absence of a Y_a component in the testis. The results of immunodiffusion studies do, however, point to some interesting possibilities. These studies suggest that there is a close antigenic relationship between the Y_a and Y_c species in the tissues which contain both species (i.e. liver, kidney and small intestinal mucosa), and further, that there is identity between the antigenic determinants of hepatic Y_a-ligandin and Y_c-ligandin in the testis.

However, the presence of a reaction of partial identity between testis Y fraction and antiserum to Y_a/Y_c-ligandin bears the implication that the Y_c-ligandin components of liver and testis are antigenically related but not identical, and are thus different in structure. It is feasible that a difference in structure between the Y_c-ligandin in testis and that in liver could underlie the lack of in vivo conversion to Y_a-ligandin in the testis and the presence of such a conversion in the liver.

The findings of the present study also show conclusively, that hepatic Y_a-ligandin possesses both catalytic and organic anion-binding properties; and although no definite conclusions may be drawn concerning these properties in hepatic Y_c-ligandin, the greater GSH S-transferase catalytic activity of hepatic Y_a-ligandin compared with Y_a/Y_c-ligandin suggests that hepatic Y_c-ligandin may not contribute much towards GSH S-transferase catalytic activity. This contrasts with the finding of considerable 1-chloro-2,4-dinitrobenzene-conjugating activity in testis, which only possesses the Y_c component of ligandin. Although the hypothesis of a structural difference between hepatic and testicular Y_c-ligandin might account for this apparent discrepancy, the factor introduced by the other GSH S-transferases, as well as the existence of size heterogeneity in these enzymes, makes satisfactory interpretation of these data impossible.

As stated earlier, the role of ligandin in the cell is not clearly defined. However, it must be borne in mind that ligandin may perform different essential functions in

different tissues. The factors determining the intracellular role of ligandin in a particular tissue could include its concentration, the morphological subtypes (Y_a and Y_c) of ligandin present, and the milieu of substrates and non-substrate ligands present in that tissue. Thus the high concentrations of ligandin in the liver, kidney and small intestinal mucosa may facilitate the transport of small molecules by these tissues, and further, provide an important detoxification mechanism. In the steroid producing tissues, ligandin may be of less importance in transport processes, but may be essential to the biosynthesis of steroid hormones (see Chapter IV.4). A "polyfunctional" role for ligandin is an attractive concept in terms of the economy of the cell and of the organism. The functional significance of ligandin heterogeneity is unknown. Indeed, many questions remain to be answered concerning the individual properties and possible functions of the size heteromers of ligandin, and further studies on homogenous forms of the Y_a and Y_c components of ligandin should prove valuable in answering these questions.

4. The Diagnostic Role of Ligandin

Considerable release of ligandin into the circulation takes place following experimentally (CCl_4) induced hepatocellular necrosis, and this is accompanied by a significant fall in the concentration of ligandin in the liver but not in the kidney. Ligandin release into the plasma following CCl_4 poisoning, and its response to different doses of the toxin, were similar in pattern to the analogous behaviour of cytoplasmic enzymes in general. However, in terms of elevation

above normal levels, plasma ligandin appeared more sensitive than the SGOT as an index of CCl_4 induced hepatocellular necrosis. Plasma ligandin elevation was not as marked as the SGOT following acute bile duct ligation, and returned to normal levels by 24h, at which time SGOT was still elevated. The reason for this latter finding is not clear, but it may reflect the more rapid removal of ligandin from the circulation. It was indeed found that ligandin is cleared from the circulation at a rapid rate, although considerable individual variation in the overall clearance rate of this protein was evident. It is also clear from the present study, that urinary excretion is important in the elimination of ligandin from the circulation, although it was not established whether this represents the sole route of clearance for this protein. Plasma ligandin thus appears to be a sensitive index of hepatocellular necrosis and its value in detecting more subtle forms of liver damage requires further study.

The present study confirms earlier reports of ligandinuria occurring following $HgCl_2$ poisoning and has elaborated further on this phenomenon. Massive ligandinuria occurs soon after $HgCl_2$ poisoning and may precede the onset of azotaemia. Ligandinuria is accompanied by ligandinaemia, with depletion of renal ligandin levels. It was further shown that $K_2Cr_2O_7$ leads to a lesser degree of ligandinuria of relatively late onset. Assuming a later time of onset of $K_2Cr_2O_7$-induced necrosis of the pars convoluta of the proximal renal tubules, it can be concluded that ligandin is present mainly in the pars recta, with considerably smaller

quantities present in the pars convoluta of the proximal renal tubules. These studies further emphasise that a sensitive assay for ligandin may prove invaluable in the detection of renal tubular necrosis.

5. The Direction of Future Work

The RIA for ligandin in the rat in itself provides a new tool for studying many aspects of ligandin as well as hepatic and renal damage in the rat. The value of this technique for quantitative work on rat ligandin needs no further comment. The assay of ligandin in plasma and urine may be of value as an aid to screening potentially hepatotoxic and nephrotoxic drugs administered to rats, while many other applications for the rat ligandin RIA as a research tool can be envisaged. Of great importance, however, is that the present study with the ligandin RIA in the rat motivates strongly towards the establishment of a similar assay for human ligandin, which will allow the assessment of plasma and urine ligandin measurement in the diagnosis of hepatic and renal tubular damage in man. Finally, an RIA for ligandin in the human being could contribute much towards the understanding of the intracellular role of ligandin, by permitting the measurement and immunochemical characterization of ligandin in liver biopsy specimens from patients with conditions of isolated impairment of hepatic uptake and/or storage of organic anions.

There are many questions surrounding ligandin. It is this that has made the execution of the present study an in-

structive and stimulating venture to me personally. It is my sincere hope that the new developments presented in this work will serve to advance the understanding and study of this fascinating molecule.

APPENDICES

APPENDIX A

REAGENTS, MATERIALS AND SOURCES OF SUPPLY

REAGENTS, SPECIAL MATERIALS AND SOURCES OF SUPPLY

Unless stated to the contrary, all reagents used in the present study were of the highest grade available.

Ames Co., Hillbrow, Transvaal, R.S.A.

Multistix (Labstix)

Aldrich Chemical Co. Inc., Milwaukee, Wisconsin, U.S.A.

3,4-Dichloronitrobenzene (1,2-Dichloro-4-nitrobenzene)

1-Chloro-2,4-dinitrobenzene

p-Nitrobenzyl chloride

Bayer Pharmaceuticals, Leverkusen, Germany.

Trasylol

Beckman Instruments Inc., Fullerton, California, U.S.A.

Desicote

Pentachlorophenol

Thiodiglycol

Boehringer Mannheim, Mannheim, Germany.

Ovalbumin (egg white)

Aldolase (rabbit muscle)

British Drug Houses (BDH), Poole, England.

Acrylamide (laboratory reagent)

Ammonium persulphate

Bilirubin

Bromophenol blue

Diethylbarbituric acid

Ethanolamine (laboratory reagent)

Folin & Ciocalteu's phenol reagent (laboratory reagent)

Glutathione (GSH) (reduced)

Glycerol

Glycine

α-Ketoglutaric acid

Malate dehydrogenase (pig heart)

Mercuric chloride

N,N'-bis-methylene acrylamide (laboratory reagent)

N,N,N',N'-tetramethylethylene diamine (TEMED) (laboratory reagent)

Potassium iodide

Potassium sodium tartrate

Riboflavin

Sodium diethylbarbiturate

Sodium dodecyl sulphate

Sodium iodate monohydrate

Sulphuric acid

Urea

Difco Laboratories, Detroit, Michigan, U.S.A.

Agar noble

Complete Freund's adjuvant

Trypsin (practical grade)

E. Merck, Darmstadt, Germany.

Amidoblack

L-Aspartic acid

Carbon tetrachloride

Dipotassium hydrogen phosphate

Ethanol

Potassium dihydrogen phosphate

Sodium azide

Sodium carbonate

Sodium citrate

Tris-(hydroxymethyl)-aminomethane (Tris)

Evans Medical Ltd., Liverpool, England.

Heparin (mucous)

Hopkin and Williams Ltd., Essex, England.

Acetone

EDTA

Chloroform

Methanol

Hynson, Westcott and Dunning Inc., Baltimore, Maryland, U.S.A.

Sulphobromophthalein sodium (BSP)

LKB Produkter, Bromma, Sweden.

Ampholines: pH 3.5-10 (40% w/v); pH 7-9 (40% w/v); pH 8-9.5 (40% w/v) and pH 9-11 (20% w/v)

May and Baker (MLB), Dagenham, England.

Chloramine-T

Cupric sulphate

Disodium hydrogen phosphate

Phenobarbital sodium

Phosphoric acid

Potassium dichromate

Potassium hydroxide

Sodium acetate

Sodium chloride

Sodium dihydrogen phosphate

Sodium hydroxide

Sodium iodide

Sodium metabisulphite

Sucrose

Trichloroacetic acid (TCA)

Miles Laboratories, Epping, Cape, R.S.A.

Bovine serum albumin (Fraction V) (BSA)

Human serum albumin (crystalline)

2-Mercaptoethanol

NADH

Natal Cane By-Products Ltd., Merebank, Natal, R.S.A.

Diethyl ether (anaesthetic grade)

Packard Instruments Co. Inc., Downers Grove, Illinois, U.S.A.

Instagel scintillation fluid

Permutit South Africa, Johannesburg, R.S.A.

Zerolit De-acidite resin, FF-1P SRA-68

Pharmacia Fine Chemicals, Uppsala, Sweden.

Blue dextran

Sephadex G-25; G-50; G-75 and G-100

QAE-Sephadex A-50

Protea Laboratory Services (Pty.) Ltd., Johannesburg.

Acetic Acid (Glacial)

Hydrochloric acid

Protea Laboratory Services (Pty.) Ltd., Johannesburg, R.S.A.

Acetic Acid (Glacial)

Hydrochloric acid

Saphar ML Laboratory (Pty.) Ltd., Ophirton, Johannesburg, R.S.A.

Sodium chloride injection BP 0.9% (w/v) (normal saline)

Sigma Chemical Co., St. Louis, Missouri, U.S.A.

Carbonic anhydrase (bovine erythrocyte)

Coomassie brilliant blue R-250

Cytochrome c (horse heart)

Dithiothreitol (DTT)

Dowex AG 1-X2 (200 mesh)

Lysozyme (egg white)

Myoglobin (horse heart)

TEAE-cellulose

The Radiochemical Centre, Amersham, Buckinghamshire, England.

Sodium (^{125}I) iodide

(^{35}S) Sulphobromophthalein sodium

Toyo Kagaka Sangyo Co. Ltd., Tokyo, Japan.

Toyo 514 chromatography paper

Wellcome Research Laboratories, Beckenham, England.

Donkey anti-rabbit globulin

Whatman Biochemicals Ltd., Maidstone, Kent, England.

CF II cellulose

Filter paper no. 1 and no. 53

The following were received as gifts: goat anti-rat ligandin IgG (GAL-IgG) from Drs. G. Fleischner and I.M. Arias of the Liver Research Centre, Albert Einstein College of Medicine, Bronx, New York; and human γ-globulin from Dr. J. de la Harpe of the Department of Clinical Science, University of Cape Town. Non-immune rabbit serum (NIRS) was provided by Dr. T. Wainer and the staff of the University of Cape Town Medical School Animal Housing Facility.

APPENDIX B

EXPERIMENTAL METHODS

APPENDIX B - LIST OF CONTENTS

I INTRODUCTORY NOTE

(a) Unless otherwise stated, all solutions were made up in distilled water, hereafter also denoted by the formula: H_2O.

(b) Percentage compositions in the case of solid reagents are w/v; and in the case of liquid reagents are v/v.

II PREPARATION OF CYTOSOL

(References: 107, 158, 159)

1. Initial Tissue Preparation

(a) All steps were performed at $4^{o}C$.

(b) Immediately after removal, liver, kidney, heart and lung, were perfused via the hilar vessels with ice cold 0.9% saline. Testis and ovary were perfused in situ via the aorta. Other tissues were washed in saline, but were not perfused prior to homogenization.

(c) Small intestine, colon and stomach were washed with cold saline; stomach was opened lengthwise, while small intestine and colon were inverted over a glass rod. These tissues were then laid on a thin glass plate chilled from below by ice chips, and the mucosa scraped off by means of a glass slide.

(d) Pancreas was removed as follows: the common bile duct was cannulated by means of a thin polyethylene tube attached to a syringe filled with cold saline. The bile duct was ligated proximally, and the pancreas perfused with saline. The distended tissue was easily identified, and

carefully dissected free from its surrounding attachments.

(e) Except in the case of mucosa, all tissues were blotted firmly between gauze swabs prior to weighing.

(f) Tissues were rapidly weighed on disposable plastic weighing boats; mucosa, pancreas, thyroid and pituitary, however, were immediately placed into preweighed glass test tubes containing a small volume of homogenization buffer, and reweighed.

2. Homogenization

(a) Homogenization was carried out in 0.01M sodium phosphate buffer pH 7.4/0.25M sucrose. In the case of most tissues, sufficient buffer was added to yield a 25% homogenate. In the case of tissues of low weight (viz: colon and stomach mucosa, thyroid, pituitary, bladder, pancreas, ovaries, adrenals and tissues from newborn animals), a minimum of 4 ml of buffer was routinely added, yielding final homogenate strengths between 5-20%. For immunodiffusion experiments, sufficient tissue was used to permit preparation of 25% homogenates in order to allow uniform comparison of qualitative results.

(b) After initial fragmentation with scissors, tissues were homogenized in a motor driven teflon-pestle glass homogenizer (Arthur H. Thomas Co., Pennsylvania) at 250 rpm for 7 strokes. Muscle tissue required initial disruption for 3s with an Ultra-Turrax homogenizer (Optolabor, Johannesburg).

3. Centrifugation

(a) Tissue homogenates were centrifuged at 109,000xg (max) for 2h in a Beckman model L3-50 ultracentrifuge. When a large volume of cytosol was prepared (viz: for ligandin purification), homogenate was first centrifuged at 27,000 xg in a Sorvall RC2-B centrifuge, and the supernatant centrifuged at 100,000 xg thereafter.

(b) After centrifugation, the supernatant fraction (cytosol) was carefully removed without disturbing the pellet or floating lipid, and either used immediately or stored at -20°C.

III PREPARATION OF MOLECUAR SIEVE MATERIALS AND COLUMNS

(Reference: 299)

Procedure:

1. Swelling and equilibration of gels

(a) 10-40g of dry Sephadex beads are swollen in 1-2 l H_2O in a boiling water bath for 1h (G-25), 3h (G-75) or 6h (G-100).

(b) At 3 intervals during swelling, stir the slurry, allow to settle and decant the fines.

(c) Allow the slurry to cool at 4°C, during which time, decant the supernatant and replace with appropriate eluent buffer (see text). Repeat 3 times.

2. Column packing

(a) Using a spirit-level, clamp the column vertically in a 4°C cold room with a gel reservoir attached.

(b) Insert the lower bed support or flow adaptor.

(c) Inject eluent into the outflow tubing to flush out bubbles, then close outlet.

(d) Pour cold eluent into column to fill 25% of its volume.

(e) Dilute gel slurry with cold eluent and pour into column and reservoir.

(f) Allow the gel particles to settle for 10-20 min, then open the outlet. (Note: G-100 in 90 x 2.5 cm columns should not be packed under a pressure greater than 50 cm H_2O).

(g) When eluent is within 5 cm of the packed gel surface, close the outlet.

(h) In the case of pump-driven columns, the upper flow adaptor is now installed, taking care not to trap any air bubbles.

3. Running of columns

(a) Allow column to stabilize prior to sample application by allowing at least 3 bed volumes of eluent to pass through.

(b) In the present study, columns were eluted either by pump-driven upward eluent flow mode, or by descending

eluent flow mode using a constant pressure reservoir (Mariotte flask). Flow rates were at least 10% less than the flow at which columns were packed.

4. Calibration of columns

The following procedures were employed in the present study:

(a) The void volume (Vo) of columns was determined by chromatography of a 0.3% solution of blue dextran.

(b) Marker proteins used to calibrate columns included 0.4-0.8% solutions of BSA, ovalbumin, carbonic anhydrase and cytochrome c. Molecular weights are given in Method V.A.5.

(c) The volume of samples loaded onto columns was generally between 0.5-1 ml cm^{-2} column cross sectional area.

(d) Elution volumes (Ve) were determined from the elution peaks of samples studied.

(e) Relative mobility (R_f) was calculated from the relationship: $R_f = Ve/Vo$.

(f) Linear plots of log molecular weight standard proteins vs $1/R_f$ were used to interpolate the molecular size of unknown samples, as recommended by Fisher (299).

IV PREPARATION OF ION-EXCHANGE MATERIALS AND COLUMNS

(Reference: 373)

Procedure:

1. TEAE-cellulose

(a) Wash 400g of the anion-exchange cellulose as

follows:

i) 0.1M HCl for 1h

ii) H_2O until pH = 5-6

iii) 0.1M NaOH for 1h

iv) H_2O until pH = $\sim$ 8

v) 10 litres of acetone

(b) Remove acetone by air-drying in fume cupboard.

(c) Equilibrate the cellulose with 3 x 10l washes of the eluent buffer (see text), with decantation to remove the fines.

(d) Fill $\frac{1}{4}$ of the column (see text) with eluent, then add the cellulose suspended in 4l of eluent.

(e) Pack the cellulose by negative-pressure suction.

(f) Elute the column by gravity flow (a 10l reservoir was utilized in the present study).

(g) Equilibrate the column at $4^{o}C$ for 24h with eluent buffer prior to sample application, check that the effluent pH is the same as that of the eluent buffer.

2. QAE Sephadex A-50

(a) Swell 5g of the resin in 1l eluent buffer (see text) for 24h at $4^{o}C$.

(b) Degas the resin slurry in a vacuum flask.

(c) Pack the column (see text) under gravity flow in the manner described for molecular sieve materials, and equilibrate at $4^{o}C$ for 12h with eluent buffer prior to sample

application. Check the effluent pH.

(d) After sample application, elute by descending eluent flow using a constant pressure reservoir (Mariotte flask).

V POLYACRYLAMIDE GEL ELECTROPHORESIS IN SDS

(References: 300, 301)

A Discontinuous System (300)

Reagents:

(a) 30% Acrylamide/0.8% bis-acrylamide (N,N'-bis-methyllene acrylamide) solution. In the present study acrylamide and bis-acrylamide were recrystallized before use from chloroform and acetone respectively, by the procedure of Loening (374). The solution is filtered before use.

(b) N,N,N',N'-tetramethylethylene diamine (TEMED).

(c) 10% SDS solution.

(d) 0.004% riboflavin solution.

(e) 3M Tris:HCl buffer pH 8.9 (resolving gel buffer stock).

(f) 0.5M Tris:phosphate buffer pH 6.7 (spacer gel buffer stock).

(g) 0.005M Tris:glycine buffer pH 8.6 (tank buffer stock).

(h) Sample buffer, comprised of glycerol 2 ml, 10% SDS 2 ml, 2-mercaptoethanol 0.02 ml, resolving gel buffer 2.5 ml, 1 ml 0.02% bromophenol blue solution and H_2O to 10 ml.

Note: (a), (b) and (d) are stored in dark bottles at 4^oC.

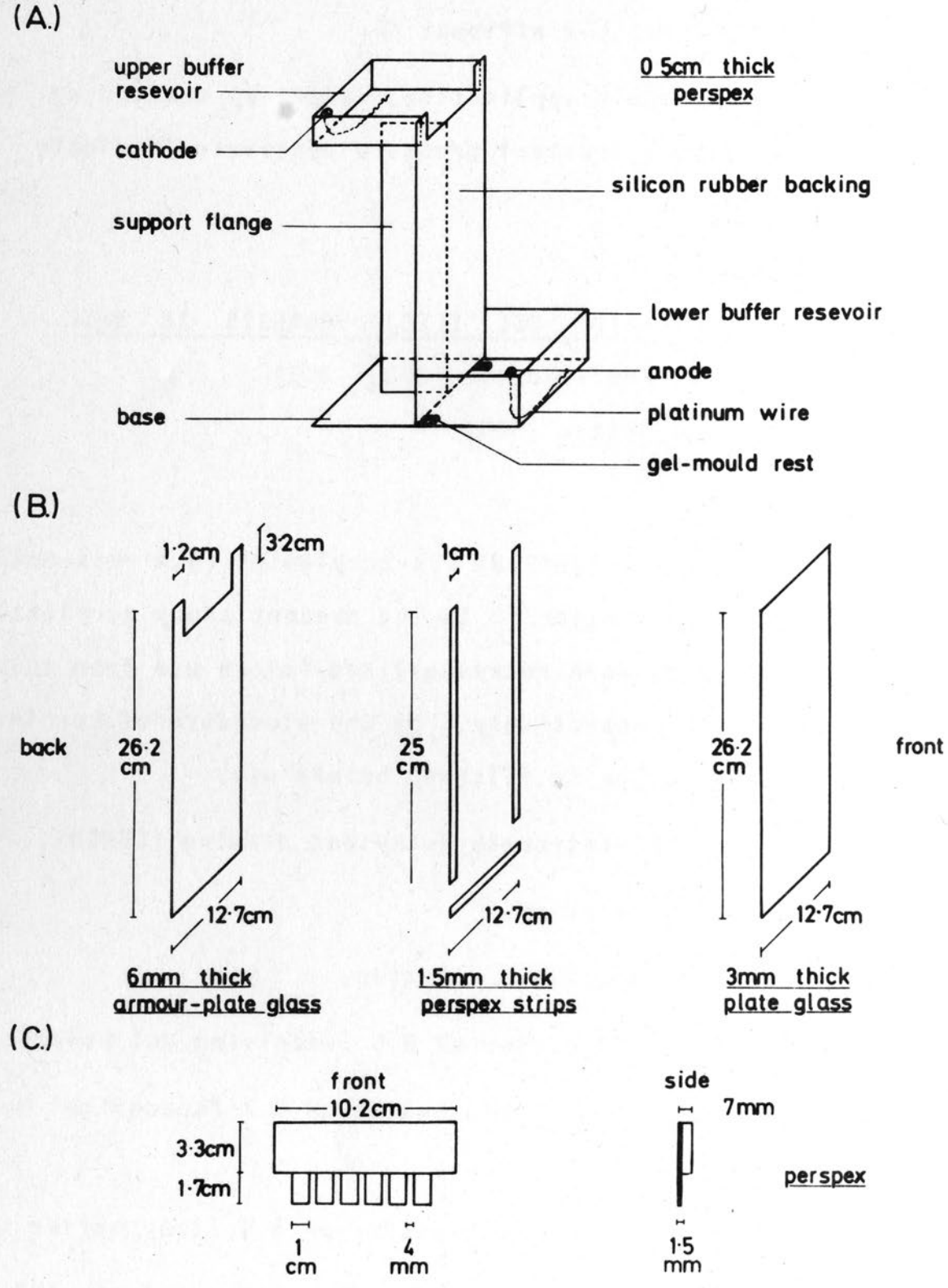

Fig. A.1. Apparatus for slab discontinuous PAGE in SDS. (A), Vertical electrophoresis tank; (B), glass plates and perspex strips for construction of gel mould; (C), perspex sample application-bay template.

Apparatus:

(a) Tube gels: Shandon PAGE apparatus with 65 x 5 mm glass tubes. (Shandon Southern Instruments, Surrey, U.K.).

(b) Slab gels: see Fig. A.1.

(c) Shandon Vokam 2541 power supply.

(d) Bulldog clamps or Waverly clips.

(e) Fluorescent (neon) light source.

1. Preparation of gel solutions

(a) Resolving gel mixture: add the following in a measuring cylinder:

i) Acrylamide/bis-acrylamide solution: x ml, where x = required % gel strength x 5/3

ii) buffer (e) : 6.25 ml

iii) 10% SDS : 0.5 ml

iv) TEMED : 0.025 ml

v) riboflavin : 0.4 ml

vi) H_2O : to 50 ml

Mix and pour into a round bottomed vacuum flask.

(b) 3% Spacer gel mixture: add and mix as above:

i) acrylamide/bis-acrylamide : 1.00 ml

ii) buffer (f) : 1.25 ml

iii) 10% SDS : 0.1 ml

iv) TEMED : 0.025 ml

v) riboflavin : 0.1 ml

vi) H_2O : to 10 ml

2. Preparation of slab gels

(a) Wash glass plates and perspex strips in detergent, rinse with H_2O and dry with paper towels. Do not siliconize.

(b) Position perspex strips between front and back plates to form a "U"-seal and clamp plates together. Ensure good contact between the ends of the perspex strips (see Fig. A.1).

(c) Seal the sides and bottom of the glass-perspex mould with hot 1.2% agar.

(d) Stand the mould upright with the back plate facing you.

(e) Degas the resolving gel mixture on an oil pump and pour into the space between the glass plates, up to 3 cm from the upper edge of the back plate.

(f) Degas 10 ml H_2O and layer to 0.5 cm on top of the gel solution using a Pasteur pipette.

(g) Position neon lights on either side of gel, switch on and allow gel to polymerize ($\sim$ 1h).

(h) Degas the spacer gel mixture. Remove water from top of gel, rinse with spacer mixture, then pour same on top of polymerized resolving gel.

(i) Insert sample application-bag template (see Fig. A.1) and allow to light-polymerize for 3-4h.

(j) When spacer gel is polymerized, remove template and bottom perspex strip.

3. Preparation of tube gels

(a) Siliconize tubes with Desicote and seal bottom ends with parafilm. Stand upright.

(b) The procedure is then identical in principle to that given above for slab gels; except that water is overlaid on the spacer gel as well. Use a Pasteur pipette to fill tubes. The top of the spacer gel should be ∿ 1 cm from top of tube. Remove parafilm after gels polymerized.

4. Electrophoresis procedure

(a) Prepare the tank buffer from 50 ml glycine buffer (g), and 5 ml 10% SDS made to 500 ml with H_2O.

(b) For slab gels: Fill lower reservoir of tank, wet bottom edge of gel and clamp gel plate into position. Now fill the upper reservoir with tank buffer.

(c) For tube gels: Fill lower reservoir and pass tubes through rubber grommets and wet lower ends of gels. Now fill upper reservoir and flush bubbles out of tube tops.

(d) Connect apparatus to power source (anode : lower reservoir).

(e) Mix samples (20-50 µl) with equal volumes of sample buffer, and heat at 100°C for 2 min.

(f) With a Hamilton microsyringe carefully load 5-20 µl (2-50 µg) of reduced sample into the sample bags (slab gels) or on top of gels (tube gels).

(g) For tube gels: run at 3mA/gel until the marker dye

front has migrated to within 1 cm of the lower end.

(h) For slab gels: run at 10 mA for 16h, or until the front is within 4 cm of the lower edge.

5. Molecular weight estimation

(a) The following proteins were used as standards for PAGE-SDS estimation of molecular weight of ligandin (monomer molecular weights given in parentheses are from the data provided by Weber and Osborn (301)): human serum albumin (68,000), human γ-globulin H chain (50,000), ovalbumin (43,000), aldolase (40,000), carbonic anhydrase (29,000), human γ-globulin L chain (23,500), myoglobin (17,200), lysozyme (14,300) and cytochrome c (11,700).

(b) R_f was calculated from the distance migrated by protein bands (measured from top of gel to front of band) divided by the distance migrated by the marker dye front. Unknowns were interpolated from linear plots of log standard protein molecular weight vs R_f.

B Continuous System (301)

Reagents:

(a) 22.2% Acrylamide (recryst.) / 0.6% bis-acrylamide (recryst.).

(b) 0.2M sodium phosphate buffer pH 7.2/0.2% SDS (gel buffer).

(c) 1.5% ammonium persulphate - freshly prepared.

(d) TEMED.

(e) Sample reagents: glycerol, 2-mercaptoethanol, 0.05% bromophenol blue, 10% SDS and 0.01M sodium phosphate buffer pH 7.0.

Apparatus

Shandon apparatus and power supply as for discontinuous system.

Procedure:

(a) Degas 15 ml gel buffer, mix with 13.5 ml degassed acrylamide/bis-acrylamide solution.

(b) Degas ammonium persulphate solution and add 1.5 ml to gel mixture, followed by 0.045 ml of TEMED. Mix.

(c) Set up tubes, fill and layer as described above. Allow gels to polymerize ($\sim$ 10 min).

(d) Set up tubes in apparatus (see above), use gel buffer diluted 1:1 with H_2O for tank buffer.

(e) Prepare samples by adding to 200 µl protein solution : 100 µl each of 10% SDS, 2-mercaptoethanol and glycerol, and 50 µl bromophenol blue solution. Make to 1 ml with phosphate buffer, mix and incubate at 37^{o}C for 2h (or else heat as described for discontinuous system).

C Staining of PAGE-SDS gels (301) and Autoradiography

Procedure:

(a) Tube gels: loosen gels by injecting H_2O between gel and glass tube using a 22 gauge needle. Expel (using a

rubber teat) into perforated plastic tubes.

(b) Slab gels: prize off back plate by inserting a blade between glass and gel and at the same time, lifting the plate. Invert over staining dish and let gel peel off into fixative.

(c) Fix gels for 2h in 5% TCA.

(d) Stain for 2.5h in 0.2% Coomassie brilliant blue in methanol:H_2O:acetic acid = 50:50:7 (filter before use).

(e) Destain for 24h in 5% methanol/7% acetic acid with several changes.

(f) Autoradiography (^{125}I) may be performed on gels that are stained or simply fixed. Place gels on glass plate, and cover with thin plastic food wrapping. Place Kodak PE-4006 x-ray film (in packet) squarely on gel and compress with a heavy glass plate. After 24h, open pellet in darkroom, place film in Kodak DX-80 developer for 2 min, wash for 2 min, then place in Kodak FX-40 x-ray fixer for 3 min, wash for 30 min and hang up to dry.

VI ISOELECTRIC FOCUSING

(Reference: 302)

Reagents:

(a) 30% Acrylamide (recryst.)/1% bis-acrylamide (recryst).

(b) Carrier ampholytes (ampholines) pH 3.5-10 (40%), pH 7-9 (40%), pH 8-9.5 (40%) and pH 9-11 (20%) ranges.

(c) TEMED.

(d) 2% Ammonium persulphate (freshly prepared).

(e) Glycerol.

(f) 0.02M H_3PO_4 (anolyte).

(g) 0.4% Ethanolamine (catholyte).

(h) 0.05% Bromophenol blue.

(a), (b) and (c) are stored in dark bottles at 4°C.

Apparatus:

(a) Shandon apparatus (as for PAGE-SDS) or MRA water cooled apparatus M 137 (MRA Corp. Boston Mass.) with 10 x 0.3 cm plastic tubes.

(b) Power supply (as for PAGE-SDS).

Procedure:

1. Gel preparation

(a) Shandon and MRA tubes are prepared as for PAGE-SDS, but MRA tubes are not siliconized.

(b) Prepare ampholyte solution for pH 7-10 range by mixing pH 7-9 ampholines 1 ml, pH 8-9.5 ampholines 0.5 ml and pH 9-11 ampholines 2 ml.

(c) In a measuring cylinder, combine (with mixing) in the following order:

i) H_2O 5 ml

ii) acrylamide/bis-acrylamide 3 ml

iii) TEMED 0.01 ml

iv) glycerol 1.2 ml

v) ampholyte: for pH 7-10 range : 0.85 ml of mixture prepared in (b), or for pH 3.5-10 range, 0.6 ml pH 3.5-10 ampholine. Make up to 11.8 ml with H_2O. This will yield 7.5% gels with 2% (w/v) ampholines.

(d) Degas the gel mixture and the ammonium persulphate separately. Add 0.2 ml of the latter to the gel solution, mix and pipette with gel tubes. Overlay with degassed H_2O, and allow to polymerize at 4^oC ($\sim$ 15 min).

(e) Place gel tubes in apparatus (see PAGE-SDS), MRA tubes require toweling wick held in place by rubber bands at bottom ends. Now transfer apparatus to cold room (4^oC).

2. Running gels

(a) If using MRA apparatus, connect cooling jacket inlet to cold water source. Electrolyte solutions should be pre-cooled to 4^oC. Fill upper and lower reservoirs with anolyte and catholyte solutions respectively. Pre-run gels at 1 mA/gel for 45 min.

(b) Prepare sample by mixing 200 µl of protein solution (50-200 µg in low ionic strength buffer or H_2O), 100 µl ampholine (as used in gel), 100 µl glycerol and 600 µl bromphenol blue solution.

(c) Switch off power supply. Load 50-100 µl of sample onto gels with a microsyringe.

(d) Commence run by applying 100V and increasing by 50V every 30 min up to 400V. Maintain this voltage for $\sim$ 4h at which stage current should be at a constant, low level.

3. Determination of pH gradient

(a) Remove gels from tubes (see PAGE-SDS). Two are selected for pH gradient determination. Measure length of all gels.

(b) Slice pH gels in a perspex-brass gel slicer. This is readily constructed to suit any gel size and is based on an "egg slicer" principle. The slicer used in the present study cut the gel into 2 mm segments.

(c) Each slice is eluted in 0.5 ml H_2O at room temperature on a shaker tray for 2h. The pH of eluate is then measured.

4. Staining of gels

Method 1. (303)

Reagents:

(a) 100 ml 2% Coomassie brilliant blue.

(b) 100 ml 2N H_2SO_4.

(c) 10M KOH.

(d) Solid TCA.

(e) Add (b) to (a) and allow precipitate to sediment.

(f) Filter green supernatant.

(g) Add (c) dropwise till blue tint appears.

(h) Measure volume and add TCA 12g/100 ml and mix.

This is the stain fixative.

Procedure:

(a) Stain gels for 15 min to 1h.

(b) Remove background stain by immersion for 5 min in 0.2% H_2SO_4.

(c) Store gels in H_2O.

Method 2. (281)

Procedure:

(a) Wash gels 5 times in 500 ml 5% TCA with hourly changes.

(b) Stain for 2h in 0.1% Coomassie brilliant blue in acetic acid:ethanol:H_2O = 2:9:9 (filtered)

(c) Destain in acetic acid:ethanol:H_2O = 2:5:13.

5. Determination of pI

(a) Draw graph of pH gradient vs length of gel.

(b) Measure stained gel and find correction factor = prestaining length ÷ post-staining length.

(c) Measure migration of protein bands in cm and multiply by correction factor. Read pI for corrected length of migration off graph.

VII IMMUNODIFFUSION

(Reference: 307)

Materials and Reagents:

(a) Agar - Noble: 1.2g.

(b) 0.05M sodium phosphate buffer pH 7.4/0.15M NaCl (PBS).

(c) Sodium azide: 100 mg.

(d) 9.5 x 8.5 cm clean glass plates, 1 mm thick. Clean with ethanol prior to use.

(e) A horizontal platform and spirit-level.

Procedure:

(a) Combine the agar and sodium azide and 100 ml PBS;

(b) Heat in a conical flask stoppered with a small inverted volumetric flask on a magnetic stirrer, until the solution clarifies. Do not allow to boil.

(c) Remove the flask and place in a hot water bath ($\sim 60^{o}C$).

(d) Warm the glass plates in an oven, and place on the horizontal platform (to be strictly horizontal).

(e) Using a 10 ml graduated pipette, pour 10 ml of agar solution onto each plate, allowing the solution to cover the entire plate.

(f) Allow plates to cool for 1h. These can then be stored in an air-tight moisture box at $4^{o}C$, or used immediately.

(g) For immunodiffusion experiments, the desired pattern of wells can be cut using an LKB 2117 Multiphor template and borers. In the present study, wells of 4 mm diameter (10 µl capacity) were routinely employed.

(h) Place antigen samples in peripheral wells, and antiserum in the centre well, using a 10 µl Oxford pipette.

(i) Keep in a strictly horizontal position in a box at room temperature for 48h and for 24-72h at $4^{o}C$.

VIII IMMUNOELECTROPHORESIS

(Reference: 308)

Materials and Reagents:

(a) 0.14 veronal buffer pH 8.7/0.2% sodium azide.

(b) Agar - Noble: 1g.

(c) (d) and (e) as in Immunodiffusion.

(d) 8.5 x 4 cm strips of Whatman No. 1 filter paper.

Apparatus:

(a) Shandon electrophoresis tank SA 2692.

(b) Power supply (as in PAGE-SDS).

Procedure:

(a) Make 25 ml of veronal buffer to 100 ml with H_2O and add agar.

(b) (b) to (f) as in Immunodiffusion.

(c) Cut pattern of wells and troughs as in (g) under Immunodiffusion.

(d) Fill the buffer tanks of the electrophoresis apparatus with veronal buffer (diluted 1+1 with H_2O).

(e) Position the gel plates in the electrophoresis apparatus.

(f) Moisten the filter paper wicks and place in contact with the ends of the plate and the buffer tanks.

(g) Using a 10 µl Oxford repette, place the samples in the wells.

(h) Close the apparatus lid and run at a current of 12 mA/plate for 1.5 to 2h.

(i) At the end of this time, switch off current and remove wicks from gel plates.

(j) Add antiserum (30-50 µl) to troughs with a Hamilton syringe.

(k) (i) as in Immunodiffusion.

IX STAINING OF AGAR GELS

(Reference: 375)

Procedure:

(a) Wash agar plates for 3-5 days in 0.9% saline. 0.1% sodium azide (4-5 changes).

(b) Thereafter, wash for 24h in H_2O (2-3 changes).

(c) Stain plates in amidoblack stain (1g in 500 ml 5% acetic acid, filtered prior to use) for 6h.

(d) Destain in 5% acetic acid for 12h.

(e) Store stained gels in a moisture box.

X QUANTITATIVE RADIAL IMMUNODIFFUSION

(Reference: 309)

Reagents:

(a) 0.1M veronal buffer pH 8.6/0.05% sodium azide.

(b) Agar - Noble: 3g.

(c) Specific antiserum. (The present study employed rabbit antiserum 982/28/10 diluted 1:4 with veronal buffer).

(d) Desicote siliconizing solution.

Apparatus:

(a) 10 x 7 cm photographic glass plates, 1 mm thick.

(b) A 1mm thick brass "U"-frame having the same branch lengths as the glass plates, and a branch width of 8 mm.

(c) Bulldog clamps.

Procedure:

1. Preparation of the agar

(a) Add the 3g of agar to 100 ml veronal buffer, and place in a boiling water-bath.

(b) Stir until agar is dissolved, replacing evaporation losses with H_2O.

(c) Pour agar into well stoppered test tubes and store at 4^oC.

2. Preparation of agar-antiserum plates

(a) The agar mould is first constructed by placing the "U"-frame upon a clean glass plate, and covering this with another glass plate, the lower surface of which has been siliconized. The three pieces of the mould are clamped tightly together.

(b) Melt $\sim$ 6 ml of agar in a tube in a boiling water-bath and allow to cool to 60^oC.

(c) Bring the diluted antiserum (6 ml) to 55^oC.

(d) Mix equal volumes of the agar and antiserum using a pipette pre-heated to 60^oC in the water-bath. Avoid bubbling.

(e) Using the same heated pipette, pour the antiserum-agar mixture ($\sim$ 5 ml) into the mould, holding the latter in a slightly slanted position with the tip of the pipette applied to the lower corner of the slit.

(f) After solidification (15 min) remove the clamps and

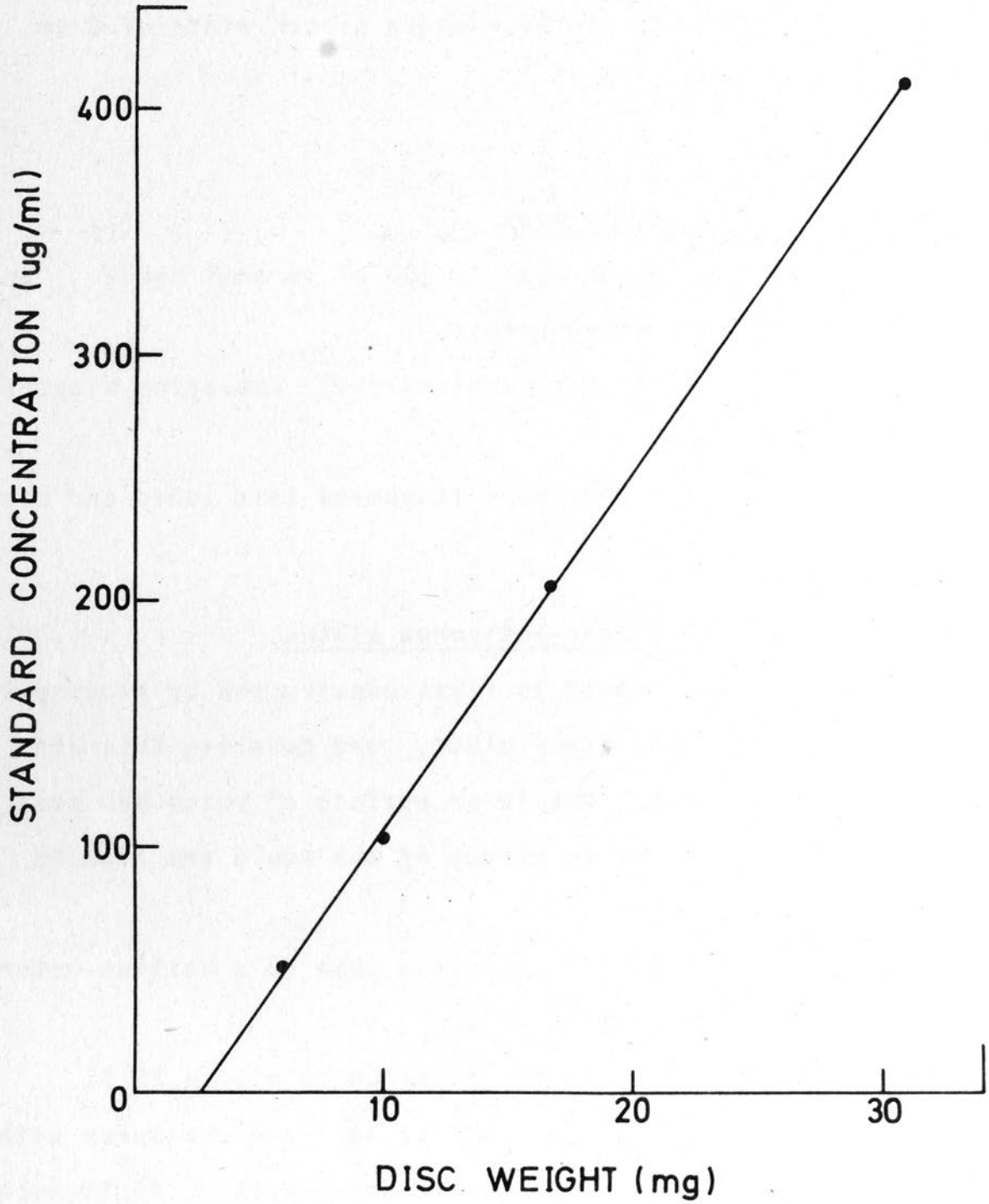

Fig. A.2. Standard curve of quantitative radial immunodiffusion technique for measuring ligandin. Each point represents the mean of duplicate determinations. The abscissa intercept represents the disc weight of the antigen well. (For details of the procedure, see Method X).

carefully slide off the siliconized top plate; then remove the brass frame.

3. Application of antigen samples

(a) Using the LKB apparatus described in Immunodiffusion, cut 2 mm diameter wells.

(b) With the plates in a moisture box and in a strictly horizontal position, place antigen solutions (2 µl) in antigen wells by means of a Hamilton microsyringe. In the present study, pure ligandin was used as a standard. At least 4 standard concentrations were employed (51 to 410 µg/ml) in duplicate on each plate. Tissue samples were assayed in duplicate at 1:2 and 1:4 dilutions of 100,000xg supernatants.

(c) Close moisture box and keep plates at room temperature for 48h and 4°C for a further 72h.

4. Estimation of unknown sample values

(a) Stain plates with amidoblack (see above).

(b) Photograph plates at standard magnification.

(c) Carefully cut out precipitin discs and weigh accurately.

(d) Construct a standard curve by plotting the standard concentrations vs the weight of standard precipitin discs (Fig. A.2).

(e) Interpolate unknown values from the standard curve, and express results in µg/mg supernatant protein.

XI IODINE MONOCHLORIDE IODINATION

(Reference: 314)

Reagents:

(a) Protein sample: 0.2-0.5 ml (1 - 15 mg).

(b) 0.033M Iodine monochloride (ICl)/1M HCl: made up as follows:

i) Dissolve 150 mg NaI in 8 ml 6M HCl.

ii) To this, add 108 mg sodium iodate monohydrate in 2 ml H_2O with forceful injection to prevent iodide precipitation.

iii) Dilute with H_2O to 40 ml.

iv) Shake with CCl_4. If the solvent is faint red, repeat this step.

v) Remove CCl_4 by aerating with moist air for 1h and make solution up to 45 ml with H_2O.

(c) 1M Glycine/0.25M NaCl solution.

(d) Na ^{125}I.

(e) 1M NaOH.

(f) 2M NaCl.

Procedure:

(a) Put 1.8 ml glycine-NaCl in a tube; add 0.2 ml 1M NaOH.

(b) Put 0.9 ml 2 ml NaCl in a second tube; add 0.1 ml ICl.

(c) From tube (b) take 0.3 ml, and place in a third tube with 1 mCi (10 µl) Na ^{125}I.

(d) Adjust pH of protein solution to pH 8.5 with solu-

tion in tube (a) (glycine buffer) if necessary.

(e) Similarly adjust pH of ^{125}I solution in tube (c) with ∿ 12 drops glycine buffer (tube (a)). Solution de-colourizes just prior to this point.

(f) With a Pasteur pipette, vigorously inject Na ^{125}I solution into protein sample.

(g) Dialyse the reaction mixture against 3 x 1l volumes of 0.05 sodium phosphate buffer pH 7.4/0.15M NaCl, containing 3g de-acidite resin.

XII CHROMATOELECTROPHORESIS

(Reference: 313)

Materials and Reagents:

(a) Radioactive sample: reaction mixture or purified label.

(b) 0.05M sodium phosphate buffer pH 7.5/0.15M NaCl (PBS).

(c) 0.05M Veronal buffer pH 8.6 (tank buffer).

(d) Human plasma coloured with a few crystals of bromophenol blue.

(e) Toyo 514 paper cut into 3.5 x 50 cm strips.

Apparatus:

(a) Electrophoresis tank.

(b) Power supply (as for PAGE-SDS).

Procedure:

(a) To 5-50 µl of radioactive sample, add 5 µl "blue

plasma" and PBS up to 150 µl.

(b) Wet the paper strip in tank buffer and blot off excess moisture between paper towels.

(c) Apply 100 µl of sample along a line 3.5 cm from anodal end of the paper strip.

(d) Place ends of the strip in buffer tank, and apply a current of 400V.

(e) Continue electrophoresis until blue front has migrated 12-15 cm from the origin.

(f) Remove strip and suspend in an oven until dry.

(g) Cut dried strip into 1 cm portions for determination of radioactivity. For routine purposes, when the characteristic migration of "intact", "damaged" and "free" fractions are established, the strip may be cut into 3 portions for determination of the radioactivity attributable to these fractions.

XIII SPECTROPHOTOMETRY

(a) All spectrophotometric analyses were performed using a Pye-Unicam S.P. 1700 double-beam spectrophotometer.

(b) All cuvettes were 1 cm in path-length. Quartz cuvettes were used for all readings below 320 nm.

(c) Small volumes were read in 1 ml Beckman cuvettes (quartz); otherwise 3 ml cuvettes were used.

XIV DETERMINATION OF PROTEIN CONCENTRATION

(Reference: 298)

Reagents:

(a) 3% $Na_2 CO_3$ in 0.1M NaOH.

(b) 2% $CuSO_4$.

(c) 2% Potassium sodium tartrate.

(d) Folin & Ciocalteu's phenol reagent, dilute 1:1 before use.

(e) Human serum albumin (HSA), (crystalline), 1 mg/ml standard stock.

Procedure:

(a) Make Reagent 1 by mixing 2 ml (c), 2 ml (b) and 96 ml (a).

(b) Perform in triplicate: pipette 200 µl of sample, and 200, 100, 50, 20 and 10 µl of HSA standard solution into test tubes, and make up to 0.5 ml with H_2O. Use tubes with just 0.5 ml H_2O as blanks.

(c) Add 5 ml Reagent 1 to all tubes. Mix well and let stand 10 min.

(d) Add 0.5 ml phenol reagent (1:1 diluted) to tubes. Mix immediately and leave to stand 30 min.

(e) Read absorbance at 660 nm.

(f) Interpolate unknowns from standard curve of absorbance vs standard protein concentration.

XV GSH S-TRANSFERASE ASSAYS

(Reference: 155)

Principle:

Spectrophotometric measurement of the formation of GSH adducts from electrophilic substrates by the GSH S-transferases.

Reagents:

(a) 30 mM 1-chloro-2,4-dinitrobenzene in 95% ethanol.

(b) 30 mM 3,4-dichloronitrobenzene (1,2-dichloro-4-nitrobenzene) in 95% ethanol.

(c) 30 mM p-nitrobenzyl chloride in 95% ethanol.

(d) 0.9 mM BSP in H_2O.

(e) 100 mM reduced GSH, freshly prepared and kept on ice under N_2.

(f) 0.1M potassium phosphate buffer pH 7.5.

(g) 0.1M potassium phosphate buffer pH 6.5.

Procedure:

1. General

(a) The assays are performed at 25°C.

(b) Assay mixture:

i)	Buffer	2.75 ml
ii)	Substrate	0.1 ml
iii)	GSH	0.15 ml
iv)	Enzyme	0.01 ml (up to 0.05 ml)

mixed together in a cuvette.

(c) Include a reference blank in every assay, which includes all the reactants except enzyme.

2. Specific

(a) 100 mM GSH stock (5 mM final) is used in all except the 1-chloro-2,4-dinitrobenzene assay, for which the stock is diluted to 20 mM (1 mM final).

(b) The 3,4-dichloronitrobenzene and BSP assays employ the pH 7.5 phosphate buffer, while the 1-chloro-2,4-dinitrobenzene and p-nitrobenzyl chloride assays are run at pH 6.5.

(c) The change in absorbance (ΔA) is measured for 6 min at the following wave lengths: 1-chloro-2,4-dinitrobenzene, 340 nm; 3,4-dichloronitrobenzene, 345 nm; BSP, 330 nm; p-nitrobenzyl chloride, 310 nm.

3. Calculation:

For 1 cm path-length cuvettes, results are derived from the general formula:

$$\frac{\Delta A/min}{\Delta \varepsilon} \times \frac{EV}{TV} \times 10^3 \times \frac{1}{cP} = \mu mol/min/mg \text{ protein}$$

where EV is the final assay volume, TV is the sample volume, cP is the concentration of protein in enzyme sample and $\Delta\varepsilon$ is the difference in molar extinction coefficient (M^{-1} cm^{-1}), and is = 9600, 8500, 1900 and 4500 for 1-chloro-2,4-dinitrobenzene, 3,4-dichloronitrobenzene, p-nitrobenzyl chloride and BSP respectively.

XVI SGOT DETERMINATION

(Reference: 337)

Principle:

First reaction: α-ketoglutarate + aspartate $\rightleftarrows$ L-gluta-

mate + oxaloacetate (transamination).

Second reaction: oxaloacetate + NADH + H^+ ⇄ L-malate + NAD^+.

The rate of NADH oxidation is measured spectrophotometrically.

Reagents:

(a) 0.1M sodium/potassium phosphate buffer pH 7.4.

(b) 0.2M L-aspartic acid, (pH to 7.4 with KOH).

(c) 0.1M α-ketoglutaric acid (pH to 7.4 with KOH).

(d) Reduced NADH.

(e) Malate dehydrogenase (pig heart) 5 mg/ml solution.

Procedure:

(a) Prepare assay mixture for 36 estimations by mixing together:

i)	NADH	0.0144g
ii)	Phosphate buffer	75.6 ml
iii)	L-aspartic acid	18 ml
iv)	Malate dehydrogenase	50 µl

(b) Mix 0.2 ml serum (or plasma) with 2.6 ml of assay mixture in a cuvette, and allow to stand for 15 min.

(c) Add 0.2 ml α-ketoglutaric acid, mix and measure the change in absorbance (ΔA) at 340 nm (at 25°C) for 5 min.

(d) Calculate activity from the formula:

$$\Delta A/min \times 2420 = mU/ml$$

XVII DIFFERENCE SPECTROPHOTOMETRY METHOD FOR MEASUREMENT OF BILIRUBIN - LIGANDIN BINDING

(Reference: 164)

Principle:

The binding of bilirubin to ligandin induces a red shift in the absorption maximum of the pigment. The change in absorbance (ΔA) at the maximum (λ_{max}) on titration of increasing amounts of bilirubin to a known amount of ligandin is used to calculate the parameters of bilirubin binding to ligandin.

Reagents:

(a) Recrystallized bilirubin (method of Ostrow et al (331)):

i) Dissolve 100 mg bilirubin in 15 ml chloroform ($CHCl_3$).

ii) Filter through Whatman No. 53 paper.

iii) Evaporate $CHCl_3$ in a boiling water-bath to 2 ml.

iv) Add 1 ml methanol and evaporate the remaining $CHCl_3$.

v) The red crystals which form at this stage are centrifuged down at 2500 xg for 30 min, washed with cold methanol and dried in vacuo in a desiccator (in the dark).

vi) Repeat i - v twice.

vii) Dissolve $\sim$ 5 mg bilirubin in 10 ml 10 mM NaOH. This is kept at $4^{o}C$ in the dark (cover glass container with silver tin foil).

viii) Using 10 mM NaOH as a reference blank, measure

the absorbance (A) of 10, 20 and 30 µl aliquots of the bilirubin solution in 2 ml 10 mM NaOH at the absorption maximum of the solution (437 nm), and obtain the concentration of the stock solution using an ε mM of 52 mM^{-1} cm^{-1} for bilirubin (25) by the formula (for 1 cm path-length cuvettes):

$$\text{stock bilirubin (mM)} = \frac{A_{437}}{52} \times \frac{2}{\text{Volume of bilirubin aliquot (ml)}}$$

In the present study, the calculated and predicted stock bilirubin concentrations were identical (0.92 mM).

ix) The stock solution should be used as soon as possible, and the absorbance spectrum should be checked for oxidation products and flocculant formation as described by Lee and Gartner (376).

(b) 0.05M Tris:HCl buffer pH 8.2/0.1M KCl.

(c) ∿ 20 µM ligandin stock solution in buffer (b). The actual concentration is determined by estimation of protein concentration (298) in triplicate after dialysis of ligandin against this buffer, assuming a molecular weight of 46,000 for ligandin.

Procedure:

1. Demonstration of the difference spectrum and $\Delta\varepsilon$ calculation

(a) Add 10 µl of bilirubin stock solution with a microsyringe to sample cuvette containing 2.5 ml protein stock solution and also to reference cuvette containing 2.5 ml of buffer (b).

(b) Scan between wave lengths 300-600 nm. In the present study, a difference spectrum was obtained identical to that described by Tipping et al (164) with a λ_{min} at 410 nm and λ_{max} at 474 nm.

(c) Read A at λ_{max}, and repeat with increasing amounts of bilirubin added in 10 µl aliquots to both sample and reference cuvettes (up to 70 µl).

(d) Plot the ΔA against the molar ratio of bilirubin to protein. In accord with Tipping et al (164), this plot was linear up till a bilirubin:protein ratio of 1. The difference in molar extinction coefficient ($\Delta\varepsilon$) is obtained from A values in this range (completely bound bilirubin) by the formula (for 1 cm path-length cuvettes):

$$\Delta\varepsilon\ (M^{-1}\ cm^{-1}) = \Delta A / \text{bilirubin (M)}$$

In the present study, a value of 20,700 $M^{-1}\ cm^{-1}$ for $\Delta\varepsilon$ was obtained (cf 20,400 reported by Tipping et al (114)).

2. Estimation of binding parameters

(a) Proceed as above, except use diluted protein stock solution ($\sim$ 5 µM in buffer) and diluted bilirubin stock solution ($\sim$ 0.5 mM in 10 mM NaOH).

(b) The concentration of bound bilirubin is calculated for each reading from the value of $\Delta A/\Delta\varepsilon$, while free bilirubin concentration (L) is equal to the difference between this value and total bilirubin concentration.

(c) The data are plotted according to the method of Scatchard (317) as detailed in Chapter XIV.

XVIII MEASUREMENT OF BSP BINDING TO LIGANDIN BY EQUILIBRIUM DIALYSIS

(Reference: 167)

Reagents:

(a) 0.01M sodium phosphate buffer pH 7.4.

(b) (^{35}S) BSP 20 mg (specific activity = 42.5 mCi/mmol) in 1l buffer (a) (24 µM, 5.8×10^{13} cpm/ml).

(c) 12 µM ligandin solution in buffer (a) (See difference spectrophotometry (c) above).

(d) Instagel scintillation fluid.

Apparatus:

(a) Glass equilibrium dialysis cells. The cells employed in the present study were each constructed from 2 semi-elliptic glass chambers flanged at the open ends. The chambers were held together at the flanges by means of spring clamps, with the dialysis membrane interposed and held in place by 2 silicone rubber "O" rings. The two chambers were each capable of holding 1.5 ml. The interior of each chamber was accessible via a 2 mm diameter sampling port. Dialysis membranes were cut from Thomas dialysis tubing (no. 3782-D22), which had been boiled in 1% Na_2CO_3 and rinsed in H_2O.

(b) Packard Tri-Carb 2650 liquid scintillation counter (employed in the present study).

Procedure:

1. Equilibrium dialysis

(a) Assemble dialysis cells (8 were used in present

study, two for each concentration of BSP).

(b) Into one chamber (A) of each cell, pipette 0.5 ml buffer, 0.5 ml protein solution and 0.5 ml (^{35}S) BSP solution. To the other chamber (B) is added 1 ml of buffer and 0.5 ml (^{35}S) BSP. Different concentrations of BSP are added to different cells by making doubling dilutions of the stock, and using 0.5 ml of these dilutions.

(c) Seal sampling ports well with parafilm and clamp cells horizontally on a shaker (to agitate gently).

(d) After 72h remove cells. Preliminary experiments confirmed that this period (167) was adequate for equilibration. Blank dialyses using protein solution only, revealed no loss of protein by adsorption after this period of time.

(e) Remove two 500 µl aliquots from each chamber, and pipette each aliquot into a separate counting vial. To each vial add 10 ml Instagel.

(f) Count radioactivity in each vial for 5 min. Similarly, count duplicate 500 µl aliquots of stock (^{35}S) BSP solution and each dilution used in the experiment. Use external standard method for quench correction.

2. Calculation

(a) Obtain mean counts for each chamber of each cell.

(b) Correct (x 3) to 1.5 ml for A and B chambers.

(c) % Recovery of counts = $\frac{\text{cpmA + cpmB}}{\text{Total cpm added}} \times 100$

(= 98% in present study).

(d) Bound counts = cpmA - cpmB = x

(e) Bound BSP (μmol) = x/y, where y = cpm/μmol of (^{35}S) BSP.

(f) Free BSP (μM) = $\frac{\text{cpmB}}{y} \times \frac{1000}{1.5} = L$

(g) $\bar{\nu}$ = Bound BSP (μmol)/Ligandin (μmol) in chamber A.

(h) Plot data (317) as detailed in Chapter XIV.

XIX AMINO ACID ANALYSIS

(References: 329, 330)

Procedure:

1. Hydrolysis

(a) Dialyse 3 mg of protein solution against 2l H_2O with 2 changes for 48h.

(b) Estimate protein concentration (298) and accurately transfer identical volumes of protein solution in H_2O (∿ 1 mg) to three pyrex hydrolysis tubes (cleaned with chromic acid) and lyophilize.

(c) Add 1 ml 6N HCl to each tube, and freeze in solid CO_2-ethanol.

(d) Evacuate tubes on an oil pump to < 50 microns, then flush with N_2. Seal tubes under vacuum.

(e) Place 3 tubes in oven with temperature controlled at 110°C and hydrolyse for ∿ 24 ∿ 48 and ∿ 72h respectively.

(f) Remove HCl on rotary evaporator, and dissolve residue in 1 ml 0.2M sodium citrate buffer, pH 2.2/0.5% thiodiglycol/0.01% pentachlorophenol.

2. Analysis

In the present study, 0.2 ml of each sample was loaded per column on a Beckman model 120C amino acid analyser. Chromatographic peaks were identified and integrated by on-line computer, and results given in nmoles amino acid/sample.

3. Calculation

(a) Correct values of serine and threonine to zero hydrolysis time by the formula:

$$\text{Log } A_o = (t_2/t_2-t_1) \text{ Log } A_1 - (t_1/t_2-t_1) \text{ Log } A_2$$

where A_1, A_2 and A_o are the quantities of amino acid present after t_1, t_2 and zero hours of hydrolysis respectively.

(b) Correct the value of amide-NH_3 at first hydrolysis period for the nmoles of threonine and serine destroyed by this time.

(c) Moles amino acid/mole protein = $\frac{X \cdot Z}{\Sigma X \cdot Y}$

where X is nmoles amino acid/sample

Y is the molecular weight of amino acids

Z is the molecular weight of the protein

(taken as 45,000 for Ya-ligandin).

4. Estimation of Tryptophan (330):

(a) Mix 0.9 ml dilute protein solution in H_2O with 0.1 ml 1M NaOH.

(b) Zero the spectrophotometer at 280 nm on 0.1M NaOH.

(c) Using 0.1M NaOH as a reference, determine the

absorbance (A) of the protein solution at 280, 294.4, 320 and 360 nm.

(d) Plot A_{320} and A_{360} values vs wave length; extrapolate line to the left, and subtract extrapolated values at 280 and 294.4 nm from respective A values (haze correction).

(e) The molar ratio of tyrosine to tryptophan is calculated:

$$\text{Mtyr/Mtryp} = \frac{0.592 \cdot A_{294.4} - 0.263 \cdot A_{280}}{0.263 \cdot A_{280} - 0.17 \cdot A_{294.4}}$$

(f) Tryp content is thus obtained from the tyr value yielded by the chromatographic analysis (see above).

APPENDIX C

STATISTICAL METHODS

STATISTICAL METHODS

(References: 377-379)

1. The mean and measures of dispersion

(a) Calculation of the mean ($\bar{X}$):

$$\bar{X} = \frac{\Sigma X}{n}$$

where n = number of estimates and ΣX is the sum of all the estimates.

(b) Calculation of standard deviation (s) and related parameters:

i) for $n < 30$: $s = \sqrt{\frac{\Sigma(X - \bar{X})^2}{n - 1}}$

ii) The standard error of the mean (SEM) $= \frac{s}{\sqrt{n}}$

iii) The percentage coefficient of variation (%CV) $= \frac{s}{\bar{X}} \times 100$

iv) The variance $= s^2$

2. Tests of hypotheses and significance

(a) Parametric and non-parametric tests:

When research data may appropriately be analysed by a parametric test, that test will be more powerful than any other in rejecting the null hypothesis (H_0) when it is false. Appropriateness in this case is the fulfilment of the following criteria:

i) The observations must be independent.

ii) The observations must be drawn from a normally distributed population.

iii) These populations must have the same variance.

iv) The variables involved must have been measured in at least an interval scale.

It should be readily appreciated that data of the nature produced in the present study fulfils criteria i) and iv). Also, provided there was no obvious skew distribution of data, normality was assumed. (The t test is robust to any slight deviation from normality in data). Homogeneity of variance was assessed by the F test:

$$F = s_1^2/s_2^2$$

where s_1^2 is the larger of the two variances of the sample populations to be compared, and s_2^2 the smaller. Significance is determined from the "upper significance limits of the F-distribution" table (379) with $n_1 - 1$ degrees of freedom for numerator and $n_2 - 1$ degrees of freedom for denominator. F-values < table values at P = 0.05 show no significant difference in size between the two variances.

(b) Levels of significance:

Values of P were determined from appropriate tables (377-379) for the t test, Wilcoxon test and correlation coefficient. Two-tailed tests were used in determinations of P, and H_o was accepted for P > 0.05.

(c) Student's t test (parametric data):

i) Unpaired data: To compare the means ($\bar{X}_1$ and $\bar{X}_2$) of two

small samples (n_1 and n_2) from normal population with a common variance:

$$t = \frac{\bar{X}_1 - \bar{X}_2}{S\sqrt{\frac{1}{n_1} + \frac{1}{n_2}}}$$

where S is an estimate of the pooled variance:

$$S^2 = \frac{1}{n_1 + n_2 - 2}\left[\Sigma X_1^2 - \frac{(\Sigma X_1)^2}{n_1} + \Sigma X_2^2 - \frac{(\Sigma X_2)^2}{n_2}\right]$$

for degrees of freedom = $n_1 + n_2 - 2$

ii) Paired data: To compare data from a series of matched pairs for the effects of different treatment, or self-matched paired-data from before and after treatment:

$$t = \bar{D}/SEM_{\bar{D}}$$

where $\bar{D}$ is the mean of the differences between pairs, and $SEM_{\bar{D}}$ the standard error of the mean;

for degrees of freedom = n - 1 where n is the number of pairs.

(d) Wilcoxon matched-pairs signed-ranks test (non-parametric paired data):

i) For each matched pair, determine the signed (±) difference (d) between the two values.

ii) Rank the d's without respect to sign. With tied d's, assign the average of the tied ranks (i.e. first 3 tied, rank (1 + 2 + 3)/3 = 2; next rank = 4).

iii) Affix to each rank the sign (±) of the d which it repre-

sents.

iv) Determine T = the smaller of the sums of the like-signed ranks.

v) n = total no. of d's with a sign (excludes d = 0).

vi) For n < or = 25, critical T values are read from the appropriate table, for n degrees of freedom.

3. Least squares regression line

A line of the form

$$Y = a + bX$$

is fitted to each of two sets of data, each set being of the form:

$$(X_1Y_1)\ \ (X_2Y_2).....(XnYn)$$

where

$$a = \frac{(\Sigma Y)(\Sigma X^2) - (\Sigma X)(\Sigma XY)}{n\Sigma X^2 - (\Sigma X)^2}$$

and

$$b = \frac{n\Sigma XY - (\Sigma X)(\Sigma Y)}{n\Sigma X^2 - (\Sigma X)^2}$$

and the correlation coefficient (r):

$$r = \frac{n\Sigma XY - (\Sigma X)(\Sigma Y)}{\sqrt{\left[n\Sigma X^2 - (\Sigma X)^2\right]\left[n\Sigma Y^2 - (\Sigma Y)^2\right]}}$$

APPENDIX D

SPECIMEN OUTPUT OF RIARUN PROGRAMME

(References: 297, 316)

```
                    ANALYSIS OF RADIOIMMUNOASSAY
                    -------- -- ---------------

   NAME OF ASSAY: LIGANDIN
   TYPE OF ASSAY: DB AB
   NO. OF ASSAY:  25/2/77
   PREPARED BY:   N.M.BASS

   TOTAL CPM =                                  8398.5
   NONSPECIFIC CPM (MEAN) =                      132.0
   COUNTING TIME FOR ASSAY =                       1.0
   COUNTS BOUND (ABOVE NONSPECIFIC) IN
     1.00 MINUTES FOR ZERO DOSE=                4545.5
   STANDARD DEVIATIONS USED FOR C.L. =             2.0
   NO. OF POINTS ON STANDARD CURVE =                24

   COEFFICIENTS OF VARIATION    MODEL 1
      DUE TO PIPETTING ERROR =                                .0100
      FRACTION OF SUPERNATANT LEFT WITH PPT =                 .0050
      FRACTION OF PPT REMOVED WITH SUPERNATANT =              .0150

   COUNTER DID NOT SUBTRACT BACKGROUND
   MACHINE CODE FOR UNKNOWNS IS HAND

   SAMPLE VOLUME =       1.0000

   DOSE OF LABELLED ANTIGEN =              .1000
   REACTION VOLUME =                       .9000
   MOLECULAR WEIGHT =                   .44000+16
   SPECIFIC ACTIVITY (CPM/MOLE) =       .39473+21
   UNITS OF DOSE(X) =                  NANOGRAM
   TEMPERATURE =         4.0000 DEGREES CENTIGRADE

                                                          STD.     DEGS. OF
                                    MEAN      VARIANCE    DEV.     FREEDOM
                                    ----      --------    ----     -------
   BOUND @COUNTS,ZERO DOSE        4677.55     8651.89    93.0155      3
   BOUND @COUNTS,INF. DOSE         132.05      392.71    19.8169      3
              TOTAL COUNTS        8398.50     5361.07    73.2193      3

PIPETTING ERROR = V1 =     .00030
                  V2 =     .00002
                  V3 =     .00090
```

Above: input data and average values of cpm for T, B_0 and NSB.

Below: weighted and unweighted regression analysis for logit plot

```
LIGANDIN  DB AB     25/2/77   N.M.BASS

(B/T) =  .549873
      0
UNWEIGHTED REGRESSION      LOGIT (Y) =    2.820087  -   .807017 * LOG X
----------  ----------                                            E
SLOPE =                      -.807017     STD. DEV. SLOPE =   .031528
INTERCEPT Y' =               2.820087     STD. DEV. INTCPT=   .102535
NUMBER OF STANDARDS =       24
MEAN X' =                    2.202708
MEAN Y' =                    1.042464
SUM OF WEIGHTS =            24.000000
RESIDUAL VARIANCE =           .136575
CORRELATION COEFF. =         -.983623

SUM OF SQUARES OF X AROUND MEAN X =  137.398680
SUM OF SQUARES OF Y AROUND MEAN Y =   92.489105
WEIGHTED REGRESSION        LOGIT (Y) =    3.416137  -   .955973 * LOG X
----------  ----------                                            E
SLOPE =                      -.955973     STD. DEV. SLOPE =   .029949
INTERCEPT Y' =               3.416137     STD. DEV. INTCPT=   .124900
NUMBER OF ITERATIONS =          4
NUMBER OF STANDARDS =       24
MEAN X' =                    4.035288
MEAN Y' =                    -.412808
SUM OF WEIGHTS =          2163.144775
RESIDUAL VARIANCE =          2.350756
CORRELATION COEFF. =         -.989376

SUM OF SQUARES OF X AROUND MEAN X = 2620.934611
SUM OF SQUARES OF Y AROUND MEAN Y = 2446.945768
                      TABLE OF DOSE LEVELS

              Y-VALUE     X-VALUE       X-HIGH        X-LOW
              -------     -------       ------        -----
                 .1        354.92        548.08       256.37
                 .2        151.96        195.30       122.04
                 .3         86.47        106.47        71.31
                 .4         54.47         66.45        44.97
                 .5         35.64         43.84        28.98
                 .6         23.32         29.39        18.31
                 .7         14.69         19.42        10.75
                 .8          8.36         12.17         5.17
                 .9          3.58          6.72          .99

THE MINIMUM DETECTABLE DOSE:
          X-VALUE =     2.637
          Y-VALUE =      .22
```

```
LIGANDIN  DB AB      25/2/77    N.M.BASS

(B/T) =  .549873
      0

DIFFERENCE BETWEEN SLOPE OF PTS.  13 TO  24 AND
 POINTS 1 TO  12 OF STD. VALS. ON LOGIT CURVE=  -.302985
THE COMBINED VARIANCE =                         2.370325
THE T VALUE FOR EQUALITY OF SLOPES=            -1.133298
THE STUDENT'S T VALUE FOR  20 D. F. =           2.086284

NO SIGNIFICANT NON-LINEARITY IN LINEAR SEGMENT TEST

PARABOLIC REGRESSION:                                          2
  LOGIT(Y) =  3.13232  -  .79239 * LOG X  -  .02152 * (LOG X)
                             E                      E

LINEAR REGRESSION SS=            2395.22913
PARABOLIC REGRESSION SS =        2398.21808

T TEST FOR LINEARITY =              1.13496
THE STUDENT'S T VALUE FOR  21 D.F.=  2.07994

NO SIGNIFICANT NON-LINEARITY IN PARABOLIC TEST
```

Above: test for linearity of logit plot.

Below: values used during the regression analysis.

```
LIGANDIN  DB AB      25/2/77    N.M.BASS

(B/T) =  .549873
      0

 VALUES USED DURING THE REGRESSION ANALYSIS

                BOUND &#
 I     XX(I)     COUNTS    Y(I)     LN(X)  WORKING LOGIT(Y)  WEIGHT     MEAN   STD. DEV.
       0.0       4806.   1.0282
       0.0       4669.    .9981
       0.0       4652.    .9943
       0.0       4584.    .9794                                        1.0000     .0205
 1      .20       4580.    .9786  -1.609        2.892           .08
 2      .20       4493.    .9594  -1.609        2.140           .08     .9690     .0136
 3      .40       4558.    .9737   -.916        3.336           .31
 4      .40       4516.    .9645   -.916        2.646           .31     .9691     .0065
 5      .80       4486.    .9579   -.223        2.116          1.14
 6      .80       4428.    .9452   -.223        2.483          1.14     .9505     .0066
 7     1.60       4454.    .9509    .470        2.969          4.04
 8     1.60       4475.    .9555    .470        3.062          4.04     .9532     .0032
 9     3.20       4254.    .9069   1.163        2.276         13.48
10     3.20       4172.    .8887   1.163        2.056         13.48     .8978     .0128
11     6.40       3881.    .8247   1.856        1.546         40.63
12     6.40       3965.    .8432   1.856        1.682         40.63     .8340     .0131
13    12.80       3586.    .7598   2.549        1.144        102.86
14    12.80       3600.    .7629   2.549        1.160        102.86     .7613     .0022
15    25.60       2564.    .5351   3.243         .139        199.14
16    25.60       2514.    .5241   3.243         .094        199.14     .5296     .0078
17    51.20       2167.    .4477   3.936        -.209        269.68
18    51.20       2209.    .4570   3.936        -.170        269.68     .4523     .0066
19   102.00       1344.    .2665   4.625       -1.012        242.71
20   102.00       1368.    .2719   4.625        -.985        242.71     .2692     .0038
21   205.00        744.    .1345   5.323       -1.849        145.02
22   205.00        785.    .1437   5.323       -1.781        145.02     .1391     .0065
23   410.00        569.    .0960   6.016       -2.238         62.47
24   410.00        542.    .0902   6.016       -2.311         62.47     .0931     .0041
     9999.9        159.    .0059
     9999.9        135.    .0007
     9999.9        119.   -.0028
     9999.9        115.   -.0038                                        .0000     .0044
```

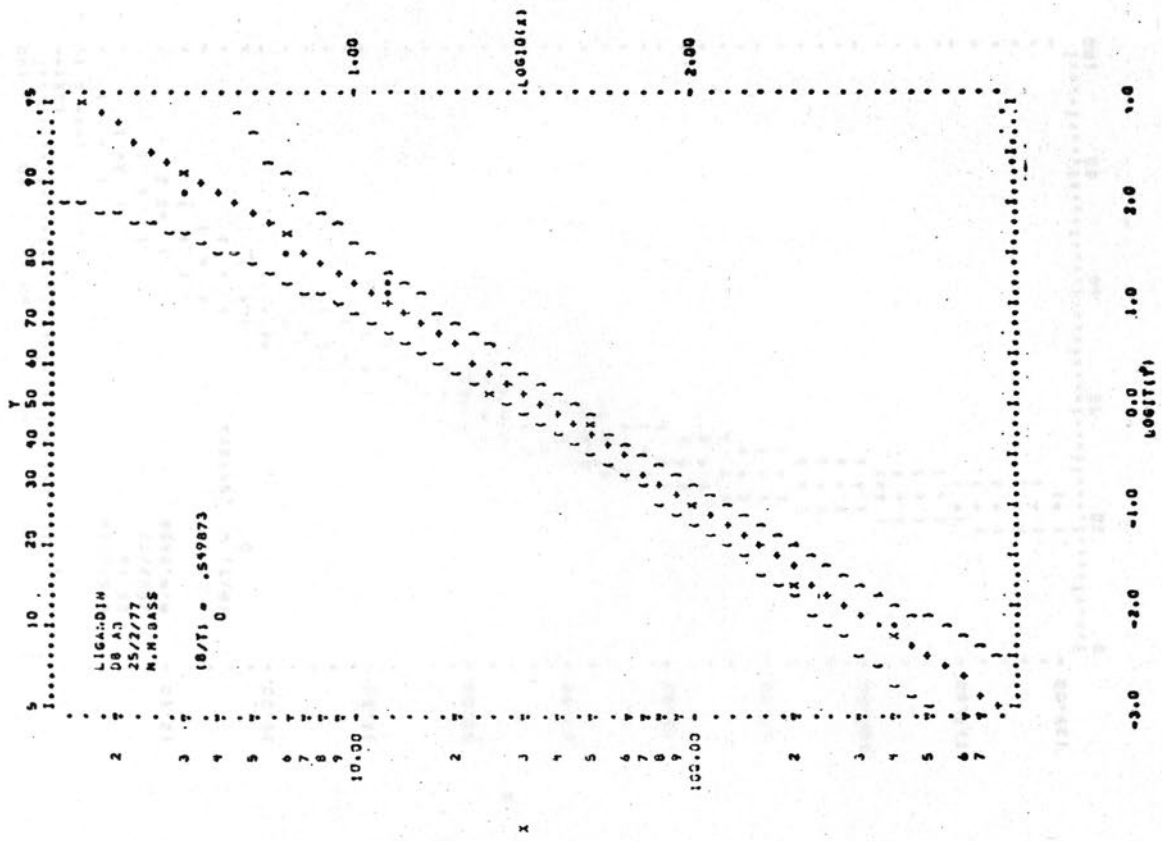

Above: plot of logit Y vs Log X, Y = B/B_0; X = dose of unlabelled antigen.

Below: plot of Y vs Log X.

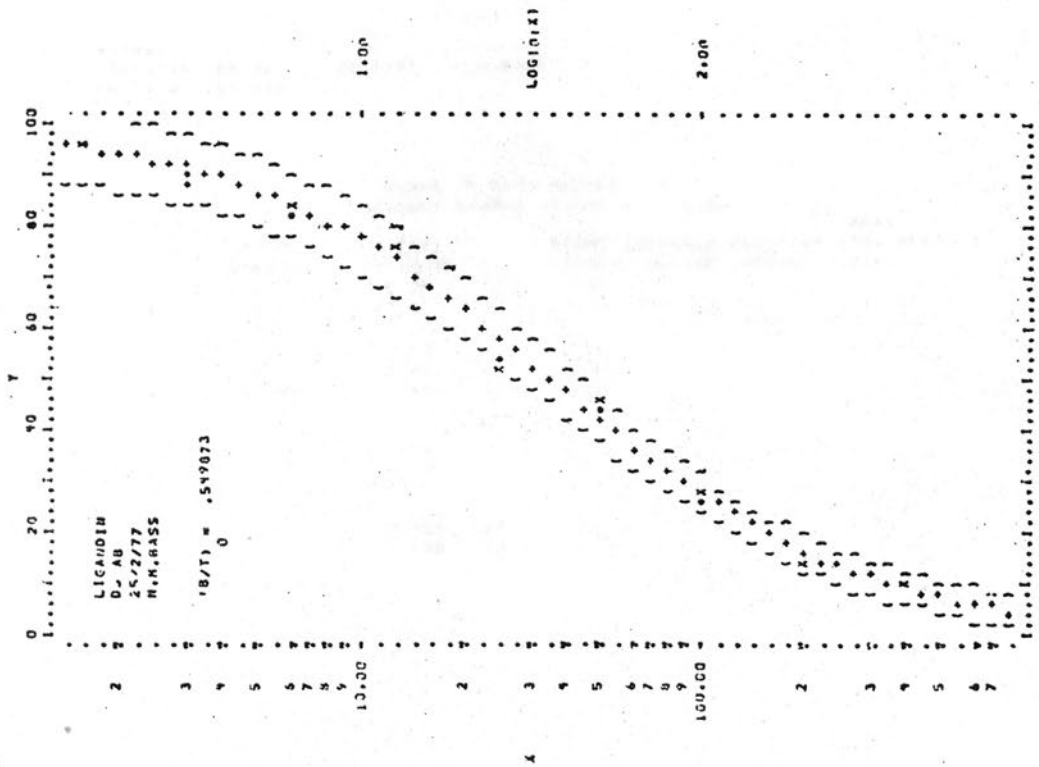

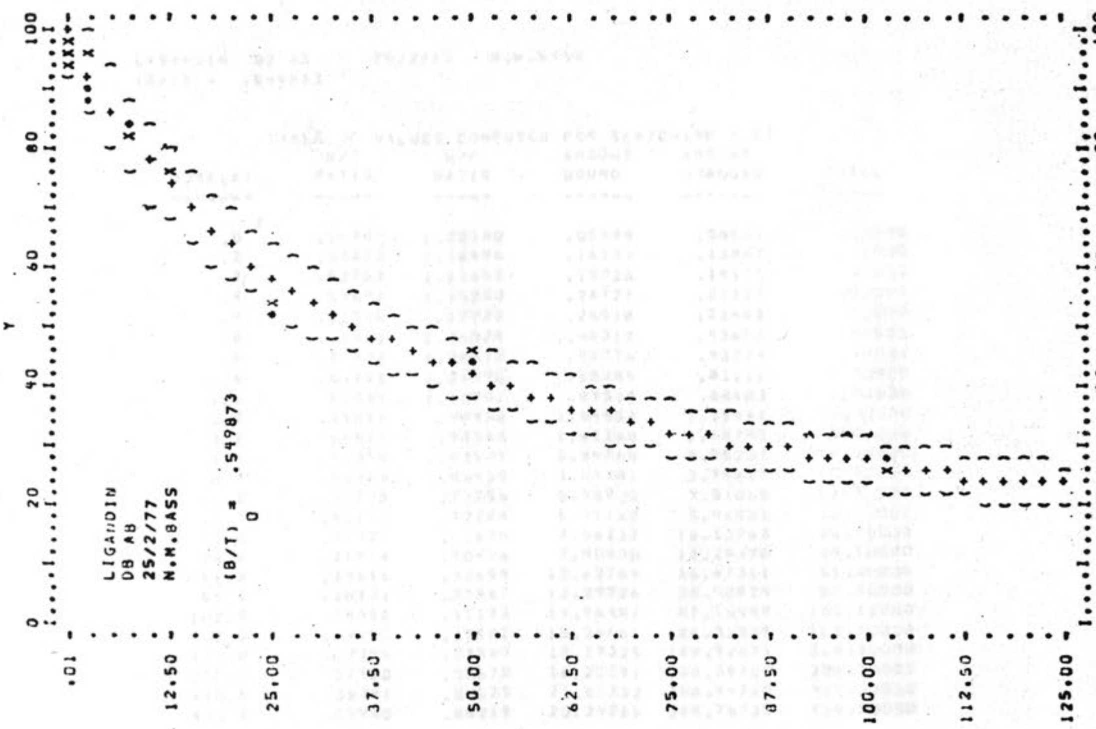

Above: plot of Y vs X

Below: calculation of unknowns

```
••••••
LIGANDIN  DB AB     25/2/77    N.M.BASS
(B/T) =  .549873
    0
                          - 1-

                 BLOCK OF DATA NUMBER   1
              CONSTANT SAMPLE VOLUME =     1.00
```

NO	Y FOR UNKNOWN	POTENCY ESTIMATE	C.V.	BOUND COUNTS	SAMPLE VOLUME	FRACTION RECVRY	MEAN STD. DEV. C.V.
1.1	.6280	20.60	12.	2987.			
1.2	.6158	21.76	12.	2931.			21.18
							.82
							3.85
2.1	.7480	11.42	17.	3532.			
2.2	.7502	11.28	17.	3542.			11.35
							.10
							.86
3.1	.6934	15.18	14.	3284.			
3.2	.7106	13.93	15.	3362.			14.55
							.88
							6.06
4.1	.8107	7.784	22.	3817.			
4.2	.8171	7.448	23.	3846.			7.62
							.24
							3.11

••••••

```
LIGANDIN  DB AB      25/2/77   N.M.BASS
(B/T) =  .549873
     0

          TABLE OF VALUES COMPUTED FOR SCATCHARD PLOT
              B/T       B/F       AMOUNT      AMOUNT
  DOSE(X)     RATIO     RATIO     BOUND       UNBOUND      TOTAL
  -------     -----     -----     ------      -------      -----

      .0      .54987   1.22160    .05499       .04501      .10000
      .2      .53810   1.16496    .16143       .13857      .30000
      .2      .52752   1.11651    .15826       .14174      .30000
      .4      .53542   1.15250    .26771       .23229      .50000
      .4      .53035   1.12927    .26518       .23482      .50000
      .8      .51463   1.06028    .46317       .43683      .90000
      .8      .51973   1.08218    .46776       .43224      .90000
     1.6      .52298   1.09590    .88889       .81111     1.70000
     1.6      .52539   1.10701    .89317       .80683     1.70000
     3.2      .49866    .99466   1.64558      1.65442     3.30000
     3.2      .48867    .95568   1.61260      1.68740     3.30000
     6.4      .45349    .82972   2.94768      3.55232     6.50000
     6.4      .46366    .86450   3.01381      3.48619     6.50000
    12.8      .41778    .71756   5.38935      7.51065    12.90000
    12.8      .41951    .72268   5.41167      7.48833    12.90000
    25.6      .29424    .41694   7.56237     18.13763    25.70000
    25.6      .28818    .40486   7.40630     18.29370    25.70000
    51.2      .24616    .32654  12.62789     38.67211    51.30000
    51.2      .25131    .33567  12.89226     38.40774    51.30000
   102.0      .14556    .17173  14.96401     87.13599   102.10000
   102.0      .14563    .17182  15.26661     86.83339   102.10000
   205.0      .07396    .07989  15.17325    189.92675   205.10000
   205.0      .07900    .08575  16.20291    188.89709   205.10000
   410.0      .05281    .05575  21.65732    388.44268   410.10000
   410.0      .04960    .05219  20.34265    389.75735   410.10000

SLOPE OF FIRST HALF OF POINTS =                    -.10387
BOUND INTERCPT. FOR FIRST HALF OF POINTS =        11.13687

SLOPE OF SECOND HALF OF POINTS =                   -.04027
BOUND INTERCPT. FOR SECOND HALF OF POINTS=        20.24505

THE COMBINED VARIANCE =                             .00605
THE T VALUE FOR EQUALITY OF SLOPES =               2.74506
THE STUDENT'S T VALUE FOR  20 D.F. =               2.08628

SIGNIFICANT NONLINEARITY IN LIN. SEG TEST

PARABOLIC REGRESSION:
     (B/F) =   1.15041   +   -.10238 * BOUND  +   .00240 * (BOUND)**2

LINEAR REGRESSION SS =                            3.88872
PARABOLIC REGRESSION SS =                         4.07740
T TEST FOR LINEARITY =                            4.43963
THE STUDENT'S T VALUE FOR  21 D.F. =              2.07994

SIGNIFICANT NONLINEARITY IN PARABOLIC TEST
```

Above: table of values computed for Scatchard plot, and test for linearity.

Below: unweighted regression of Scatchard plot.

```
LIGANDIN  DB AB      25/2/77   N.M.BASS
(B/T) =  .549873
     0

UNWEIGHTED REGRESSION OF B/F RATIO ON AMOUNT BOUND

MEAN B/F =                    .670776     STD. DEV. B/F =              .424426
MEAN BOUND =                 6.986743     STD. DEV. BOUND =           7.170011
CORRELATION COEFF. =         -.968806

SLOPE =                      -.057348     STD. DEV. SLOPE =            .003128
COEFF. OF VAR. OF SLOPE =    -.054536
B/F INTERCEPT =              1.071453     STD. DEV. INTERCEPT =        .030974
BOUND INTERCEPT =           18.683305
RESIDUAL VARIANCE =           .011566
UNWEIGHTED REGRESSION OF AMOUNT BOUND ON B/F RATIO

SLOPE =                    -16.366457     STD. DEV. SLOPE =            .892566
COEFF. OF VAR. OF SLOPE =    -.054536
RECIPROCAL OF SLOPE =        -.061101
BOUND INTERCEPT =           17.964971     STD. DEV. INTERCEPT =        .704264
B/F INTERCEPT =              1.097670
RESIDUAL VARIANCE =          3.300751
```

2-3-4-75 PARAMETER CURVE FITTING

2 PARAMETER MODEL:

IT	STEP	RES.VAR.	K11	Q1	QSUM	K1101	KQSUM	K1202
			.057348	18.663305				
1	1/ 1.	.98208-02	.079852	12.929055	12.929045	.992487	.992487	
2	1/ 1.	.13625-01	.079011	14.351143	14.351143	1.133901	1.133901	
3	1/ 1.	.21935-02	.083146	13.664252	13.664252	1.134131	1.134131	
4	1/ 1.	.21509-02	.082849	13.743043	13.743043	1.139079	1.139079	
5	1/ 1.	.21463-02	.082997	13.725581	13.725581	1.139188	1.139188	
6	1/ 1.	.21463-02	.082989	13.727029	13.727029	1.139193	1.139193	

3 PARAMETER MODEL:

IT	STEP	RES.VAR.	K11	Q1	ASMP	QSUM	K1101	KQSUM	K1202
			.082989	6.863519	.050000				
1	1/ 1.	.16179+00	.070809	14.372627	.029227	14.372627	1.017695	1.017695	
2	1/ 1.	.54436-02	.093942	10.008433	.047950	10.800433	1.015348	1.015348	
3	1/ 1.	.57376-02	.092295	11.917919	.042068	11.917919	1.099960	1.099960	
4	1/ 1.	.18235-02	.095775	11.499118	.045157	11.499118	1.101323	1.101323	
5	1/ 1.	.18078-02	.095517	11.544221	.045102	11.544221	1.102673	1.102673	
6	1/ 1.	.18082-02	.095607	11.533912	.045135	11.533912	1.102727	1.102727	

4 PARAMETER MODEL

IT	STEP	RES.VAR.	K11	Q1	K12	Q2	QSUM	K1101	KQSUM	K1202
			.165978	6.863519	.041995	13.727029				
1	1/ 2.	.17266+00	.127756	10.179615	.011599	10.442849	20.622464	1.300505	1.421111	.120606
2	1/ 1.	.37211-01	.120019	8.567061	.003751	18.266274	24.773335	1.046490	1.115035	.068699
3	1/ 1.	.57336-02	.099433	10.129800	.005302	19.749578	29.865378	1.006791	1.111376	.104655
4	1/ 1.	.25771-02	.101726	10.574332	.002912	23.030599	33.400881	1.076114	1.143177	.067062
5	1/ 1.	.19367-02	.103249	10.302571	.003781	22.904389	33.206960	1.063684	1.150286	.086602
6	1/ 1.	.18573-02	.103668	10.282130	.003584	23.763659	34.045788	1.065929	1.151109	.085180
7	1/ 1.	.18570-02	.103638	10.282827	.003608	23.719196	34.002093	1.065690	1.151270	.085581
8	1/ 1.	.18569-02	.103654	10.281825	.003604	23.730920	34.012745	1.065749	1.151286	.085537
9	1/ 1.	.18569-02	.103653	10.281830	.003605	23.727959	34.009769	1.065737	1.151285	.085548

5 PARAMETER MODEL

IT	STEP	RES.VAR.	K11	Q1	K12	Q2	ASMP	QSUM	K1101	KQSUM	K1202
			.165978	6.863519	.041995	13.727029	.050000				
1	1/ 1.	.22779+00	.158973	7.343464	.024978	7.080291	.028664	19.923705	1.090309	1.267158	.176849
2	1/ 1.	.99586-02	.142977	5.730406	.040277	8.579009	.029933	19.309415	.819314	1.161899	.342585
3	1/ 1.	.26132-02	.132422	6.067666	.038910	8.202306	.030908	19.269972	.803492	1.122692	.319150
4	1/ 1.	.19636-02	.117439	7.659003	.030356	6.965293	.029259	19.624296	.899431	1.110869	.211438
5	1/ 1.	.20380-02	.107048	9.629291	.019276	6.176109	.025899	15.800395	1.030262	1.118430	.088169
6	1/ 1.	.20036-02	.109792	9.203537	.019801	8.017911	.022685	17.220948	1.010478	1.129192	.118664
7	1/ 1.	.19543-02	.109907	9.247530	.019435	7.842559	.023091	17.090090	1.016369	1.129569	.113205
8	1/ 1.	.19584-02	.110103	9.209459	.019723	7.842229	.023126	17.061647	1.013990	1.129452	.115462
9	1/ 1.	.19569-02	.110121	9.206976	.019766	7.824515	.023179	17.031490	1.013878	1.129412	.115534
10	1/ 1.	.19569-02	.110131	9.205256	.019780	7.822693	.023188	17.028149	1.013761	1.129406	.115625

Above: calculation of 'best-fit' Scatchard plot model.

Below: selection of 'best-fit' Scatchard plot model with estimation of the equilibrium constant and binding capacity of the major binding site.

COMPARISON OF SCATCHARD PLOT MODELS

CASE	PARMTRS	D.F.	VV	SS	DELT SS	F	T
1	2	22	.21463-02	.47219-01			
					.9247-02	5.114	2.080
2	3	21	.18082-02	.37972-01			
					.8399-03	.449	2.086
3	4	20	.18569-02	.37137-01			

BEST FIT IS A 3 PARAMETER MODEL
REVISED ESTIMATES OF K AND Q BASED ON FIT

BINDING SITE NO. 1

ESTIMATE OF K-EQ = .40442+12 LITERS/MOLE
ESTIMATE OF BINDING CAPACITY Q = .27267-11 MOLES/LITER
DELTA F = R T LN(K) = FREE ENERGY CHANGE = 14.71090 KCAL/MOLE

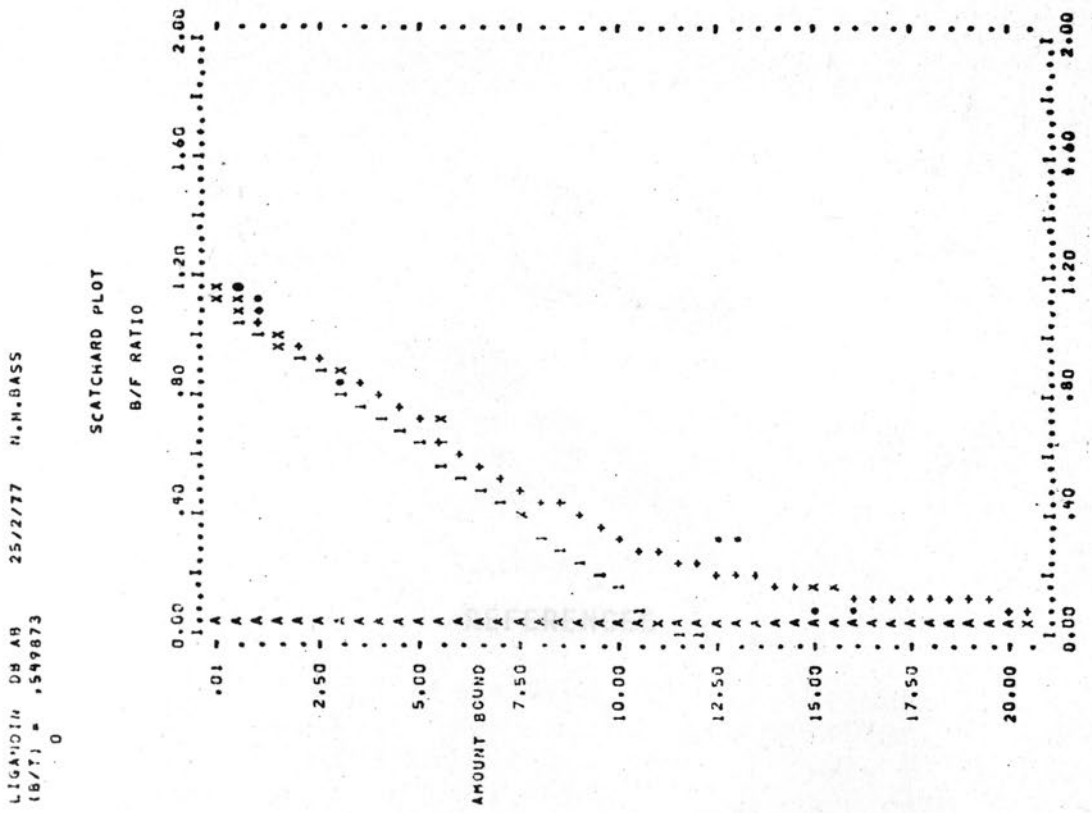

Above: Scatchard plot for binding of ligandin to specific antibody.

Below: RIA optimization routine.

```
                ASSAY OPTIMIZATION
                        INPUT DATA

                              K-EQ =          .40+12 LITERS/MOLE
                     SPEC. ACTIVITY =          .39+21 CPM/MOLE
                      REACTION VOL. =        .00090 LITERS
                      COUNTING TIME =       1.00
          (SPEC.ACT.)*(VOL)*(TIME) =          .36+18
                                V1 =         .010
                                V2 =         .005
                                V3 =         .015
       CONDITIONS FOR MAXIMAL SENSITIVITY
     (TO MINIMIZE THE LEAST DETECTABLE DOSE)

              TRACER CONCENTRATION=          .21-12 MOLES/LITER
           ANTIBODY CONCENTRATION=          .83-12 MOLES/LITER
     MIN. DETECTABLE CONCENTRATION=          .23-12 MOLES/LITER
                        INITIAL B/T=         .24
                        INITIAL B/F=         .32
       B/T AT MIN. DETECTABLE DOSE=         .23
       B/F AT MIN. DETECTABLE DOSE=         .30
      B/B0 AT MIN. DETECTABLE DOSE=         .95
     TOTAL COUNTS IN INITIAL TUBE=    73210.
            NUMBER OF ITERATIONS =       27

BASED ON THE ABOVE INPUT DATA, AND A NUMBER OF OTHER
ASSUMPTIONS (SEE RIAINTERPRET), WE SUGGEST  THE FOLLOWING
CHANGES FOR YOUR NEXT ASSAY:

      USE    8.717 TIMES AS MUCH TRACER
      USE     .305 TIMES AS MUCH ANTIBODY

$FIN
```

REFERENCES

1. Litwack, G., Ketterer, B. and Arias, I.M. (1971) Nature 234, 466-467.

2. Arias, I.M. (1972) Semin. Haematol. 9, 55-70.

3. Fleischner, G. and Arias, I.M. (1970) Amer. J. Med. 49, 576-589.

4. Ketterer, B., Tipping, E., Beale, D. and Meuwissen, J. (1975) In: Proceedings of the XIth International Cancer Congress, Florence, 1974, Vol. 2, pp. 25-29. Excerpta Medica, Amsterdam.

5. Ketterer, B., Tipping, E., Meuwissen, J. and Beale, D. (1975) Biochem. Soc. Trans. 3, 626-630.

6. Arias, I.M., Fleischner, G., Listowsky, I., Kamisaka, K., Mishkin, S. and Gatmaitan, Z. (1976) In: The Hepatobiliary System (Taylor, W., ed.) pp. 81-103. Plenum Publishing Corp., New York.

7. Fleischner, G.M. and Arias, I.M. (1976) In: Progress in Liver Diseases (Popper, H. and Schaffner, F., eds.) Vol. 5, pp. 172-182. Grune and Stratton, New York.

8. Kamisaka, K., Listowsky, I., Fleischner, G., Gatmaitan, Z. and Arias, I.M. (1976) In: Bilirubin Metabolism in the Newborn. The 2nd International Symposium, Jerusalem, 1974, Birth Defects: Original Article Series, Vol. 12, pp. 156-167. Excerpta Medica, Amsterdam.

9. Arias, I.M. and Jansen, P. (1976) In: Jaundice (Goresky, C.A. and Fisher, M.M., eds.) pp. 175-188. Plenum Publishing Corp., New York.

10. Arias, I.M., Fleischner, G., Kirsch, R., Goldstein, E., Feinfeld, D. and Gatmaitan, Z. (1976) In: The Liver : Quantitative Aspects of Structure and Function. Proceedings of the 2nd International Gstaad Symposium, Gstaad, 1975 (Preisig, R., Bircher, J. and Paumgartner, G., eds.) pp. 439-447. Editio Cantor, Aulendorf.

11. Arias, I.M., Fleischner, G., Kirsch, R., Mishkin, S. and Gatmaitan, Z. (1976) In: Glutathione : Metabolism and Function (Arias, I.M. and Jakoby, W., eds.) Kroc Foundation Series Vol. 6, pp. 175-188. Raven Press, New York.

12. Jusko, W.J. and Gretch, M. (1976)
Drug Metab. Rev. 5, 43-140.

13. Smith, G.J., Ohl, V.S. and Litwack, G. (1977)
Cancer Res. 37, 8-14.

14. Ketterer, B., Ross-Mansell, P. and Whitehead, J.K. (1967)
Biochem. J. 103, 316-324.

15. Habig, W.H., Pabst, M.J., Fleischner, G., Gatmaitan, Z., Arias, I.M. and Jakoby, W.B. (1974)
Proc. Nat. Acad. Sci. U.S. 71, 3879-3881.

16. Alpert, S., Mosher, M., Shanske, A. and Arias, I.M. (1969)
J. Gen. Physiol. 53, 238-247.

17. Billing, B.H. and Lathe, G.H. (1958)
Amer. J. Med. 24, 111-121.

18. Tarchanoff, J.F. (1874)
Op. cit. Billing and Lathe (17).

19. Mann, F.C., Sheard, C., Bollman, J.L. and Baldes, E.J. (1925)
Amer. J. Physiol. 74, 497-510.

20. Reyes, H., Levi, A.J., Levine, R., Gatmaitan, Z. and Arias, I.M. (1971)
Ann. N.Y. Acad. Sci. 179, 520-528.

21. Lester, R. and Troxler, R.F. (1969)
Gastroenterology 56, 143-169.

22. Klatskin, G. (1961)
Ann. Rev. Med. 12, 211-246.

23. Martin, N.H. (1949)
J. Amer. Chem. Soc. 71, 1230-1232.

24. Ostrow, J.D. and Schmid, R. (1963)
J. Clin. Invest. 42, 1286-1299.

25. Blauer, G. and King, T.E. (1970)
J.Biol. Chem. 245, 372-381.

26. Odell, G.B. (1974)
Ann. N.Y. Acad. Sci. 226, 224-237.

27. Chronszczewsky, N. (1866)
Op. cit. Hanzon (43).

28. Rosenthal, S.M. and White, E.C. (1924)
J. Pharmacol. Exp. Ther. 24, 265-288.

29. Rosenthal, S.M. and White, E.C. (1925)
J. Amer. Med. Assoc. 84, 1112-1114.

30. Baker, K.J. and Bradley, S.E. (1966)
J. Clin. Invest. 45, 281-287.

31. Deutchman, G., Gratzl, M. and Ullrich, V. (1974)
Biochim. Biophys. Acta 371, 470-481.

32. Baker, K.J. (1966)
Proc. Soc. Exp. Biol. Med. 122, 957-963.

33. Dragstedt, C. and Mills, M.A. (1936)
Proc. Soc. Exp. Biol. Med. 34, 467-468.

34. Cantarow, A., Wirts, C.W., Snape, W.J. and Miller, L.L. (1948)
Amer. J. Physiol. 154,211-219.

35. Ingelfinger, F.J., Bradley, S.E., Mendeloff, A.I. and Kramer, P. (1948)
Gastroenterology 11, 646-657.

36. Mendeloff, A.I., Kramer, P., Ingelfinger, F.J. and Bradley, S.E. (1949)
Gastroenterology 13, 222-234.

37. Weech, A.A., Vann, D. and Grillo, R.A. (1941)
J. Clin. Invest. 20, 323-332.

38. Schoenfield, L.J., Foulk, W.T. and Butt, H.R. (1964)
J. Clin. Invest. 43, 1409-1418.

39. Dragstedt, C.A. and Mills, M.A. (1937)
Amer. J. Physiol. 119, 713-719.

40. Cohn, C., Levine, R. and Streicher, D. (1947)
Amer. J. Physiol. 150, 299-303.

41. Brauer, R.W., Pessoti, R.L. and Krebs, J.S. (1955)
J. Clin. Invest. 34, 35-43.

42. Snell, A.M., Greene, C.H. and Rountree, L.G. (1927)
A.M.A. Arch. Intern. Med. 40, 471-487.

43. Hanzon, V. (1952)
Acta Physiol. Scand. 28, 1-268, Suppl. 101.

44. Mendeloff, A.I. (1949)
Proc. Soc. Exp. Biol. Med. 70, 556-558.

45. Hunton, D.B., Bollman, J.L. and Hoffman, H.N. (1960)
Gastroenterology 39, 713-724.

46. Hunton, D.B., Bollman, J.L. and Hoffman, H.N. (1961)
J. Clin. Invest. 40, 1648-1655.

47. Leevy, C.M., Bender, J., Silverberg, M. and
Naylor, J. (1963)
Ann. N.Y. Acad. Sci. 111, 161-175.

48. Stege, T.E., Loose, L.D. and Di Luzio, N.R. (1975)
Proc. Soc. Exp. Biol. Med. 149, 455-461.

49. Klein, R.I. and Levinson, S.A. (1933)
Proc. Soc. Exp. Biol. Med. 31, 179-181.

50. Cantarow, A. and Wirts, C.W. (1943)
Amer. J. Digest. Diseases 10, 261-266.

51. Rosenthal, S.M. and Lillie, R.D. (1931)
Amer. J. Physiol. 97, 131-141.

52. Shore, M.L. and Zilversmit, D.B. (1954)
Amer. J. Physiol. 177, 436-440.

53. Andrews, W.H.H. (1955)
Lancet (ii), 166-169.

54. Brauer, R.W., Shill, O.S. and Krebs, J.S. (1959)
J. Clin. Invest. 38, 2202-2214.

55. Krebs, J.S. and Brauer, R.W. (1949)
Fed. Proc. 8, 310.

56. Tovey, J.E. (1967)
Clin. Chim. Acta 15, 149-154.

57. Elton, N.W. (1935)
Amer. J. Clin. Path. 5, 40-54.

58. Forsgren, E. (1918-1935)
Op. cit. Hanzon (43).

59. Kremer, J. (1933)
Op. cit. Hanzon (43).

60. Novikoff, A.B. and Essner, E. (1960)
Amer. J. Med. 29, 102-131.

61. Arias, I.M. (1961)
In: Progress in Liver Disease (Popper, H. and
Schaffner, F.) Vol. 1, pp. 187-201. Grune and
Stratton, New York.

62. Tanturi, C.A. and Ivy, A.C. (1938)
Amer. J. Physiol. 121, 61-74.

63. Pavel, I. (1949)
Op. cit. Hanzon (43)

64. Combes, B. (1964)
In: The Liver (Rouiller, C. ed.) pp. 1-35.
Academic Press, New York.

65. Sperber, I. (1959)
Pharmacol. Rev. 11, 109-134.

66. Cantarow, A. and Wirts, C.W. (1941)
Proc. Soc. Exp. Biol. Med. 47, 252-254.

67. Brauer, R.W. and Pessoti, R.L. (1949)
J. Pharmacol. Exp. Ther. 97, 358-370.

68. Andrews, W.H.H. and Del Rio Lozano, I. (1961)
Quart. J. Exp. Physiol. 46, 238-256.

69. Bradley, S.E., Ingelfinger, F.J., Bradley, G.P. and Curry, J.J. (1945)
J. Clin. Invest. 24, 890-897.

70. Brauer, R.W. and Pessoti, R.L. (1950)
Amer. J. Physiol. 162, 565-574.

71. Combes, B., Wheeler, H.O., Childs, A.W. and Bradley, S.E. (1956)
Trans. Assoc. Amer. Physicians 64, 276-284.

72. Weinbren, K. and Billing, B.H. (1956)
Brit. J. Exp. Pathol. 37, 199-204.

73. Arias, I.M., Johson, L. and Wolfson, S. (1961)
Amer. J. Physiol. 200, 1091-1094.

74. Billing, B.H., Maggiore, Q. and Cartter, M.A. (1963)
Ann. N.Y. Acad. Sci. 111, 319-325.

75. Bradley, S.E. (1959)
In: The Harvey Lectures, pp. 131-155.

76. Wheeler, H.O., Meltzer, J.I. and Bradley, S.E. (1960)
J. Clin. Invest. 39, 1131-1144.

77. Klaasen, C.D. and Plaa, G.L. (1967)
Amer. J. Physiol. 213, 1322-1326.

78. Goresky, C.A. (1964)
Amer. J. Physiol. 207, 13-26.

79. Goresky, C.A. (1965)
Can. Med. Assoc. J. 92, 851-857.

80. Schmid, R., Axelrod, J., Hammaker, L. and Swarm, R. (1958)
J. Clin. Invest. 37, 1123-1130.

81. Tisdale, A., Klatskin, G. and Kinsella, E.D. (1959)
Amer. J. Med. 26, 214-227.

82. Philp, J.R., Grodsky, G.M. and Carbone, J.V. (1961)
Amer. J. Physiol. 200, 545-547.

83. Combes, B. (1962)
Clin. Res. 10, 54.

84. Whelan, G., Hoch, J. and Combes, B. (1970)
J. Lab. Clin. Med. 75, 542-557.

85. Barnhart, J.L. and Combes, B. (1976)
Amer. J. Physiol. 231, 399-407.

86. Klaasen, C.D. and Plaa, G. (1968)
J. Pharmacol. Exp. Ther. 161, 361-366.

87. Fauvert, R.E. (1959)
Gastroenterology 37, 603-616.

88. Richards, T.G., Tindall, V.R. and Young, A. (1959)
Clin. Sci. 18, 499-511.

89. Barber-Riley, G., Goetzee, A.E., Richards, T.G. and Thompson, J.Y. (1961)
Clin. Sci. 20, 149-159.

90. Billing, B.H., Williams, R. and Richards, T.G. (1964)
Clin. Sci. & Mol. Med. 27, 245-257.

91. Barret, P.V.D., Berk, P.D., Menken, M. and Berlin, N.I. (1968)
Ann. Intern. Med. 68, 355-377.

92. Berk, P.D., Howe, R.B., Bloomer, J.R. and Berlin, N.I. (1969)
J. Clin. Invest. 48, 2176-2190.

93. Quarfordt, S.H., Hilderman, H.L., Valle, D. and Waddell, E. (1971)
Gastroenterology 60, 246-255.

94. Snapp, F.E., Gutman, M., Li, T.W. and Ivy, C.A. (1947)
J. Lab. Clin. Med. 32, 321-322.

95. Hargreaves, T. and Lathe, G.H. (1963)
Nature 200, 1172-1176.

96. Berthelot, P. and Billing, B.H. (1966)
Amer. J. Physiol. 211, 395-399.

97. Barber-Riley, G. (1962)
Nature 194, 184-185.

98. Hammaker, L. and Schmid, R. (1967)
Gastroenterology 53, 31-37.

99. Andriole, V.T. (1963)
J. Lab. Clin. Med. 61, 730-744.

100. Goetzee, A.E., Richards, T.G. and Tindall, V.R. (1960)
Clin. Sci. 19, 63-78.

101. Cornelius, C.E., Ben-Ezzer, J. and Arias, I.M. (1967)
Proc. Soc. Exp. Biol. Med. 124, 665-667.

102. Burnstine, R.C. and Schmid, R. (1962)
Proc. Soc. Exp. Biol. Med. 109, 356-358.

103. Brown, W.R., Grodsky, G.M. and Carbone, J.V. (1964)
Amer. J. Physiol. 207, 1237-1241.

104. Bernstein, L.H., Ben-Ezzer, J., Gartner, L. and Arias, I.M. (1966)
J. Clin. Invest. 45, 1194-1201.

105. Grodsky, G. (1967)
In: Bilirubin Metabolism (Bouchier, I.A.D. and Billing, B. eds.) pp. 159-166. Blackwell Scientific Publications, Oxford.

106. Cornelius, C.E. and Gronwall, R.R. (1965)
Fed. Proc. 24, 144.

107. Levi, A.J., Gatmaitan, Z. and Arias, I.M. (1969)
J. Clin. Invest. 48, 2156-2167.

108. Miller, J.A. and Miller, E.C. (1953)
In: Advances in Cancer Research (Greenstein, J.P. and Haddow, A., eds.) Vol. 1, pp. 339-396. Academic Press, New York.

109. Sariff, A.M. and Heidelberger, C. (1976)
In: Glutathione : Metabolism and Function (Arias, I.M. and Jakoby, W.B., eds.) Kroc Foundation Series Vol. 6, pp. 317-338. Raven Press, New York.

110. Miller, E.C. and Miller, J.A. (1947)
Cancer Res. 7, 468-480.

111. Miller, E.C., Miller, J.A., Sapp, R.W. and Weber, G.M. (1949)
Cancer Res. 9, 336-343.

112. Price, J.M., Miller, J.A., Miller, E.C. and Weber, G.M. (1949)
Cancer Res. 9, 96-102.

113. Sorof, S. and Cohen, P.P. (1951)
Cancer Res. 11, 376-382.

114. Sorof, S., Cohen, P.P., Miller, E.C. and Miller, J.A. (1951)
Cancer Res. 11, 383-387.

115. Sorof, S., Young, E.M., McCue, M.M. and Fetterman, P.L. (1963)
Cancer Res. 23, 864-882.

116. Pitot, H.C. and Heidelberger, C. (1963)
Cancer Res. 23, 1694-1700.

117. Abell, C.W. and Heidelberger, C. (1962)
Cancer Res. 22, 931-946.

118. Ketterer, B. (1972)
Biochem. J. 126, 3p - 4p.

119. Sorof, S., Sani, B.P., Kish, V.M. and Meloche, H.P. (1974)
Biochemistry 13, 2612-2620.

120. Ketterer, B. and Christodoulides, L. (1969)
Chem. Biol. Interact. 1, 173-183.

121. Litwack, G. (ed.) (1975)
Biochemical Actions of Hormones Vol. 3. Academic Press, New York.

122. Baulieu, E.E. (1975)
Biochem. Pharmacol. 24, 1743-1748.

123. Bradlow, H.L., Dobriner, K. and Gallagher, T.F. (1954)
Endocrinology 54, 343-352.

124. Bellamy, D., Phillips, J.G., Chester Jones, I. and Leonard, R.A. (1962)
Biochem. J. 85, 537-545.

125. Hanngren, A., Hansson, E., Sjöstrand, E. and Ullberg, S. (1964)
Acta Endocrinol. 47, 95-104.

126. Gelehrter, T. (1976)
N. Engl. J. Med. 294, pp. 522-526; 589-595; 646-651.

127. Litwack, G., Sears, M.L. and Diamondstone, T.I. (1963)
J. Biol. Chem. 238, 302-305.

128. Litwack, G., Fiala, E.S. and Filosa, R.J. (1965)
Biochim. Biophys. Acta 111, 569-571.

129. Fiala, E.S. and Litwack, G. (1966)
Biochim. Biophys. Acta 124, 260-266.

130. Morey, K.S. and Litwack, G. (1968)
Fed. Proc. 27, 524.

131. Morey, K.S. and Litwack, G. (1969)
Biochemistry 8, 4813-4821.

132. Litwack, G., Filler, R., Rosenfield, S.A., Lichtash, N., Wishman, C. and Singer, S. (1973)
J. Biol. Chem. 248, 7481-7486.

133. Litwack, G. (1976)
In: Glutathione : Metabolism and Function. (Arias, I.M. and Jakoby, W.B. eds.) Kroc Foundation Series Vol. 6, pp. 285-299. Raven Press, New York.

134. Litwack, G. and Morey, K.S. (1970)
Biochem. Biophys. Res. Comm. 38, 1141-1148.

135. Singer, S. and Litwack, G. (1971)
Cancer Res. 31, 1364-1368.

136. Krebs, J. and Brauer, R. (1958)
Amer. J. Physiol. 194, 37-43.

137. Combes, B. (1959)
J. Clin. Invest. 38, 1426-1433.

138. Meltzer, J.I., Wheeler, H.O. and Cranston, W.I. (1959)
Proc. Soc. Exp. Biol. Med. 100, 174-179.

139. Javitt, N.B., Wheeler, H.O., Baker, K.J., Ramos, O.L. and Bradley, S.E. (1960)
J. Clin. Invest. 39, 1570-1577.

140. Combes, B. and Stakelum, G.S. (1960)
J. Clin. Invest. 39, 1214-1222.

141. Grodsky, G.M., Carbone, J.V. and Fanska, R. (1961)
Proc. Soc. Exp. Biol. Med. 106, 526-530.

142. Combes, B. and Stakelum, G.S. (1961)
J. Clin. Invest. 40, 981-988.

143. Baumann, E. and Preusse, C. (1879)
Ber. Dtsch. Chem. Ges. 12, 806-810.

144. Barnes, M.M., James, S.P. and Wood, P.B. (1959)
Biochem. J. 71, 680-690.

145. Booth, J., Boyland, E. and Sims, P. (1961)
Biochem. J. 79, 516-524.

146. Chasseaud, L.F. (1976)
In: Glutathione : Metabolism and Function (Arias, I.M. and Jakoby, W.B. eds.) Kroc Foundation Series Vol. 6, pp. 77-114. Raven Press, New York.

147. Johnson, M.K. (1966)
Biochem. J. 98, 44-55.

148. Boyland, E. and Williams, K. (1965)
Biochem. J. 94, 190-197.

149. Boyland, E. and Chasseaud, L.F. (1969)
Adv. Enzymol. 32, 173-219.

150. Kaplowitz, N., Percy-Robb, I.W. and Javitt, N.B. (1973)
J. Exp. Med. 138, 483-486.

151. Kaplowitz, N., Percy-Robb, I.W. and Javitt, N.B. (1973)
Gastroenterology 65, 549.

152. Ketterer, B., Christodoulides, L., Enderby, G. and Tipping, E. (1974)
Biochem. Biophys. Res. Comm. 57, 142-147.

153. Fjellstedt, T.A., Allen, R.H., Duncan, B.K. and Jakoby, W.B. (1973)
J. Biol. Chem. 248, 3702-3707.

154. Pabst, M.J., Habig, W.H. and Jakoby, W.B. (1973)
Biochem. Biophys. Res. Comm. 52, 1123-1128.

155. Habig, W.H., Pabst, M.J. and Jakoby, W.B. (1974)
J. Biol. Chem. 249, 7130-7139.

156. Pabst, M.J., Habig, W.H. and Jakoby, W.B. (1974)
J. Biol. Chem. 249, 7140-7150.

157. Habig, W.H., Pabst, M.J. and Jakoby, W.B. (1976)
Arch. Biochem. Biophys. 175, 710-716.

158. Fleischner, G., Robbins, J. and Arias, I.M. (1972)
J. Clin. Invest. 51, 677-684.

159. Kirsch, R., Fleischner, G., Kamisaka, K. and Arias, I.M. (1975)
J. Clin. Invest. 55, 1009-1019.

160. Fleischner, G., Kamisaka, K., Habig, W., Jakoby, W. and Arias, I.M. (1975)
Gastroenterology 69, 821.

161. Kamisaka, K., Habig, W.H., Ketley, J.N., Arias, I.M. and Jakoby, W.B. (1975)
Eur. J. Biochem. 60, 153-161.

162. Kornguth, M.L., Monson, R.A. and Kunin, C.M. (1974) J. Inf. Dis. 129, 552-558.

163. Ketterer, B., Tipping, E., Beale, D. and Meuwissen, J.A.T.P. (1976) In: Glutathione : Metabolism and Function (Arias, I.M. and Jakoby, W.B. eds.) Kroc Foundation Series Vol. 6, pp. 243-257. Raven Press, New York.

164. Tipping, E., Ketterer, B., Christodoulides, L. and Enderby, G. (1976) Biochem. J. 157, 211-216.

165. Koskelo, P., Sundberg, L. and Håkansson, U. (1976) Ann. Clin. Res. 8, Suppl. 17, 244-245.

166. Kamisaka, K., Listowsky, I. and Arias, I.M. (1973) Ann. N.Y. Acad. Sci. 226, 148-153.

167. Kamisaka, K., Listowsky, I., Gatmaitan, Z. and Arias, I.M. (1975) Biochemistry 14, 2175-2180.

168. Listowsky, I., Kamisaka, K., Ishitani, K. and Arias, I.M. (1976) In: Glutathione : Metabolism and Function (Arias, I.M. and Jakoby, W.B., eds.) Kroc Foundation Series Vol. 6, pp. 233-242. Raven Press, New York.

169. Jakoby, W.B., Habig, W.H., Keen, J.H., Ketley, J.N. and Pabst, M.J. (1976) In: Glutathione : Metabolism and Function (Arias, I.M. and Jakoby, W.B. eds.) Kroc Foundation Series Vol. 6, pp. 189-211. Raven Press, New York.

170. Nemoto, N., Gelboin, H.V., Habig, W.H., Ketley, J.N. and Jakoby, W.B. (1975) Nature 255, 512.

171. Habig, W.H., Keen, J.H. and Jakoby, W.B. (1975) Biochem. Biophys. Res. Comm. 64, 501-506.

172. Christ-Hazelhof, E., Nugteren, D.H. and Van Dorp, D.A. (1976) Biochim. Biophys. Acta 450, 450-461.

173. Benson, A.M., Talalay, P., Keen, J.H. and Jakoby, W.B. (1977) Proc. Nat. Acad. Sci. U.S. 74, 158-162.

174. Ketley, J.N., Habig, W.H. and Jakoby, W.B. (1975) J. Biol. Chem. 250, 8670-8673.

175. Jakoby, W.B., Ketley, J.N. and Habig, W.H. (1976) In: Glutathione : Metabolism and Function (Arias, I.M. and Jakoby, W.B. eds.) Kroc Foundation Series Vol. 6, pp. 213-223. Raven Press, New York.

176. Mannervik, B. and Askelöf, P. (1975) FEBS Lett. 56, 218-221.

177. Keen, J.H., Habig, W.H. and Jakoby, W.B. (1976) J. Biol. Chem. 251, 6183-6188.

178. Sokoloff, J., Berk, R.N., Lang, J.H. and Lasser, E.C. (1973) Radiology 106, 519-523.

179. Bloomer, J.R., Berk, P.D., Vergalla, J. and Berlin, I.N. (1973) Clin. Sci. Mol. Med. 45, 505-516.

180. Corrocher, R., De Sandre, G., Pacor, M.L. and Hoffbrand, A.V. (1974) Clin. Sci. Mol. Med. 46, 551-554.

181. Kirsch, R.E., Vinik, A.I., Frith, L.O'C., Gordon, B., Grant, B.J. and Saunders, S.J. (1975) FEBS Lett. 52, 300-303.

182. Lichter, M., Fleischner, G., Kirsch, R., Levi, A.J., Kamisaka, K. and Arias, I.M. (1976) Amer. J. Physiol. 230, 1113-1120.

183. Ketterer, B., Srai, K.S. and Christodoulides, L. (1976) Biochim. Biophys. Acta 428, 683-689.

184. Ketterer, B., Srai, K.S. and Tipping, E. (1976) Biochem. Soc. Trans. 4, 202-204.

185. Klaasen, C.D. (1975) J. Pharmacol. Exp. Ther. 195, 311-319.

186. Klaasen, C.D. (1976) Toxicol. Appl. Pharmacol. 38, 85-100.

187. Carulli, N., Ponz de Leon, M., Maneti, F. and Ferrari, A. (1976) Gut 17, 581-587.

188. Grodsky, G.M., Kolb, H.J., Fanska, R.E. and Nemechek, C. (1970) Metabolism 19, 246-252.

189. Meuwissen, J.A.T.P., Ketterer, B. and Mertens, B.B.E. (1972) Digestion 6, 293.

190. Strange, R.C., Nimmo, I.A. and Percy-Robb, I.W. (1976) Biochem. J. 156, 427-433.

191. Tipping, E., Ketterer, B., Christodoulides, L. and Enderby, G. (1976) Eur. J. Biochem. 67, 583-590.

192. Tipping, E., Ketterer, B., Christodoulides, L. and Enderby, G. (1976) Biochem. J. 157, 461-467.

193. Woolley, P.V., Hunter, M.J. and Arias, I.M. (1976) Biochim. Biophys. Acta 446, 115-123.

194. Wolkoff, A.W., Ketley, J.N., Waggoner, J.G., Jakoby, W.B. and Berk, P.D. (1976) Gastroenterology 71, 936.

195. Meuwissen, J.A.T.P. (1975) Digestion 12, 276.

196. Meuwissen, J.A.T.P. and Ketterer, B. (1975) In: Proceedings of the Bilirubin Meeting, Hemsedal, Norway, 1974. (Bakken, A.F. and Fog, J. eds.) pp. 48-57. Paediatric Research Institute, Oslo.

197. Tiribelli, C., Frezza, M., Panfili, E., Sandri, G. and Sottocasa, G.L. (1975) In: Proceedings of the Bilirubin Meeting, Hemsedal, Norway, 1974. (Bakken, A.F. and Fog, J., eds.) pp. 58-61. Paediatric Research Institute, Oslo.

198. Clifton, G., Kaplowitz, N., Kuhlenkamp, J. and Wallin, J.D. (1974) Clin. Res. 22, 521.

199. Clifton, G., Kaplowitz, N., Kuhlenkamp, J. and Wallin, J.D. (1975) Clin. Res. 23, 120.

200. Kornguth, M.L., Monson, R.A. and Kunin, C.M. (1976) Arch. Biochem. Biophys. 174, 339-343.

201. Reyes, H., Levi, A.J., Gatmaitan, Z. and Arias, I.M. (1971) J. Clin. Invest. 50, 2242-2252.

202. Levi, A.J., Gatmaitan, Z. and Arias, I.M. (1970) N. Engl. J. Med. 283, 1136-1139.

203. Foliot, A., Housset, E., Ploussard, J.P., Petite, J.P. and Infante, R. (1973) Biomedicine 19, 488-491.

204. Levine, R.I., Reyes, H., Levi, A.J., Gatmaitan, Z. and Arias, I.M. (1971) Nature New Biol. 231, 277-279.

205. Davis, D.R. and Yeary, R.A. (1975)
Proc. Soc. Exp. Biol. Med. 148, 9-13.

206. Foliot, A., Drocourt, J.L., Etienne, J.P., Housset, E., Fiessinger, J.N. and Christoforov, B. (1977)
Biochem. Pharmacol. 26, 547-548.

207. Matsushita, Y., Nakagawa, S., Umeyama, H. and Moriguchi, I. (1976)
Chem. Pharm. Bull. 24, 1650-1654.

208. Reyes, H., Levi, A.J., Gatmaitan, Z. and Arias, I.M. (1969)
Proc. Nat. Acad. Sci. U.S. 64, 168-170.

209. Baldwin, R.W., Barker, C.R. and Moore, M. (1968)
Brit. J. Cancer 22, 776-786.

210. Bannikov, G.A. and Chipysheva, T.A. (1972)
Bull. Exp. Biol. Med. 73, 77-80.

211. Bannikov, G.A., Guelstein, V.I. and Tchipysheva, T.A. (1973)
Int. J. Cancer 11, 398-411.

212. Fleischner, G.M., Robbins, J.B. and Arias, I.M. (1977)
Biochem. Biophys. Res. Comm. 74, 992-1000.

213. Kaplowitz, N., Kuhlenkamp, J. and Clifton, G. (1975)
Biochem. J. 146, 351-356.

214. Clifton, G., Kaplowitz, N., Wallin, J.D. and Kuhlenkamp, J. (1975)
Biochem. J. 150, 259-262.

215. Kaplowitz, N., Clifton, G., Kuhlenkamp, J. and Wallin, J.D. (1976)
Biochem. J. 158, 243-248.

216. Hales, B.F. and Niems, A.H.(1976)
Biochem. J. 160, 223-229.

217. Hales, B.F. and Niems, A.H. (1976)
Biochem. J. 160, 231-236.

218. Fleischner, G.M., Kamisaka, K., Gatmaitan, Z. and Arias, I.M. (1976)
In: Glutathione : Metabolism and Function (Arias, I.M. and Jakoby, W.B. eds.) Kroc Foundation Series Vol. 6, pp. 259-265. Raven Press, New York.

219. Sarrif, A.M., Danenberg, P.V., Heidelberger, C. and Ketterer, B. (1976)
Biochem. Biophys. Res. Comm. 70, 869-877.

220. Sarrif, A.M., Bertram, J.S., Kamarck, M. and Heidelberger, C. (1975)
Cancer Res. 35, 816-824.

221. Darby, F.J. and Grundy, R.K. (1972)
Biochem. J. 128, 175-177.

222. Boyer, J.L., Schwarz, J. and Smith, N. (1976)
Gastroenterology 70, 254-256.

223. Chasseaud, L.F. (1973)
Drug Metab. Rev. 2, 185-220.

224. Levi, A.J., Gatmaitan, Z. and Arias, I.M. (1969)
Lancet 2, 139-140.

225. Combes, B. and Stakelum, G.S. (1962)
J. Clin. Invest. 41, 750-757.

226. Bell, J.U. and Ecobichon, D.J. (1974)
Can. J. Biochem. 53, 433-437.

227. Levi, A.J., Gatmaitan, Z. and Arias, I.M. (1969)
Gastroenterology 56, 401.

228. Conney, A.H. (1967)
Pharmacol. Rev. 19, 317-366.

229. Stein, L.B., Mishkin, S., Fleischner, G., Gatmaitan, Z. and Arias, I.M. (1976)
Amer. J. Physiol. 231, 1371-1376.

230. Fleischner, G., Meijer, D.K.F., Levine, W.G., Gatmaitan, Z., Gluck, R. and Arias, I.M. (1975)
Biochem. Biophys. Res. Comm. 67, 1401-1407.

231. Eichholtz, A. and Howell, K.E. (1972)
Gastroenterology 62, 647-667.

232. Oxender, D.L. and Quay, S. (1955)
Ann. N.Y. Acad. Sci. 264, 358-371.

233. Scharschmidt, B.F., Waggoner, J.G. and Berk, P.D. (1975)
J. Clin. Invest. 56, 1280-1292.

234. Klaasen, C.D. (1973)
J. Pharmacol. Exp. Ther. 184, 721-728.

235. Paumgartner, G., Probst, P., Kraines, R. and Leary, C.M. (1970)
Ann. N.Y. Acad. Sci. 170, 134-147.

236. Gartner, L.M. and Arias, I.M. (1972)
Amer. J. Physiol. 222, 1091-1099.

237. Clarenburg, R. and Kao, C. (1973)
Amer. J. Physiol. 225, 192-200.

238. Schanker, L.S. (1965)
In: The Biliary System (Taylor, W., ed.) pp. 469-480.
Blackwell Scientific, Oxford.

239. Meijer, D.K.F., Weitering, J.G. and Vonk, R.J. (1976)
J. Pharmacol. Exp. Ther. 198, 229-239.

240. Arias, I.M. (1975)
In: Drugs and the Liver (Gerok, W. and Sickinger, K. eds.) pp. 165-176. F.K. Schattauer, Stuttgart.

241. Gartner, L.M. and Arias, I.M. (1969)
Pediat. Res. 3,171-180.

242. Vest, M.F. (1962)
J. Clin. Invest. 41, 1013-1020.

243. Pegg, D.G., Bernstein, J. and Hook, J.B. (1976)
Proc. Soc. Exp. Biol. Med. 151, 720-725.

244. Pegg, D.G. and Hook, J.B. (1977)
J. Pharmacol. Exp. Ther. 200, 65-74.

245. Klaasen, C.D. (1970)
J. Pharmacol. Exp. Ther. 175, 289-300.

246. Meijer, D.K.F., Keulemans, K., Weitering, J.G. and Vonk, R.J. (1976)
Digestion 14, 470-471.

247. Levi, A.J. and Kenwright, S. (1976)
In: The Liver : Quantitative Aspects of Structure and Function. Proceedings of the 2nd International Gstaad Symposium, Gstaat, 1975. (Preisig, R., Bircher, J. and Paumgartner, G. eds.) pp. 169-171.
Editio Cantor, Aulendorf.

248. Paumgartner, G. and Reichen, J. (1976)
Clin. Sci. Mol. Med. 51, 169-176.

249. Schwenk, M., Burr, R., Schwarz, L. and Pfaff, E. (1976)
Eur. J. Biochem. 64, 189-197.

250. Accatino, L. and Simon, F.R. (1976)
J. Clin. Invest. 57, 496-508.

251. Bloomer, J.R. and Zaccaria, J. (1976)
Amer. J. Physiol. 230, 736-742.

252. Van Bezooijen, C.F.A., Grell, T. and Knook, D.L. (1976)
Biochem. Biophys. Res. Comm. 69, 354-361.

253. Horne, D.W., Briggs, W.T. and Wagner, C. (1976)
Biochem. Biophys. Res. Comm. 68, 70-76.

254. Barnhart, J.L. and Clarenburg, R. (1973)
Amer. J. Physiol. 225, 497-507.

255. Tiribelli, C., Panfili, E., Sandri, G., Frezza, M. and Sottocasa, G.L. (1974)
In: Diseases of the Liver and Biliary Tract (Leevy, C.M., ed.) pp. 55-59. S. Karger, Basel.

256. Tiribelli, C., Lunazzi, G.C., Frezza, M. and Sottocasa, G.L. (1976)
Digestion 14, 470.

257. Berk, P.D., Bloomer, J.R., Howe, R.B. and Berlin, N.I. (1970)
Amer. J. Med. 49, 296-305.

258. Berk. P.D., Blaschke, T.F. and Waggoner, J.G. (1972)
Gastroenterology 63, 472-481.

259. Black, M., Fevery, J., Parker, D., Jacobsen, J., Billing, B.H. and Carson, E.R. (1974)
Clin. Sci. Mol. Med. 46, 1-17.

260. Martin, J.F., Vierling, J.M., Wolkoff, A.W., Scharschmidt, B.F., Vergalla, J., Waggoner, J.G. and Berk, P.D. (1976)
Gastroenterology 70, 385-391.

261. Auclair, C., Hakim, J., Boivin, P., Troube, H. and Boucherot, J. (1976)
Enzyme 21, 97-107.

262. Kirschenbaum, G., Shames, D.M. and Schmid, R. (1976)
J. Pharmacokinetics and Biopharmaceut. 4, 115-155.

263. Frezza, M. and Tiribelli, C. (1974)
Digestion 10, 314-315.

264. Dhumeaux, D. and Bertelot, P. (1975)
Gastroenterology 69, 988-993.

265. Okuda, K., Ohkubo, H., Musha, H., Kotoda, K., Abe, H. and Tanikawa, K. (1976)
Gut 17, 588-594.

266. Chowdhury, J.R., Jansen, P.L.M., Fischberg, E., Daniller, A.I. and Arias, I.M. (1976)
Gastroenterology 71, 901.

267. Hamada, S., Torikuza, K., Miyake, T. and Fukase, M. (1970)
Biochim. Biophys. Acta 201, 479-492.

268. Dillman, W., Surks, M.I. and Oppenheimer, J.H. (1974) Endocrinology 95, 492-498.

269. Defer, N., Dastugue, B., Sabuteur, M.M., Thomopoulous, P. and Kruh, J. (1975) Biochem. Biophys. Res. Comm. 67, 995-1004.

270. Kamisaka, K., Gatmaitan, Z., Moore, C.L. and Arias, I.M. (1975) Pediat. Res. 9, 903-905.

271. Laperche, Y. and Oudea, P. (1976) J. Pharmacol. Exp. Ther. 197, 235-244.

272. Filler, R., Morey, K.S. and Litwack, G. (1974) Biochem. Biophys. Res. Comm. 60, 431-439.

273. Kirsch, R., Fleischner, G., Feinfeld, D., Goldstein, E., Kamisaka, K. and Arias, I.M. (1975) Clin. Res. 23, 431.

274. Feinfeld, D., Fleischner, G., Goldstein, E., Arias, I.M. and Bourgoignie, J. (1975) Clin. Res. 23, 361.

275. Mishkin, S., Stein, L., Gatmaitan, Z. and Arias, I.M. (1972) Biochem. Biophys. Res. Comm. 47, 997-1003.

276. Kamisaka, K., Listowsky, I., Gatmaitan, Z. and Arias, I.M. (1975) Biochim. Biophys. Acta 393, 24-30.

277. Ockner, R.K. and Manning, J.A. (1974) J. Clin. Invest. 54, 326-338.

278. Mishkin, S., Stein, L., Fleischner, G., Gatmaitan, Z. and Arias, I.M. (1975) Amer. J. Physiol. 288, 1634-1640.

279. Tipping, E., Ketterer, B., Christodoulides, L. and Enderby, G. (1975) Biochem. Soc. Trans. 3, 680-683.

280. O'Doherty, P.J.A. and Kuksis, A. (1975) FEBS Lett. 60, 256-258.

281. Ketterer, B., Tipping, E., Hackney, J.F. and Beale, D. (1976) Biochem. J. 155, 511-521.

282. Grabowski, G.A., McCoy, K.E., Williams, G.C., Dempsey, M.E. and Hanson, R.F. (1976) Biochim. Biophys. Acta 441, 380-390.

283. Na-Rideout, M.Y.C., Elson, C. and Shrago, E. (1976)
Biochem. Biophys. Res. Comm. 71, 809-816.

284. Yalow, R.S. and Berson, S.A. (1960)
J. Clin. Invest. 39, 1157-1175.

285. Odell, W.D. and Daughaday, W.H. (eds.) (1971)
Principles of Competitive Protein-Binding Assays.
Lippincott, Philadelphia.

286. Kirkham, K.E. and Hunter, W.M. (eds.) (1971)
Radioimmunoassay Methods. Churchill Livingstone,
Edinburgh.

287. Skelley, D.S., Brown, L.P. and Besch, P.K. (1973)
Clin. Chem. 19, 146-186.

288. Sönksen, P.H. (ed.) (1974)
Brit. Med. Bull. 30, 1-103.

289. Roberts, R., Sobel, B.E. and Parker, C.W. (1976)
Science 194, 855-857.

290. Temler, R.S. and Felber, J.P. (1976)
Biochim. Biophys. Acta 445, 720-728.

291. Foti, A.G., Herschman, H. and Fenimore Cooper, J.
(1977)
Clin. Chem. 23, 95-99.

292. Murray, T.M., Arnold, B.M., Tam, W.H., Hitchman,
A.J.W. and Harrison, J.E. (1974)
Metabolism 23, 829-837.

293. Arnold, B.M., Kuttner, M., Swaminathan, R., Care,
A.D., Hitchman, A.J.W., Harrison, J.E. and Murray,
T.M. (1975)
Can. J. Physiol. Pharmacol. 53, 1129-1134.

294. Stone, M.J., Willerson, J.T., Gomez-Sanchez, C.E.
and Waterman, M.R. (1975)
J. Clin. Invest. 56, 1334-1339.

295. Taubman, M.B., Kammerman, S. and Goldberg, B. (1976)
Proc. Soc. Exp. Biol. Med. 152, 284-287.

296. Berson, S.A. and Yalow, R.S. (1968)
Clin. Chim. Acta 22, 51-69.

297. Rodbard, D. (1974)
Clin. Chem. 20, 1255-1270.

298. Lowry, O.H., Rosebrough, N.J., Farr, A.L. and
Randall, R.J. (1951)
J. Biol. Chem. 193, 265-275.

299. Fischer, L. (1972)
In: Laboratory Techniques in Biochemistry and Molecular Biology (Work, T.S. and Work, E., eds.) Vol. 1, pp. 151-391. North-Holland Co., Amsterdam.

300. Maizel, J.V. (1971)
In: Methods in Virology (Maramorosch, R. and Kroprowsky, H., eds.) Vol. 5, pp. 179-246. Academic Press, New York.

301. Weber, K. and Osborn, M. (1969)
J. Biol. Chem. 244, 4406-4412.

302. Wrigley, C.W. (1972)
Methods Enzymol. 22, 559-564.

303. Malik, N. and Berrie, A. (1972)
Anal. Biochem. 49, 173-176.

304. Camacho, A., Carrascosa, J.L., Vinuela, E. and Salas, M. (1975)
Anal. Biochem. 69, 395-400.

305. Hayashi, M. and Natori, Y. (1976)
J. Biochem. 79, 221-224.

306. Hurn, B.A.L. and Landon, J. (1971)
In: Radioimmunoassay Methods (Kirkham, K.E. and Hunter, W.M., eds.) pp. 121-142. Churchill Livingstone, Edinburgh.

307. Ouchterlony, P. (1958)
Prog. Allergy 5, 1-78.

308. Graber, P. (1959)
Methods Biochem. Anal. 7, 1-38.

309. Mancini, G., Carbonara, O. and Heremans, J.F. (1965)
Immunochemistry 2, 235-254.

310. Hunter, W.M. (1971)
In: Radioimmunoassay Methods (Kirkham, K.E. and Hunter, W.M., eds.) pp. 3-23. Churchill, Livingstone, Edinburgh.

311. Hunter, W.M. (1974)
Brit. Med. Bull. 30, 18-23.

312. Greenwood, F.C., Hunter, W.M. and Glover, J.S. (1963)
Biochem. J. 89, 114-123.

313. Berson, S.A., Yalow, R.S., Bauman, A., Rothschild, M.A. and Newerly, K. (1956)
J. Clin. Invest. 35, 170-190.

314. McFarlane, A.S. (1958)
Nature 182, 53.

315. Morgan, C.R. and Lazarow, A. (1963)
Diabetes 12, 115-126.

316. Rodbard, D. and Lewald, J.E. (1970)
Acta Endocrinol. 64, Suppl. 147, 79-103.

317. Scatchard, G. (1949)
Ann. N.Y. Acad. Sci. 51, 550-670.

318. Hunter, W.M. and Ganguli, P.C. (1971)
In: Radioimmunoassay Methods (Kirkham, K.E. and Hunter, W.M., eds.) pp. 243-257. Churchill Livingstone, Edinburgh.

319. Feldman, H. and Rodbard, D. (1971)
In: Principles of Competitive Protein-Binding Assays (Odell, W.D. and Daughaday, W.H., eds.) pp. 158-203. Lippincott, Philadelphia.

320. Israel, J.B. and Arias, I.M. (1976)
Adv. Int. Med. 21, 77-96.

321. Tidball, C.S. (1964)
Amer. J. Physiol. 206, 239-242.

322. Yam, J., Reeves, M. and Roberts, R.J. (1976)
J. Lab. Clin. Med., 87, 373-383.

323. Thomas, F.B., Baba, N., Greenberger, N.J. and Salsburg, D. (1972)
J. Lab. Clin. Med. 80, 548-558.

324. Stripp, B., Menard, R.H. and Gillette, J.R. (1974)
Life Sciences 14, 2121-2130.

325. Greengard, O. (1971)
Essays Biochem. 7, 159-205.

326. Halac, E. and Sicignano, C. (1969)
J. Lab. Clin. Med. 73, 677-685.

327. Kim, J.K., Hirsch, G.H. and Hook, J.B. (1972)
Pediat. Res. 6, 600-605.

328. Weber, K. and Kuter, D.J. (1971)
J. Biol. Chem., 246, 4505-4509.

329. Moore, S. and Stein, W.H. (1963)
Methods Enzymol. 6, 819-831.

330. Beaven, G.H. and Holiday, E.R. (1952)
Adv. Protein Chem. 7, 319-386.

331. Ostrow, J.D., Hammaker, L. and Schmid, R. (1961)
J. Clin. Invest. 40, 1442-1452.

332. Clermont, R.J. and Chalmers, T.C. (1967)
Medicine 46, 197-207.

333. Wilkinson, J.H. (1970)
Clin. Chem. 16, 882-890.

334. Wolf, P.L. and Williams, D. (1973)
Practical Clinical Enzymology, John Wiley and Sons,
New York.

335. Schmidt, E. and Schmidt, F.W. (1976)
FEBS Lett. 62, (Suppl.) 362-379.

336. Recknagel, R.O. (1967)
Pharmacol Revs. 19, 145-208.

337. Karmen, A. (1955)
J. Clin. Invest. 34, 131-133.

338. Espinosa, E. and Insunza, I. (1962)
Proc. Soc. Exp. Biol. Med. 111, 174-177.

339. Espinosa, E. (1974)
Clin. Exp. Immunol. 16, 153-162.

340. Arakawa, Y., Bull, D.M., Schott, C.F. and Davidson,
C.S. (1976)
Gastroenterology 71, 118-122.

341. Felber, J.P. and Temler, R.S. (1971)
In: Radioimmunoassay Methods (Kirkham, K.E. and
Hunter, W.M., eds.) pp. 658-663. Churchill Livingstone,
Edinburgh.

342. Hirayama, C., Kawasaki, H. and Morotomi, I. (1967)
Experientia 23, 528-529.

343. Javitt, N.B. (1965)
Fed. Proc. 24, 166 (Abstr.)

344. Datta, D.V., Singh, S. and Chuttani, P.W. (1973)
Indian J. Med. Res. 9, 1351-1359.

345. Zimmerman, H.J., Kodera, Y. and West, M. (1965)
J. Lab. Clin. Med. 66, 315-323.

346. Cohen, P.P. (1955)
Methods Enzymol. 2, 178-184.

347. Klaasen, C.D. and Plaa, G.L. (1968)
Toxicol. Appl. Pharmacol. 12, 132-139.

348. Chinsky, M. and Sherry, S. (1957)
Arch. Int. Med. 99, 556-568.

349. Trams, G.E. and Symeonidis, A. (1957)
Am. J. Pathol. 33, 13-25.

350. Posen, S. (1970)
Clin. Chem. 16, 71-84.

351. Tyson, J.W., Meade, J.H., Dalrymple, G.V. and Marven, H.N. (1967)
J. Nuc. Med. 8, 558-569.

352. Durst, A., Dishon, T., Rosenmann, E. and Boss, J.H. (1971)
Lab. Invest. 25, 35-41.

353. Boss, J.H., Rosenmann, E., Dishon, T., Slavin, S. and Eliakim, M. (1976)
Res. Exp. Med. 167, 51-59.

354. Appert, H.E., Dimbiloglu, M., Pairent, F.W. and Howard, J.M. (1968)
Surg. Gyn. Obstet. 127, 1281-1286.

355. Zbinden, G. (1969)
In: The Kidney (Rouiller, C. and Muller, A.F., eds.)
Vol. 2, pp. 401-475. Academic Press, New York.

356. Clarkson, T.W. (1972)
Ann. Rev. Pharmacol. 12, 375-406.

357. Rodin, A.E. and Crowson, C.N. (1962)
Amer. J. Path. 41, 297-307.

358. Gritzka, T.L. and Trump, B.F. (1968)
Amer. J. Path. 52, 1225-1277.

359. Biber, T.U.L., Mylle, M., Baines, A.D., Gottschalk, C.W., Oliver, J.R. and MacDowell, M.C. (1968)
Am. J. Med. 44, 664-705.

360. McDowell, E.M., Nagle, R.B., Zalme, R.C., McNeil, J.S., Flamenbaum, W. and Trump, B.F. (1976)
Virchows Arch. B Cell Path. 22, 173-196.

361. Rodin, A.E. and Crowson, C.N. (1962)
Am. J. Path. 41, 485-499.

362. Zalme, R.C., McDowell, E.M., Nagle, R.B., McNeil, J.S., Flamenbaum, W. and Trump, B.F. (1976)
Virchows Arch B Cell Path. 22, 197-216.

363. Wright, P.J. and Plummer, D.T. (1974)
Biochem. Pharmacol. 23, 65-73.

364. Schmidt, U. and Guder, W.G. (1976)
Kidney International 233-242.

365. Robinson, D., Price, R.G. and Dance, N. (1966)
Biochem. J. 102, 533-538.

366. Amador, E., Dorfman, L.E. and Wacker, E.C. (1965)
Ann. Intern. Med. 62, 30-40.

367. Rosenmann, E., Durst, A., Dishon, T. and Boss, J.H. (1970)
Israel. J. Med. Sci. 6, 311-313.

368. Wellwood, J.M., Lovell, D., Thompson, A.E. and Tighe, J.R. (1976)
J. Pathol. 118, 171-182.

369. Flanigan, W.J. and Oken, D.E. (1965)
J. Clin. Invest. 44, 449-457.

370. Bank, N., Mutz, B.F. and Aynedjian, H.S. (1967)
J. Clin. Invest. 46, 695-704.

371. Wada, T., Aizawa, K., Kan, K., Kitamoto, K., Kuroda, S., Oguwa, M. and Kato, E. (1974)
Amer. J. Path. 77, 175-179.

372. Tapp, E., Carroll, R. and Kovacs, K. (1965)
Arch. Path. 79, 629-634.

373. Peterson, E.A. (1970)
In: Laboratory Techniques in Biochemistry and Molecular Biology (Work, T.S. and Work, E., eds.) Vol. 2, pp. 223-397. North-Holland Publishing Co., Amsterdam.

374. Loening, U.E. (1967)
Biochem. J. 102, 251-257.

375. Clausen, J. (1970)
In: Laboratory Techniques in Biochemistry and Molecular Biology (Work, T.S. and Work, E., eds.) Vol. 1, pp. 397-557. North-Holland Publishing Co., Amsterdam.

376. Lee, K. and Gartner, L.M. (1976)
Pediat. Res. 10, 782-788.

377. Snedecor, G.W. and Cochran, W.G. (1967)
Statistical Methods. Iowa State University Press, Ames, Iowa.

378. Siegel, S. (1956)
Nonparametric Statistics. McGraw-Hill, Kogakusha, Tokyo.

379. Diem, K. and Lenter, C. (eds.) (1970)
Documenta Geigy Scientific Tables. Ciba-Geigy Ltd., Basle.